Mechanisms for Elimination of Low-Dose Hyper-Radiosensitivity

-

A study of cellular effects following exposure to low doses of ionizing radiation

Håvar Andreas Sollund

Thesis for the Degree of
Master of Science

Department of Physics
Faculty of Mathematics and Natural Sciences
University of Oslo

January 2009

Acknowledgements

The work presented in this thesis was carried out at the Biophysics group, Department of Physics, University of Oslo. Most of the experimental work, however, was performed at the Department of Radiation Biology, Institute for Cancer Research at The Norwegian Radium Hospital. I would therefore like to thank the Head of Department Professor Dag Rune Olsen, group leader Professor Johan Moan and Senior Scientist Trond Stokke for the use of their research facilities.

Many thanks are owed to many persons, whose help and assistance have been invaluable to me during this period.

First I want to thank my supervisors Professor Dr. Philos Erik O. Pettersen and Ph.D. Nina F. Jeppesen Edin for enthusiastic and professional guidance. Whenever I needed help, in the lab or for discussing experimental results, I was always met with an open door and good mood. Their tutoring has been very inspiring, and has been greatly appreciated.

I also wish to thank:
Joe A. Sandvik for all assistance at the cell lab.
Kirsti Solberg Landsverk and Idun Dale Rein for skillful technical assistance with flow cytometry. Cell sorting was used for a large part of the present study, and it would not have been possible without their help.
Knut Vedeld for reading through the manuscript, and for many interesting discussions on scientific topics.
All students and employees at the group for creating a wonderful work environment.
My parents and friends for all their love and support.

Finally I wish to thank my girlfriend, Patrycja Mikolajewska, who not only has been an amazing support and inspiration during this work, but also assisted me whenever an extra pair of hands was needed in the lab, and even plated some of the experiments.

Oslo, January 2009

Håvar Andreas Sollund

Summary

In the present study, T-47D cells were γ-irradiated at acute dose rates by a ^{60}Co source, and their low-dose response was extensively studied using the Puck and Marcus [1956] clonogenic assay. T-47D cells have previously been found to express pronounced low-dose hyper-radiosensitivity (HRS) when irradiated acutely by ^{60}Co γ-rays [Edin, 2003; Edin et al., 2007; Edin et al., 2008c; Edin et al., 2008b; Edin et al., 2008a]. Surprisingly, the results presented in this thesis were not in accordance with the previous reports as no HRS response could be detected, although the cells were irradiated at similar dose rates and using the same radiation quality. In a series of experiments designed to elucidate the mechanisms causing this contradiction, different aspects of the experimental procedure were changed, and the impact of these changes on the low-dose response of the cells was examined. The effects of preparing single-cell suspensions in different ways, of maintaining the temperature at 37°C during irradiation, of avoiding centrifugation, of diminishing the pipetting error and of reducing the Perspex shielding to avoid modification of the ^{60}Co γ-ray spectrum were all explored. Furthermore, experiments were performed on different cell batches to ensure that the inconsistencies were not caused by spontaneous genetic changes in the cell stock. Finally, it was speculated whether exposure to alkaline conditions during plating might be involved in the HRS removal, since considerably longer time was spent on the plating procedure per experiment in the present study than in experiments by Edin. This hypothesis was not tested, however. Thus, despite repeated investigations of the low-dose response, the presence of HRS was never successfully retrieved.

Low-dose HRS is thought to reflect the failure of an early G_2 checkpoint to arrest G_2-phase cells irradiated with less than ~0.3 Gy, and exaggerated HRS responses would be expected when irradiating G_2-enriched cell populations [Marples et al., 2003; Short et al., 2003]. Therefore, in another attempt to detect HRS in the T-47D cells, the low-dose response of G_2-enriched cell populations was measured. G_2 enrichment was obtained using Hoechst 33342-based fluorescence-activated cell sorting (FACS). For comparison, similar experiments were performed on T-47D-P cells. These cells had been given a priming dose of 0.3 Gy at a low dose rate (0.3 Gy/h) on August 17th, 2005, after which HRS was permanently eliminated [Edin et al., 2007; Edin et al., 2008b]. Consistent with the dose-response measurements on asynchronous cultures, no signs of HRS were observed in the G_2-enriched T-47D cell populations. This indicates that the removal of HRS was not caused by an insufficient amount of G_2 cells, an observation that was corroborated by flow-cytometric measurements of DNA content in asynchronous cultures at the time of irradiation (~18 hours after trypsinization). The experiments with G_2 enrichment also demonstrated that G_2 is a relatively radioresistant phase for T-47D cells, i.e., the radiosensitivity in G_2 phase is not higher than the average sensitivity in other phases of the cell cycle. The radiosensitivity of T-47D-P cells appeared to be slightly increased in G_2 phase, although the dose response of asynchronous T-47D-P cells corresponded well with that of asynchronous unprimed cultures.

Flow-cytometric measurements revealed a substantially lower fraction of G_0/G_1 cells in exponentially growing T-47D-P cells compared to unprimed T-47D cells. This difference probably reflects the shorter doubling time of the primed cells.

In studies by Edin et al. [2007; 2008c; 2008b] and Fenne [2008] the low-dose survival of T-47D-P cells was higher than predicted by the linear-quadratic model, with surviving fractions even exceeding 1 for doses up to ~0.3 Gy. A similar consistent trend of higher cloning efficiencies in low-dose irradiated flasks than in controls was not observed in the present study, but surviving fractions at the lowest doses did tend to exceed 1 when medium was changed weekly. Interestingly, a similar elevated low-dose survival was not measured when medium change during colony growth was omitted. This corresponds well with a hypothesis previously put forward by Fenne [2008], suggesting that challenge-irradiation improves the cellular attachment to the flask surface. However, the data are much too sparse to establish a connection between the elevated survival and change of medium.

Another hypothesis explains the enhanced clonogenicity of irradiated T-47D-P cells by radiation-induced recruitment of G_0-phase cells into the cell cycle [Fenne, 2008]. To test this hypothesis FACS was employed to select populations of G_0/G_1-phase cells that were subsequently incubated for different periods of time, ranging from 14-24 hours. The cell-cycle distributions were then measured by flow cytometry, and the fraction of cells remaining in G_0/G_1 in unirradiated controls was compared to the corresponding fraction in cell populations given a small radiation dose (0.2 Gy). No stimulation of irradiated G_0 cells into the cell cycle could be observed using this assay, but the measurements were not precise enough to exclude the possibility that such recruitment does occur.

T-47D-P cells that had been selected in G_0/G_1 phase and irradiated with 0.2 Gy showed a delayed exit from G_1 phase. This was evident from significantly greater G_0/G_1 fractions in irradiated than in unirradiated cell populations 14 hours ($P = 0.0065$) and 15 hours ($P = 0.021$) after plating, and it was also reflected by delayed entry into G_2/M at later times. Thus, it appears that the cells are arrested in G_1 in response to very low radiation doses. Normally wild-type p53 status is required for a marked G_1 arrest [Kastan et al., 1991; OConnor et al., 1997], and since T-47D cells contain only mutated single copies of the p53 gene [Casey et al., 1991; Nigro et al., 1989], this result was unexpected. However, a rapid p53-independent checkpoint pathway has been reported to block the G_1/S transition transiently (for a few hours only) in response to genotoxic stress [Bartek and Lukas, 2001; Kastan and Bartek, 2004]. Consistent with these reports, the observed G_1 delay in T-47D-P cells was quite short, as the differences in G_0/G_1 fractions measured after 14 and 15 hours had disappeared after 16 and 17 hours. Because of relatively few measurements and high uncertainties in the analyses of the DNA histograms, supplementary investigations are needed to corroborate these findings. It should also be investigated whether unprimed T-47D cells exhibit a similar delay.

Table of Contents

Abbreviations and Designations

AR:	Adaptive response
ATM:	Ataxia telangiectasia mutated
ATR:	Ataxia telangiectasia related
BRCA1:	Breast cancer 1 (human tumor-suppressor gene)
CCM:	Cell conditioned medium
Cdc:	Cell division cycle gene
Cdk:	Cyclin-dependent kinase
CFU:	Colony-forming unit
Chk:	Checkpoint kinase
DNA:	Deoxyribonucleic acid
DNR:	The Norwegian Radium Hospital
DSB:	Double-strand break
ERK1/2:	Extracellular signal regulated protein kinase 1 and 2
FACS:	Fluorescence-activated cell sorting
FSC:	Forward-scattered light
HCO_3^-:	Bicarbonate (hydrogen carbonate)
HDR:	High dose rate
H_2O_2:	Hydrogen peroxide
HR:	Homologous recombination
HRS:	Hyper-radiosensitivity
ICCM:	Irradiated-cell conditioned medium
IDRE:	Inverse dose-rate effect
IR model:	Induced repair model
IRR:	Increased radioresistance
LAF:	Laminar air flow
LDR:	Low dose rate
LPR:	Lysing and permeabilizing reagent
LQ model:	Linear-quadratic model
MRN complex:	Mre11-Rad50-Nbs1 complex

Nbs1:	Nijmegen breakage syndrome 1
NHEJ:	Nonhomologous end-joining
NO:	Nitric oxide
NTCP:	Normal tissue complication probability
N_2O_3:	Nitrous anhydride
$ONOO^-$:	Peroxynitrite
PARP1:	Poly(ADP-ribose) polymerase 1
PBS:	Phosphate-buffered saline
PE:	Plating efficiency
PI:	Propidium iodide
pRb:	The retinoblastoma protein
RBE:	Relative biologic effectiveness
RNA:	Ribonucleic acid
RNase:	Ribonuclease
RNS:	Reactive nitrogen species
ROS:	Reactive oxygen species
SSB:	Single-strand break
SSC:	Side-scattered light
SSD:	Source-surface distance
T-47D-P:	T-47D cells given a 0.3 Gy priming dose at 0.3 Gy/h
TCP:	Tumor control probability
TGF-β:	Transforming growth factor β
TLD:	Thermoluminescent dosimetry
UIO:	University of Oslo

1 Introduction

The aim of radiotherapy is to deliver a lethal dose to the tumor while incurring minimal damage to surrounding normal tissues. This is often a complicated task, and treatment of cancer by radiation therapy generally involves a trade-off between maximizing the tumor control probability (TCP) and maintaining the normal tissue complication probability (NTCP) at an acceptable level. It is a primary objective of radiobiology to improve the therapeutic ratio (ratio of TCP to NTCP), and many of the strategies used in clinical radiation therapy are firmly based on radiobiologic laboratory experiments.

Over the last two decades several new radiobiologic phenomena, such as genomic instability, adaptive responses, bystander effects and low-dose hyper-radiosensitivity (HRS), have been described after low doses of ionizing radiation. These phenomena have been extensively studied and characterized over the past few years, revealing large variability with widely differing responses depending on the model system studied [Schwartz, 2007]. Consequently, the modeling of low-dose radiation effects will be a highly complex process, and it is now clear that low-dose cell survival for a majority of cell lines cannot be predicted by simply back-extrapolating measurements made at higher doses [Bonner, 2004; Marples and Collis, 2008]. In particular, many mammalian cell lines exhibit HRS to acute radiation doses below ~0.5 Gy, while a transition towards increased radioresistance (IRR) is observed as the dose is increased above ~0.3 Gy. The presence of HRS is thought to reflect a dose threshold for the activation of an early G_2-phase checkpoint, in which cells irradiated in G_2 are arrested [Marples et al., 2003; Marples et al., 2004]. At the lowest doses the failure to activate this checkpoint results in premature entry of radiation-damaged G_2 cells into mitosis, leading to increased cell death.

The potential clinical implications of HRS are an area of current debate [Marples and Collis, 2008]. In conventional external-beam radiotherapy the total radiation dose to the tumor volume is typically divided into fractions of 2 Gy that are given with 24-hour intervals, although many alternative treatment protocols exist. The surrounding tissues will generally receive much smaller doses, and especially with the advent of intensity-modulated radiation therapy there is a risk of exposing normal tissues to repeated dose fractions in the HRS range, possibly resulting in increased complication probability [Honore and Bentzen, 2006]. Thus HRS can negate the predicted benefits of reducing the radiation dose to normal tissues. Conversely, in the case of HRS-proficient tumors, HRS can be exploited clinically by using multiple low-dose fractions to improve tumor curability. A combined chemo-radiotherapy approach to enrich the G_2/M-phase fraction in the tumor by chemical cell synchronization prior to irradiation has shown considerable promise in experiments and is now being tested clinically [Dey et al., 2003; Marples and Collis, 2008; Spring et al., 2004]. However, low-dose fractionated treatment strategies will be successful only if there is a hypersensitive response to each dose in a fractionated regimen. It has previously been demonstrated that HRS can be abrogated in response to pretreatment with DNA damaging agents such as a priming dose of X-rays [Joiner et al., 1996; Marples and Joiner, 1995], and in studies using radiotherapy alone, HRS *in vitro* did not translate into improved outcomes of ultrafractionated irradiation *in vivo* [Krause

et al., 2005; Krause et al., 2003]. For the possible clinical utilization of the HRS response, investigations of mechanisms causing HRS elimination are therefore of great interest.

Previous studies by our group have provided valuable new insights into the nature of processes concerning HRS removal [Edin, 2003; Edin et al., 2007; Edin et al., 2008c; Edin et al., 2008b; Edin et al., 2008a]. T-47D breast cancer cells were found to display a pronounced HRS-response when irradiated with ^{60}Co γ-rays at acute dose rates [Edin, 2003; Edin et al., 2007], but HRS was abolished in response to diverse forms of pretreatment, such as priming doses of radiation, chronic moderate hypoxia and treatment with medium transferred from cell cultures irradiated at low dose rates [Edin et al., 2007; Edin et al., 2008c; Edin et al., 2008b; Edin et al., 2008a]. Surprisingly, the recovery of HRS following a small priming dose was demonstrated to depend on dose rate, and irradiating the cells with a priming dose of 0.3 Gy at a low dose rate (0.3 Gy/h) eliminated HRS permanently [Edin et al., 2007; Edin et al., 2008b]. The first culture that was primed in this way, in the following denoted T-47D-P, has at present time been cultivated for more than three years without recovering HRS. Interestingly, the T-47D-P cells consistently respond to the lowest doses of challenge-irradiation with surviving fractions above 1, i.e., clonogenicity seems to be enhanced by low doses of radiation [Edin et al., 2008b; Edin et al., 2007]. Studies of the growth pattern of T-47D-P cells by means of time-lapse filming failed to identify the mechanisms behind the elevated survival, but it was hypothesized that the effect is caused either by radiation-induced recruitment of G_0-phase cells into the cell cycle, or by a decrease in the loss of clonogenic units at medium change due to improved cellular surface attachment triggered by challenge-irradiation [Fenne, 2008].

A method for internal irradiation of cells at ultra-low dose rates (~0.01 Gy/h) by incorporation of tritium into cellular protein has previously been described by Søvik [2002] and Bjørhovde [2006]. The purpose of the present study was originally to determine possible thresholds in priming dose and dose rate for abrogation of HRS by tritium decay. However, in the preliminary experiments with unprimed T-47D cells HRS could not be detected in response to acute ^{60}Co γ-irradiation. Thus, an identification of the mechanisms responsible for removing HRS in the unprimed cells became the main focus of the study, and different aspects of the experimental procedure that could influence the low-dose behavior were investigated in a series of dose-response measurements. At the same time the previous work by Fenne [2008] was continued by performing experiments designed to test whether recruitment of G_0 cells can explain the elevated low-dose survival of T-47D-P cells. Pure G_0/G_1-phase T-47D-P cell populations were collected, and the rate of exit from G_1 was monitored. Furthermore, low-dose responses of G_2-enriched populations of T-47D and T-47D-P cells were examined, since the "early" G_2-phase checkpoint is so important for the HRS response. Cells from specific cell-cycle phases were selected by means of fluorescence-activated cell sorting (FACS).

2 Theory

2.1 Cell Biology

2.1.1 The Cell Cycle

The sequence of processes by which the cell duplicates its contents, including the vast amount of DNA in its chromosomes, and then distributes organelles and chromosome copies into two genetically identical daughter cells, is referred to as the cell cycle. The cell cycle is commonly divided into interphase, in which the cells grow and duplicate its DNA, and M phase (*M* for *m*itosis), which includes the segregation of replicated chromosomes during mitosis and the cytoplasmic division during cytokinesis. Interphase cells are easily distinguished from mitotic cells by the use of a light microscope. Interphase is further divided into three subphases; G_1, S and G_2, respectively. Using autoradiography, these phases were first discovered and described by Howard and Pelc [1953]. In a typical human cell M phase lasts for no more than an hour, while the much longer interphase occupies the rest of the cell cycle (see for instance table 4.1, p. 50 in Hall and Giaccia [2006]).

Accurate transmission of genetic information from one cell to its progeny is a necessity for the survival of organisms. In order to accomplish such a difficult task, the cell must first replicate its DNA with extreme accuracy. This occurs during S phase (*S* for *s*ynthesis). Thereafter the cell must segregate the identical sister chromatids equally into its two daughter cells during mitosis, which the cell achieves by constructing a spindle of microtubules, stretching from one pole of the cell to the other. The microtubules will attach to specialized regions of the chromosomes, called the kinetochores, and pull the chromatids apart. However, the most time-consuming undertaking within a cell's lifespan is the growth and doubling of protein mass and organelles. Partly to allow time for this growth, gap phases are inserted between the S and M phases. G_1 phase is the first phase of the cell cycle, and also the one with the greatest variation in length between different cells under different circumstances. The gap between S phase and mitosis is called G_2. In addition, the gap phases are important for monitoring the internal and external environment, making sure that conditions are suitable before triggering S or M phase. Unfavorable extracellular conditions will often yield insufficient amounts of extracellular signals (growth factors), causing the cell to be delayed in G_1 or enter a quiescent state G_0. The cell might remain in G_0 for long periods of time (permanently in the case of a terminally differentiated cell), or re-enter the cell cycle if conditions are favorable. However, once the cell progresses through a restriction point near the end of G_1, it is committed to DNA replication even if growth factors are removed [Alberts et al., 2002, p. 986].

2.1.2 Cell-Cycle Regulation

Progression through the cell cycle is regulated by a constantly present, but periodically activated family of protein kinases, known as cyclin-dependent kinases (Cdks). In its active state these Cdks initiate important cell-cycle events such as DNA replication and

mitosis by phosphorylating a number of protein substrates. The activity of the Cdks is controlled by a complex network of enzymes and other proteins. Most importantly they are not active unless bound to a cyclin subunit, forming a Cdk-cyclin complex. The cyclins are synthesized and degraded at specific stages of the cycle, giving rise to a cyclically varying concentration (hence their name). Moreover, the onset of cyclin synthesis or degradation is regulated by different mechanisms, for instance will production of cyclin D (G_1-cyclin) require preceding mitogenic stimulation, as described in chapter 2.1.1. In this way, the activation of different Cdk-cyclin complexes triggers the next event in the cycle at the appropriate time (see fig. 2.1). There are also many possibilities for fine-tuning Cdk activity and cell-cycle progression through interactions with other kinases, phosphatases and Cdk inhibitor proteins.

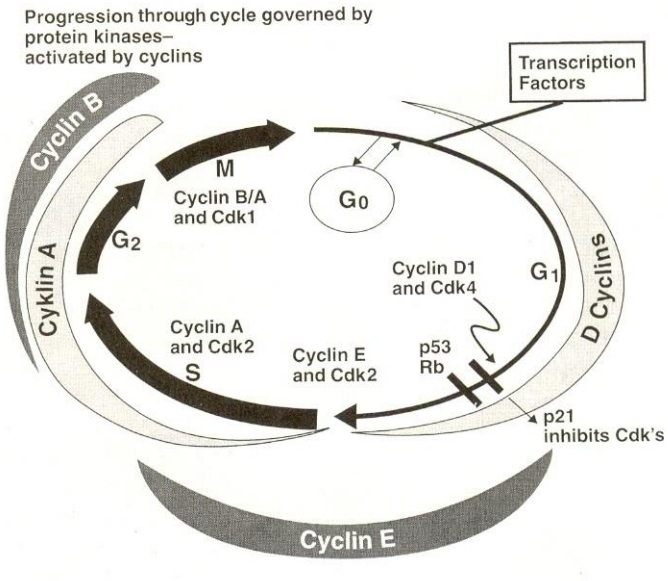

Figure 2.1
The diagram shows how different phases of the cell cycle are regulated by the periodic activation of various Cdk-cyclin complexes. These protein kinases are required for the phosphorylation of protein substrates that trigger cell-cycle progression. Also shown are the tumor-suppressor proteins p53 and pRb. The inhibitory actions of these proteins prevent premature entry into S phase (see Ch. 2.1.3) [Hall and Giaccia, 2006, fig. 4.4].

2.1.3 Checkpoints

Cell-cycle progression can be halted at several checkpoints along the cycle. These checkpoints are necessary to ensure that the events of the cell cycle are completed in the correct order [Hartwell and Weinert, 1989], and also to ensure that genomic integrity is maintained. The restriction point in late G_1 has already been mentioned. A cell will pass this checkpoint only if sufficient growth factor binding to membrane receptors triggers intracellular signal pathways resulting in increased transcription of D-type cyclins. The binding of these cyclins to Cdk 4 or Cdk 6 yields rising concentration of active G_1-Cdks. These Cdk complexes phosphorylate the Rb protein, an inhibitor of cell-cycle

progression. Both copies of the Rb gene are mutated or missing in children with retinoblastoma. Such a gene, for which a loss-of-function mutation can lead to tumorigenesis, is called a tumor-suppressor gene. In its active form, pRb binds to the gene regulatory protein E2F. Phosphorylation of pRb makes it inactive, freeing E2F. The liberated E2F increases the transcription of cyclin E and cyclin A, leading to increased Cdk-cyclin activity. This results in a positive feedback loop, since the active Cdks will phosphorylate more pRb. Furthermore, they will phosphorylate Cdk inhibitor proteins like p27, marking them for degradation [Alberts et al., 2002, p.1005]. Once a cell in this way passes the restriction point, it is committed to enter S-phase.

Two other important checkpoints are the DNA replication checkpoint and the spindle-attachment checkpoint [Alberts et al., 2002, p.1000-1003]. The first of these checkpoints prevents entry into mitosis by keeping the phosphatase Cdc25C (Cdc – *C*ell *d*ivision *c*ycle gene) inactive until DNA replication is complete. Cdc25C is needed to remove an inhibitory phosphate from M-Cdk in order to trigger mitosis [Alberts et al., 2002, p.1000; Hall and Giaccia, 2006, p.297]. The second checkpoint arrests the cell in metaphase, when the chromosomes are aligned at the equator of the mitotic spindle, until all kinetochores are properly attached to microtubules.

Cell-cycle progression can also be blocked at DNA damage checkpoints, following exposure to chromosome-damaging chemicals or ionizing radiation [Alberts et al., 2002, p.1007-1008]. There are damage checkpoints in late G_1- and in S-phase, both arresting the cell to give time for repair, and thus avoiding the replication of damaged DNA. In addition, two molecularly distinct checkpoints have been shown to function at the G_2/M interface [Xu et al., 2002]. These checkpoints seek to prevent the cell from entering mitosis with unrepaired DNA, as this is potentially lethal to the cell, and also involves a risk of mutation in cancer-associated genes if the cell is able to divide despite its DNA damages.

The ATM (*a*taxia *t*elangiectasia *m*utated) protein contributes in initiating checkpoint pathways in G_1, S and G_2 phases of the cell cycle [Xu et al., 2002]. If the cell's DNA is damaged by ionizing radiation in G_1, the ATM dimer autophosphorylates, dissociates and releases active ATM monomers [Bakkenist and Kastan, 2003]. The activated ATM monomers phosphorylate the tumor-suppressor gene p53 and the ubiquitin ligase Mdm2 [Hall and Giaccia, 2006, p. 297], which normally keeps p53-levels in the cell low by marking it for degradation through ubiquitylation [Alberts et al., 2002, p. 995 and 1008]. ATM also phosphorylates the checkpoint kinase Chk2, after which Chk2 also participates in the phosphorylation of p53. This Chk2-mediated phosphorylation results in stabilization of p53 by disrupting Mdm2 binding [Hirao et al., 2000; Kastan and Lim, 2000]. These phosphorylation events are followed by quickly increasing levels of activated p53, stimulating expression of the p21 gene (also known as WAF1 or CIP1). Thereafter, the Cdk inhibitor protein p21 will arrest the cell in G_1 as long as DNA damage persists, and p53 levels remain high. If the DNA damage is so severe that repair is impossible, p53 can initiate suicide by programmed cell death, so-called apoptosis [Alberts et al., 2002, p. 1008 and 1345]. Alternatively, p53 is capable of inducing sustained and even permanent G_1 arrest through the pathway described above [Kastan

and Bartek, 2004]. In this way, the cell will not endanger the health of the entire organism by propagating damaged DNA, thus risking harmful mutations and development of cancer. The importance of this checkpoint for maintaining genomic integrity is well illustrated by the fact that p53 is mutated in at least half of all human cancers [Alberts et al., 2002, p. 1008]. Wild-type p53 status has been reported to be required for radiation-induced G_1 arrest [Kastan et al., 1991; OConnor et al., 1997]. Note, however, that p53 acts as a transcription factor, and processes such as transcription and protein synthesis are too slow to account for the rapid inhibition of G_1/S-Cdks seen upon DNA damage [Bartek and Lukas, 2001]. A rapid p53-independent pathway has been observed to induce a transient G_1 block in response to UV and ionizing radiation [Bartek and Lukas, 2001; Kastan and Bartek, 2004; Mailand et al., 2000]. This pathway operates by targeting the phosphatase Cdc25A, marking it for degradation. Cdc25A is required to remove an inhibitory phosphate from Cdk2 molecules, and degradation of Cdc25A will therefore keep G_1/S-Cdks inactive. The ubiquitylation of Cdc25A is mediated by the Chk1 and Chk2 kinases, which are phosphorylated and activated by ATM and ATR (*a*taxia *t*elangiectasia *r*elated, a kinase related to and often participating in damage responses together with ATM).

The S-phase checkpoint can occur throughout S phase, i.e., it is not located at a specific stage of the phase like the G_1 and G_2/M checkpoints (see fig. 2.2). In contrast to the p53-mediated G_1 checkpoint, the S-phase checkpoint arrests the cells transiently, while inhibiting replication-origin firing and protecting the integrity of stalled replication forks [Kastan and Bartek, 2004]. More than one pathway is thought to activate the S-phase checkpoint. However, cells lacking functional key proteins like ATM or Nbs1 (*N*ijmegen *b*reakage *s*yndrome) are defective in this checkpoint [Kastan, 2001; Zhao et al., 2000].

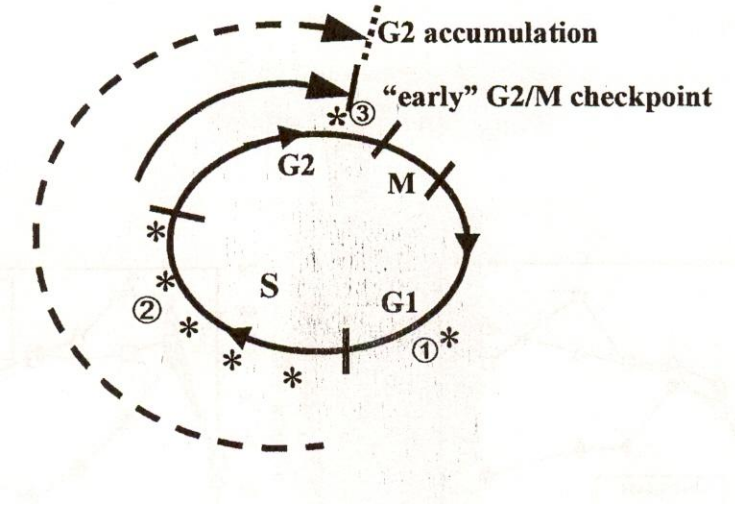

Figure 2.2
Important checkpoints activated by ionizing radiation are found at several locations in the cell cycle. The checkpoints are labeled with asterisks. (1), The p53-dependent G_1 checkpoint; (2), The ATM-dependent S-phase checkpoint, occurring throughout S phase; (3), The ATM-dependent "early" G_2/M checkpoint inhibits cells that are irradiated in G_2 from entering mitosis (indicated by unbroken arrow). G_2 accumulation reflects the arrest of cells that are in S (or G_1) phase at the time of irradiation (indicated by dashed arrow). [Xu et al., 2002, fig. 3]

As mentioned before, there are two distinct mechanisms for G_2 arrest induced by ionizing irradiation [Xu et al., 2002]. The so-called "early" G_2/M checkpoint probably occurs

about 30 minutes prior to chromosome condensation. This checkpoint is very transient, ATM dependent and dose independent between 1 and 10 Gy. However, there is a dose threshold for activation of the checkpoint, implicating that the arrest is less effective at doses below ~0.3-0.4 Gy [Krueger et al., 2007a; Marples et al., 2003; Xu et al., 2002]. This is utterly important in the context of low-dose hyperradiosensitivity and will be discussed later (see Ch. 2.4.4). The "early" G_2/M checkpoint prevents cells that were in G_2 at the time of irradiation (or exposure to DNA damaging agents) from entering into mitosis.

The other mechanism for G_2 arrest has been known for decades and was first described by Sinclair [1968]. G_2 accumulation, or the Sinclair checkpoint, is measurable only several hours after irradiation, is dose dependent and is ATM independent. This checkpoint causes an accumulation in G_2 of cells that were in earlier phases of the cell cycle at the time of irradiation. Cells lacking the S-phase checkpoint, like AT and Nbs cells, show a prolonged G_2 arrest and enhanced G_2/M accumulation [Xu et al., 2002]. Multiple kinase signaling pathways are assumed to be participating in the regulation of G_2/M checkpoints [Hall and Giaccia, 2006, p. 297-298].

2.2 Radiation Physics

2.2.1 Ionizing Radiation and Radioactive Decay

Common for all ionizing radiations is their ability to ionize atoms and molecules of the absorber. The radiation must therefore carry kinetic or quantum energies in excess of 4-25 eV, which is the energy needed to cause the escape of a valence electron, in order to be termed "ionizing" [Attix, 1986, p. 2].

It is common to distinguish between directly and indirectly ionizing radiations. Directly ionizing radiations deposit energy and cause ionizations through many small, direct Coulomb-force interactions with atoms of the absorber. Hence, fast charged particles are directly ionizing. On the other hand, neutrons and electromagnetic radiations such as X- and γ-rays, are referred to as indirectly ionizing radiations. These radiations first transfer their energy to charged particles in the absorber, which in turn deliver the energy in a directly ionizing manner. In contrast to the directly ionizing radiations, neutrons and photons deposit their energy in a relatively few large interactions.

Two radiation sources were used in the experimental work of this thesis. Most importantly, a ^{60}Co unit was applied to irradiate cell flasks. In addition a few experiments were performed where tritium was incorporated into the proteins of the cells (see Materials and Methods, Ch. 3.3.3), giving the cells a radiation dose prior to external irradiation. In both cases the radiation originates from radioactive decay.

Radioactive decay is the spontaneous emission of energy from an unstable nucleus. The energy is emitted as particulate or electromagnetic radiation. The disintegration is a random process at the atomic level. Consequently, a prediction of when a particular atom will decay is impossible, but given a large number of similar atoms the decay rate is

predictable. The number of decaying nuclei per unit time, dN/dt, is, at any time, proportional to the total number of radioactive nuclei N:

$$-\frac{dN}{dt} = \lambda N \tag{2.1}$$

where the constant of proportionality, λ, is generally known as the decay constant. The straight-forward solution to the first-order differential equation (2.1), is

$$N(t) = N_0 e^{-\lambda t} \tag{2.2}$$

where N_0 is the initial number of radioactive nuclei.

The activity A is simply defined to equal the decay rate:

$$A = \lambda N \tag{2.3}$$

The SI unit of activity is the becquerel (Bq), defined as one decay per second:

$$1Bq = 1s^{-1}$$

The expectation value of the time required for half of the initial number of nuclei to disintegrate is known as the half-life, $T_{\frac{1}{2}}$. $T_{\frac{1}{2}}$ is found by setting $N(t) = \frac{N_0}{2}$ and solving for t in equation (2.2):

$$T_{\frac{1}{2}} = \frac{\ln 2}{\lambda} \tag{2.4}$$

2.2.2 Interaction of Radiation with Matter

Charged particles (directly ionizing) deposit energy through Coulomb-force interactions with nearly every atom they pass. The incident particles can interact with the electrons or the nuclei of the atoms, as all these particles are charged and thereby surrounded by Coulomb electric force fields. In most of these interactions the energy transferred from the incident particles to the atoms of the absorber are deposited as tiny energy packets (soft or glancing collisions). However, larger energy depositions might also occur (hard or knock-on collisions). Although hard collisions are rare compared to soft collisions, the primary particle generally loses comparable fractions of its initial energy on these two processes [Attix, 1986, p. 162]. Hard collisions often give rise to secondary electrons with sufficient kinetic energy to deposit energy a distance away from the track of the primary particle. Such secondary electrons are called δ-rays.

The expectation value of the rate of energy *T* lost by a charged particle per unit of path length *x*, is called its stopping power, *dT/dx*. A similar, but slightly different quantity is the linear energy transfer (LET), *dE/dl*, or the average energy *dE* locally imparted by a

charged particle in traversing a distance of *dl* [Hall and Giaccia, 2006, p. 106-107]. Since δ-rays might transport energy away from the primary track, the stopping power will overestimate the locally imparted energy. The linear energy transfer is therefore defined as the energy dE_Δ lost by a charged particle in traversing a distance *dl* due to soft and hard collisions minus the total kinetic energies of δ-rays with individual energies in excess of a cutoff value Δ [Attix, 1986, p. 179].

Compared to charged particles, X- and γ-ray photons interact with matter in a distinctly different manner. Most importantly, they carry no charge; hence no Coulomb interactions will occur with the atoms of the absorber. For the energies used in radiotherapy, three types of interaction are dominating: photoelectric effect, Compton scattering and pair production. The cross sections for these types of interaction depend on the energy of the incoming photon and the atomic number *Z* of the absorber. In carbon (whose atomic number $Z = 6$ is close to the effective atomic numbers of biologic materials) the Compton effect dominates for photon energies ranging from 100 keV to 20 MeV [Attix, 1986, p. 147]. Only γ-rays with energies of ~1 MeV were used in the experiments of this thesis, which means that the vast majority of interactions were Compton events.

The cross section of the Compton effect has a very weak dependence on *Z*, since the binding energy of the electron is nearly negligible compared to the energy of the incoming photon. In a Compton event the photon is deflected from its original path by transferring energy and momentum to the electron. The fraction of energy lost by a 1 MeV photon may vary from 0 to 80%, with a mean value of approximately 45% [Attix, 1986, p. 135]. The resulting energetic secondary electrons will subsequently give rise to tracks of excitations and ionizations (as described above), capable of causing biologic damage.

2.2.3 Cobalt-60 [^{60}Co]

^{60}Co is a radioactive nuclide with a half-life of 5.2718 years (1925.1 days). Cobalt unit γ-rays are emitted at the energies 1.173 MeV and 1.332 MeV. Both photons are emitted at every disintegration event (probabilities of 0.999 and 1.000, respectively), and they are accompanied by a 317.9 keV β-particle [Mayles et al., 2007, table M.4]. These low-energetic β-particles are filtered out by the capsule walls of the treatment unit. Compton events within the source itself result in the incident (on the cell flasks) beam having a continuum of energies that are slightly lower than the energies of the two decay photons. Typically, about 25% of the primary photons are lost due to self-attenuation [Mayles et al., 2007, p. 242-243 and 452].

The LET of ^{60}Co γ-rays is very low, 0.3 keV/μm according to Dertinger and Jung [1970, table 4, p. 43] or 0.2 keV/μm according to Hall and Giaccia [2006, table 7.1].

2.2.4 Tritium

Tritium [^{3}H] is a radioactive hydrogen isotope with a half-life of 12.32 years. Tritium disintegrates into the stable helium isotope ^{3}He accompanied by the emission of a β-particle and an anti-neutrino:

$$^3\mathrm{H} \longrightarrow {}^3\mathrm{He} + \beta + \overline{\nu}$$

The energy released in this reaction is constant, and is shared between the electron and the anti-neutrino (plus a small amount of recoil energy given to the nucleus). The electron can obtain a continuum of energies, the maximum energy being 18.6 keV and the mean energy being 5.75 keV [Feinendegen, 1967]. This corresponds to a maximum and mean range in water of 6 μm and 1 μm, respectively [ICRP, 1983]. For comparison, the diameter of T-47D cells was found to be 14±1 μm by Bjørhovde [2006] and 14±2 μm by Palmer et al. [2003], while the nucleus diameter was found to be 11±1 μm by Bjørhovde [2006].

The radiation originating from tritium decay is generally considered to be of low LET [Pouget and Mather, 2001; Radford, 2002]. The emitted electron can, however, produce regions of relatively high LET, particularly near track ends [Morstin et al., 1993]. Since the electron has a mean energy of 5.75 keV, and a mean range of 1 μm in water, the LET should be of the order of 5-6 keV/μm. Tritium administered to cells in vitro as tritiated amino acids yields relative biologic effectiveness (RBE, see discussion by Hall and Giaccia [2006, chapter 7]) values 2 to 3 times higher than ^{60}Co γ-rays at low doses [Straume and Carsten, 1993].

2.2.5 Dosimetry

The following precise definition of absorbed dose is taken from Attix [1986, p. 26-27]:
Assume that matter of mass m is contained in a finite volume V. The energy imparted by ionizing radiation to the mass m is defined as

$$\epsilon = (R_{in})_u - (R_{out})_u + (R_{in})_c - (R_{out})_c + \Sigma Q \tag{2.5}$$

where $(R_{in})_u$ and $(R_{in})_c$ are the radiant energies of all the uncharged and charged radiation entering V, while $(R_{out})_u$ and $(R_{out})_c$ are the corresponding energies leaving V. ΣQ is the net energy derived from rest mass in V (>0 if $m \rightarrow E$, <0 if $E \rightarrow m$).

The absorbed dose at any point P in V is then defined as

$$D = \frac{d\epsilon}{dm} \tag{2.6}$$

where $d\epsilon$ is the expectation value of the energy imparted for an infinitesimal volume dv at point P, and dm is the mass in dv. The preferred unit for absorbed dose is the gray:

$$1\mathrm{Gy} = 1\mathrm{J/kg}$$

Many different dosimeters are used to determine the absorbed dose. In general, dosimeters consist of two parts. The first component is a sensitive volume, i.e., a compound that experiences changes when exposed to radiation. The other component is a device that converts these changes into measurable signals [Henriksen and Maillie, 2003, p. 47].

Thermoluminescence Dosimetry (TLD)
Thermoluminescent dosimeters consist of crystals with an empty conduction band. If one of these crystals is irradiated with ionizing radiation, some electrons gain enough energy to make a transition from the valence band to the conduction band. The phosphors used for TL dosimeters contain imperfections that can trap electrons at an energy state in between the conduction and the valence band. The number of electrons trapped increases with the incident radiation intensity and the absorbed dose, and the electrons can persist in this metastable excited state for extended periods of time. When the irradiated phosphors are subsequently heated, the electrons gain enough energy to be raised back into the conduction band and release energy (light photons) by recombining with a positive hole. The emitted light is detected by a photomultiplier tube, and converted to an electrical current which is amplified and recorded. The intensity of the light (luminescence) is a measure of the dose [Attix, 1986, p. 395-411; Metcalfe et al., 1997, p. 159-163].

Several different phosphor materials with different characteristics and sensitivities are available. Most common is lithium fluoride crystals with impurities of magnesium and titanium (LiF: Mg, Ti). LiF has an effective atomic number of 8.14, which is close to tissue (Z_{eff} = 7.51) and water (Z_{eff} = 7.78) equivalence [Metcalfe et al., 1997, p. 167]. TL dosimeters also have a very broad sensitivity range, from several Gy down to ~10^{-5} Gy. They can normally be reused after reading, making TLD an economic method of measuring dose. These advantages, combined with their small size and absence of wire connections, have made TLD dominating in personal dosimetry [Metcalfe et al., 1997, Ch. 3.9]. TLD was used to determine the dose rates for different ^{60}Co-irradiation setups (see Ch. 3.3.2).

Tritium Dosimetry
The dosimetry of the incorporated tritium was estimated by Åste Søvik [2002]. The so-called MIRD (Medical Internal Radionuclide Dose) schema was used. This mathematical framework was originally derived to facilitate the calculation of mean absorbed organ doses from distributed sources of radioactivity in the context of nuclear medicine. However, the formalism is readily extended to be applicable also at the subcellular level [Howell, 1994]. A detailed description of the MIRD mathematical formalism is given by Bjørhovde [2006].

To accommodate the MIRD framework to cellular dimensions, a model introduced by Goddu et al. [1997] was applied. Within this model the cell is regarded as two concentric spheres; one with radius R_C, representing the cytoplasm, and one with radius R_N,

representing the nucleus. Both spheres have density 1 g/cm^3, and the distribution of radioactivity is homogenous within each sphere. The model contains several reasonable simplifications. For instance, δ-electrons are ignored, the dose contribution from emitters outside the cell is considered negligible, and since the electron range is short compared to the dimensions of the cell and its nucleus, the curvature of electron paths is ignored. The model estimates the average dose rate to a population of cells with incorporated radionuclides, such as tritium. The average dose rate to the nucleus is given by

$$\dot{D_N} = A_C \left[f_N S(N \leftarrow N) + f_{Cy} S(N \leftarrow Cy) \right] \tag{2.7}$$

where A_C is the intracellular activity, $S(N \leftarrow N)$ is the dose to the nucleus per unit activity in the nucleus, $S(N \leftarrow Cy)$ is the dose to the nucleus per unit activity in the cytoplasm, and f_N and f_{Cy} are the fractions of intracellular activity in the nucleus and the cytoplasm, respectively. The cellular S values are functions of R_C and R_N, and have been calculated by Goddu et al. [1997]. For T-47D cells the activity of the cell nucleus and the cytoplasm plus the incorporation kinetics, were found experimentally using a liquid scintillation counter [Bjørhovde, 2006].

2.3 Radiobiology

2.3.1 Direct and Indirect Action of Radiation

The principal target for cell killing and other cytotoxic and mutagenic effects of ionizing radiation on cells, is the DNA [Hall and Giaccia, 2006, p. 35; Pouget and Mather, 2001].

Direct action of radiation occurs if the radiation particles interact directly with the critical targets of the cell, causing biologic change by ionizing or exciting atoms within these targets. However, typically 80% of the cell consists of water [Hall and Giaccia, 2006, p. 12]. If the radiation interacts with water molecules (or other molecules surrounding the targets), free radicals are produced. These radicals are atoms carrying an uncoupled electron in the outer shell, making them highly reactive. When they are produced in the vicinity of the critical targets, they are able to diffuse towards and damage these targets. This is called indirect action of radiation. Hydroxyl radicals (OH·) arising from ionization of water are estimated to inflict about two thirds of the X-ray damage to DNA in mammalian cells [Hall and Giaccia, 2006, p. 12]. Although this estimate is generally accepted, it is somewhat debated, and some reports even suggest that DNA damage by indirect action is negligible in mammalian cells [Pohlit and Drenkard, 1985].

Direct action of radiation is the dominant process for high-LET radiations (such as α-particles and fast neutrons), while indirect action of radiation is dominant for sparsely ionizing, low-LET radiations (such as X- and γ-rays and electrons).

2.3.2 Radiation Damage

Radiation damage is conventionally divided into three categories: (1) lethal damage, which is irreversible, irreparable and results in cell death, (2) potentially lethal damage, and (3) sublethal damage. The potentially lethal damages cause cell death under normal circumstances, but if the post-irradiation environment is suboptimal for growth, they might be repaired. Sublethal damage is readily repaired under normal conditions, but accumulation of additional sublethal damage sufficiently close in space and time, can cause formation of lethal damage. The increase in survival observed if a radiation dose is split into two fractions separated by a time interval, is attributed to repair of sublethal damage [Hall and Giaccia, 2006, p. 65-70].

Even though cytoplasmic irradiation and irradiation of the cell membrane have been shown to be secondary targets for ionizing radiation [Cohen-Jonathan et al., 1999; Pouget and Mather, 2001], and there is evidence suggesting involvement of the nuclear membrane in radiation-induced cell killing, damages to the DNA are the most important [Hall and Giaccia, 2006, p. 36]. Such damages include purine and pyrimidine base damages, sugar damages, DNA-protein cross-links, DNA-DNA cross-links and strand breaks [Ward, 1988].

Strand breaks can be divided into single- and double-strand breaks (SSBs and DSBs, respectively). Apart from the small risk of misrepair, the SSBs are of little biologic consequence, as they are easily repaired using the opposite strand as a template. DSBs are on the other hand considered to be the most deleterious lesions caused by ionizing radiation [Bryant, 1985; Burma et al., 2006]. To deal with such lesions, mammalian cells adopt two repair mechanisms: (1) nonhomologous end-joining (NHEJ), in which the broken ends are simply juxtaposed and ligated, generally resulting in the loss of one or more nucleotides, or (2) homologous recombination (HR), which is an error-free process where information is copied from the undamaged homologous chromosome or sister chromatide. HR occurs primarily in late S/G_2, when sister chromatides are available, but that does not imply that the error-prone NHEJ mechanism stops occurring in this phase of the cell cycle [Hall and Giaccia, 2006, p. 60-64]. In addition to the mutations suffered from NHEJ, DSBs might result in deletions (loss of DNA fragments), translocations (chromosome fragments are interchanged), or asymmetric chromosomal aberrations (rings, dicentrics, anaphase bridges). Asymmetric aberrations are lethal for the cell in most cases [Hall and Giaccia, 2006, Ch. 2]. In fact, there is virtually a one-to-one correlation between cell survival and the average number of asymmetric chromosomal aberrations per cell [Hall and Giaccia, 2006, p. 36-37 and 45] in cells dying a mitotic death (see chapter 2.3.3). It is important to be aware, however, that a variety of damages with different degrees of complexity and lethality, are termed DSBs [Goodhead, 1989; Goodhead, 1994; Radford, 2002].

Around 1000-2000 instances of base damage, 850-1000 single-strand breaks and 40 double-strand breaks are produced per mammalian cell per Gy of low-LET radiation [Goodhead, 1994; Hall and Giaccia, 2006, p. 19; Pouget and Mather, 2001].

2.3.3 Dose-Survival Measurements

The most frequent mode of radiation-induced cell killing is the mitotic death, in which cells die attempting to divide because of chromosomal aberrations [Cohen-Jonathan et al., 1999; Hall and Giaccia, 2006, p. 36]. Death occurs within a few cell division cycles following irradiation, often after the formation of daughter cells containing micronuclei. Mitotic cell death usually leads to necrosis [Cohen-Jonathan et al., 1999]. In this process the cell typically swell and burst, causing an inflammatory response in tissues. In addition to necrosis, some irradiated cells will undergo a process similar to senescence, remaining metabolically active, but no longer being clonogenic [Cohen-Jonathan et al., 1999]. It has been shown that p53 and pRb play a critical role in the induction of this process [Ben-Porath and Weinberg, 2005].

Cells can also disintegrate through another mechanism, termed apoptosis. This form of programmed cell death is more advantageous for neighboring cells, as the dying cell after a series of morphologic events finally separates into many membrane-bound fragments containing its organic components. These apoptotic bodies are subsequently phagocytosed by macrophages or neighboring cells, and the components reused [Alberts et al., 2002, p. 1011; Hall and Giaccia, 2006, p. 36]. Apoptosis after irradiation seems commonly to be a p53-dependent process [Hall and Giaccia, 2006, p. 36]. However, p53-mutated cells do not completely lose the ability to undergo apoptosis, they are just less efficient in this respect [Roos and Kaina, 2006].

To measure the ability of ionizing radiation to inactivate cells, an appropriate end-point must be established. In radiobiology, it is conventional to regard the loss of reproductive integrity rather than cell death as the criterion for inactivation. Consequently, it is not sufficient to remain metabolically active in order to be counted as a surviving cell - the cell must also be able to divide. A surviving cell is defined as a cell able to form a colony of 40-50 cells [Steel, 1997].

In vitro radiation response is normally measured using an assay for clonogenicity, scoring the ability of a single cell to produce a viable colony in concordance with the definition above [Puck and Marcus, 1956]. The dose-response curve resulting from this assay is typically plotted in a semi-logarithmic plot, based on the assumption that the increased number of inactivated cells dN because of a dose increment dD, should be proportional to the number of surviving cells $N(D)$ and to the added dose:

$$dN = -f(D)NdD \tag{2.8}$$

Equation (2.8) gives the following expression for the surviving fraction S:

$$\ln S = \ln \frac{N}{N_0} = -\int_0^D f(D)dD \tag{2.9}$$

Hence the cell survival curve is plotted with the surviving fraction as the logarithmic ordinate and the dose as the linear abscissa. In some cases, as for the densely ionizing, high-LET radiations, the proportionality factor $f(D)$ is independent of dose, and the curve simply becomes a straight line. For low-LET radiations like X- and γ-rays, the curve has an initial linear slope, followed by a shoulder region, before it often straightens again at very high doses [Hall and Giaccia, 2006, p. 32] (see fig. 2.3).

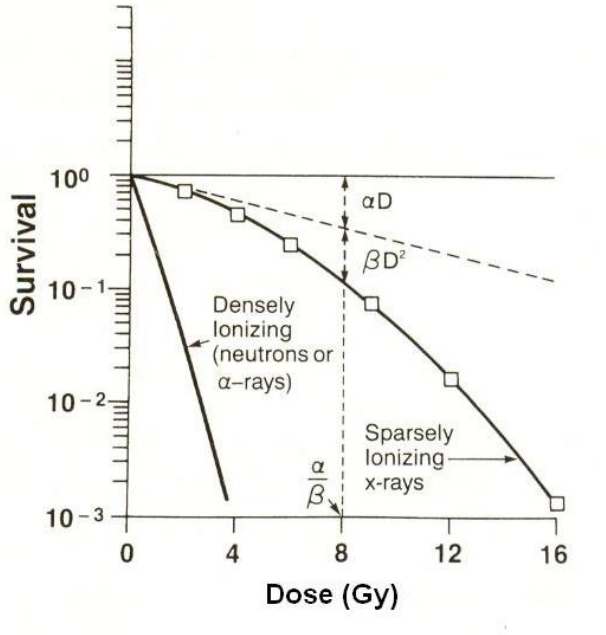

Figure 2.3
The surviving fraction of cells is plotted on a logarithmic scale against dose on a linear scale. High-LET radiations (α-particles, low-energy neutrons) produce linear dose-response curves, while low-LET radiations (X- and γ-rays) produce dose-response curves with an initial linear slope followed by a shoulder region. At the dose α/β, the linear and quadratic components of cell-kill are equal. [Hall and Giaccia, 2006, fig. 3.3, modified]

The best fit to the survival curves, at least within the dose range relevant for clinical radiotherapy, is often obtained by the linear-quadratic (LQ) model, as first described by Sinclair [1966]. In this model, one assumes $f(D) = \alpha + \beta D$, resulting in the following famous expression for cell survival as a function of dose:

$$S = e^{-\alpha D - \beta D^2} \tag{2.10}$$

This equation was later derived by Chadwick and Leenhouts [1973], based on the assumptions that DNA is the critical target and the critical damage is a double-strand break in the DNA helix. A single particle breaking both strands was deduced to give rise to the linear (α) term, while two particles each breaking a strand close enough in time and space to produce a DSB, would make $\ln S$ proportional to the square of the dose (β term) in a first-order approximation.

The dose α/β, at which the linear and quadratic components of cell-kill are equal, is commonly used as a measure of the size and shape of the shoulder region of the curve. A significant shoulder indicates extensive repair of sublethal damage, and corresponds to low α/β-values, typically found in late responding tissues. High α/β-doses are common in tumor- and early responding tissues (for a discussion of how this is exploited in fractionated radiotherapy, see Hall and Giaccia [2006, Ch. 22]).

At low doses cell-survival values often tend to deviate from the linear-quadratic model. This is due to an effect in which cells die from excess sensitivity to small doses of ionizing radiation, but become more resistant per unit dose as the dose increases. The effect has been termed low-dose hyper-radiosensitivity, and will be discussed thoroughly in chapter 2.4.

2.3.4 The Age-Response Function and the Dose-Rate Effect

Many of the experiments in this study were performed on synchronized cell populations. Cells exhibit a variation in radiosensitivity as they progress through the cell cycle. Cells are generally most radiosensitive in the G_2 and M phases, while they tend to be most resistant in late S phase. This resistance is probably due to the increase in homologous recombination repair occurring as DNA replication approaches an end. For cells with a significantly long G_1 phase, a second resistant period is evident in early G_1, followed by a sensitive period toward the end of the phase [Hall and Giaccia, 2006, Ch. 4]. For T-47D cells, however, it was shown by Furre et al. [2003] that radiosensitivity is not higher in G_2 as compared with the average sensitivity in other cell cycle phases. In addition Edin et al. [2007] found that T-47D cells in G_1 were more resistant than asynchronous populations for doses smaller than 1 Gy, and more radiosensitive for doses larger than 1 Gy.

Dose rate, i.e., the amount of dose absorbed per unit time, is also of great importance for the cellular response to ionizing radiation. A lowered dose rate will generally yield a reduction in cell kill. This is attributed to an increase in repair of sublethal damage during irradiation, as a result of the prolonged exposure time. The dose-rate effect is most pronounced between 0.01 and 1 Gy/min, above and below which little change is observed in the cell-survival curve [Hall and Giaccia, 2006, p. 71]. Some cell lines have for a limited dose-rate interval been shown to exhibit an inverse dose-rate effect, in which decreasing the dose rate results in increased cell killing [Furre et al., 1999; Mitchell et al., 2002; Mitchell et al., 1979]. Mitchell et al. [1979] proposed that this was a manifestation of redistribution, since the irradiated cells will accumulate in G_2 (see Ch. 2.1.3). Consequently, an asynchronous cell population becomes a population of radiosensitive G_2 cells under continuous low-dose-rate irradiation, and cell survival per unit dose will decrease. At sufficiently low dose rates, however, the cells will escape the G_2 block and proliferation will offset cell killing from irradiation. This hypothesis has been tested several times with contradictory results [Cao et al., 1983; Furre et al., 1999; Mitchell et al., 2002]. Cao et al. [1983] suggested that the effect might be due to a lack of induction of repair processes at low dose rates, and Mitchell et al. [2002] hypothesized that the inverse dose-rate effect reflects the phenomenon of low-dose hyperradiosensitivity (HRS) after finding evidence of inverse dose-rate effect in HRS-proficient cells, but not in HRS-deficient cell lines. However, T-47D cells have been shown to express HRS [Edin et al., 2007; Edin et al., 2008c], but lack an inverse dose-rate effect [Furre et al., 2003]. Furthermore, NHIK3025 cervix cancer cells have been shown to be HRS-deficient [Edin, 2003], but still demonstrate inverse-dose rate effect [Furre et al., 1999].

2.4 Low-Dose Hyper-Radiosensitivity and Increased Radioresistance

2.4.1 The Induced Repair Model

Over the last two decades it has been identified a region of high sensitivity in the dose response of mammalian cells at doses below ~0.5 Gy when given at acute dose rates. This phenomenon, which also has been observed in a number of nonmammalian systems [Joiner et al., 2001], is termed low-dose hyper-radiosensitivity (HRS). As the dose is increased above ~0.3 Gy a more radioresistant response per unit dose emerges. The transition from HRS toward higher resistance is called increased radioresistance (IRR). At values greater than 1 Gy, the cell survival curve is well described by the linear-quadratic model (see Ch. 2.3.3). To adequately describe the low-dose region of the survival data, a modification of the LQ-representation was proposed [Joiner and Johns, 1988; Marples and Joiner, 1993], replacing α in equation (2.10) by

$$\alpha = \alpha_r \left(1 + \left(\frac{\alpha_s}{\alpha_r} - 1\right) e^{-D/d_c}\right) \tag{2.11}$$

This expression is termed the induced repair (IR) model. The low-dose value of α describing the region of HRS (α_s) is distinct from the initial slope of the curve (α_r) using the LQ model. The dose d_c is the transition point, indicating the change from low-dose (HRS) to high-dose (IRR) survival response. By fitting survival data with the IR model, the presence of HRS is deduced by values of α_s and α_r whose confidence limits do not overlap, and a value of d_c significantly greater than zero [Marples et al., 2003]. For an example of a typical cell survival curve with evidence of HRS, see figure 2.4.

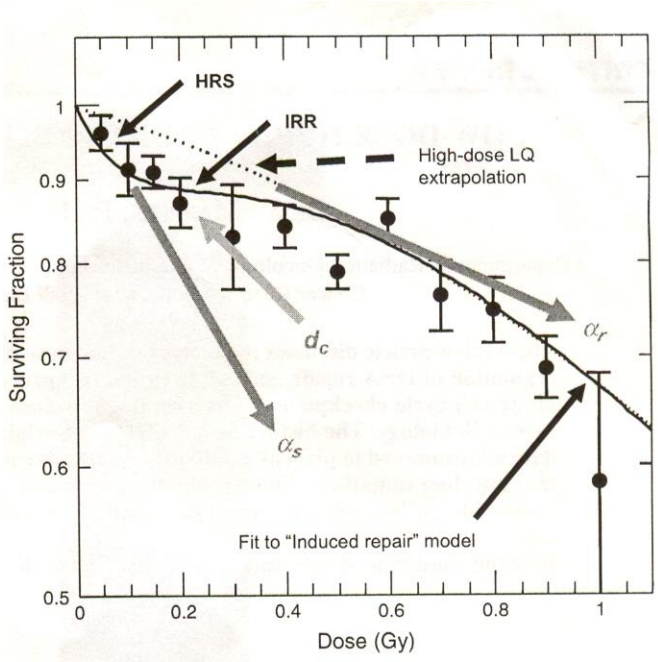

Figure 2.4
The solid line shows a fit to low-dose data by the induced repair model. α_s is the initial slope of the cell survival curve, which changes into α_r as the HRS/IRR transition occurs. At the dose d_c the transition is 63% complete. The dashed line is a low-dose extrapolation from the linear-quadratic model applied to high-dose data. [Marples and Collis, 2008, fig. 1]

2.4.2 The Dependence of HRS on LET

The X-ray survival response over 0-0.2 Gy found in V79 cells was almost indistinguishable from that of high-LET neutrons. However, while an IRR response making the survival curve less steep was evident after X-irradiation, the survival curve for neutrons continued with constant slope [Marples and Joiner, 1993]. A correspondence between the extent of IRR and LET was later shown [Marples et al., 1996]. Furthermore, Dionet et al. [2000] observed a likely HRS/IRR response in human melanoma cells after irradiation with low-dose-rate high-LET neutrons, indicating that IRR was not specific to low-LET radiation damage, but rather a general response to radiation injury. It has also been shown that cells surviving a small acute dose of neutrons were adapted to subsequent doses of X-irradiation [Marples and Skov, 1996], suggesting that high-LET radiation can activate repair processes protecting cells against low-LET radiation. The dependence of HRS/IRR on LET gives strong circumstantial evidence for the involvement of DNA-repair mechanisms in overcoming HRS.

2.4.3 IRR Response Requires Threshold Level of DNA Damage

A connection between HRS and DNA damage has also been established by chemically inhibiting DNA repair, and thereby extending the HRS response to higher doses [Marples and Joiner, 2000]. In agreement with this, a lack of an IRR response was found in DNA-repair deficient cell lines [Skov et al., 1994], clearly indicating that IRR is a result of the activation of DNA repair pathways. Moreover, pretreatment with hydrogen peroxide eliminated HRS in subsequently X-irradiated V79 cell populations, given that the concentration was sufficiently high [Marples and Joiner, 1995]. HRS can also be abrogated by priming doses of X- or γ-rays. While priming doses of 0.2 Gy or greater eliminated HRS, a priming dose of 0.05 Gy gave only limited protection against a second exposure [Marples and Joiner, 1995]. The data from these dual-treatment experiments with H_2O_2 and X-rays indicate that a threshold level of DNA damage needs to be exceeded for the full induction of repair processes.

Priming T98G cells with low-dose-rate ($\leq$ 0.60 Gy/h) ^{60}Co γ-rays did not remove HRS to subsequent acute-dose-rate irradiation in asynchronously growing cells, but HRS was removed in confluent cultures given that the dose-rate exceeded a threshold (0.30 Gy/h to a total dose of 5 Gy removed HRS, 0.30 Gy/h to a total dose of 2 Gy did not) [Mitchell and Joiner, 2002]. In addition, as mentioned in Ch. 2.3.4, HRS-proficient cells were reported to demonstrate an inverse dose-rate effect, and lowering the dose rate from 1 Gy/h down to 0.02-0.05 Gy/h enhanced net radiosensitivity by a factor of 4 [Mitchell et al., 2002]. This supports the notion that DNA damage must exceed some threshold to induce an IRR response. In fact, it has been shown that DNA damage introduced at a reduced rate does not activate ATM and its associated repair pathways, thereby contributing to the increased cell-killing from low-dose-rate irradiation [Collis et al., 2004]. However, the dependence of the HRS/IRR transition on dose rate is far from trivial, and other reports have demonstrated that low-dose-rate priming successfully removes HRS to subsequent challenge doses [Edin et al., 2007; Skov et al., 1995]. This will be discussed further in chapter 2.4.7.

2.4.4 HRS Can Be Explained by Ineffective Arrest of Radiation-Injured G_2 Cells

The dose-response activation pattern of ATM coincides with the transition from HRS to IRR, with weak phosphorylation after X-ray doses of 0.1-0.2 Gy, and thereafter a gradual increase until expression is saturated at doses greater than 0.5 Gy [Bakkenist and Kastan, 2003; Krueger et al., 2007a]. Krueger et al. [2007a] showed that when ATM was either inhibited or lacking, no IRR response was seen. In addition chemical stimulation of ATM induced low-dose radioresistance. However, the same ATM activation pattern was observed in HRS-deficient cells as in cells exhibiting HRS, indicating that ATM activity alone does not determine the survival transition from HRS to IRR.

As described in chapter 2.1.3, two distinct radiation-inducible cell-cycle checkpoints were found in the G_2 phase. The Sinclair checkpoint, which is ATM independent, arrests radiation-damaged G_1- and S-phase cells. The second checkpoint, the so-called "early" G_2 checkpoint, is ATM dependent and is dose independent over the dose range 1-10 Gy, with a specific activation threshold of around ~0.3 Gy [Krueger et al., 2007a; Xu et al., 2002]. Consequently, the low-dose activation threshold and dose-range of activation for the "early" checkpoint is commensurate with that observed for transition from HRS to IRR. Since this checkpoint prevents G_2-phase cells from prematurely entering mitosis with unrepaired DNA damage, it is hypothesized that HRS reflects the failure of this checkpoint to allow time for repair in G_2-phase cells irradiated with doses less than ~0.3 Gy. This argument implies that exaggerated HRS/IRR responses would be seen in G_2-enriched cell populations. Such exaggerated responses have indeed been reported [Marples et al., 2003; Short et al., 2003].

Using flow cytometry it is possible to assess which cells are stained positive for phosphorylated histone H3, which is a marker for mitosis, and thus distinguish G_2 cells from mitotic cells. A mitotic ratio can then be determined by calculating the ratio of irradiated versus unirradiated mitotic cells in matched cell cultures. Studies of the dose response of the mitotic ratio in several HRS-proficient and HRS-deficient cell lines have revealed that cells exhibiting HRS have a constant mitotic ratio up to ~0.3 Gy after which a sharp decrease in the ratio is evident, indicating that entry of radiation-damaged G_2 cells is not inhibited before the threshold level of damage is exceeded. In contrast, cells deficient in HRS show a gradually decreasing mitotic ratio with increasing dose, starting already at the lowest doses measured [Krueger et al., 2007a; Marples et al., 2003]. These findings verify the strong association between the HRS/IRR transition and the induction of the "early" G2 checkpoint.

Since the pattern of ATM activity is the same whether the cells exhibit HRS/IRR or not, but the ATM-dependent "early" G_2 checkpoint is functional even after doses that are insufficient to induce full ATM activation in HRS-deficient cells, Krueger et al. [2007a] suggest that these cells have a dissociation between ATM activity and the checkpoint function.

2.4.5 The Molecular Basis of HRS

The induction of increased radioresistance in V79 cells after X-irradiation was inhibited by treatment with a non-toxic concentration of the protein synthesis inhibitor cycloheximide [Marples and Joiner, 1995]. This demonstrates the need for protein synthesis in the development of IRR.

Pretreatment with H_2O_2 can abrogate HRS [Marples and Joiner, 1995] to subsequent radiation exposures, indicating that the formation of DNA strand breaks is important for activation of IRR. In support of this the double-strand break repair-deficient murine cell line XR-V15B exhibits an exponential survival response to irradiation with no evidence of IRR (however, so does UV20 cells, deficient in an incision step of excision repair, making them sensitive to crosslinking agents) [Skov et al., 1994]. It has also been demonstrated that poly(ADP-ribose) polymerase-1 (PARP-1) activation is required for the development of IRR [Chalmers et al., 2004; Marples and Joiner, 2000]. PARP-1 binds rapidly and directly to DNA strand-breaks [Herceg and Wang, 2001], and deficiency in functional PARP-1 can result in severely impaired base excision repair and genomic instability [Shall and de Murcia, 2000]. Also functional DNA-PK (DNA-dependent protein kinase) activity seems to be necessary for overcoming HRS [Marples et al., 2002; Vaganay-Juery et al., 2000]. The DNA-PK complex consists of the DNA-PK catalytic subunit (PRKDC, also called DNA-PK_{CS}) and the Ku heterodimer (G22p1 and Xrcc5, also known as Ku70 and Ku 80). Their activity depends on DNA double-strand breaks, and they are key components of the nonhomologous end-joining repair (NHEJ) pathway [Collis et al., 2005]. Both PARP-1 and DNA-PK influence the homologous recombination pathway, as well as NHEJ [Shrivastav et al., 2008]. Together these data suggest that strand breaks, and perhaps in particular DSBs, are the most important DNA lesions triggering operation of the "early" G_2/M checkpoint and the IRR response.

Exactly how radiation-induced DSBs are initially recognized remains to be elucidated, but the Mre11-Rad50-Nbs1 (MRN) complex seems to play a key role. Current models for ATM activation posit that DSB production alters the chromatin structure to initiate ATM activation [Bakkenist and Kastan, 2003; Berkovich et al., 2007]. The MRN complex, through interactions with Nbs1, physically recruits ATM to DNA lesions, and promotes full ATM kinase activity [Berkovich et al., 2007; Williams et al., 2007]. Thereafter ATM phosphorylates a number of substrates to regulate cellular checkpoint responses, most notably the "early" G_2 checkpoint in regard to HRS/IRR, and DNA repair [Kastan and Bartek, 2004]. Since ATM activity does not directly regulate the HRS/IRR transition [Krueger et al., 2007a], it is likely, although not experimentally verified, that also the MRN complex is relatively insignificant in regulating this transition. Indeed, Xu et al. [2002] proved the "early" G_2/M checkpoint to be independent of Nbs1 activity.

Short et al. [2005] found that the influence of RAD51-mediated repair events may increase at low doses (<1Gy), suggesting a change in the balance of repair events toward homologous recombination (HR) in hyper-radiosensitive cells. In concordance with this, HRS-proficient cells displayed more unrepaired DNA breaks processed by the RAD51 repair pathway than HRS-deficient cells in a study of the low-dose radiosensitivity of cells isolated from a rat colon tumor [Thomas et al., 2008]. As described in chapter 2.3.2,

the importance of HR repair increases in the late stages of the cell cycle. A schematic diagram of the proteins linked with HRS/IRR is shown in figure 2.5.

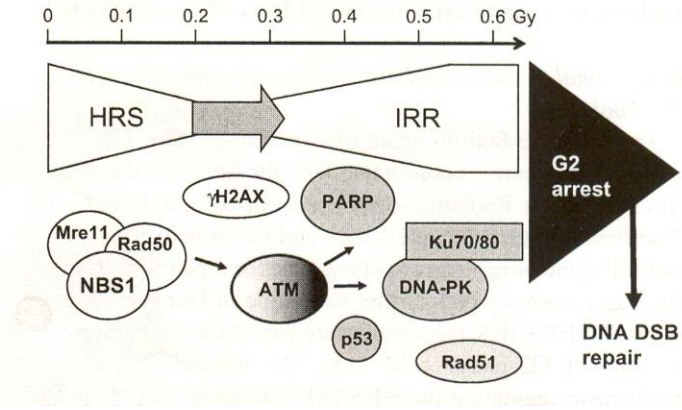

Figure 2.5
A schematic representation of the proteins linked with low-dose hyper-radiosensitivity and increased radioresistance. The filled circles show proteins demonstrated to directly effect the HRS/IRR transition, while the open circles are used for proteins believed to play an accessory role. ATM is gradually shaded to illustrate dose-dependent activation. [Marples and Collis, 2008, fig. 3]

Although not included in figure 2.5, several additional proteins have been implicated in the regulation of the "early" G_2/M checkpoint. Most notably, the checkpoint has been shown to be BRCA1 dependent [Xu et al., 2002], and the rapid decrease in the proportion of mitotic cells was significantly attenuated when the mitogen-activated protein kinase ERK1/2 was inhibited [Yan et al., 2007].

2.4.6 Apoptosis as Mode of Death in HRS

As previously described, HRS has been shown to reflect the premature entry into mitosis of G_2-phase cells with unrepaired DNA injury. Typically, going through mitosis with unrepaired double-stand breaks would lead to lethal chromosomal aberrations and mitotic death, usually involving necrosis. Somewhat surprisingly, Enns et al. [2004] demonstrated that HRS is linked with a p53-dependent activation of caspase-3, leading to apoptosis. Since such a mode of death neither requires radiation-produced chromosomal breakage nor implies cell-cycle specificity, it seemed to contradict the concept of HRS being specific to G_2-phase cells with unrepaired DNA damage. Despite these objections, the association between HRS and p53-dependent apoptosis was corroborated by Krueger et al. [2007b], and the findings were reconciled with previous reports linking HRS to evasion of the "early" G_2-phase checkpoint arrest (see Ch. 2.4.4).

In the studies by Enns et al. [2004] and Krueger et al. [2007b] a total of 14 cell lines were tested for HRS (7 cell lines were HRS proficient), and post-irradiation caspase-3 levels were examined in 12 of them (the two lines not tested for apoptosis were HCT116 p53 wild-type and HCT116 p53-null cells, and these were only tested for dose response by the clonogenic assay. The p53 wild-type cells exhibited HRS, the p53-null cells did not). Without exception in the panel of cell lines tested, HRS proficiency was accompanied by

significantly elevated caspase-3 levels after low-dose irradiation, indicating apoptosis. Conversely, neither of the HRS-deficient cell lines showed this response. Apparently the apoptotic response seems independent of p53 status, since the T98G cells (the only cell line tested in both studies) are p53 mutant and still exhibits HRS, while MR4 and MCF7 cells are p53 wild-type and HRS deficient. However, although the mutated p53 in T98G cells is not functional for instance in p21 activation, the p53-depentendent apoptosis does not seem to be suppressed [Enns et al., 2004; Krueger et al., 2007b]. MCF7 cells lack caspase-3 [Jaenicke et al., 1998], while MR4 might have increased cellular resistance to p53-dependent apoptosis due to activation of Mdm2 (see Ch. 2.1.3) as a result of Ras transformation [Krueger et al., 2007b]. Indeed, the dependence of p53 was confirmed when the p53-inhibitor pifithrin ablated HRS in A549 and T98G cells [Enns et al., 2004]. Krueger et al. [2007b] also showed that the increased levels of active caspase-3 in response to low doses of ionizing radiation disappeared in G_1-enriched cell populations, thereby implicating S- or most likely G_2-phase specificity.

The experimental results cited above argue a strong case for the involvement of p53-dependent apoptosis in the HRS phenomenon. Nevertheless, care should be taken to avoid inductive reasoning, as a large number of cell lines with disparate p53 status have been demonstrated to exhibit HRS. Some recent reports have shown the occurrence of HRS although no or only infrequent apoptosis was detected [Simonsson et al., 2008; Chandna et al., 2002; Thomas et al., 2008]. Still the findings of Enns et al. [2004] and Krueger et al. [2007b] implicate that apoptosis is a common, and perhaps the dominating, mode of death in the context of HRS.

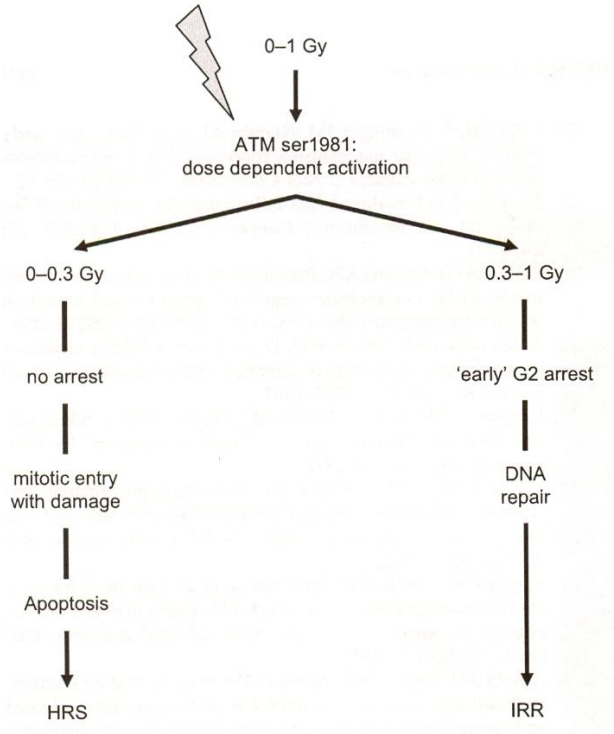

Figure 2.6
The current understanding of the HRS phenomenon. Within this framework, activation of the early G_2 checkpoint is the key event, facilitating DNA repair in cells irradiated in G_2 and thereby triggering the IRR response. While this checkpoint is active even at the lowest doses examined in HRS-deficient cells, a threshold dose of ~0.3Gy is observed in HRS-proficient cells. At lower doses, radiation-damaged G_2 cells enter mitosis with unrepaired DNA, resulting in apoptosis. [Krueger et al., 2007a, fig. 8]

The current view is thus that cell killing in the HRS region reflects the caspase-3-mediated apoptotic death of cells that failed to undergo an ATM-dependent, early G_2-phase arrest. The transition to IRR reflects induction of the "early" G_2 checkpoint, allowing time for repair and thereby increasing cell survival (see fig. 2.6).

2.4.7 Mechanisms for Elimination of HRS – Relationships Between HRS/IRR and the Adaptive Response

The "adaptive response" (AR) is the term most often used to describe the increased radioresistance observed in cells when they are irradiated with higher doses ("challenge" doses) several hours after a relatively small conditioning ("priming") dose. The AR has been observed in many different organisms (including human cells *in vitro* and animal models *in vivo*) and using many different endpoints, among others cell survival, gene mutations and chromosomal aberrations [Dimova et al., 2008]. AR can also be induced by other stress stimuli than priming doses of ionizing radiation, such as DNA damaging chemicals (cisplatin, bleomycin, hydrogen peroxide), restriction endonucleases and hyperthermia [Cregan et al., 1999; Szumiel, 2005]. The induction of an adaptive response has been found to be highly dependent on the experimental design. The adapting dose, dose rate, the time between priming and challenge doses, culture conditions and stage of the cell cycle are factors that have been shown to influence the magnitude of the response [Cregan et al., 1999; Dimova et al., 2008].

The HRS/IRR transition is another manifestation of induced resistance, and is thus closely related to the AR phenomenon. It was speculated for a while that the adaptive response and HRS/IRR are consequences of the same underlying mechanisms [Joiner et al., 1996; Joiner et al., 2001]. In support of this, pretreatment with chemicals like hydrogen peroxide and cisplatin or a small priming dose of radiation abolished HRS to a second challenge dose [Edin et al., 2007; Marples and Joiner, 1995; Short et al., 2001; Wouters and Skarsgard, 1997]. However, Wouters and Skarsgard [1997] argued that although a small priming dose abrogated HRS to doses less than 1 Gy, it did not induce a classical AR with increased radioresistance to higher doses, and therefore concluded that these phenomena were distinct. Differences in response to certain priming agents have also been demonstrated. For instance, incorporated tritium-labeled thymidine is an effective priming agent for AR and removes HRS, while bleomycin only primes for the adaptive response [Skov, 1999]. After the discovery of the "early" G_2/M checkpoint and the recognition of its importance for HRS/IRR, the search for similarities with the adaptive response in order to elucidate common underlying mechanisms seems to have stopped.

Still it is interesting to note the dependence of the adaptive effect on priming dose and dose rate. Studies on human lymphocytes, the most thoroughly studied cells in the context of AR, by Shadley and Wiencke [1989] convincingly showed that the level of adaptation is related to the dose rate of the priming irradiation. In these cells, using chromatid deletions as an endpoint, there is an inverse relationship between priming dose and the required dose rate. Lower priming doses are effective when given at higher dose rates, higher doses have to be applied at low dose rates. According to Feinendegen [1999]

the adaptive responses that have been examined all decline if the priming dose exceeds 0.1-0.2 Gy and disappear with doses above 0.5 Gy, while the lowest measured dose to induce AR is approximately the average hit size for X- and γ-rays (about 1 mGy for 100 keV X-rays). These findings suggest the existence of an optimal priming dose and dose rate, depending on the cell line.

The dose rate can also influence the ability of priming irradiation to remove HRS. This was demonstrated by Edin et al. [2007] on T-47D cells. When the priming dose of 0.3 Gy was delivered at an acute dose rate (40 Gy/h) 6 hours prior to challenge irradiation, HRS was abolished, but the cells restored low-dose HRS when challenge doses were given 24 hours after priming. If the priming dose of 0.3 Gy was delivered at 0.3 Gy/h, however, the abrogation of HRS persisted for intervals up to 14 weeks between doses (after 28 passages). Later work by Edin et al. [2008c; 2008b] showed that HRS was still abolished more than 2 years after the low-dose-rate (LDR) priming. Consequently, the transition seems to be permanent. Indeed, using the method for assessment of anti-phospho-histone H3 staining (as described in Ch. 2.4.4) it was shown that the primed cells have a gradually decreasing mitotic ratio after low-dose irradiation, in contrast to unprimed T-47D cells, which exhibit a constant mitotic ratio at the lowest doses [Edin et al., 2008b]. In the present study, more experiments have been performed on these primed cells, denoted T-47D-P cells.

However, the influence of dose rate on priming, as just outlined for T-47D cells, seems to be dependent on the cell line. As described in chapter 2.4.3, similar priming of HRS-proficient T98G cells produced quite different results [Mitchell and Joiner, 2002]. In those cells HRS was not removed with LDR (5, 10, 30 and 60 cGy/h) priming in asynchronously growing cells, for priming doses of 2 and 5 Gy. In confluent cultures HRS was abrogated when the priming dose was delivered at 30 cGy/h to a total dose of 5 Gy, and when the priming dose was delivered at 60 cGy/h. HRS was recovered again within four hours. However, 2 and 5 Gy were the only priming doses tested. Marples and Joiner [1995] found that a high-dose-rate (HDR) priming dose of 0.2 Gy was more effective than a priming dose of 1 Gy in V79 cells, so a search for an optimal priming dose in the T98G cells might give results more in concordance with those for T-47D cells. As noted before (Ch. 2.3.4), T98G cells exhibit a strong inverse dose-rate effect (IDRE), with a higher cell kill per unit dose when the dose rate is 2 cGy/h, than after acute exposures. This is in clear contrast to T-47D cells, which lacks an IDRE [Furre et al., 2003] and seems to be able to grow indefinitely under continuous irradiation from incorporated tritium at a dose rate of 1.5 cGy/h [Bjørhovde, 2006; Pettersen et al., 2007].

In general the adaptive response seems to operate over a longer timescale (ranging from a few hours to several months) than the time needed for a return to the hypersensitive state following an initial small dose [Wouters and Skarsgard, 1997]. Typically HRS is recovered 3-6 hours after the priming exposure [Joiner et al., 2001; Short et al., 2001]. This is similar to what is observed for T-47D cells after HDR pretreatment [Edin et al., 2007]. The assumed permanent switch in low-dose radiosensitivity seen in T-47D-P cells is more reminiscent of durations sometimes seen for the adaptive response and the bystander effect.

A possible explanation for the abolition of HRS following a subthreshold priming dose is the selective killing of G_2 cells, that are sensitive because of the inactive "early" checkpoint. While the G_2 cells are absent, the response to a subsequent dose will follow LQ survival. If the second exposure is given some hours later, when the G_2 population is replenished, the cells will exhibit HRS [Bonner, 2004].

2.4.8 Mechanisms for Elimination of HRS – Relationships Between HRS/IRR and the Bystander Effect

Sometimes at low doses one can detect the induction of biologic effects in cells that are not directly traversed by an ionizing particle. This phenomenon, which has been observed in many cell types using different endpoints and radiation qualities, is known as the radiation-induced bystander effect [Hall and Giaccia, 2006, p. 35-36; Mothersill and Seymour, 2001]. Traditionally, bystander responses have been considered as detrimental, i.e., as responses inflicting damage to bystander cells. More recent reports of seemingly advantageous effects, such as enhanced cloning efficiencies and acquisition of radioresistance, call for a broader interpretation of the phenomenon, comprising all kinds of biologic effects in bystander cells [Azzam et al., 2004; Bonner, 2004; Matsumoto et al., 2007]. It has been shown that medium harvested from irradiated cell cultures can produce effects in cells that have never been in a radiation field [Mothersill and Seymour, 2001]. Thus, cells of certain cell lines produce some sort of signal(s) or factor(s) released into the medium. Moreover, these (most often) toxic substances appear not to be cell-line specific, while the ability to secrete such factors might be. This was clearly demonstrated using media transfer protocols on human keratinocyte (HaCAT) and fibroblast (MSU-1) lines [Mothersill and Seymour, 1997a]. Irradiated-cell conditioned medium (ICCM) transferred from HaCAT cells to unirradiated HaCAT cultures decreased cloning efficiency to ~60% compared to controls. The same procedure on MSU-1 cells led to no significant bystander effect on the recipient cells (although it seemed to give a slightly beneficial response). When ICCM was transferred from MSU-1 to HaCAT cells, the response was again slightly beneficial, but not significantly different from controls. However, ICCM transferred from HaCAT cultures to unirradiated MSU-1 cultures, caused the latter's survival to drop to ~2%. A recent study by Vines et al. [2008] also suggested that it is the signal produced by the irradiated cell line, and not the individual response of the cell line treated with ICCM, that determines the extent of the bystander effect.

Since cells that get no radiation hits or direct DNA damage, die in response to signals from hit cells, it is somewhat surprising to note that it is important for the magnitude of the effect whether or not the cells are DNA repair proficient. In general DNA repair-deficient cell lines produce bystander effects resulting in high levels of clonogenic death [Mothersill et al., 2004]. There is also some evidence from media transfer and co-cultivation protocols that ICCM from repair-competent cells can induce an adaptive response to subsequent irradiation or exposure to higher-dose ICCM (i.e., ICCM from cells irradiated with a higher dose than the donor cells of the "priming" ICCM) [Iyer and Lehnert, 2002; Matsumoto et al., 2000; Matsumoto et al., 2001; Maguire et al., 2007].

The characteristic bystander response induced in cultures exposed to ICCM is most often transmitted to the progeny, in other words the signal production is persistent and not reset by cell division [Mothersill et al., 2004].

Since both HRS and the bystander effect result in increased sensitivity to low radiation doses, there has been some speculation as to whether or not the two effects have similar mechanisms. However, experiments by Mothersill et al. [2002] showed a weak inverse correlation between the two phenomena. As pointed out in that study, such an inverse relationship makes it tempting to suggest that if one mechanism fails at low doses, the other will produce the necessary cell killing to avoid the risk of propagating misrepaired or damaged DNA, causing genomic instability. In the context of HRS it has been hypothesized that the reason why the DNA repair system acting on G_2 cells needs to be activated by a threshold of damage, is that it is beneficial for the organism to allow small numbers of cells with low levels of damage to die rather than risking mutation if repair is attempted, and the cells survive [Marples et al., 2004].

Using media transfer protocols, another phenomenon linking bystander effects with HRS has been found. Edin et al. [2008c] demonstrated that ICCM from T-47D cells given 0.3 Gy is able to eliminate HRS in recipient cells. The abolition of HRS is dose-rate dependent, however. Only when the dose was delivered at a low dose rate (0.3 Gy/h) did the effect occur, although a slight reduction in HRS was observed when HDR ICCM (medium from cells irradiated at high dose rate, 40 Gy/h) was transferred after six hours instead of 40 hours post-irradiation. As described in the previous section (Ch. 2.4.7), cells given LDR priming at this particular dose and dose rate seem to change phenotype, resulting in a permanent loss of HRS. Medium transferred from the T-47D-P cells retained the ability to remove HRS in recipient T-47D cells, even 14 months after the 0.3 Gy priming. Within two weeks cells that were exposed to LDR ICCM for 24 hours, recovered HRS. Hence the perpetuation of signal production (or modification) in progeny of cells exposed to ICCM, as noted above for the bystander effect [Mothersill et al., 2004], was not observed in this study. It was also showed by Edin et al. [2008c] that the ability to eliminate HRS was weakened as the concentration of ICCM was lowered. Later work has revealed that cell conditioned medium (CCM) that receives a LDR priming is able to remove HRS in recipient cells, even though cells were not present at the time of irradiation. However, LDR ICCM has no effect if serum is not present during the priming [Edin et al., 2008b].

In some cases ICCM has the ability to induce an increase in cell survival as compared to controls receiving fresh or unirradiated CCM. A significant increase in the number of viable colonies was observed for T-47D cells that received LDR ICCM or HDR ICCM compared to cells that received fresh medium at the same time [Edin et al., 2008c]. There are more reports of this phenomenon in the literature. ICCM from MSU-1 cultures irradiated with 2 Gy and from HT29 cells irradiated with 0.5 Gy both induced statistically significant increases in the relative survival of recipient cultures [Mothersill et al., 2002]. T-47D, MSU-1 and HT29 are all repair-proficient cell lines. When the hamster cell line CHO-K1 was exposed to ICCM from XRS-5 cells irradiated with 3 or 5 Gy, a doubling in the plating efficiency (PE) was observed [Mothersill et al., 2004]. XRS-5 is a DSB

repair-deficient cell line, derived from CHO cells. The increase in PE was so large that apparently every plated CHO-K1 cell survived to form a colony when ICCM was added (the effect was dose dependent, and did not occur for 0.5 and 1 Gy). The authors could not explain this result, but suggested it was related to the ability of CHO-K1 cells to seed small colonies during the growth period post-irradiation. Normally such satellite colonies are very small and easily distinguished from parent colonies because the seeding out takes place late in the colony growth. Possibly, the ICCM can cause this process to occur much earlier. The mechanisms causing the bystander-induced enhancement of survival are not known, but transforming growth factor β (TGF- β), reactive oxygen and nitrogen species have been identified as mediators of such effects [Iyer and Lehnert, 2000; Shao et al., 2001].

2.4.9 Mechanisms for Elimination of HRS – Excess Survival in Primed Cells

In T-47D cells that were primed with 0.3 Gy at a low dose rate (0.3 Gy/h), HRS was abrogated. Surprisingly, this did not result in a dose response in concordance with the linear-quadratic model at the lowest doses. Instead survival exceeded 1 for doses below ~0.5 Gy, i.e., the number of colonies in the flasks receiving low challenge doses exceeded the number of colonies in the controls [Edin et al., 2007; Edin et al., 2008c; Edin et al., 2008b; Fenne, 2008]. This is illustrated in figure 2.7, in which line A is the survival of a cell line exhibiting HRS/IRR, line B is the linear-quadratic function of clonal survival and line C shows the dose response observed for T-47D-P cells. Be aware that the controls in the latter case have been given a 0.3 Gy priming dose.

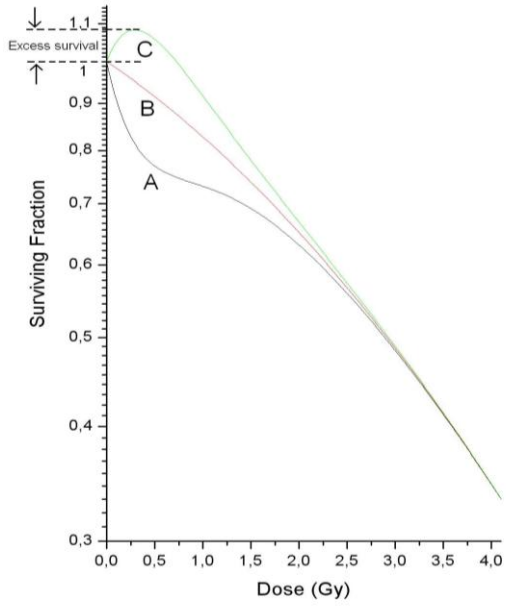

Figure 2.7
In experiments with T-47D-P cells, the survival tends to increase after low radiation doses, as compared to controls. Curve A is a fit to the observed survival data in unprimed T-47D cells, using the induced repair model [Edin, personal communication]. Curve B is a fit to the same data using the linear-quadratic model (extrapolating from the high-dose response). Curve C is a dose-response curve illustrating the observed survival for T-47D-P cells (the curve is fictitious, i.e., it does not represent a fit to a measured data set).

The reason for the excess survival in LDR primed cells is not clear. Siri Fenne [2008] investigated the growth pattern of T-47D-P cells by means of time-lapse filming. The purpose of the study was to see if clonogenic units gave rise to more than one colony

each by seeding small colonies during the growth period, or if other differences in growth pattern could explain the elevated surviving fractions. Surprisingly, it was found that effects increasing the number of colonies did occur, but to a larger extent in the controls (priming only), than in cultures receiving a challenge dose. Consequently, it seems that such effects counteract and partially mask the real increase in reproductive capability among the plated challenge-irradiated cells.

2.5 Flow Cytometry

Flow cytometry is a technology capable of measuring and analyzing multiple physical characteristics of single cells, as they flow in a fluid stream through one or more laser beams. The technique can be used to measure cell size, relative granularity and internal complexity, and fluorescence intensity. Flow cytometry has become an invaluable technique in radiobiology, allowing radiation effects to be considered at the cellular and molecular level on a cell-by-cell basis [Wilson and Marples, 2007]. Since flow cytometry was used quite extensively for cell sorting in the present study, the principles of operation will be briefly described.

2.5.1 Principles of Flow Cytometry

The cell sample is injected into a stream of sheath fluid (buffer) within a flow chamber. The chamber is designed with a gradually decreasing diameter, and through so-called hydrodynamic focusing, the sample core is focused in the center of the stream. The core pressure is always greater than the sheath fluid pressure, and the flow rate is regulated by modifying the pressure difference and thereby changing the width of the core. Thus, the cells can be forced to pass through the laser beam one cell at a time, confined to the stream center for optimal illumination.

When cells pass through the laser intercept, they scatter light. Forward-scattered light (FSC) consists mostly of diffracted light detected just off the axis of the incident laser beam, and it is proportional to cell size. Side-scattered light (SSC), which is detected at approximately 90 degrees to the beam direction, consists mostly of reflected and refracted light, indicating a change in refractive index. Measurements of SSC are therefore suited to reveal cell granularity or internal complexity. By staining the cells with a fluorescent dye, the laser can also be used to induce fluorescence. The emitted photons are detected, and the amount of fluorescent signal is proportional to the number of fluorochrome molecules in the cell. The cells can for instance be stained with a dye that becomes fluorescent when it binds to DNA, so that the fluorescence will be directly proportional to the DNA content. Flow cytometers can simultaneously measure the fluorescence pulse height, width and area. They are measured as three independent entities, although derived from the same signal. Aggregates of cells are larger in size and will produce a signal with a greater pulse width than singlets. Pulse area is the most accurate measure of total cell fluorescence and hence DNA content. Thus the cell-cycle distribution can be determined from a histogram of fluorescence pulse area against cell number, since cells in G_2/M will have exactly twice the amount of DNA as cells in G_0/G_1, while S-phase fluorescence will constitute a continuum of signal intensities in between these two peaks.

The scattered and fluorescent light is collected by a lens system and filtered before reaching a photodetector. The stronger FSC signal is usually detected by a photodiode, while photomultiplier tubes are used to detect SSC and fluorescence. The light signal is quantitatively transformed into an electric signal by the detector. Finally, the resulting voltage pulse is assigned a digital value (a channel number) by an analog-to-digital converter.

2.5.2 Fluorescence-Activated Cell Sorting

The first demonstration of fluorescence-activated cell sorting (FACS) was made by Herzenberg and colleagues [Bonner et al., 1972]. Herzenberg's machine was later commercialized by Becton Dickinson, who trademarked the acronym FACS.

The sorting is commonly achieved by using a vibrating mechanism to break up the sample stream into individual droplets. When the sheath velocity and the vibration speed are kept constant, the distance between drops will be fixed. The system is tuned so that the probability of finding more than one cell per droplet is very low. A voltage charge is applied to droplets containing a cell that meets the sorting criteria, and the drops will subsequently be deflected by charged plates present on either side of the vibrating stream. The deflected droplets are collected in the appropriate collection tubes depending on the charge of the droplet, while the uncharged drops are wasted (see fig. 2.8).

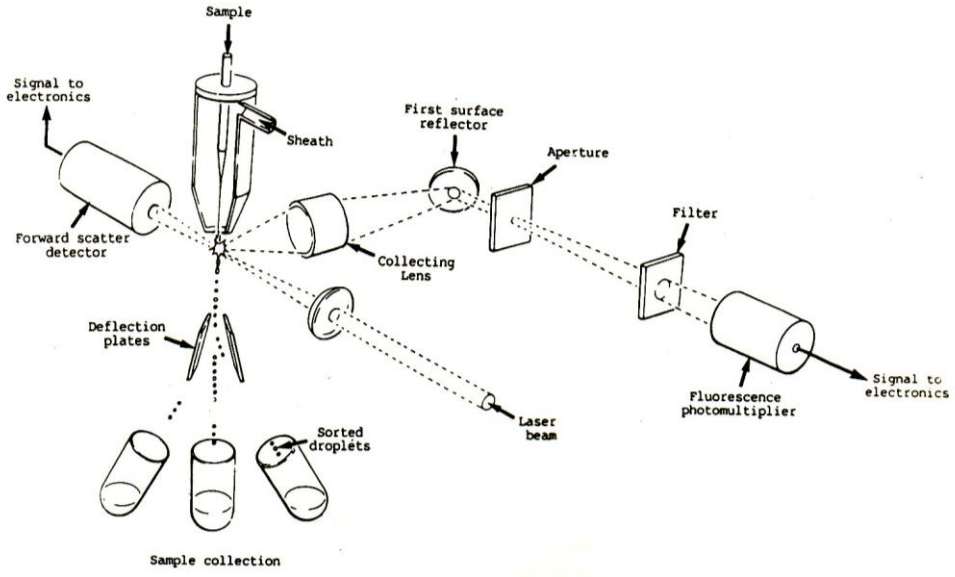

Figure 2.8
Typical layout of an electrostatic fluorescence-activated cell sorter. Cells meeting the desired sorting criteria are contained in droplets given a certain voltage charge. These droplets will be deflected by charged plates on either side of the stream and collected by the appropriate sample tubes. [Watson, 1991, fig. 6.1].

To sort cells, it is first necessary, however, to identify the cells of interest. This is achieved by drawing a region around the relevant populations on a data acquisition plot. Typically a dot plot of FSC vs. SSC is used to recognize cells of a specific size and structure. An appropriate boundary encircling only the desired cells is then drawn on the plot. This is called gating. If the cells are stained with a fluorescent dye, other gates can be defined based on fluorescence intensity, restricting the analysis to a small subset of the original cell population. For instance, doublets of G_0/G_1 cells, having the same DNA content as G_2/M cells, can be excluded by gating on fluorescence pulse area versus pulse width, utilizing the fact that the pulse width will be greater for aggregates. Furthermore, one can select cells of different cell-cycle phases. By specifying a narrow gate around the G_1 peak in a DNA histogram, it is possible to sort out a population consisting exclusively of G_1 cells.

A relatively non-toxic staining agent is required if the cells are supposed to be grown after sorting. The bisbenzimide Hoechst 33342, so-called vital Hoechst, is a common DNA-binding (binds to A-T basepairs) dye for this purpose, reported to provide adequate-resolution DNA staining at the expense of minimal toxicity and marginal mutation [Arndt-Jovin and Jovin, 1977; Durand and Olive, 1982], although significant increase in cell-kill has been observed in stained cells pre-exposed to high radiation doses [Pallavicini et al., 1979; Siemann and Keng, 1986].

Cell sorters can be used to plate known number of cells into appropriate vessels for clonogenicity studies, thereby improving the accuracy of the Puck and Marcus assay (see Ch. 2.3.3) and enabling a detailed investigation of the low-dose region of the cell-survival curve [Durand, 1986; Skarsgard et al., 1996]. The combination of this technique with vital Hoechst staining, has been exploited to explore the extent of HRS in different cell cycle phases [Marples et al., 2003; Short et al., 2003].

3 Materials and Methods

3.1 The Cell Line

Most cultured cells have a limited lifespan before they stop dividing in a process called senescence, most often due to telomere shortening. The cells of an established cell line, however, have acquired the ability to divide indefinitely in culture, either through random mutations or deliberate modifications. Especially important is the expression of the telomerase gene, which is turned off in normal human somatic cells [Alberts et al., 2002, p. 474].

Human breast cancer cells of the line T-47D were used in the experimental work of this thesis. The T-47D cell line was isolated by Dr. I. Keydar in 1974 from a pleural effusion obtained from a patient with an infiltrating ductal carcinoma of the breast. These aneuploid cells have a chromosome number range from 60 to 70 with a mode of 66. When grown in culture, T-47D cells exhibit epithelial morphology and form monolayers [Keydar et al., 1979]. The cells have normal Rb function [Åmellem et al., 1998; Stokke et al., 1993], but contain only mutated single copies of the p53 gene [Casey et al., 1991; Nigro et al., 1989]. The doubling time for T-47D cells kept in exponential growth under favorable conditions have been measured to be 37 ± 2 hours [Stokke et al., 1993].

Experiments were also performed with T-47D cells that had been primed with 0.3 Gy at 0.3 Gy/h. These cells are termed T-47D-P cells (see Ch. 2.4.7 and 2.4.9). The priming dose was given on August 17th, 2005 by Nina F.J. Edin. The cells were γ-irradiated with a ^{60}Co source that was shielded by a 10 cm thick block of Roos metal. Since then the cells have been passaged continuously for more than three years. During this period they have been kept in cryostorage (-196°C) twice, for 42 days in late 2006 and for two weeks in the spring of 2008. The doubling time of T-47D-P cells must be shorter than that of unprimed cells, since smaller proportions of the primed cells has to be subcultured in order to keep the cell density at a constant level. As a crude approach, the doubling time can be estimated to ~25-30 hours (typically ~1/8 of the cells is transferred to a new cell flask twice per week).

3.2 Cell Cultivation

Cells were grown both in the Biophysics group's cell laboratory at the Department of Physics, University of Oslo (UIO), and in a small provisional laboratory adjoining the ^{60}Co γ-irradiation facility at The Norwegian Radium Hospital (DNR). Most of the work was performed at DNR.

3.2.1 Equipment, Chemicals and Sterile Techniques

Whenever cells, or chemicals to be used on cells, would be exposed to air, the work was performed in a LAF (Laminar air flow) bench. The cabinet was disinfected with 70% ethanol before and after working in it. Two LAF benches were employed; an OAS LAF

VB 2040 (Odd A. Simonsen AS, Oslo, Norway) at UIO and a Gelaire LAF class 100 (Solberg & Andersen AS, Norway) at DNR.

All the equipment used when working with the cells was sterile. Gloves were sanitized by washing them with 70% ethanol and allowing them to air dry for 30 seconds before commencing work, and they were discarded after use. The exterior surfaces of equipment and materials put into the cabinet (e.g., medium bottle, trypsin bottle and motor-driven pipetting device) were sanitized by wiping with a tissue soaked with 70% ethanol. Sterile polystyrene pipettes (Sarstedt, Nümbrecht, Germany) were disposed of after use. Glass equipment and screw caps were kept in soap water (Decon 90, Decon Laboratories Ltd., UK) for at least 24 hours. Screw caps and small glass bottles and flasks were subsequently washed in a dishwasher (Electrolux BW100) without using detergent, while large glass bottles were kept under running water for 1-2 hours before being rinsed thoroughly with Milli-RO water (Milli-RO, Millipore, MA, USA). Finally, equipment of glass and metal was wrapped in double layers of aluminum foil and dry-heat sterilized in a Termaks oven (Termaks, Bergen, Norway) at 180^{o}C for approximately three hours. Screw caps, cloth and rubber materials were packed in sealed autoclave paper bags and autoclaved (Labo Autoclave, Sanyo) at 121 ^{o}C for 25 minutes. Rubber tops and pyrex screw caps, plus glass equipment and bottle necks were burnt prior to use in a propane flame (at UIO) or ethanol flame (at DNR).

The cells were grown as monolayer cultures in RPMI (Roswell Park Memorial Institute) 1640 medium (JHR Biosciences, Lenexa, KS, USA) supplemented with 10% fetal bovine serum (Euroclone, Devon, UK), 2mM L-glutamine (Sigma, Saint Louis, MO, USA), 1% penicillin/streptomycin (Euroclone, Devon, UK) and 200 units/liter insulin (Sigma, Saint Louis, MO, USA). All the nutrients, vitamins and inorganic salts required to sustain cell growth are contained in the RPMI 1640 medium, while the added fetal bovine serum and insulin provide growth factors necessary for cell proliferation. The amino acid L-glutamine is rapidly decomposed and fresh L-glutamine was therefore added to the medium regularly (after three weeks if the medium bottle was kept in refrigerator). RPMI 1640 was supplemented with the pH indicator phenol red (Merck, Germany), which gradually changes color from yellow to red over the pH range 6.6 to 8.0.

The proteolytic enzyme trypsin was employed to make cells detach from their substrate and break protein bonds between adjacent cells during subculturing (see Ch. 3.2.2). A chelating agent called EDTA, which binds Ca^{2+} necessary for cell-cell adhesion, was added to enhance the effect of the trypsin. Medium and trypsin were prepared at the cell laboratory at UIO and sterilized by filtration (Millex GP Filter Units, 0.22 μm, Millipore, Carrigtwohill, Ireland). The cells were grown in sterile plastic flasks (Nunc AS, Roskilde, Denmark). At DNR the cells were incubated in a semi-sterile incubator (Thermo Forma model 371, Dipl.ing. Houm AS, Oslo, Norway) with the lids unscrewed at 37^{o}C, 95% humidity and 5% CO_2. At UIO a non-CO_2 incubator (National, Heinicke Instruments Co., Hollywood, FL, USA) was used. The flasks were therefore flushed with CO_2 and sealed prior to incubation at 37^{o}C.

3.2.2 Maintenance of the Cell Line

As cells grow and divide, nutrients and growth factors are depleted, and fresh medium therefore has to be added. In addition it is necessary to monitor the cell density to avoid confluence, which can cause contact inhibition and nutrient depletion. Too low density will also repress proliferation, as cell growth depends on growth stimulating substances secreted by the cells. To ensure optimal growth conditions, the cells were kept in exponential growth by subculturing twice per week, Monday and Friday.

Subculturing
First the old culture medium was removed and discarded. Then the cell layer was rinsed twice with trypsin/EDTA solution (2 ml each time in 25 cm^2 flasks, 5 ml in 75 cm^2). After each rinsing the trypsin was removed with a pipette. The cells were detached upon ~5 minutes of incubation at 37 ^oC, as a small amount of trypsin remained in the flask. The side of the flask was gently tapped if necessary to release any remaining attached cells. The trypsin was then inactivated by adding medium, as serum contains trypsin inhibitors. In order to separate the cells, a pipette was used to pump the suspension gently. Afterwards the desired amount of cell suspension was added to a new flask. This flask had been pre-filled with fresh medium (total content of medium, including suspension, was 5 ml for a 25 cm^2 flask and 15 ml for a 75 cm^2 flask). Finally the cell flasks were placed in an incubator with the lids unscrewed (DNR) or flushed with CO_2 and put in the incubator with the lids closed (UIO).

Medium change
The old medium was removed and fresh medium added every Wednesday.

3.3 Clonogenic Survival of Asynchronous Cell Populations

3.3.1 Plating

The cells were plated, irradiated and incubated at DNR after plating. Prior to seeding the cells were often grown at UIO. During transportation from UIO to DNR the cell flasks were sealed and enclosed in a thermos bag. Normally the cells were transported by car, taking ~15 minutes, although public transportation was used at a few occasions. The cells were incubated at DNR for at least one day before plating took place.

Since it proved hard to find any expression of HRS in the asynchronous cell populations, different seeding techniques were applied. The purpose was to elucidate the influence of various treatments that might trigger a stress response in the cells and thereby alter their low-dose radiosensitivity. The method of seeding that is described here was used for experiments T1-T8, T16, T18, T22, P1-P7 and H1-H4. All deviations from this procedure will be described in detail when the data from these experiments are presented in the Results and Analysis section (Ch. 4).

The medium was removed and the cells trypsinized, as described in Ch. 3.2.2. This time, however, the trypsin was not removed after the second rinsing. Instead the cell flask (25 cm^2) was incubated with 3 ml of trypsin for a few minutes. When the cells had detached

from the surface, the suspension was gently pumped using a 2-ml cannula mounted on a 10-ml syringe. A microscope (Nikon Eclipse TS100, Japan) was consulted to examine the separation of the cells. The single-cell suspension was then transferred to a test tube containing the same amount of medium as the amount of trypsin (normally 3 ml), and centrifuged (Labofuge I, Heraeus Christ, Dipl.ing. Houm AS, Oslo, Norway) at 2000 rpm for approximately 3 minutes. After removing the trypsin and medium, the resulting pellet was resuspended in fresh medium using a 2-ml pipette. The cell suspension was diluted further, and a sample was then counted using a disposable Bürker-chamber plate containing ten chambers (Kova glasstic slide 10, Hycor Biomedical, Garden Grove, CA, USA). Each chamber consists of 3×3 squares, and each of these nine compartments has a volume of 10^{-4} ml. The number of cells was counted in five of the squares, whereupon the highest and lowest values were crossed out. Two chambers were counted in this way, and finally the average cell number from the 2 sets was calculated. The number of cells per ml of cell suspension was found by multiplying this average by 10^4. When the concentration of cells was known, the appropriate dilutions were made.

For all the low doses (including 2 Gy) 200 cells were seeded per flask (25 cm^2). This was performed by making a suspension containing 200 cells/ml and adding 1 ml of suspension to each flask (previously filled with 4 ml of medium). For doses higher than 2 Gy, the cell numbers were increased depending on the irradiation dose. Five parallel flasks were seeded for every dose, and ten flasks were seeded as controls (sham-irradiated). The cells were irradiated 16-20 hours after trypsinization.

3.3.2 External Irradiation

The irradiations were performed with a ^{60}Co source (Theratron 780C/T1000, MDS Nordion, Canada) that was installed at DNR on April 30th, 2007. A sketch of the head of this treatment unit is shown in figure 3.1. As seen from this diagram, the source is moved from a safe to an exposed position during irradiation.

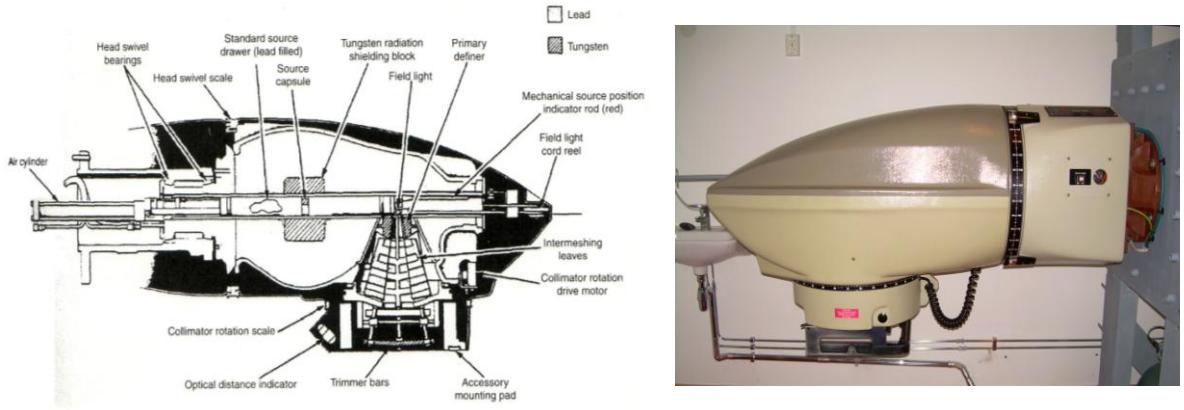

a) **b)**

Figure 3.1
a) Diagram of a Theratron 780 treatment unit. The source drawer mechanism, the collimator and the shielding are shown. [Mayles et al., 2007, fig. 12.1] b) Picture of the Theratron unit installed at DNR.

The half-life of ^{60}Co is 1925.1 days, and ^{60}Co γ-rays are emitted at two well-defined energies (1.173 MeV and 1.332 MeV, see Ch. 2.2.3). Three different setups were used for the irradiations. The dose rates were measured by Thorbjørn Furre, using LiF thermoluminescence dosimeters (see Ch. 2.2.5). The readout process and dose calculations followed the procedures standard at DNR.

Setup A:
The source was shielded by three slabs of Perspex (water-equivalent material). Each slab was 20 mm thick. The cell flasks were put on a 10 mm thick Perspex plate, resting on two wooden boards (47×95 mm^2) placed edgeways, see figure 3.2 a). This setup resulted in a source-surface distance (SSD) of 66.5 cm. Maximum field size was used (approximately 40×40 cm^2 at 80 cm SSD), and that applies also for setup B and C. The dose rate was measured to be 1.02 Gy/min on August 24th, 2007. Experiments T1, T2 and H1 were irradiated using setup A.

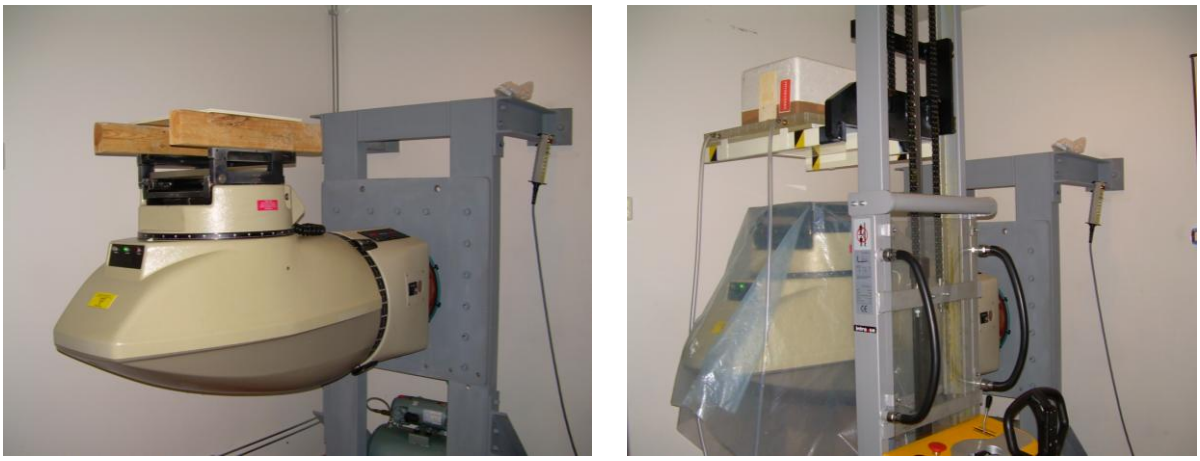

a) **b)**

Figure 3.2
a) The picture shows setup A and B. These setups were identical apart from three Perspex slabs shielding the source in setup A. The slabs were placed directly on the accessory mounting pad (one slab is seen on the picture). b) The picture shows setup C. A Perspex slab with inbuilt water heating was held at the correct SSD by a mobile lifting jack. The hoses were used to connect the slab to a water bath with an integral pump.

Setup B:
This setup was equivalent to setup A except for the three Perspex slabs, which were removed. The dosimetry was performed with the 10 mm Perspex plate placed directly on the metal mounting base, i.e., without the wooden boards. Hence the measured dose rate of 1.88 Gy/min (August 21st, 2007) had to be corrected according to the inverse square law for the difference in SSD, yielding the dose rate 1.38 Gy/min. The longest exposure time with this setup was approximately one and a half minute, needed for a 2 Gy irradiation. Thus the change in surrounding temperature should not affect the cells much. Nevertheless, a heating oven was turned on in the cobalt-unit room the day before the irradiations took place. In addition a Styrofoam hood was put over the cell flasks to

diminish heat dissipation. Experiments T3-T10, P1-P3 and H2-H4 were irradiated using setup B.

Setup C:
A Perspex slab (36 mm thick) with a built-in water passageway was used in this setup, see figure 3.3. Water was pumped through the slab by a water bath with an integral pump (Optima GR150, Grant Instruments, Cambridge, UK). The water was preheated to a temperature of 39.8°C, found through calibration to give a temperature of 37°C inside the cell flask at relatively protracted exposures. The water-heating slab was placed on top of a 15 mm thick Perspex plate mounted on a mobile lifting jack (see fig. 3.2 b)). The SSD was 85.1 cm, corresponding to a distance of 80 cm from the source to the lower surface of the Perspex plate. A Styrofoam hood was used to cover the cell flasks. The dose rate for this setup was measured to be 0.700 Gy/min on March 6th, 2008. Experiments T11-T24, A1-A3, P4-P7, plus the experiments with G_2-enriched cell populations, were irradiated using setup C.

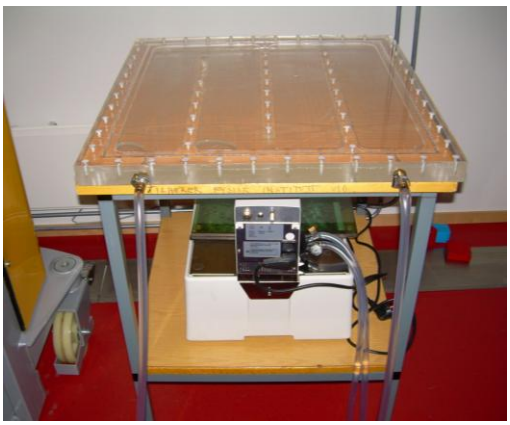

Figure 3.3
A Perspex slab with a built-in water passageway was used in Setup C. The water was kept at 39.8°C by a water bath with an integral pump. This maintained a temperature of 37°C in the cell flasks during protracted exposures.

Since the field size and SSD were fixed within each setup, the measured dose rates only needed to be corrected for the reduction in the activity of the source when exposure times were calculated (see Ch. 2.2.1). However, the so-called shutter effect should also be considered when performing low-dose irradiations. This is discussed in appendix H.

3.3.3 Tritium Irradiation

The cells in experiments H1-H4 had been primed by continuous low dose-rate β-irradiation. This was done by incorporation of tritium-labeled valine (TRK533, L-[3,4(n)-^{3}H]valine, 1.0 mCi/ml, Amersham, GE healthcare, Buckinghamshire, UK) into cellular protein. Valine is an essential amino acid for human cells, and is thus required in the growth medium. The amount of tritium-labeled valine added to the medium corresponded to a specific activity of 1.6 Ci/mol. In order to maintain the specific activity at a constant level, the concentration of unlabeled valine in the medium was high (1mM). Consequently, any amount of unlabeled valine released from protein degradation would be insufficient to alter the specific activity, and under steady-state conditions the fraction of labeled valine molecules in the cells would equal the corresponding fraction in the

medium. Calculations of specific activity and recipe for medium supplemented with tritium-labeled valine are given in appendix F.

The dose rate delivered to the cells was found using the method described by Goddu et al. [1997] (see Ch. 2.2.5). Initially, there is a non-linear increase in the dose rate, but eventually a balance is reached between synthesis and degradation of protein containing tritium-labeled valine. Under such steady-state conditions the dose rate was found to be (0.015 ± 0.004) Gy/h [Bjørhovde, 2006; Pettersen et al., 2007].

The cells in experiment H1 were grown in medium supplemented with tritium-labeled valine for 26 weeks, corresponding to a dose of (65 ± 17) Gy. 17 hours before challenge irradiation with the ^{60}Co unit, they were plated in medium without tritium-labeled valine and with normal concentration of cold valine (0.171 mM in stem solution).

The cells in experiments H2-H4 were grown in medium with tritium-labeled valine for 48 hours, 96 hours and 1 week, respectively. This corresponded to the following doses:

H2 – 48 hours of tritium incorporation, D = (0.3 ± 0.1) Gy
H3 – 96 hours of tritium incorporation, D = (0.9 ± 0.2) Gy
H4 – 1 week (168 hours) of tritium incorporation, D = (2.0 ± 0.5) Gy

Dose calculations are given in appendix G. The cells were plated in normal medium 17-18 hours before challenge irradiation. After plating, the cells in experiments H1-H4 were kept in normal medium until fixation.

3.3.4 Incubation and Fixation

After plating and irradiation the cells were incubated until colonies were sufficiently large to be easily spotted by the unaided eye. The colonies were then fixed and stained. The T-47D-P cells normally needed 14-15 days for colonies to reach the sufficient size, while unprimed (and tritium-primed) T-47D cells needed 18-19 days. During this growth period, the medium (5 ml) was changed once a week in the initial experiments T1-T5, P1-P3 and H1, but in the subsequent experiments medium was not changed. Edin et al. [2008c] showed that medium change does not influence final surviving fraction in T-47D cells.

The cells were rinsed twice with PBS (phosphate-buffered saline) prior to fixation in absolute ethanol for 5 minutes. Next, the cells were stained with methylene blue for approximately 5 minutes, before they were gently rinsed with water to remove excess staining. Finally they were left to dry until the colonies were to be counted.

3.4 Calculation of Cell Survival

3.4.1 Surviving Fraction

Cell colonies were counted using a counter with a simple magnifier (New Brunswick Scientific, New Brunswick, NJ, USA). To be scored as a survivor, a colony needs to consist of more than 50 cells, and thus satisfy the criterion described in chapter 2.3.3. Colonies with a cell number close to this limit were examined in a microscope (Nikon Eclipse TS100, Japan).

As previously mentioned, five flasks of cells were plated for each radiation dose. Since the standard error of the control group influences the standard errors of all other groups, ten flasks were plated as controls and subsequently sham-irradiated. From the control group the percentage of seeded cells that grow into colonies can be calculated. This quantity is termed the plating efficiency (PE):

$$PE = \frac{N(C)}{N_0(C)} \tag{3.1}$$

where $N(C)$ is the mean number of surviving colonies in the control flasks, and $N_0(C)$ is the number of cells seeded per control flask.

Let $N(B)$ represent the mean number of counted colonies in the group given treatment B, and let $N_0(B)$ represent the number of cells seeded per flask in this group. The quantity $N_E(B) = N_0(B) \cdot PE$ is the expected number of surviving colonies if no additional treatment is given to the cells, compared to the controls. The surviving fraction for each set of five flasks given treatment B is then given by

$$F(B) = \frac{N(B)}{N_0(B) \cdot PE} = \frac{N(B)}{N_E(B)} \tag{3.2}$$

The standard error of the mean number of colonies is

$$\Delta N(B) = \sqrt{\frac{1}{n(n-1)} \sum_{i=1}^{n} \Big(N_i(B) - N(B) \Big)^2} \tag{3.3}$$

where n is the number of flasks in the set and $N_i(B)$ is the number of colonies in flask i.

The surviving fraction $F(B)$ is a function of two variables, $N(B)$ and $N_E(B)$. Hence the standard error of the surviving fraction is given by

$$\Delta F(B) = \sqrt{\left(\frac{\partial F(B)}{\partial N_E(B)} \cdot \Delta N_E(B) \right)^2 + \left(\frac{\partial F(B)}{\partial N(B)} \cdot \Delta N(B) \right)^2}$$

$$= \sqrt{\left(-\frac{N(B)}{\left(N_E(B)\right)^2} \cdot \Delta N_E(B) \right)^2 + \left(\frac{1}{N_E(B)} \cdot \Delta N(B) \right)^2} \tag{3.4}$$

Since the number of cells seeded per flask, $N_0(B)$, is (at least ideally) a constant, the relative standard error of $N_E(B)$ should equal the relative standard error of the mean colony number in control flasks, $N(C)$, implicating that

$$\Delta N_E(B) = \frac{N_0(B)}{N_0(C)} \cdot \Delta N(C) \tag{3.5}$$

3.4.2 Correction for Multiplicity

Ideally only single cells are plated and subsequently irradiated. If this is the case, the surviving fractions found from colony counting reveal directly the probability of survival for a single cell irradiated with a given dose. However, since protracted exposure to trypsin is harmful for the cells, it is not possible to produce a suspension consisting exclusively of single cells. In addition, the time between plating and radiation exposure was quite long (16-20 hours) in these experiments, so that some of the plated cells would divide before irradiation commenced. Consequently, some colony-forming units (CFUs) would consist of more than one cell, and such CFUs would have a higher probability of survival than single cells. To determine the individual cellular radiosensitivity, a correction for this multiplicity is needed.

To measure the multiplicity, 5000 cells were seeded in an additional flask during plating. These cells were fixed at the time of irradiation, and 200-300 cell units were counted under microscope to calculate the mean multiplicity. It has been shown that the increased cell density in this flask does not affect the value of the multiplicity [Edin et al., 2008c].

Multiplicity corrections were first developed by Elkind and Whitmore [1967], but the derivation outlined here is taken from Melvik [1983].

The multiplicity, or the mean number of cells per CFU, is given by

$$M = \sum_{i=1}^{n} x_i \cdot i \tag{3.6}$$

where x_i is the fraction of CFUs consisting of i cells.

Assume that the survival probability (the probability of maintaining clonogenic capacity, see Ch. 2.3.3) of a single cell is constant, i.e., independent of the number of cells in the CFU and independent of the inactivation of other cells in the CFU. If this probability is denoted by S, the fraction of cells losing their colony-forming ability is $(1 - S)$. Since

independent cell survival is assumed, the probability of inactivating a CFU containing m cells is $(1-S)^m$, which implies a survival probability of

$$F = 1 - (1-S)^m \tag{3.7}$$

for this particular CFU.

For a population of cell units containing up to n cells the expected surviving fraction F can be calculated:

$$F = \sum_{i=1}^{n} x_i \left(1 - (1-S)^i\right) \tag{3.8}$$

By equating the expected surviving fraction with the observed surviving fraction, the actual single-cell survival probability S can be deduced from equation (3.8). This problem is readily solved numerically for all values of n. For the special case of $n = 2$, when all cell units are either singlets or doublets, an analytical solution can be obtained. x_1 and x_2 are found from

$$M = x_1 + 2x_2 \quad \wedge \quad x_1 + x_2 = 1$$

Inserting the values for x_1 and x_2 into equation (3.8) and solving for S gives

$$S = \frac{M - \sqrt{M^2 - 4(M-1)F}}{2(M-1)} \tag{3.9}$$

CFUs consisting of more than two cells did occur in the present experiments. As an approximation the surviving fractions were still calculated from equation (3.9). The deviations from the exact solution was found to be less than 1% for cell units containing up to three cells [Lorentzen, 2001].

The standard error ΔM in the observed multiplicity M was found by counting some of the flasks several times. Different (although sometimes overlapping) regions of the flask surfaces were examined. The standard error was found to be $\Delta M = 0.03$.

The survival probability S in the doublet approximation (3.9) is a function of both F and M, resulting in the following expression for the standard error:

$$\Delta S = \sqrt{\left(\frac{\partial S}{\partial F} \cdot \Delta F\right)^2 + \left(\frac{\partial S}{\partial M} \cdot \Delta M\right)^2}$$

$$= \sqrt{\left(\frac{\Delta F}{\sqrt{M^2 - 4(M-1)F}}\right)^2 + \left(\frac{-1 + \frac{M-2(M-1)F}{\sqrt{M^2-4(M-1)F}}}{2(M-1)^2} \cdot \Delta M\right)^2} \qquad (3.10)$$

It is important, however, to be aware of the limitations in this model. As pointed out, these equations are based on the assumption of independent cell survival. The validity of this assumption is debated. The importance of intercellular communication for cell inactivation has been demonstrated through investigations of bystander effects (see Ch. 2.4.8), and it is clear today that radiation damage can cause cells to influence the viability of other cells both by secreting factors into the medium and through direct cell-cell contact [Hall and Giaccia, 2006, p. 35-36]. There is evidence that at least for some cell lines, microcolonies appear to respond to irradiation as a unit rather than as individual cells, with the uncorrected surviving fractions being relatively constant irrespective of the number of cells in the colony at the time of irradiation [Cummins et al., 1999; Mothersill and Seymour, 1997b]. Several reports have also shown an altered radiosensitivity for cells within microcolonies compared with cells irradiated singly [Moussa et al., 2000].

Furthermore, there are examples of increased survival in irradiated cells as compared to controls, resulting in surviving fractions greater than 1 (see Ch. 2.4.9). Such "probabilities" violate the fundamental axioms of probability theory, on which the equations given above are based. This can result in complex solutions of equation (3.8). Whenever surviving fractions greater than 1 were measured in the present experiments, multiplicity corrections were not performed. Despite the objections given above, all other surviving fractions were corrected for multiplicity, as this is still believed to give the most accurate estimates of the actual single-cell survival probabilities.

3.4.3 Mean Value Calculations

Assume that n identical experiments are performed to find the value of the parameter μ. In addition we assume that the measurements are taken from a population with a normal distribution centered around the true value μ. The measured value in each experiment is denoted S_i with an uncertainty ΔS_i. The best estimate of μ can then be obtained through the method of maximum likelihood.

The probability of measuring the value S_i in a single experiment is given by the Gaussian density function

$$P(S_i;\mu) = \frac{1}{\sqrt{2\pi(\Delta S_i)^2}} e^{-\frac{1}{2}\left(\frac{S_i-\mu}{\Delta S_i}\right)^2} \qquad (3.11)$$

The total probability of obtaining the set $\{S_i\}$ of measured values equals the product of all $P(S_i;\mu)$. This product, called the likelihood function, can be used to obtain the estimate $\widehat{\mu}$ of μ that yields the highest probability of obtaining the measured set of values $\{S_i\}$. The likelihood function is in this case given by

$$\mathcal{L}(\widehat{\mu}) = \prod_{i=1}^{n} \frac{1}{\sqrt{2\pi(\Delta S_i)^2}} e^{-\frac{1}{2}\left(\frac{S_i-\widehat{\mu}}{\Delta S_i}\right)^2} = C_1 e^{-\frac{1}{2}\sum_i \left(\frac{S_i-\widehat{\mu}}{\Delta S_i}\right)^2} \tag{3.12}$$

where C_1 is a constant. For numerical convenience, it is usually preferable to maximize the function $\ell(\widehat{\mu})$ defined as

$$\ell(\widehat{\mu}) = \ln \mathcal{L}(\widehat{\mu}) = C_2 - \frac{1}{2}\sum_i \left(\frac{S_i - \widehat{\mu}}{\Delta S_i}\right)^2 \tag{3.13}$$

The maximum of $\ell(\widehat{\mu})$ will coincide with the maximum of $\mathcal{L}(\widehat{\mu})$, since the logarithm is a monotonic function. The maximum occurs for

$$\frac{\partial \ell(\widehat{\mu})}{\partial \widehat{\mu}} = \sum_i \frac{S_i - \widehat{\mu}}{(\Delta S_i)^2} = \sum_i \frac{S_i}{(\Delta S_i)^2} - \sum_i \frac{\widehat{\mu}}{(\Delta S_i)^2} = 0 \tag{3.14}$$

which implies that the best estimate of μ is given by

$$\widehat{\mu} = \frac{\sum_i S_i/(\Delta S_i)^2}{\sum_i 1/(\Delta S_i)^2} \tag{3.15}$$

This is a weighted average of the measurements, and the weight factors are inversely proportional to the square of the uncertainty.

Uncertainties in the mean values
The uncertainty in the estimate $\widehat{\mu}$ is in general given by [Orear, 1982]

$$\sigma_{\widehat{\mu}} = \left(\sum_i \frac{1}{(\Delta S_i)^2}\right)^{-\frac{1}{2}} \tag{3.16}$$

However, if the set of measurements is poorly fitted by the normal distribution, as is often the case when the number n of measurements is small, the estimate of uncertainty obtained from (3.16) is erroneously small. In the present study this was true in the high-dose region, where just three measurements were performed for each dose. For this reason it was chosen to estimate uncertainties by calculating the standard error in the arithmetic mean value $\bar{S}$ of the n measurements. The standard error is given by

$$\Delta\bar{S} = \sqrt{\frac{1}{n(n-1)}\sum_{i=1}^{n}\left(S_i - \bar{S}\right)^2} \tag{3.17}$$

3.4.5 Presentation of Survival Data

The survival curves are plotted in the conventional manner, with the surviving fraction S as a function of dose D in a semi-logarithmic plot. In appendices A and B all the raw data are listed and plots of all the measurements are included.

When parallel experiments (normally performed in triples) are presented in the Results and Analysis section, two graphs are plotted for each set of experiments:

1) A plot of the measurement values from single experiments.
2) A plot of the mean values from the parallel experiments.

Note that the standard errors of control flasks are not plotted, but they are inherent in the calculation of errors for the other survival data (eq. (3.4)), and in the calculation of weighted mean values (eq. (3.4), (3.10) and (3.15)). In graphs of type 1) and 2) the measurement data are plotted against two survival curves. The first of these is a fit to the mean values found by pooling all the data from experiments with asynchronous T-47D cells performed in the present study. These data were fitted by the LQ model (see Ch. 4.1). The curve fittings were performed both in Origin (version 7, OriginLab Co., Northampton, MA, USA) and in IDL by a program developed by Opstad [2005]. Both programs used the method of least squares, weighting the errors. The second survival curve is a fit to survival data from ^{60}Co-irradiation of T-47D cells, measured by Edin [personal communication]. These dose-response measurements were performed with the new ^{60}Co treatment unit (see Ch. 3.3.2), i.e., in the same period of time as the experiments of the present study. The IR model gave the best fit, and the parameters obtained by Edin are given in table 3.1.

Mean values from pooled survival data of asynchronous T-47D cells are also plotted in the form of effect per unit dose, and the LQ model was fitted to the data points by linear regression in Origin. An LQ response will follow a straight line in such plots:

$$-\frac{\ln S}{D} = \alpha + \beta D \tag{3.18}$$

It is evident from this equation that the line will have a y-intercept equal to α. In the IR model (see Ch. 2.4.1) α is replaced by

Program	α_s (Gy^{-1})	α_r (Gy^{-1})	β (Gy^{-2})	d_c (Gy)
IDL/Opstad [2005]	1.141 ± 0.131	0.164 ± 0.0054	0.0253 ± 0.0005	0.485 ± 0.052

Table 3.1: IR-model parameter values obtained by Edin [personal communication]
The IR model was fitted to the mean values from experiments performed by Edin, using T-47D cells and the same ^{60}Co unit for irradiations as in the present study. A program developed by Opstad [2005] was used for the curve fitting.

$$\alpha = \alpha_r \left(1 + \left(\frac{\alpha_s}{\alpha_r} - 1\right) e^{-D/d_c}\right) \tag{3.19}$$

Back-extrapolation from the high-dose region will now produce a y-intercept equal to α_r, while the low-dose data points will approach α_s as $D \to 0$. This kind of plot is therefore particularly suited to reveal the presence of HRS.

3.5 Clonogenic Survival of G_2-Enriched Cell Populations

3.5.1 Experiments

For each cell line three sets of experiments were performed, and in each set of experiments, three methods were used to obtain G_2-enriched cell populations:

1) G_1-phase cells were sorted and incubated for 24 hours (T-47D-P) or 29-30 hours (T-47D) prior to irradiation (experiments denoted PX and TX).
2) Cells in early S phase were sorted and incubated for 14 hours before irradiation (denoted PY and TY).
3) G_2-phase cells were collected directly and incubated for only 15 minutes before irradiation took place (denoted PZ and TZ).

This produced a total of 18 experiments (PX1-PX3, PY1-PY3, PZ1-PZ3, TX1-TX3, TY1-TY3, TZ1-TZ3) measuring low-dose survival in cell populations with high fractions of G_2 cells.

3.5.2 Cell Sorting

Many cells were needed for these experiments, since large parts of the cell populations are wasted during the sorting. The cells were therefore grown in 75 cm^2 flasks, and they were first rinsed with 5 ml of trypsin and then incubated with the same amount. After ~5 min. of incubation, the cells detached. The suspensions were gently pumped using a syringe with a cannula until most of the cells were separated from each other. 5 ml of medium was then added, and the suspensions were centrifuged (as described in Ch. 3.3.1). Next, the cells were resuspended in 6 ml of fresh medium and incubated at 37°C for 15 minutes with 8 μM of the staining agent Hoechst 33342 (Riedel-de Haën, Seelze, Germany). Halfway through the incubation period, the suspensions were stirred using a vortex shaker. After staining, the test tubes were centrifuged one more time and 3 ml of medium was removed from each sample, thereby increasing the cell density to produce a higher flow rate. The cells were resuspended in the remaining medium and filtered through sterile 70 μm cell strainers (BD Falcon, Bedford, MA, USA). The cell samples were put on ice, and immediately brought to the flow cytometry lab for sorting. The ice was mixed with water to avoid subzero temperatures.

The cells were sorted in a FACS DiVa flow cytometer (Becton Dickinson, San Jose, CA, USA). Three populations (four samples) of cells were collected:

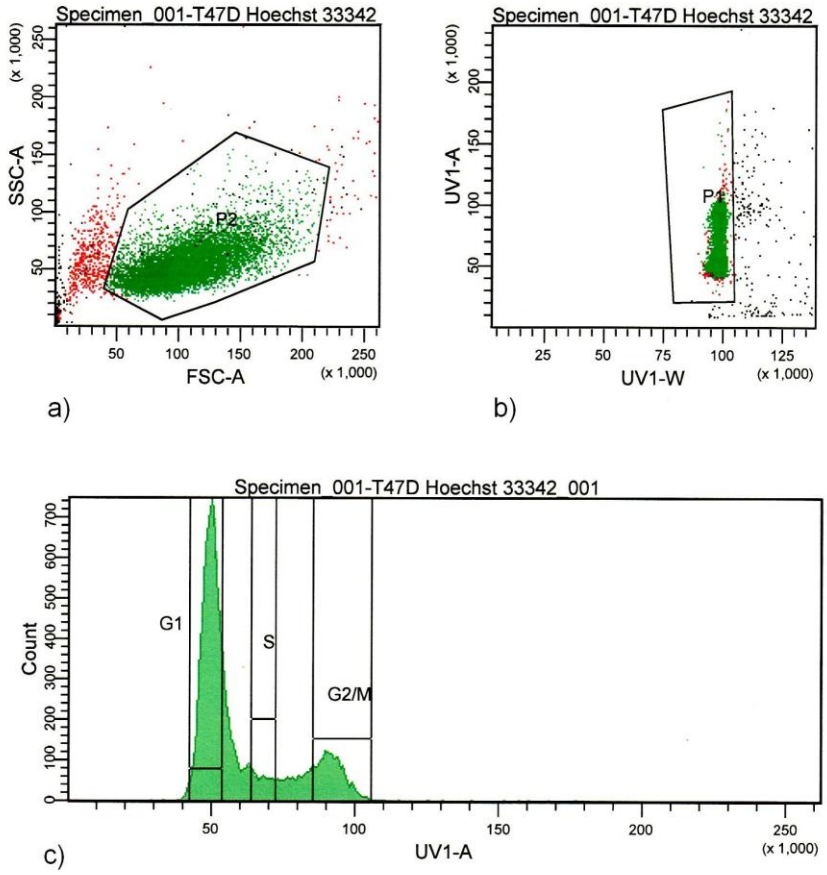

Figure 3.4
a) Dot plot of forward-scatter (FSC) versus side-scatter (SSC). The cells in the P2 region were analyzed further. b) Dot plot of fluorescence pulse area (UV1-A) versus pulse width (UV1-W). The cells outside region P1 were excluded. c) The DNA histogram that was obtained, with gating for the different cell-cycle phases (the figures are taken from the first experiment with T-47D-P cells).

1) 500 000 + 100 000 G_1-phase cells
2) 100 000 cells from early S phase
3) 100 000 G_2-phase cells

The flow cytometer was equipped with one argon laser tuned to 488 nm, and one krypton laser tuned to UV. Five parameters were measured. These were forward light scatter (FSC), side scatter (SSC), Hoechst 33342 fluorescence pulse height and pulse width, and integrated Hoechst 33342 intensity (DNA content). The data were gated in three ways. Gating on FSC versus SSC was used to eliminate cell debris and dead cells. FSC can be used to estimate particle size or cell size, while SSC is a measure of cell granularity. Dead cells have lower forward-scatter and often higher side-scatter than living cells. Only the cells enclosed by the P2 boundary in the dot plot shown in figure 3.4 a) were sorted. To exclude aggregates of cells, the data were also gated on Hoechst 33342 fluorescence pulse area (UV1-A) versus pulse width (UV1-W), as shown in figure 3.4 b). The dots to the right of the P1 boundary, having a too-high pulse width, represent clumps of two or

more cells (see Ch. 2.5.1). Finally, cells of different phases were selected by gating on a histogram of fluorescence pulse area against the number of cells counted. This is shown in figure 3.4 c). The cells were collected in tubes pre-filled with 1 ml of fresh medium. The tubes were put back on ice as soon as the desired number of cells was sorted.

3.5.3 Plating and Irradiation

The cells were transferred to larger test tubes and centrifuged. The buffer/medium supernatant was removed, and the cells washed in 5 ml of fresh, pre-warmed medium. After another round of centrifuging, the cells were resuspended in 8 ml of fresh medium. 1 ml of this cell suspension was subsequently mixed with 59 ml of medium to produce a stock solution containing approximately 200 cells/ml. 200 cells were then plated in each flask, as described in chapter 3.3.1.

The G_1- and S-phase cells were plated simultaneously (except for the 2 first experiments with T-47D-P, when S-phase cells were plated in between plating of G_1 and G_2 cells, see comments in appendix B.1), and the G_2 cells were plated immediately after this. The plating of one cell population took ~1 hour. For the G_1- and S-phase cell populations, 5000 cells were seeded in an extra flask to establish the multiplicity. This was not relevant for the G_2 cells, since the time span between plating and irradiation was insufficient for mitosis to occur.

The cells were irradiated when the fraction of G_2-phase cells was believed to be close to its peak. The incubation times prior to irradiation for the different cell populations are given in chapter 3.5.1. Setup C was used for the irradiations (see Ch. 3.3.2).

3.5.4 Incubation and Fixation

The cells were incubated until the colonies could be readily spotted by the unaided eye. The colonies seemed to grow slightly slower than normal after the staining and sorting treatment described above. To ensure complete removal of the Hoechst dye, all the medium (5 ml) in the flasks were changed after one week (except for the first experiment with T-47D-P cells). The cells were fixed as described in chapter 3.3.4.

3.5.5 Cell-Cycle Distribution after 24 hours

The 500 000 extra G_1 cells were plated in a 75 cm^2 flask. These cells were incubated for 24 hours, then harvested and washed once with 5 ml of PBS, before being fixed in 70% methanol (1.5 ml PBS + 3.5 ml methanol) and stored at -20°C.

The fixed cells were washed with PBS and prepared for analysis on a flow cytometer using the Coulter DNA prep reagents kit (Beckman Coulter, Fullerton, CA, USA), which comprises reagents for lysing, permeabilizing and staining cells in a two-step process. The cells were first resuspended in 200 µl of DNA prep LPR (containing <0.1% potassium cyanide) and subsequently resuspended in 2 ml of the DNA prep stain (containing 50 µg/ml propidium iodide (PI) and 4 KU/ml bovine pancreatic RNase type

III-A) without removing the DNA prep LPR. The lysing and permeabilizing reagent (LPR) maintains intact cells, allowing measurements of light scatter to accompany DNA fluorescence measurements. PI-staining of double-stranded RNA is prevented by the RNase.

The cells were incubated with the staining reagents for 1 hour and filtered before the DNA content was measured on a FACS DiVa flow cytometer (see Ch. 3.5.2). The DNA histograms were subsequently analyzed in the specialized software program ModFit (version 5.1, Verity Software House, Topsham, ME, USA) to obtain the cell-cycle distributions.

3.6 Selection of G_1 cells

G_0/G_1-phase T-47D-P cells were sorted and incubated for different periods of time ranging from 14-24 hours. The cell-cycle distributions were then measured by flow cytometry, and the fraction of cells remaining in G_0/G_1 in unirradiated controls was compared to the same fraction in cell populations given a small radiation dose. The purpose was to examine whether T-47D-P cells are recruited from G_0 when irradiated with a small dose.

3.6.1 Cell Sorting

The cells were harvested, stained and sorted as described in chapter 3.5.2. Three experiments were performed, and eight samples, each containing 500 000 G_1 cells, were collected per experiment. Some of the sorted cells were reanalyzed by the flow cytometer to ensure that only G_0/G_1 cells had been collected (see fig. 3.5).

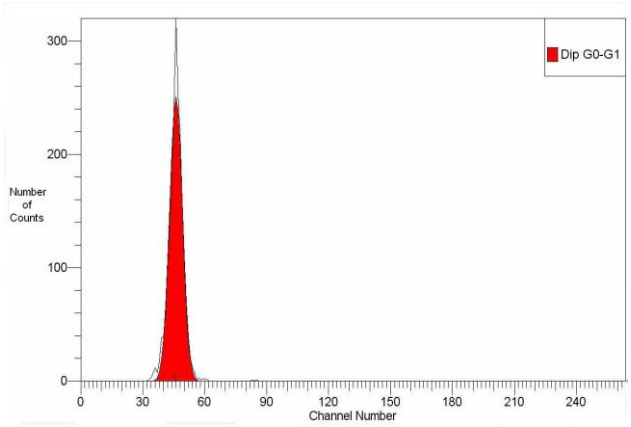

Figure 3.5
Samples of the sorted G_0 /G_1 cells were reanalyzed by the flow cytometer. Only one peak was visible in the resulting histograms, and analyses in Modfit determined the G_0 /G_1 fractions to be close to 100% (the figure is taken from the third experiment, see appendix C).

3.6.2 Plating and Irradiation

The cells were washed with fresh medium as described in chapter 3.5.3, and 500 000 cells were seeded per flask. Two parallel flasks were irradiated with 0.2 Gy using setup C

(see Ch. 3.3.2) after 15 minutes of incubation, while two other parallel flasks served as unirradiated controls. Thus the eight available samples allowed the G_0/G_1 fraction to be measured at two separate times after seeding and irradiation in each experiment.

3.6.3 Cell-Cycle Distribution Measurements

The cells were harvested and washed once with PBS prior to staining with the Coulter DNA prep reagents kit (as described in Ch. 3.5.5). When staining was completed, the cells were filtered and DNA fluorescence measured on a FACS DiVa flow cytometer.

The cell-cycle distributions were determined from the measured DNA histograms using ModFit. However, since these cells were not asynchronously growing, the resulting histograms were quite atypical. In addition, an inherent distortion in the flow cytometer caused the ratio G_2/G_1 between the G_2- and G_1-peak fluorescence intensities to be approximately 1.8, rather than 2. Consequently, ModFit had some problems finding reasonable cell-cycle distribution estimates corresponding to the measured histograms. More specifically, the auto-analysis command often produced unreliable results, and a short description of how ModFit was used to calculate the distributions in such cases will therefore be given.

First of all, ModFit is initially programmed to look for a G_2 peak corresponding to a G_2/G_1 ratio in the interval 1.85-2.20. The lower boundary of this interval was assigned to be 1.50 (using the edit peak finder command). During the sorting procedure the flow cytometer measures the DNA distribution in the asynchronous cell population in order to set up the gate for collecting G_1 cells. By letting ModFit auto-analyze these "undisturbed" histograms and other histograms with clearly distinct G_0/G_1 and G_2/M peaks, the G_2/G_1 ratio was found to be ~1.80. In the majority of these cases ModFit chose the model f_dip_t1, which is suitable for fresh, diploid samples with a visible G_2/M peak. This model also contains a triplet range, called "t1", which is assigned to correct for aggregates and triplets. Based on the results from auto-analysis by ModFit, two criteria were set up for analysis of the other DNA histograms:

1) The model f_dip_t1 was used for the analyses as long as the histograms had a visible G_2/M peak.
2) The G_0/G_1 and G_2/M ranges were chosen so that the G_2/G_1 ratio would be close to 1.80. The widths of the ranges were set equal to the average widths from auto-analyzed distributions.

Based on these criteria, relatively reasonable and consistent cell-cycle distribution estimates were obtained. However, when the G_0/G_1 cells had been incubated for only 14 hours, no G_2/M peak was visible. Using f_dip_t1 would then produce erroneously low G_2/G_1 ratios, and the model f_dip_n0, especially designed to handle histograms with indistinct G_2/M peaks, was preferred for these cases (although this model automatically assumes a G_2/G_1 ratio of 2.00).

3.6.4 Hypothesis testing on G_0/G_1 fractions

A two-sample one-sided Student's *t*-test was employed to test whether the percentage of cells in G_0/G_1 was significantly greater in the irradiated populations compared to the controls. To perform this test, a null hypothesis (H_0) is developed, which is the logical counterpart, mutually exclusive and exhaustive, to an alternative hypothesis (H_1). It is the alternative hypothesis which is being evaluated. In our case, H_0 was that the percentage of control cells in $G_0/G_1 \geq$ the percentage of irradiated cells in G_0/G_1. Depending on the outcome of the test, the null hypothesis is either rejected or retained. If H_0 is rejected, H_1 is accepted. The observed significance (*P* value) is the probability of obtaining a result at least as extreme as the one that was actually observed, given that H_0 is true. Generally, one rejects H_0 if the *P* value is smaller than or equal to a pre-determined significance level. The conventional choice of $P = 0.05$ was used in this study. The *t*-test is based on the assumption that the data are normally distributed.

3.7 Cell-Cycle Distribution 18 Hours after Trypsinization

To examine the effects of trypsinization and plating on cell-cycle distribution, cells were plated and their DNA content measured by flow cytometry 18 hours after trypsinization. Asynchronous T-47D cells were trypsinized and plated as described in chapter 3.3.1, the only difference being that 500 000 cells were plated in a single flask (75 cm^2). After 18 hours, the cells were harvested, washed with PBS, stained with PI and analyzed by a flow cytometer as previously described (Ch. 3.5.5). DNA histograms from three independent experiments were subsequently analyzed in ModFit, and the average cell-cycle distribution determined.

3.8 Measurements of pH in Medium and Cell Suspension

The pH in the medium and in cell suspensions of different dilutions were measured at various stages of the plating procedure (described in Ch. 3.3.1). The measurements were performed with a standard pH meter (PHM 210, MeterLab, Radiometer-Copenhagen, Lyon, France). The pH meter was calibrated with calibration buffers (pH = 7.000 and pH = 10.01) a few minutes prior to use.

4 Results and Analysis

4.1 Acute Irradiation of Asynchronous Unprimed Cells

Asynchronous T-47D cell populations have previously been found to express a pronounced hyper-radiosensitivity (HRS) in the low-dose region [Edin, 2003; Edin et al., 2007; Edin et al., 2008c; Edin et al., 2008b; Edin et al., 2008a]. In the present study, a total of 24 cell-survival experiments were conducted with such cell populations. 21 of these experiments assessed the low-dose response (up to 2 Gy), while 3 experiments included measurements for doses up to 10 Gy. The average plating efficiency of control flasks from the 24 experiments was (76 ± 4)%. The linear-quadratic (LQ) model was fitted to the experimental mean values in Origin (see Ch. 3.4.5), and the resulting survival curve is seen in figure 4.1 a) and b). A second survival curve is shown for comparison. This curve is a fit of the induced repair (IR) model to survival data from ^{60}Co-irradiation of the same cell line, measured by Edin [personal communication].

Curve fitting was also performed in IDL, by a program developed by Opstad [2005]. Like Origin, this program uses the method of least squares, weighting the errors. Values of the α and β parameters from the fittings of the LQ model are shown in table 4.1.

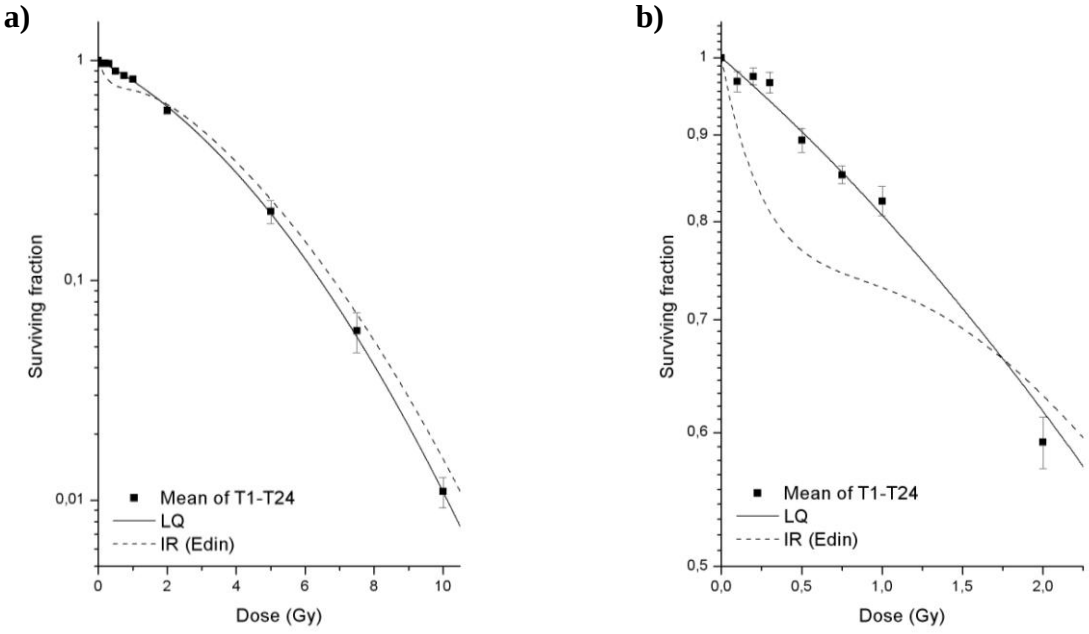

Figure 4.1
T-47D cells irradiated with single acute doses of ^{60}Co γ-radiation. The data points represent mean values from 21 experiments (0.1, 0.2, 0.3 and 0.75 Gy) or 24 experiments (0.5, 1 and 2 Gy) in the low-dose region, and from 3 experiments (5, 7.5 and 10 Gy) in the high-dose region. Vertical bars are standard errors. The curves represent a fit by the LQ model (solid line) to the data measured in the present study, and a fit by the IR model (dashed line) to survival data measured by Edin [personal communication] using the same cell line and radiation quality. a) All data are included. b) Only data in the low-dose region up to 2 Gy are shown.

Program	α (Gy^{-1})	β (Gy^{-2})	χ^2/ν
Origin	0.188 ± 0.010	0.0263 ± 0.0020	0.941
IDL/Opstad [2005]	0.188 ± 0.010	0.0264 ± 0.0019	1.062

Table 4.1: Parameter values obtained by fitting the LQ model to the data points in figure 4.1
The LQ model was fitted to the mean values from experiments T1-T24 by two different computer programs, both using the method of least squares and weighting the errors. χ^2/ν is the reduced chi-squared value, i.e., the value of chi-squared divided by the associated number of degrees of freedom.

The two programs give virtually identical results for the curve fitting, but Origin returns a slightly lower value for the reduced chi-squared (χ^2/ν). In both cases, however, the reduced chi-squared value is close to one, and the experimental data are fitted very well by the LQ model. The reduced chi-squared value is expected to be close to one. If it is much greater, the fitted curve deviates too much from the data points to be considered reasonable. If it is much lower than one, the fit is unexpectedly good, often indicating that something is wrong (for instance the standard errors might be too large).

The mean-value data points are replotted in the form of effect per unit dose as a function of dose in figure 4.2. As described in chapter 3.4.5, this kind of plot is suited to reveal the presence of HRS, since a back-extrapolation from the high-dose region will intercept the y-axis at α_r, while the low-dose data points will approach α_s. A linear-quadratic response will follow a straight line with a slope equal to β and a y-intercept equal to α.

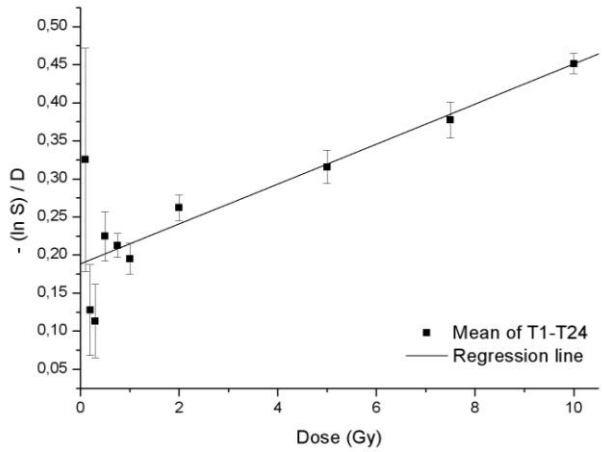

Figure 4.2
Effect per unit dose (-(ln S)/D = α+βD) is plotted as a function of dose. The straight line was found by linear regression in Origin. Since the data points (mean values from experiments T1-T24) seem to follow the line quite well, the LQ model is suited to describe the data.

New estimates for the parameters α and β could be obtained from this plot using linear regression. The regression was performed in Origin, which uses the method of least squares with the error bars as weights. The results from this analysis are given in table 4.2, and the obtained values are almost identical to those given in table 4.1. Again the LQ model gives an excellent fit to the experimental data. This is reflected in the coefficient of determination (r^2), which is equal to 0.965. The value of r^2 is a measure of how well the regression line represents the data, and while a value of 0 would implicate a random nonlinear relationship between the two variables, a perfect linear association would correspond to a value of one.

α (Gy^{-1})	β (Gy^{-2})	r^2
0.188 ± 0.010	0.0262 ± 0.0018	0.965

Table 4.2: Parameter values obtained by linear regression in the effect-per-unit-dose versus dose plot
The values of the LQ-model parameters α and β were determined by linear regression in Origin (see figure 4.2), which uses the method of least squares with the error bars as weights. The point (D=0, S=1) was not included. The coefficient of determination, r^2, is a measure of how well the regression line represents the data.

It is evident from figures 4.1 and 4.2, that the dose-response measurements followed the LQ model closely. The IR model, on the other hand, is derived from the LQ model by introducing two additional parameters (α_s and d_c, see equations 2.10 and 2.11), and the presence of HRS is often deduced from the parameter values found by fitting the IR model to dose-survival data. It is conventional to establish the presence of significant HRS by requiring non-overlapping 95% confidence limits on the α_r and α_s parameters (with $\alpha_s > \alpha_r$), and 95% confidence limits on the d_c parameter that does not include zero [Marples et al., 2003; Mitchell and Joiner, 2002]. Even though the LQ model clearly seems sufficient to describe the dose-response measured in the present study, the IR model was also fitted to the survival data in order to compare the obtained parameter values with the given criteria. The results are given in table 4.3.

From the parameter values listed in table 4.3, it is clear that none of the HRS criteria are satisfied. The α_r 95% confidence interval is contained within the confidence limits of the α_s parameter. Furthermore, d_c is not significantly greater than zero. Finally and most importantly, $\alpha_s < \alpha_r$, meaning that the initial radiosensitivity is not higher than expected from the LQ formulation. Thus there is no transition towards increased radioresistance (IRR). Note, however, that the plot in figure 4.2 shows a higher-than-expected effect at the lowest dose (0.1 Gy), although not significantly. It is also worth mentioning that the reduced chi-squared values are somewhat larger than what is seen for the LQ curve fits, so it seems that there is no gain from the introduction of two extra parameters, and the LQ model is best suited to describe the data.

The lack of HRS expression in the unprimed T-47D cells was naturally very surprising,

Program	α_s (Gy^{-1})	α_r (Gy^{-1})	β (Gy^{-2})	d_c (Gy)	χ^2/ν
Origin	0.127 ± 0.087 (-0.078-0.332)	0.204 ± 0.026 (0.144-0.265)	0.0244 ± 0.0033 (0.0166-0.0322)	0.495 ± 0.704 (-1.169-2.159)	0.985
IDL/Opstad [2005]	0.124 ± 0.090	0.203 ± 0.025	0.0245 ± 0.0033	0.478 ± 0.653	1.150

Table 4.3: Parameter values obtained by fitting the IR model to the data points in figure 4.1
The IR model was fitted to the mean values from experiments T1-T24 by two different computer programs, both using the method of least squares and weighting the errors. The numbers in parentheses are 95% confidence intervals (only calculated in Origin). χ^2/ν is the reduced chi-squared value, i.e., the value of chi-squared divided by the associated number of degrees of freedom.

as these results contradict the previous findings of Edin et al. [2007; 2008c; 2008b; 2008a]. In an attempt to explain this paradox a series of measurements was performed in the low-dose region. Different cell batches, radiation setups and plating techniques were used in order to find out what caused the observed discrepancy. This is the reason for the large number of experiments (T1-T24) performed with asynchronous T-47D cells. The results of the different experimental approaches will be presented in the following sections, although it is evident from the mean values already shown in figure 4.1 (which are the values found by pooling the results of all these experiments) that the presence of HRS was never successfully retrieved.

Unless stated otherwise, the cells were plated as described in chapter 3.3.1 and irradiated the following day (16-20 hours later).

4.1.1 The Initial Experiments

The cells were irradiated with a dose rate of 1.0 Gy/min, and the ^{60}Co source was shielded with 7 cm of Perspex (setup A, see Ch. 3.3.2). The results from these experiments (T1 and T2) are shown in figure 4.3. The observed surviving fractions seem to follow the LQ curve quite closely.

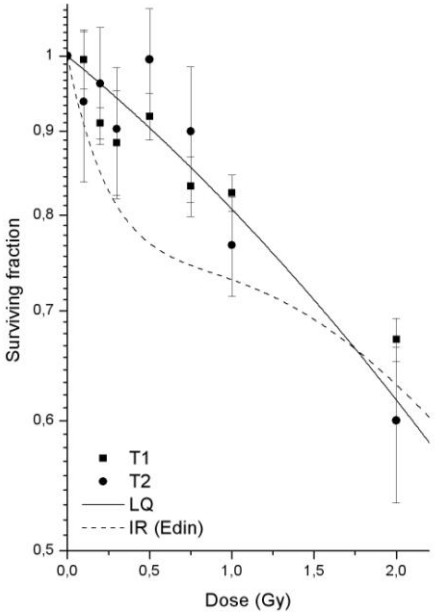

Figure 4.3
Survival of T-47D cells irradiated with single acute doses of ^{60}Co γ-rays. The data points represent single observations of two independent experiments (T1 and T2), and the vertical bars are standard errors. The curves represent a fit by the LQ model (solid line) to pooled data (T1-T24) from the present study, and a fit by the IR model (dashed line) to survival data measured by Edin [personal communication] using the same cell line and radiation quality.

4.1.2 Reduced Perspex Shielding

Because of the missing HRS response in the initial experiments, we started looking for deviations from the experimental setup previously used by Edin [Edin, 2003; Edin et al., 2007]. One difference was the Perspex shielding used to obtain the desired dose rate. A total thickness of 7 cm is quite much, and a lot of the primary photons will be scattered through Compton interactions before reaching the cell-flask surface. For a circular ^{60}Co beam with a field radius of 16.6 cm (corresponding to the field size at SSD = 66.5 cm

using setup A, see Ch. 3.3.2) the scatter-primary ratio at 7 cm depth is approximately 0.4 in water [Iwasaki, 1994]. Furthermore, the mean fraction of the incident photon's energy given to the recoiling electron in Compton interactions is about 45% for ^{60}Co photons [Attix, 1986, p. 135]. This means that the energy distribution of the photons will be substantially altered by the Perspex shielding, and the mean photon energy will be lowered. Photons of lower energy transfer less energy to fast secondary electrons, and since the stopping power of electrons is roughly inversely proportional to the square of the electron velocity, the LET will be increased (see Ch. 2.2.2). While 250 kV_p X-rays typically have a LET equal to 2.0 keV/µm, the LET of ^{60}Co γ-rays is approximately 0.2 keV/µm [Hall and Giaccia, 2006, p. 108]. At low doses reference X-rays are about twice as biologically effective as ^{60}Co γ-rays [Chen, 2004], and Edin et al. [2008a] showed that the transition to IRR set in for smaller doses following X-irradiation compared to ^{60}Co γ-irradiation, causing the HRS "dip" to be much less pronounced. Consequently, the modification of the photon spectrum introduced by the Perspex shielding could reduce the observed HRS.

The Perspex shielding was therefore reduced to 1 cm, and the dose rate increased to approximately 1.3 Gy/min (setup B). The results from these experiments (T3, T4 and T5) are shown in figure 4.4 a) and b). From these figures it is clear that HRS was not observed. In concordance with this, Monte Carlo simulations using the EGSnrc program demonstrated that the Perspex shielding caused just minor changes in the LET values [Edin, personal communication].

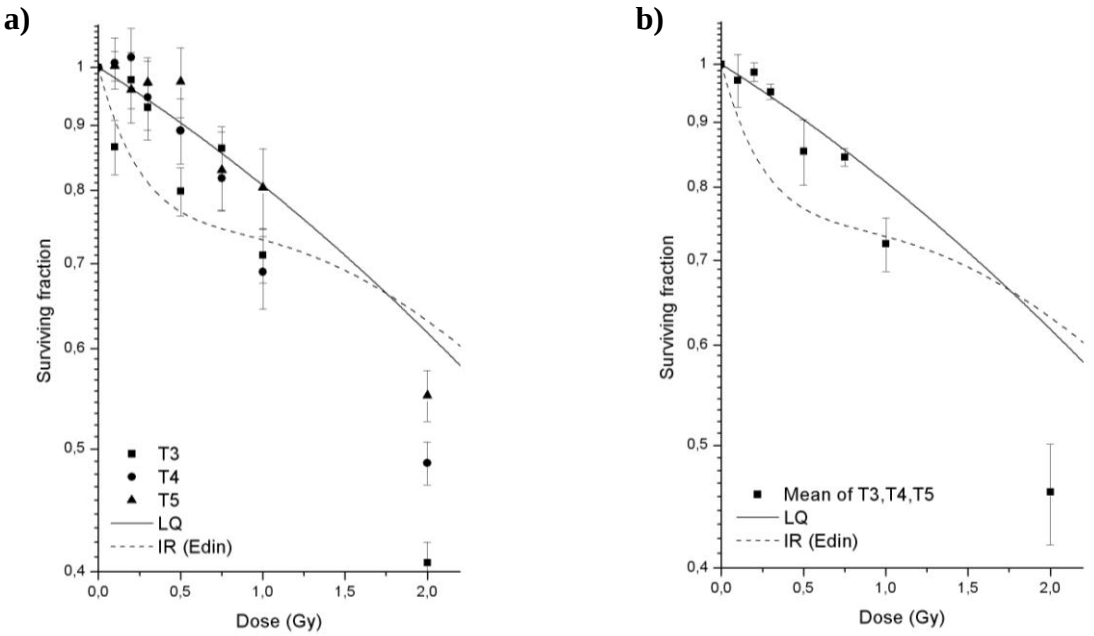

Figure 4.4
Survival of T-47D cells irradiated with single acute doses of ^{60}Co γ-rays. The curves represent a fit by the LQ model (solid line) to pooled data (T1-T24) from the present study, and a fit by the IR model (dashed line) to survival data measured by Edin [personal communication] using the same cell line and radiation quality. a) Data points represent single observations of three independent experiments (T3, T4 and T5). b) Data points represent mean values of the three experiments. Standard errors are shown by error bars.

4.1.3 New Batch of Cells

The cells used in experiments T1-T5 had been grown continuously for more than a year by reculturing twice a week. It was speculated whether the low-dose radio-sensitivity of the cells could have been modified during this time. To address this issue, a fresh batch of cells was taken from a stock kept at -196°C in a liquid nitrogen storage container. The cells were thawed on October 5th, 2007, but the experiments (T6, T7 and T8) were performed more than three months later. Irradiation was administered using setup B, and the resulting survival measurements are shown in figure 4.5 a) and b). The low-dose response showed no sign of HRS. In fact the surviving fractions tended to be slightly higher than indicated by the LQ curve.

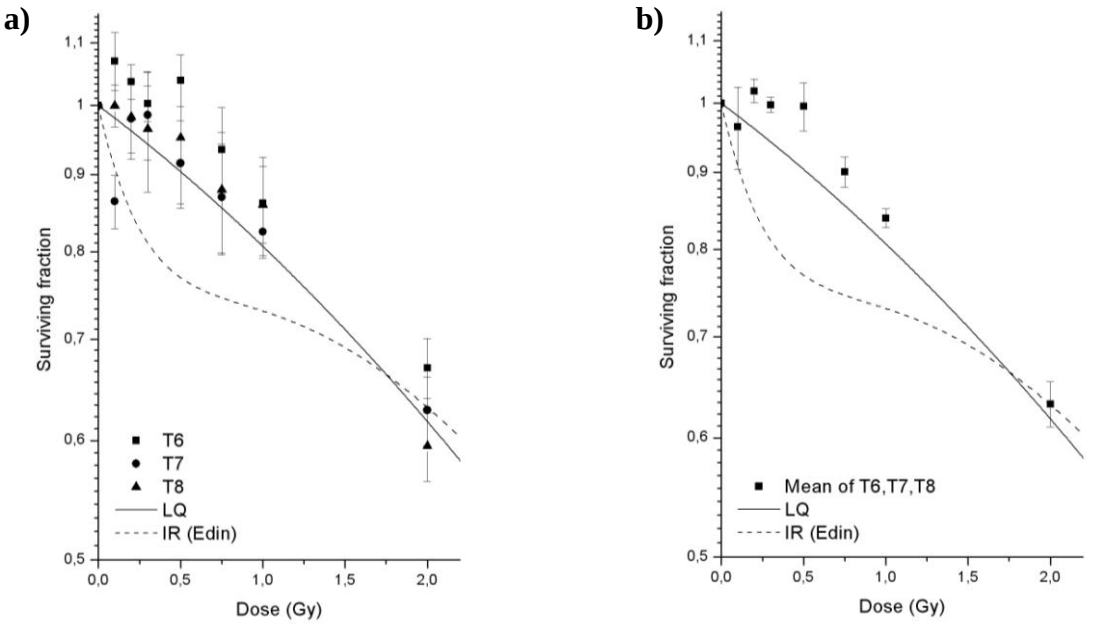

Figure 4.5
Survival of T-47D cells irradiated with single acute doses of ^{60}Co γ-rays. The curves represent a fit by the LQ model (solid line) to pooled data (T1-T24) from the present study, and a fit by the IR model (dashed line) to survival data measured by Edin [personal communication] using the same cell line and radiation quality. a) Data points represent single observations of three independent experiments (T6, T7 and T8). b) Data points represent mean values of the three experiments. Standard errors are shown by error bars.

4.1.4 Single-Cell Suspension Prepared without Syringe and Cannula

Since neither changing the batch of cells nor changing the irradiation setup helped regaining the HRS expression, it was hypothesized that some kind of stress stimulus applied on the cells during plating altered their sensitivity to low radiation doses. The plating procedure, as described in chapter 3.3.1, was therefore slightly modified. In stead of separating cells by pumping with a syringe and cannula, a 2-ml pipette was used to prepare the single-cell suspension. The pipette has a larger opening, which probably makes the pumping less harmful for the cells. Three experiments (T9, T10 and T13) were performed using this method of cell separation. T9 and T10 were irradiated using setup

B, while experiment T13 was irradiated using setup C (see Ch. 3.3.2). The results are given in figure 4.6 a) and b).

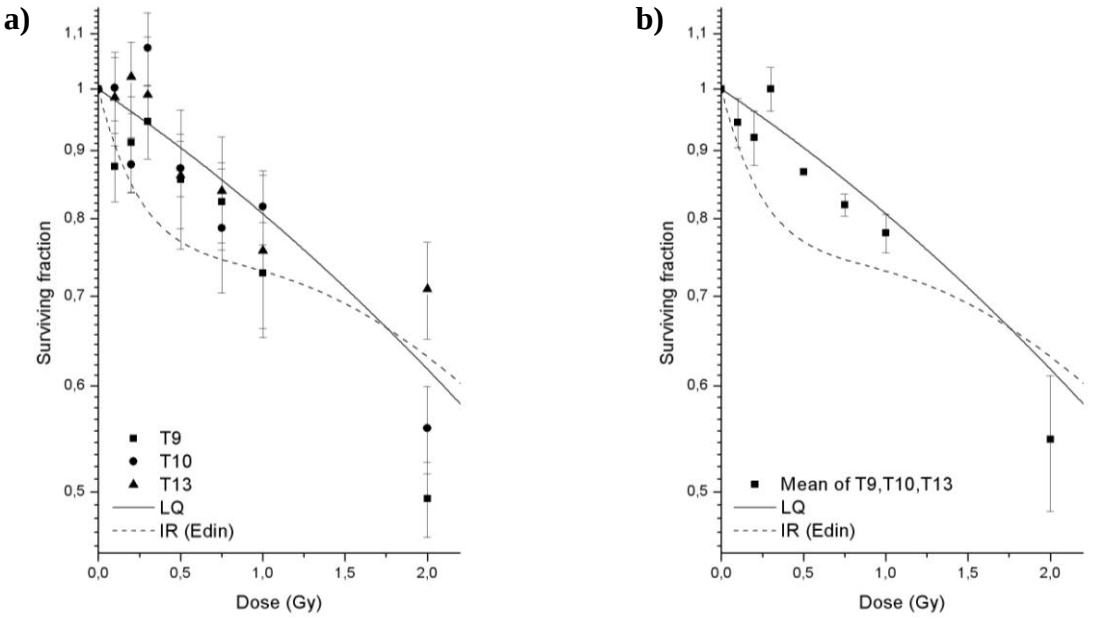

Figure 4.6
Survival of T-47D cells irradiated with single acute doses of ^{60}Co γ-rays. The curves represent a fit by the LQ model (solid line) to pooled data (T1-T24) from the present study, and a fit by the IR model (dashed line) to survival data measured by Edin [personal communication] using the same cell line and radiation quality. a) Data points represent single observations of three independent experiments (T9, T10 and T13). b) Data points represent mean values of the three experiments. Standard errors are shown by error bars.

Even though the mean surviving fractions, except for 0.3 Gy, lay below the LQ line, the typical HRS/IRR pattern was not observed, as no transition towards increased radioresistance (IRR) seemed to occur.

4.1.5 Temperature Maintained at 37°C

Temperature during irradiation has been reported to affect the radiosensitivity of T-47D cells [Christiansen, 2005]. In the study by Christiansen, cells were irradiated with 220 kV X-rays at room temperature and with the temperature maintained at 37°C. While no HRS was observed in the experiments performed at room temperature, the low-dose radio-sensitivity increased when the temperature was controlled to keep 37°C (using a water-heated copper plate). However, the radiosensitivity was elevated for the entire dose range examined, and although it was concluded that the cells exhibited HRS, curve fitting by the IR model did not produce parameter values satisfying the criteria given in chapter 4.1 (in fact $\alpha_s \approx \alpha_r$).

Three experiments were performed to examine the effect of controlling the temperature (T11, T12 and T15). Using a Perspex plate with water heating (setup C), the temperature could be maintained at 37°C in the cell flasks during irradiation. Syringe and cannula

were again applied to separate cells. However, the cells were kept longer in trypsin (total time ~10 minutes) and pumped very gently. The results of these experiments are shown in figure 4.7 a) and b).

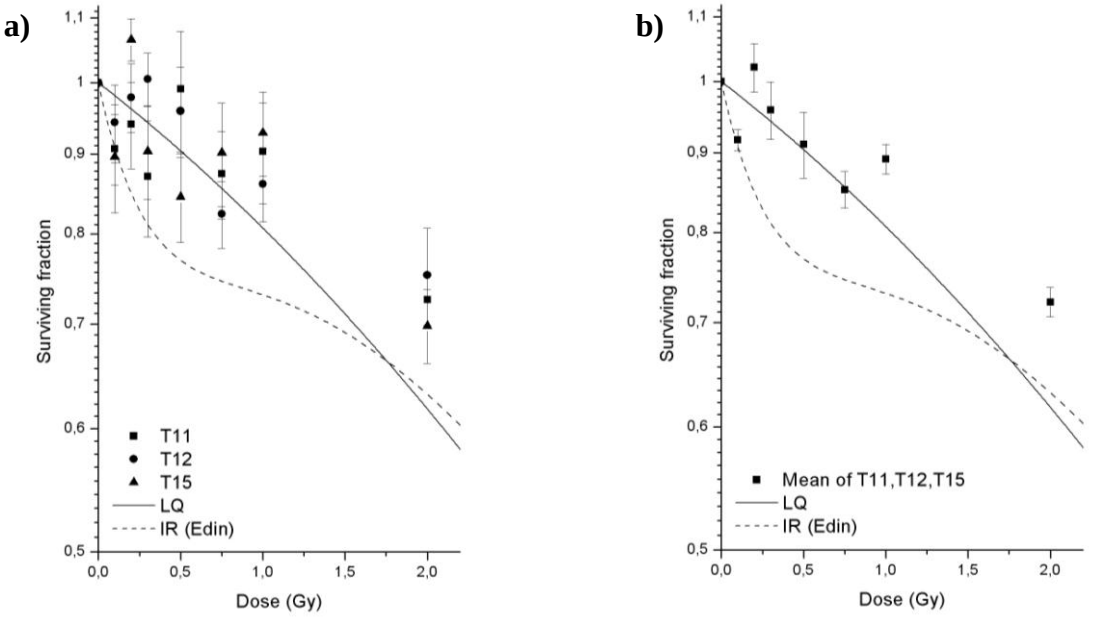

Figure 4.7
Survival of T-47D cells irradiated with single acute doses of ^{60}Co γ-rays. The curves represent a fit by the LQ model (solid line) to pooled data (T1-T24) from the present study, and a fit by the IR model (dashed line) to survival data measured by Edin [personal communication] using the same cell line and radiation quality. a) Data points represent single observations of three independent experiments (T11, T12 and T15). b) Data points represent mean values of the three experiments. Standard errors are shown by error bars.

The survival data were quite similar to those previously obtained, with the LQ curve as a good fit. The temperature effects reported by Christiansen [2005] were not observed. Note however, that both irradiation (due to lower dose rates) and transportation times were much longer in Christiansen's study than in the present one. Cell flasks were never kept outside the incubator for more than ~4 minutes (except for the largest doses delivered with setup C) in the present study.

4.1.6 Centrifugation Avoided

Parallel experiments conducted by Edin [personal communication], in which the same batch of cells, the same plating procedure and the same irradiation setup were used, showed evidence of HRS. Thus the missing HRS response in the experiments of the present study seemed to be due to some aspect of how the cells were handled. Different techniques used to separate cells had already been applied. Exposure to shear forces in the centrifuge might be another factor that causes stress and potential cell damage, especially if the rotation speed is too high. In her experiments, Edin used the same centrifuge and rotation speed as was applied in this study. But centrifugation, which is

commonly used to remove trypsin and thereby avoid protracted exposure to this harmful enzyme, is not really necessary if the trypsin is sufficiently diluted with medium, as medium contains serum which acts as a trypsin inhibitor. In these experiments the original trypsin/medium solution was diluted many times (the final trypsin concentration in the cell flasks would be ~1:20000 if trypsin was not removed).

The first experiment (T14) performed omitting centrifugation, was highly promising (see figure 4.8). Except for not being centrifuged, the cells were treated exactly as described in the previous section (Ch. 4.1.5). This is the only experiment that actually showed clear indications of HRS/IRR.

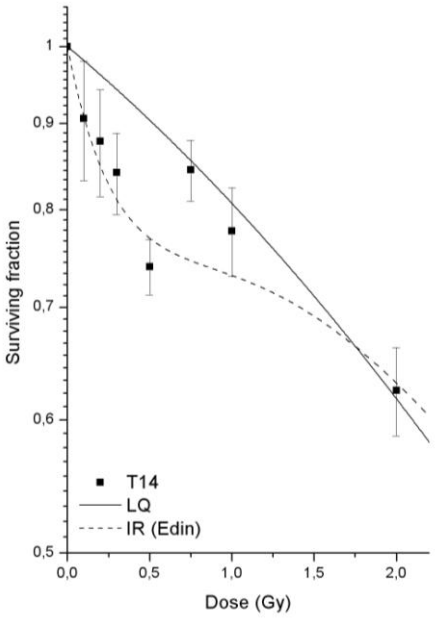

Figure 4.8
Survival of T-47D cells irradiated with single acute doses of ^{60}Co γ-rays. The data points represent surviving fractions from a single experiment (T14), and the vertical bars are standard errors. The curves represent a fit by the LQ model (solid line) to pooled data (T1-T24) from the present study, and a fit by the IR model (dashed line) to survival data measured by Edin [personal communication] using the same cell line and radiation quality.

Three additional experiments (T20, T21 and T23) without centrifugation were conducted. In these attempts to reproduce the results of experiment T14, the cells did not exhibit HRS (see figure 4.9 a) and b)).

4.1.7 Pipetting Error Diminished

Statistical uncertainty in the number of cells seeded per flask is a problem in the study of low radiation doses, because the difference between the number of surviving colonies in irradiated flasks and control flasks, small to begin with, is masked by the statistical variations. Three kinds of error will typically contribute to these variations. These are (1) errors due to inadequately controlled variables, such as temperature, pH, quality of serum, etc., (2) sampling errors due to the limited number of cells transferred in the plating procedures, and (3) dilution or pipetting errors due to inaccuracy in the volume of suspension transferred [Boag, 1975].

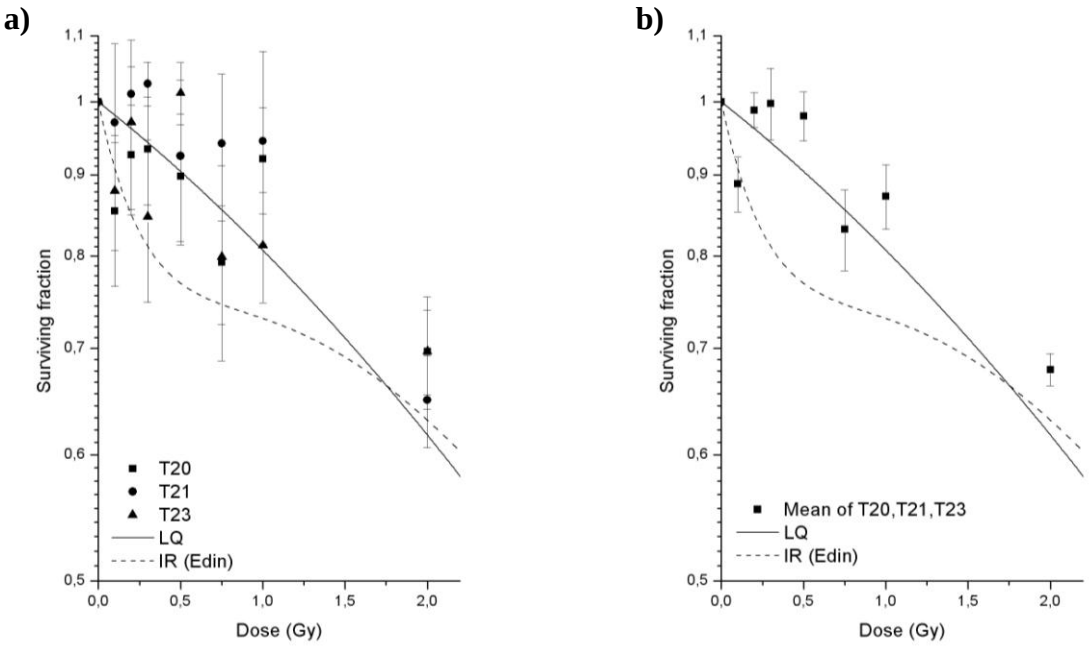

Figure 4.9
Survival of T-47D cells irradiated with single acute doses of ^{60}Co γ-rays. The curves represent a fit by the LQ model (solid line) to pooled data (T1-T24) from the present study, and a fit by the IR model (dashed line) to survival data measured by Edin [personal communication] using the same cell line and radiation quality. a) Data points represent single observations of three independent experiments (T20, T21 and T23). b) Data points represent mean values of the three experiments. Standard errors are shown by error bars.

Normally a stock solution containing 200 cells/ml was prepared for each plating. 1 ml of this suspension was manually transferred to each cell flask using a 2-ml pipette equipped with a rubber bulb. Adjustable pipettes were not used, as the disposable tips used for these pipettes have too narrow opening, causing cells to be damaged. The uncertainty of the described method was presumably ±0.05 ml or 5%. By reducing the cell concentration in the stock solution to 50 cells/ml, this accuracy was improved. Now a 5-ml pipette was filled with an electric pipette filler, and 4 ml of suspension was transferred to each flask. The absolute uncertainty of ±0.05 ml was probably unchanged, giving a relative error of only 1.25%. Results from three experiments (T17, T19 and T24) using this plating approach are shown in figure 4.10 a) and b). The cells were irradiated using setup C.

The number of actually transferred cells, assuming a uniform mixing of the stock suspension, will follow the Poisson distribution (since the cells will be randomly distributed in the medium). If one supposes that N cells are transferred, the sampling error will be $\sqrt{N}$, or $(100/\sqrt{N})$ if expressed as a percentage of N. With a pipetting error of x% the combined percentage error in the number of transferred cells will be

$$\left(x^2 + \frac{10^4}{N}\right)^{1/2} \tag{4.1}$$

The ratio of this combined error to the basic sampling error $(100/\sqrt{N})$ is

$$R = \left(1 + \frac{Nx^2}{10^4}\right)^{1/2} \tag{4.2}$$

Setting N = 200 and x = 1.25, gives R = 1.016, which means that the pipetting error is negligible compared to the sampling error. With $x = 5$, the ratio R = 1.22, implicating that the pipetting error in that case increases the combined error by 22%. Still the sampling error is by far dominating in both cases, and a big effect of reducing the pipetting error should not be expected. This is in agreement with the observed survival (see figure 4.10), which is similar to previous measurements. The mathematical argument given above is taken from Boag [1975].

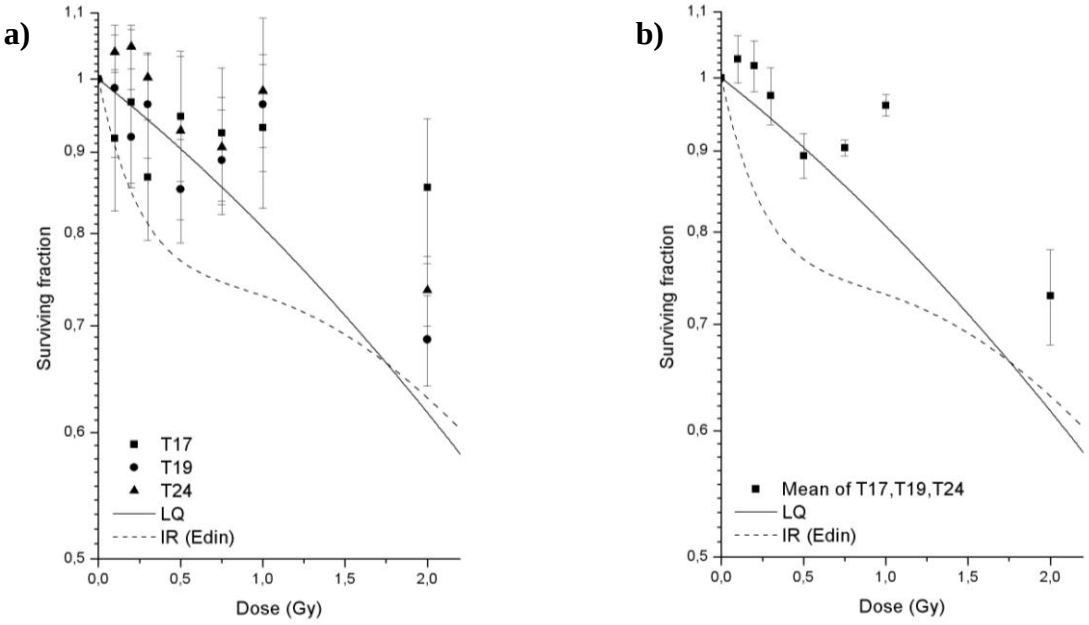

Figure 4.10
Survival of T-47D cells irradiated with single acute doses of ^{60}Co γ-rays. The curves represent a fit by the LQ model (solid line) to pooled data (T1-T24) from the present study, and a fit by the IR model (dashed line) to survival data measured by Edin [personal communication] using the same cell line and radiation quality. a) Data points represent single observations of three independent experiments (T17, T19 and T24). b) Data points represent mean values of the three experiments. Standard errors are shown by error bars.

4.1.8 Radiosensitivity in the High-Dose Range

In order to obtain a decent curve fit the radiosensitivity in the high-dose region had to be established. The cells were plated as described in chapter 3.3.1, and the temperature was maintained at 37°C during irradiation (setup C). The dose-survival measurements from three experiments (T16, T18 and T22) are shown in figure 4.11 a) and b).

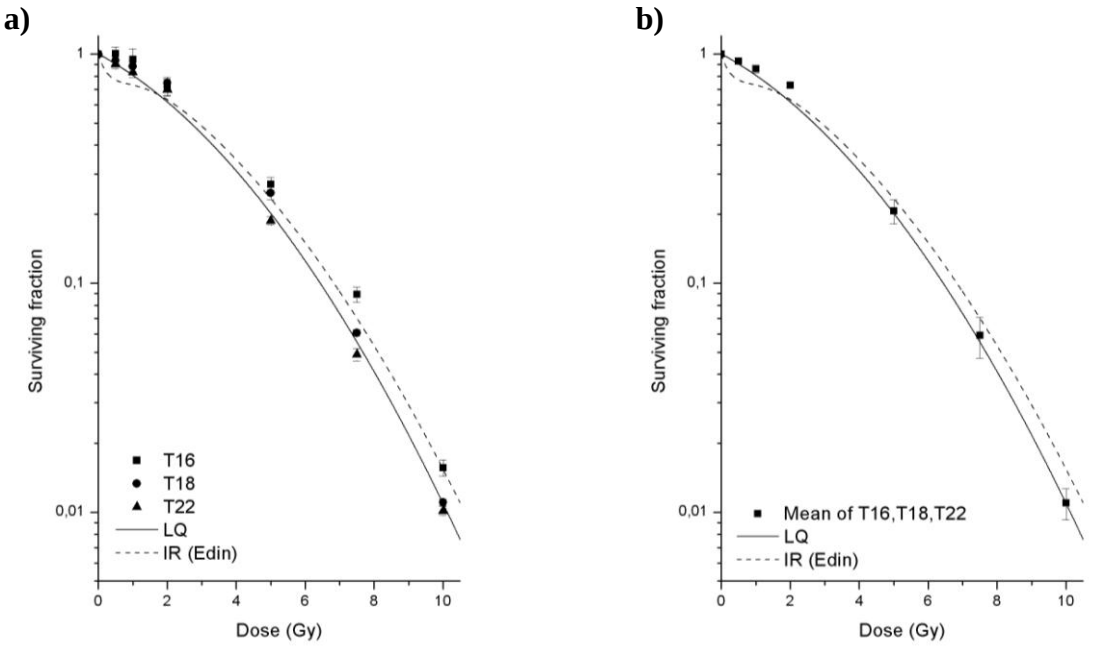

Figure 4.11
Survival of T-47D cells irradiated with single acute doses of ^{60}Co γ-rays. The curves represent a fit by the LQ model (solid line) to pooled data (T1-T24) from the present study, and a fit by the IR model (dashed line) to survival data measured by Edin [personal communication] using the same cell line and radiation quality. a) Data points represent single observations of three independent experiments (T16, T18 and T22). b) Data points represent mean values of the three experiments. Standard errors are shown by error bars.

As seen from figure 4.11, the high-dose survival observed in these experiments was in good agreement with the IR curve fitted to data measured by Edin [personal communication].

4.1.9 Plating Performed by another Person

Since I failed to detect the expression of HRS/IRR in a long series of measurements and there were indications that this might be due to how the cells were handled during plating, a final attempt to find the effect was made by letting another person perform the experiments. Three experiments (A1, A2 and A3) were plated by Patrycja Mikolajewska (PhD-student at DNR, M.Sc. in biotechnology). The resulting survival data points are plotted against the LQ and IR curve fits in figure 4.12 a) and b).

The mean surviving fractions, except for 1 Gy, are seen to follow the LQ curve quite closely, even though the results of these three experiments were not included when calculating the mean-value data points that were fitted by the LQ model. Note however that the first experiment (A1) did show an HRS-like response for the three lowest doses. Because of large dispersion in the colony numbers in these groups, they were given little weight in the mean value calculations (see Ch. 3.4.3).

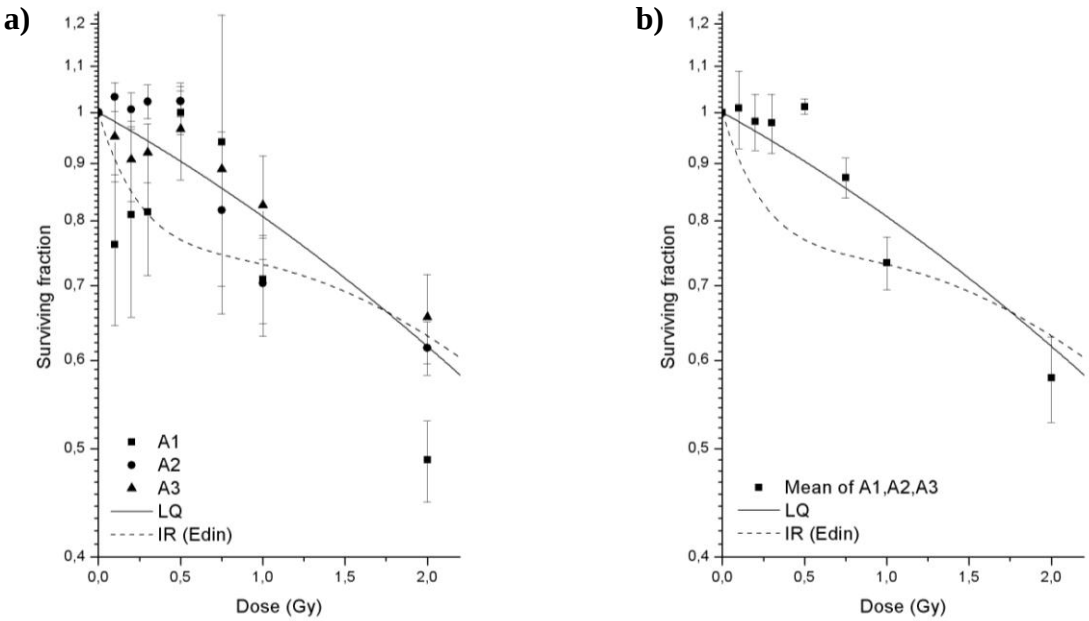

Figure 4.12
Survival of T-47D cells irradiated with single acute doses of ^{60}Co γ-rays. The curves represent a fit by the LQ model (solid line) to pooled data (T1-T24) from the present study, and a fit by the IR model (dashed line) to survival data measured by Edin [personal communication] using the same cell line and radiation quality. a) Data points represent single observations of three independent experiments (A1, A2 and A3) plated by P. Mikolajewska. b) Data points represent mean values of the three experiments. Standard errors are shown by error bars.

4.2 Acute Irradiation of Asynchronous Primed Cells

The pronounced HRS/IRR response seen in T-47D cells was permanently removed when the cells were given a low-dose-rate (0.3 Gy/h) priming dose of 0.3 Gy [Edin et al., 2007; Edin et al., 2008c; Edin et al., 2008b]. The first culture that was primed in this way has at present been cultivated continuously for more than three years (see Ch. 3.1), and HRS has not been recovered. As described in chapter 2.4.9, the survival of these cells tended to be higher than predicted by the LQ model, and even exceeded 1 at the lowest doses.

Seven experiments were performed to measure the low-dose response of T-47D-P cells, and the average plating efficiency of control flasks was (79 ± 10)%. The mean surviving fractions from these experiments are shown in figure 4.13. Note, however, that when the mean values were calculated, two of the experiments (P3-P4) were not included for reasons that are described in chapter 4.2.2. It is clear from figure 4.13 that although the surviving fractions lay slightly above the LQ curve, the survival at the lowest doses did not appear to exceed the survival of controls. A comparison with the LQ curve fitted to data from unprimed T-47D cells (see Ch. 4.1) rather suggest that the difference in dose response between primed and unprimed cells is relatively small. Thus, the results of the present study again deviate somewhat from previous observations. Since the seven experiments with T-47D-P cells were performed using slightly differing experimental setups and different batches of cells, the results of the individual experiments will be reviewed.

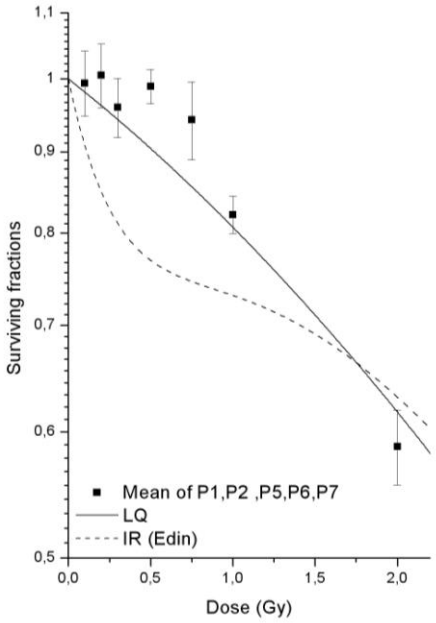

Figure 4.13
Survival of T-47D-P cells irradiated with single acute doses of ^{60}Co γ-rays. All the cells, including the controls, had been given the same priming treatment (0.3 Gy at 0.3 Gy/h). The curves represent a fit by the LQ model (solid line) to pooled survival data (T1-T24) from unprimed cells, and a fit by the IR model (dashed line) to survival data measured by Edin [personal communication] using unprimed T-47D cells and the same radiation quality. The data points represent mean values of five experiments (P1-P2 and P5-P7). Standard errors are shown by error bars.

4.2.1 The Initial Experiments

The two first experiments on T-47D-P cells were performed in January and February 2008 on cells that had been cultured continuously since the 0.3 Gy priming dose was given by Nina F. J. Edin on August 17th, 2005. The cells were irradiated at a dose rate of 1.3 Gy/min, using a 1 cm Perspex plate as support (setup B, see Ch. 3.3.2). After two weeks of incubation, the cells were fixed and stained. Medium was changed after one week. The results of the experiments seemed to be consistent with the observations of Edin et al. [2007; 2008c; 2008b] and Fenne [2008], with low-dose surviving fractions higher than 1 (see fig. 4.14).

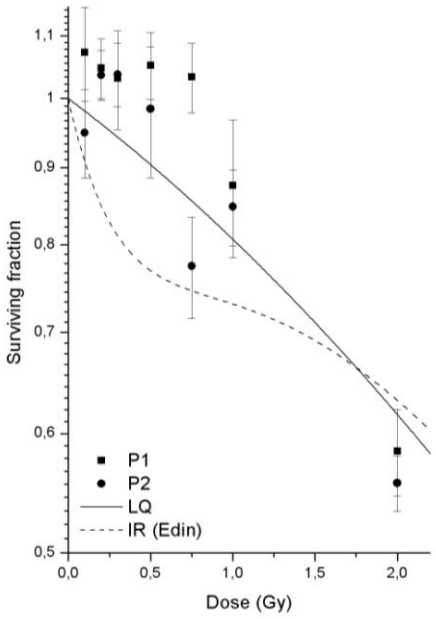

Figure 4.14
Survival of T-47D-P cells irradiated with single acute doses of ^{60}Co γ-rays. All the cells, including the controls, had been given the same priming treatment (0.3 Gy at 0.3 Gy/h). The curves represent a fit by the LQ model (solid line) to pooled survival data (T1-T24) from unprimed cells, and a fit by the IR model (dashed line) to survival data measured by Edin [personal communication] using unprimed T-47D cells and the same radiation quality. The data points represent single observations of two experiments (P1 and P2). Standard errors are shown by error bars.

4.2.2 New Batch of Cells

Due to some problems with maintaining the stock cultures in our lab, probably as a result of contaminated medium, new T-47D-P cells were thawed on March 18th, 2008. These cells had been taken from the cell culture that was primed in August 2005, and kept in a liquid nitrogen storage container since November 9th, 2006. Consequently, they had been cultured for 15 months since the priming dose was given.

Two experiments were performed on these cells (see fig. 4.15) on April 16th, that is, 28 days after thawing. One of the experiments (P3) was irradiated using setup B, and in this experiment, medium was changed after one week of incubation. The intent was to make it similar to the previous experiments (P1 and P2). The other experiment (P4) was irradiated using setup C, and medium was not changed during the colony growth period. Figure 4.15 displays the resulting surviving fractions. Surprisingly, they tend to lie below the LQ curve, and are thus markedly lower than seen in figure 4.14.

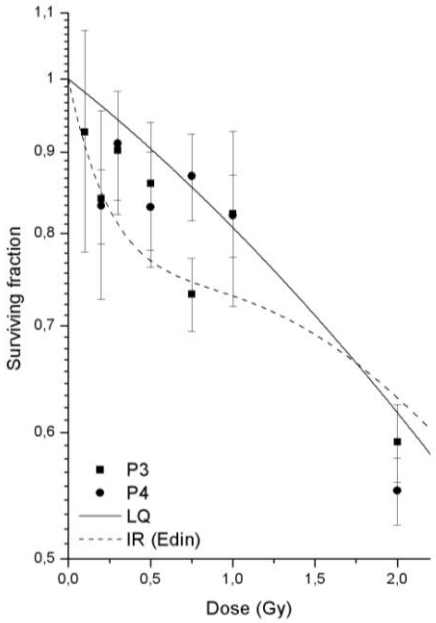

Figure 4.15
Survival of T-47D-P cells irradiated with single acute doses of ^{60}Co γ-rays. All the cells, including the controls, had been given the same priming treatment (0.3 Gy at 0.3 Gy/h). The curves represent a fit by the LQ model (solid line) to pooled survival data (T1-T24) from unprimed cells, and a fit by the IR model (dashed line) to survival data measured by Edin [personal communication] using unprimed T-47D cells and the same radiation quality. The data points represent single observations of two experiments (P3 and P4). Standard errors are shown by error bars.

As part of her thesis, Fenne [2008] had performed three experiments on T-47D cells that were thawed 19 – 26 days earlier, which proved to be too soon. Those experiments were excluded from the study because the cells seemed to be more sensitive than normal, with low surviving fractions for all doses. Since experiments P3 and P4 of the present study were performed only 28 days after thawing and showed a similar pattern of reduced survival, it was decided to exclude them from the calculation of mean values. Besides, these two experiments would have influenced the data points in figure 4.13 relatively little, and a plot of mean values based on data from all seven T-47D-P experiments is given at the end of appendix A. However, the surviving fractions in the region 0.75 – 2 Gy was not as low as in the experiments performed by Fenne, and the plating efficiencies were normal. Consequently, a total exclusion of the data from the study could not be justified, and they are therefore presented here, although it is difficult to evaluate the reliability of these results.

4.2.3 Follow-up Experiments with Temperature Maintained at 37°C

Some cells taken from the culture that had been grown continuously since priming in August 2005 had been sent to Aalborg University. These were returned to our laboratory, where they were thawed on April 11th, 2008. Three experiments were performed on these cells 9 – 11 weeks later. During irradiation the temperature was maintained at 37°C (setup C), and medium was not changed during colony growth. From figure 4.16 it is clear that the measured survival is very well fitted by the LQ curve.

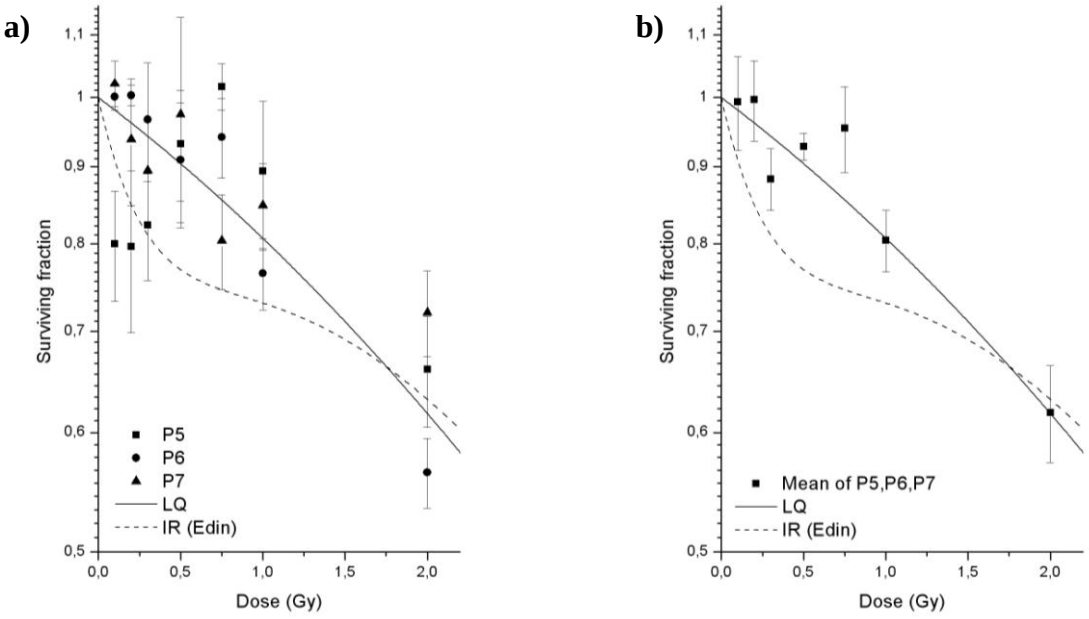

Figure 4.16
Survival of T-47D-P cells irradiated with single acute doses of ^{60}Co γ-rays. All the cells, including the controls, had been given the same priming treatment (0.3 Gy at 0.3 Gy/h). The curves represent a fit by the LQ model (solid line) to pooled survival data (T1-T24) from unprimed cells, and a fit by the IR model (dashed line) to survival data measured by Edin [personal communication] using unprimed T-47D cells and the same radiation quality. a) Data points represent single observations of three independent experiments (P5, P6 and P7). b) Data points represent mean values of the three experiments. Standard errors are shown by error bars.

Thus three series of experiments with T-47D-P cells showed three different patterns of survival in the low-dose region; higher than predicted by the LQ curve (P1 and P2), lower than predicted by the LQ curve (P3 and P4), and finally in accordance with the LQ curve (P5 – P7). It is hard to decide whether these differences are merely a consequence of statistical fluctuations and uncertainties, or whether they reflect actual effects caused by different experimental setups. These issues will be addressed further in the discussion (Ch. 5.7.1).

4.3 Acute Irradiation of Cells Primed by Incorporation of Tritium-Labeled Valine

The original intent of this thesis was to investigate whether priming doses administered at ultra-low dose rates could remove low-dose hyper-radiosensitivity in T-47D cells, and try to identify possible thresholds in dose and dose rate for the occurrence of this effect. Since it proved difficult to identify an HRS/IRR-response pattern in the unprimed cells there was no basis for such investigations. By the time it was clear that the unprimed cells consistently failed to show HRS some preliminary experiments with priming at very low dose rates had already been performed, and they are presented in this section.

The priming dose was given by continuous β-irradiation from the decay of tritium nuclides incorporated into cellular protein. As described in chapter 3.3.3, this was accomplished by growing cells in medium supplemented with tritium-labeled valine. During the first 100 hours of incorporation there was a non-linear increase in the dose rate, but when steady-state conditions were reached, the dose rate to the nucleus has been found to be (0.015 ± 0.004) Gy/h [Bjørhovde, 2006; Pettersen et al., 2007]. Four experiments (H1-H4) were performed with challenge irradiation of tritium-primed cells, and the priming doses that were given are shown in table 4.4.

The cells used in the first experiment had been given an accumulated priming dose of (65 ± 17) Gy over 26 weeks. The survival data are plotted in figure 4.17. The LQ curve seems to represent a good fit, but the data are of course too sparse to conclude anything. However, this experiment clearly showed, in agreement with previous reports [Bjørhovde, 2006; Pettersen et al., 2007], that T-47D cells are able to continue growth seemingly indefinitely at this dose rate.

The three other experiments were performed after much shorter exposure times (see table 4.4). From the resulting surviving fractions, plotted in figure 4.18, it seems clear that no HRS is observed. For experiments H2 and H4 the surviving fractions at the lowest doses are quite consistently greater than 1. Again the data are too sparse to conclude whether this might be a manifestation of a similar elevated survival as observed by Edin et al. [2007; 2008c; 2008b] and Fenne [2008] for T-47D-P cells, or whether it is merely a result of statistical fluctuations. Experiment H3 resulted in low-dose survival more in accordance with the LQ curve.

Experiment	Priming dose (Gy)	Exposure time
H1	65 ± 17	26 weeks
H2	0.3 ± 0.1	48 hours
H3	0.9 ± 0.2	96 hours
H4	2.0 ± 0.5	1 week (168 hours)

Table 4.4: Absorbed dose to the nuclei of cells primed by incorporation of tritium-labeled valine
Four experiments were performed with acute challenge irradiation of tritium-primed cells. The calculation of priming doses are outlined in appendix G and are based on measurements by Bjørhovde [2006]. The exposure time corresponds to the time the cells had been grown in medium supplemented with tritium-labeled valine. The cells were plated in normal medium 17-18 hours before challenge irradiation.

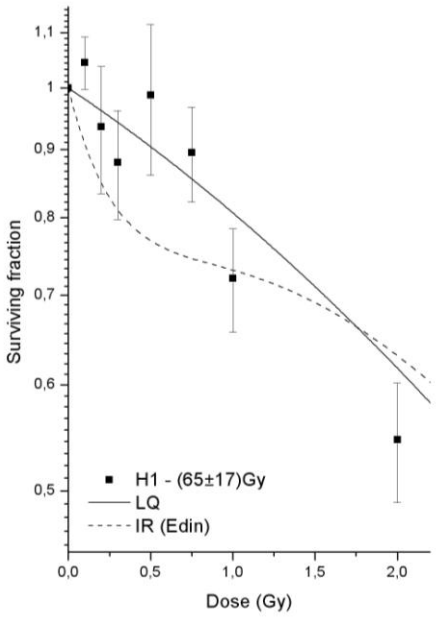

Figure 4.17
Survival of T-47D cells primed by incorporation of tritium-labeled valine and challenge-irradiated with single acute doses of ^{60}Co γ-rays. All the cells, including the controls, had been given the same priming dose, (65 ± 17) Gy. The curves represent a fit by the LQ model (solid line) to pooled survival data (T1-T24) from unprimed cells, and a fit by the IR model (dashed line) to survival data measured by Edin [personal communication] using unprimed T-47D cells and the same radiation quality. The data points represent surviving fractions measured in a single experiment (H1). Standard errors are shown by error bars.

Note that the survival of tritium-primed cells after acute challenge irradiation now has been compared to curve fits obtained from irradiation of unprimed cells grown under normal conditions. However, since the tritium-primed cells were grown in medium with an unusually high concentration of unlabeled ("cold") valine (1mM, see Ch. 3.3.3), the proper unprimed control cells should have been grown in medium with identical high concentration of "cold" valine. The studies involving tritium incorporation were stopped before such control experiments were performed.

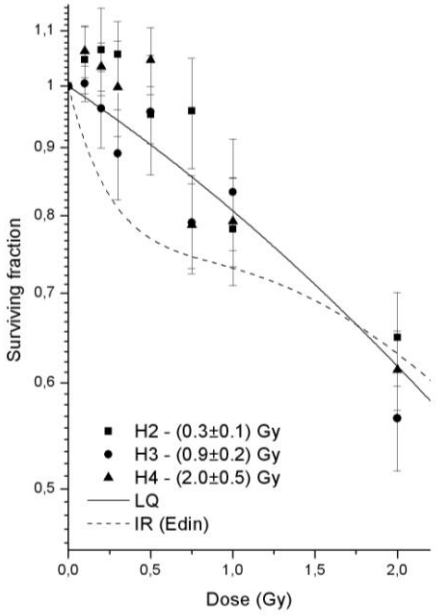

Figure 4.18
Survival of T-47D cells primed by incorporation of tritium-labeled valine and challenge-irradiated with single acute doses of ^{60}Co γ-rays. In each experiment, all the cells, including the controls, had been given the same priming dose, see table 4.4. The curves represent a fit by the LQ model (solid line) to pooled survival data (T1-T24) from unprimed cells, and a fit by the IR model (dashed line) to survival data measured by Edin [personal communication] using unprimed T-47D cells and the same radiation quality. The data points represent single observations of three experiments (H2, H3 and H4). Standard errors are shown by error bars.

4.4 Selection of G_1-phase T-47D-P cells

In studies by Edin et al. [2007; 2008c; 2008b] and Fenne [2008] the surviving fractions of T-47D-P cells for doses up to ~0.3 Gy tended to exceed 1. The initial dose-response measurements of the present study (P1 and P2, see Ch. 4.2.1) corresponded well with these observations. Later cell-survival experiments indicated a response more in accordance with a linear-quadratic description, but at that point investigations had already been started to elucidate the mechanisms behind the elevated low-dose survival.

The average plating efficiency of control flasks in the seven experiments performed on asynchronous T-47D-P cells was (79 ± 10)%. Thus approximately 20% of the plated cells will not give rise to a viable colony. This can partly be accounted for by the fact that some of the cells will be in the resting phase G_0 (see Ch. 2.1.1) when plated. It was hypothesized that more G_0-phase cells were recruited into the cell cycle among cells given a small radiation dose than among controls. Furthermore, the cells had to be stimulated out of G_0 almost immediately after irradiation, since no single-cells (except for cells migrating out of colonies) had been observed to start dividing several days after plating in the time-lapse films recorded by Fenne [2008]. The following method was applied to investigate this theory (see Ch. 3.6): first two populations of G_0/G_1-phase cells were collected by fluorescence-activated cell sorting, one of these was irradiated with 0.2 Gy and the other served as controls, before the cells were allowed to progress through the cell cycle for various amounts of time. Finally, the cell-cycle distributions of both populations were determined by means of flow cytometry. If it would turn out that significantly fewer cells remained in G_0/G_1 in the irradiated cell population, the hypothesis would be strengthened.

Three experiments were performed. Naturally, the timing was crucial in these experiments. If the cells were incubated for too long, it could result in some cells finishing mitosis and returning to G_1, while if the cells were stopped prematurely, many progressing cells would still not have left the G_1 phase. Consequently, several different times had to be investigated. In the first experiment, the cells were allowed to progress for 23 hours and 24 hours. The resulting cell-cycle distributions are given in table 4.5, and the measured DNA histograms are printed in appendix C. Note that both the control sample and the irradiated sample consisted of two individual measurements (A and B) for each incubation time.

May 8, 2008	**23 hours**				**24 hours**			
	Control		**Irradiated**		**Control**		**Irradiated**	
	A (%)	B (%)	A (%)	B (%)	A (%)	B (%)	A (%)	B (%)
G_0 / G_1	15.2	17.6	18.9	16.3	20.4	19.5	19.3	17.3
S	36.7	34.7	38.6	46.4	28.7	28.7	32.5	30.1
G_2 / M	48.1	47.7	42.5	37.3	50.9	51.8	48.2	52.7

Table 4.5: Cell-cycle distributions for sorted cells after 23 and 24 hours of incubation
G_1-phase cells were collected and incubated for 23 and 24 hours after plating, before cell-cycle distributions were measured with flow cytometry. DNA histograms were analyzed in ModFit. The irradiated cells had been given a 0.2 Gy acute dose of ^{60}Co γ-rays 15 minutes after plating.

The progression of cells through the cell cycle from 23 hours to 24 hours after plating is illustrated in figure 4.19 a). In this figure the average G_0/G_1 and G_2/M fractions at the two times are plotted (the S fractions were omitted for clarity, but can of course be deduced from the two other fractions). The spread in the two individual measurements of each sample are reflected by error bars. The figure clearly shows that the G_0/G_1 fractions at both times were almost identical for the two cell populations (irradiated and control), thus no indication of radiation-induced stimulation out of G_0 was seen at these times. The percentage of cells in G_0/G_1 also increased slightly from 23 to 24 hours, indicating that some cells were dividing already. It also appears that the irradiated cells were progressing through the cell cycle at a somewhat slower rate than the controls, since the fraction of cells in G_2/M after 23 hours was lowest for the irradiated population.

When interpreting these numbers it is important to be aware that the calculated fractions of cells in S and G_2/M are less reliable than the corresponding G_0/G_1 percentages. The reason for this is the problems ModFit had in analyzing the peculiar DNA histograms (as described in Ch. 3.6.3). A range surrounding the G_2/M peak had to be assigned as an input in this software, and in many cases the results of the calculations were very sensitive to small changes in this range. However, the G_0/G_1 peaks were always easy to identify, and ModFit gave quite consistent estimates of the G_0/G_1 fractions. These considerations apply to all three experiments.

When the cells were sorted and plated, they would experience a lag period before they continued their progression through the cell cycle. The length of this lag period was not known. Consequently, even though we knew that the doubling time of T-47D-P cells is probably around 25-30 hours (see Ch. 3.1), it was hard to know when the first cells would reach the end of the cycle and divide. Since the G_0/G_1 fractions increased slightly from 23 to 24 hours, it was decided to incubate the cells for a shorter time in the next experiment. Cell-cycle distributions were therefore determined 15 and 17 hours after plating in the second experiment (see table 4.6). Figure 4.19 b) displays how the G_0/G_1 and G_2/M fractions changed in this two-hour time span.

As in the first experiment, the irradiated cells seemed to reach the G_2 phase later than the control cells. This might reflect a delayed exit from the G_1 phase, since the fraction of G_0/G_1 cells after 15 hours were considerably higher in the irradiated cell population.

May 26, 2008	**15 hours**				**17 hours**			
	Control		**Irradiated**		**Control**		**Irradiated**	
	A (%)	B (%)	A (%)	B (%)	A (%)	B (%)	A (%)	B (%)
G_0 / G_1	42.7	43.7	49.6	47.6	27.1	24.7	22.3	30.9
S	44.7	44.6	44.2	43.2	54.3	47.1	52.6	52.4
G_2 / M	12.7	11.7	6.3	9.2	18.6	28.2	25.0	16.7

Table 4.6: Cell-cycle distributions for sorted cells after 15 and 17 hours of incubation
G_1-phase cells were collected and incubated for 15 and 17 hours after plating, before cell-cycle distributions were measured with flow cytometry. DNA histograms were analyzed in ModFit. The irradiated cells had been given a 0.2 Gy acute dose of ^{60}Co γ-rays 15 minutes after plating.

Although the data sets were confined to only two measurements each, one-sided Student's *t*-tests were performed on the G_0/G_1 fractions to check for statistical significance (see table 4.8). The null hypothesis was that the percentage of control cells in $G_0/G_1 \geq$ the percentage of irradiated cells in G_0/G_1. The tests showed that the G_0/G_1 fraction in fact was significantly higher ($P = 0.021$) in the irradiated cell population after 15 hours, but not after 17 hours ($P = 0.44$). Thus instead of finding evidence for a stimulation of G_0-phase cells into the cell cycle, a possible cell-cycle arrest was observed

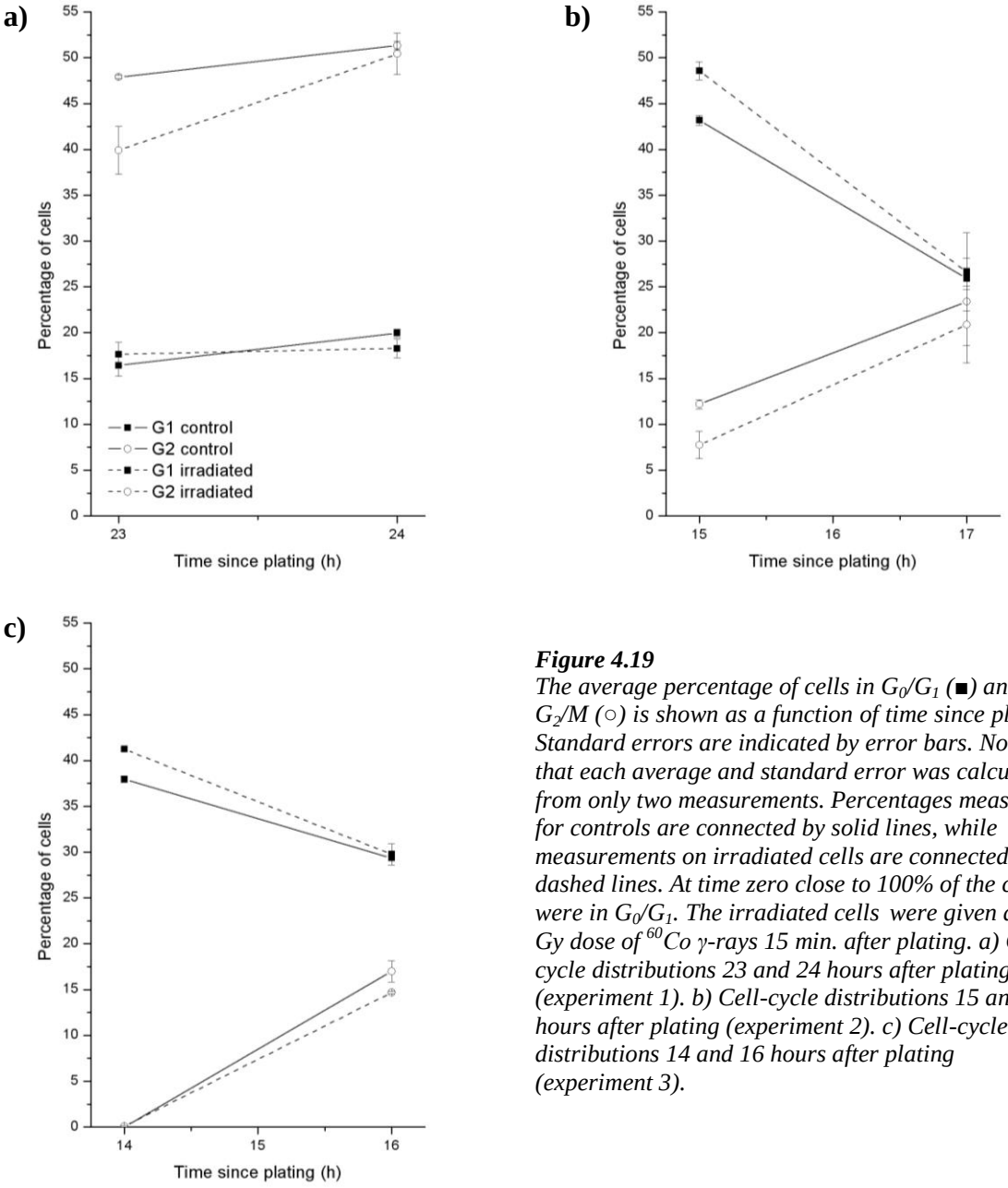

Figure 4.19
The average percentage of cells in G_0/G_1 (■) and G_2/M (○) is shown as a function of time since plating. Standard errors are indicated by error bars. Note that each average and standard error was calculated from only two measurements. Percentages measured for controls are connected by solid lines, while measurements on irradiated cells are connected by dashed lines. At time zero close to 100% of the cells were in G_0/G_1. The irradiated cells were given a 0.2 Gy dose of ^{60}Co γ-rays 15 min. after plating. a) Cell-cycle distributions 23 and 24 hours after plating (experiment 1). b) Cell-cycle distributions 15 and 17 hours after plating (experiment 2). c) Cell-cycle distributions 14 and 16 hours after plating (experiment 3).

June 16, 2008	14 hours				16 hours			
	Control		Irradiated		Control		Irradiated	
	A (%)	B (%)	A (%)	B (%)	A (%)	B (%)	A (%)	B (%)
G_0 / G_1	37.6	38.3	41.1	41.4	29.6	29.1	30.9	28.6
S	62.4	61.7	58.9	58.4	52.3	55.0	54.3	56.8
G_2 / M	0	0	0	0.2	18.1	15.8	14.8	14.6

Table 4.7: Cell-cycle distributions for sorted cells after 14 and 16 hours of incubation
G_1-phase cells were collected and incubated for 14 and 16 hours after plating, before cell-cycle distributions were measured with flow cytometry. DNA histograms were analyzed in ModFit. The irradiated cells had been given a 0.2 Gy acute dose of ^{60}Co γ-rays 15 minutes after plating.

in the G_1 phase. This was somewhat surprising, considering that the given radiation dose was as low as 0.2 Gy, and that T-47D cells lack functional p53 (see Ch. 3.1).

In the third experiment the possible G_1-phase cell-cycle arrest was investigated further by measuring cell-cycle distributions after 14 and 16 hours (see table 4.7). The pattern of cell-cycle progression resembled the observations in the previous experiment (see figure 4.19 c)). After 14 hours the G_0/G_1 fraction was again significantly greater (*$P = 0.0065$*) for the irradiated cells, but this difference had disappeared after 16 hours (*$P = 0.38$*). However, the G_1 arrest seemed to be reflected in a delayed entry into G_2 after 16 hours. No visible G_2 peak could be identified after 14 hours.

The results of the last two experiments also illustrate another important issue concerning selection of cells of a specific phase, and in particular the G_1 phase. It is seen that the average percentage of cells in G_0/G_1 is higher after 15 hours than after 14 hours. There are two important reasons for this contradiction. First, by selecting a population of G_1 cells, one does not obtain a synchronized cell population. The G_1 phase is the longest of the cell-cycle phases in T-47D cells [Stokke et al., 1993], and cells in either early or late G_1 phase will accordingly be at two completely different stages of the cell cycle, despite being in the same phase. It is evident from the present results that cell populations sorted during the same experiment, and thus taken from cell flasks that were grown in parallel and given exactly the same treatment, will progress at more or less the same rate (since the spread between the individual measurements A and B was relatively small). However, G_1-cell populations sorted in different experiments will not be identical. A second important factor contributing to discrepancies is the time required for sorting, which varied from 2.5 hours to 4 hours (4 million cells were needed. When 2 million cells were collected, these were plated, while the additional cells were being sorted). During this time the sample tubes were kept in a mixture of ice and water to prevent the Hoechst 33342 dye from being transported out of the cells. The combination of Hoechst 33342 staining and low temperature is quite harmful for cells [Durand and Olive, 1982], and induction of stress responses might of course obscure the experimental results.

Time since plating	*P* values from one-sided Student's *t*-tests
14 hours	0.0065
15 hours	0.021
16 hours	0.38
17 hours	0.44
23 hours	0.28
24 hours	0.86

Table 4.8: Results of hypothesis testing on G_0/G_1 fractions
The null hypothesis was that the percentage of control cells in $G_0/G_1 \geq$ the percentage of irradiated cells in G_0/G_1. At the 5% level the fraction of irradiated cells in G_0/G_1 was significantly greater than the fraction of control cells in G_0/G_1 after 14 and 15 hours.

4.5 Acute Irradiation of G_2-Enriched Cell Populations

It is now commonly assumed that HRS is associated with a ~0.3-Gy activation threshold of the so-called "early" G_2 checkpoint, which allows time for repair in irradiated G_2-phase cells (see Ch. 2.4.4). Consequently, exaggerated HRS/IRR responses would be expected when irradiating G_2-enriched cell populations, and such exaggerated responses have also been reported [Marples et al., 2003; Short et al., 2003]. As shown in chapter 4.1 it proved difficult to detect any low-dose hyper-radiosensitivity in the asynchronous T-47D cells. For this reason it was decided to look for HRS in G_2-enriched populations of such cells. For comparison, similar experiments were performed on T-47D-P cells.

Cells were sorted by means of fluorescence-activated cell sorting using the relatively non-toxic staining agent Hoechst 33342 (see Ch. 2.5.2 and Ch.3.5). Three methods were applied to obtain the G_2-enriched populations: 1) The cells were selected in G_1 and irradiated when it was believed that the fraction of cells that had entered G_2 was greatest. 2) Cells from early S phase were sorted, thereby giving rise to a synchronized cell population. When the cells were assumed to have reached G_2 they were irradiated. 3) G_2-phase cells were collected directly and irradiated 15 minutes after plating.

The Hoechst-based cell sorting resulted in a somewhat reduced average plating efficiency of (52 ± 4)% after 18 experiments, and the cells also needed a few days more than normal to grow into macroscopically visible colonies.

4.5.1 Cell-Cycle Distribution in Exponentially Growing Cultures

In order to properly compare the survival in G_2-enriched cell populations with the observed survival in asynchronous cells an estimate of the cell-cycle distribution in asynchronous cultures is advantageous. During the sorting procedure cells of different phases were selected by gating on a DNA histogram (see figure 3.4). Since these DNA measurements were performed on cells that had been harvested while kept in exponential growth, the resulting histograms provided a measurement of the initial cell-cycle distribution for each experiment. Three DNA histograms were thereby measured for T-47D cells. For T-47D-P cells two additional histograms were available from the

experiments with selection of G_1-phase cells (the third histogram was not saved), giving a total of 5 measurements of the DNA content. All the DNA histograms are printed in appendix C. In table 4.9 the average percentage of cells in each cell-cycle phase is shown. The average CV (coefficient of variation – the standard deviation of a peak divided by the mean channel number of the peak) for the eight histograms was (6.5 ± 0.4)%, which coincides well with the reported resolution (CV ~6%) for use of Hoechst 33342 in flow-cytometric analysis [Durand and Olive, 1982].

Cell line	G_0/G_1	S	G_2/M
T-47D	65.6 ± 1.3	22.2 ± 0.3	12.2 ± 1.0
T-47D-P	51.9 ± 2.2	31.3 ± 3.1	16.8 ± 1.5

Table 4.9: Cell-cycle distributions for exponentially growing T-47D and T-47D-P cells
The percentages of cells in the different cell-cycle phases were determined for asynchronous T-47D and T-47D-P cell cultures from DNA histograms measured by flow cytometry. Cell-cycle distributions from individual DNA histograms were obtained by analyses in ModFit. The numbers are given as average ± standard error calculated from respectively 3 and 5 histograms for T-47D and T-47D-P cells.

It is clear from table 4.9 that the fraction of cells in the G_1 phase is substantially lower for T-47D-P cells than for unprimed T-47D cells. As a result of this the S and G_2 fractions are markedly greater for the primed cells. Rather than an effect of the priming dose given three years earlier, this is probably an effect caused by the fact that the primed cells have been continuously grown in culture for such a long time. Proliferation rates will then in general increase as a result of the natural selection pressure for rapidly proliferating subpopulations of the cell culture. As described in chapter 3.1, the doubling time of T-47D-P cells was shorter than the doubling time of unprimed cells (this was not the case, though, for the first batch of T-47D cells used, which had been grown for more than a year). Population-doubling times for sublines of T-47D cells after revival from cryostorage have been reported to decrease substantially before they reached more stable levels after 16-32 weeks of passage [Reddel et al., 1988].

The difference among mammalian cell-cycle times in different circumstances is primarily caused by variation in the length of the G_1 period [Hall and Giaccia, 2006, p. 50]. Thus, it is natural to assume that the observed difference in doubling times between the primed and unprimed T-47D cells reflect a difference in the duration of the G_1 phase (this notion is also supported by experiments that will be presented in chapter 4.5.3). If the length of the G_1 period is shortened, while the lengths of the S and G_2 phases remain the same, the consequence will be a reduction in the fraction of G_1 cells. This might, at least partly, explain the observed variations between cell-cycle distributions of T-47D and T-47D-P cells.

4.5.2 Dose Response of the G_2-Enriched Populations Obtained by Selection of G_1-Phase Cells

From the first experiment with selection of G_1-phase T-47D-P cells it seemed that a high fraction (~50%) of the cells would be in G_2 24 hours after plating (see table 4.5), and on this basis it was decided to incubate the T-47D-P cells for 24 hours before commencing

irradiation. Since the unprimed cells had a longer doubling time, the time between plating and irradiation was increased to 29-30 hours for these cells. For the cells selected in G_1 the cell-cycle distributions at the time of irradiation were determined by flow cytometry. Such measurements were not performed in the S- and G_2-phase experiments, as it is more time consuming to sort cells of those phases.

The average cell-cycle distributions and multiplicities for both unprimed and primed cells are given in table 4.10. Surprisingly only (31.6 ± 1.4)% of the T-47D-P cells were in G_2 at the time of irradiation 24 hours after plating. A multiplicity of 1.096 was determined for the last experiment, which means that 9.6% of the colony-forming units (CFUs) were doublets. Some of the doublets might result from being plated in the vicinity of each other or not being separated after centrifugation, but most of them were presumably originating from cell division. So even though the majority of the cells had not yet left G_1 or S phase, almost one tenth of them had already divided. This illustrates very well that a population of G_1 cells is not a synchronized population (which was pointed out also in section 4.4), and it might partly explain why the G_2/M fraction was so much lower in these experiments than what was observed previously (see table 4.5). Differences in cell handling between the experiments, for instance how long the cell vials were kept on ice during sorting, would also contribute to the observed discrepancy. For the unprimed cells the measured G_2/M fraction was (42.0 ± 3.5)%. However, the average multiplicity was as high as 1.219 ± 0.046, indicating that approximately one out of five plated cells had divided. Consequently, the actual percentage of CFUs in G_2/M at the time of irradiation was most likely greater than 42%, as every doublet successfully separated into single-cells would count twice in the flow-cytometric analysis.

The mean surviving fractions are plotted in figure 4.20 (the surviving fractions measured in single experiments are plotted in appendix B). The dose response of unprimed T-47D cells seems to be affected very little by the high fraction of G_2 cells. In fact the LQ curve originally fitted to data from irradiation of asynchronous populations, gives an excellent fit also to the survival of the G_2-enriched populations. The dose response of the primed cells is, on the other hand, not well described by this curve, although the cells do not show any signs of low-dose hypersensitivity either. Rather the radiosensitivity appears to have increased slightly over the whole dose range examined, indicating that for T-47D-P the G_2 cells are more sensitive than the (asynchronous) population as a whole.

Experiment	Cell line	G_0 / G_1	S	G_2/M	Multiplicity
TX1-TX3	T-47D	36.3 ± 2.9	21.7 ± 1.0	42.0 ± 3.5	1.219 ± 0.046
PX1-PX3	T-47D-P	35.9 ± 2.5	32.5 ± 1.1	31.6 ± 1.4	1.096*

Table 4.10: Cell-cycle distributions and multiplicities at the time of irradiation
T-47D cells were selected in G_1 phase, plated and irradiated 29-30 hours later. T-47D-P cells were also selected in G_1 phase, but irradiated 24 hours after plating. The percentages of cells in the different cell-cycle phases at the time of irradiation were determined from DNA histograms measured by flow cytometry. Cell-cycle distributions from individual DNA histograms were obtained by analyses in ModFit. The numbers are given as average ± standard error calculated from 3 experiments.
** Multiplicity was not determined for the first two experiments (PX1-PX2).*

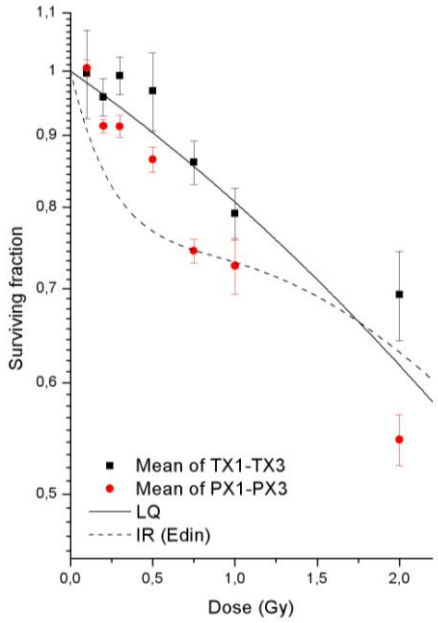

Figure 4.20
Survival of T-47D and T-47D-P cells irradiated with single acute doses of ^{60}Co γ-rays. The cells had been selected in G_1 and were irradiated 29-30 hours (T-47D) and 24 hours (T-47D-P) after plating. All T-47D-P cells, including the controls, had been given the same priming treatment (0.3 Gy at 0.3 Gy/h). The curves represent a fit by the LQ model (solid line) to pooled survival data (T1-T24) from unprimed asynchronous cells, and a fit by the IR model (dashed line) to survival data measured by Edin [personal communication] using asynchronous T-47D cells and the same radiation quality. The data points represent mean values of three experiments with T-47D cells (■) and three experiments with T-47D-P cells (●). Standard errors are shown by error bars. Note that experiments PX1 and PX2 were not corrected for multiplicity.

4.5.3 Dose Response of the G_2-Enriched Populations Obtained by Selection of S-Phase Cells

Three experiments were performed for each cell line with cells that had been selected in early S phase. Cells sorted in this way will be more or less synchronized, as the position of a cell in the DNA histogram during S phase reflects how much of its DNA that has been replicated. In the experiments with selection of G_1-phase T-47D-P cells it was demonstrated that no G_2 peak could be detected after 14 hours of incubation, but ~10-15% of the cells had reached the G_2 phase 1-2 hours later (see table 4.6 and 4.7). Thus it seemed that cells in late G_1 would need approximately 14 hours to reach G_2 (lag phase included), and it was decided to irradiate the cells that were collected in early S phase 14 hours after plating.

Multiplicities were measured in all but the first experiment (PY1). For the T-47D-P cells the average multiplicity was 1.101 ± 0.009, implying that ~10% of the cells had divided at the time of irradiation. In two of the experiments with unprimed T-47D cells (TY1 and TY3), the time between plating and irradiation was prolonged to approximately 15 hours for practical reasons. This resulted in an average multiplicity of 1.219 ± 0.036. The high increase in the fraction of divided cells indicate that a large part of the plated cells were in late G_2 or mitosis during irradiation.

Figure 4.21 displays the mean surviving fractions. Interestingly, a strong increase in the radiosensitivity is evident over the entire dose range examined. Furthermore, the survival of the unprimed T-47D cells coincides very well with the survival of the primed cells. The surviving fractions seem to decrease almost exponentially, i.e., the dose-response curve appears to be a straight line with no pronounced shoulder. For low-LET radiations

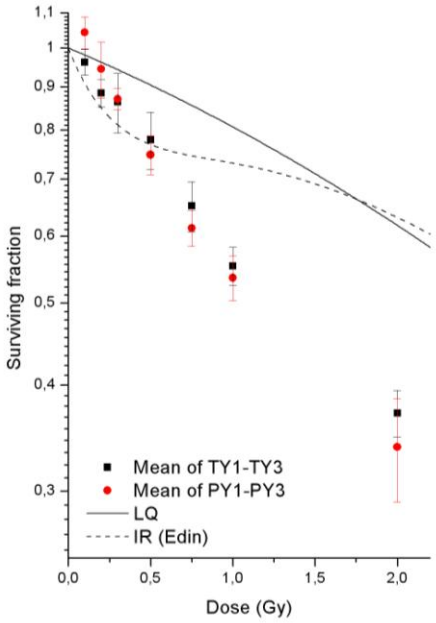

Figure 4.21
Survival of T-47D and T-47D-P cells irradiated with single acute doses of ^{60}Co γ-rays. The cells had been selected in early S phase and were irradiated 14-15 hours (T-47D) and 14 hours (T-47D-P) after plating. All T-47D-P cells, including the controls, had been given the same priming treatment (0.3 Gy at 0.3 Gy/h). The curves represent a fit by the LQ model (solid line) to pooled survival data (T1-T24) from unprimed asynchronous cells, and a fit by the IR model (dashed line) to survival data measured by Edin [personal communication] using asynchronous T-47D cells and the same radiation quality. The data points represent mean values of three experiments with T-47D cells (■) and three experiments with T-47D-P cells (●). Standard errors are shown by error bars. Note that experiment PY1 was not corrected for multiplicity.

this type of survival curve would be expected for mitotic cells (or alternatively for cells that predominantly die through apoptosis) [Hall and Giaccia, 2006, p. 37-41]. As mentioned above, it appears that a large fraction of the cells were in late G_2 or mitosis at the time of irradiation, since the multiplicities increased substantially when the time between plating and irradiation was prolonged with an hour. Mitosis is in general the most radiosensitive phase of the cell cycle [Wilson, 2004]. It is tempting to speculate whether irradiation of a cell population consisting exclusively of cells in late G_2 and mitosis, in other words cells that would attempt to divide with unrepaired radiation-induced DNA damage (similar to the G_2-cells believed to be responsible for HRS), would result in a dose-response curve with a similar initial slope as observed by Edin. Let us assume, in an attempt to explain the data presented in figure 4.21, that two cell populations were present at the time of irradiation. One population consisted of sensitive mitotic cells exhibiting purely exponential survival with slope equal to the α_s parameter measured by Edin (α_s = 1.14, see table 3.1), while the other population consisted of resistant G_2 (and G_1) cells with survival following the LQ model (α = 0.188 and β = 0.0263, see table 4.1). The fraction P of sensitive cells is not known, but can be found by curve-fitting. Thus, the survival would be described by the equation

$$S = P \cdot e^{-\alpha_s D} + (1 - P) \cdot e^{-\alpha D - \beta D^2} \qquad (4.3)$$

By fitting this two-population model with P as the only unknown parameter to the data points in figure 4.21, a very good fit was obtained (χ^2/ν = 1.01). The value of P was found to be 0.494 ± 0.024. The curve-fitting was performed in Origin (using the same algorithm as in Ch. 4.1), and the resulting dose-response curve is plotted together with the observed surviving fractions in figure 4.22.

Naturally, the obtained value of the mitotic fraction P should be interpreted as nothing but a vague estimate, as the assumptions of the two-population model were merely speculations. Besides, the fact that 10-20% of the irradiated colony-forming units were doublets consisting of two G_1 cells complicates the analysis further, although multiplicity corrections were performed. However, the goodness-of-fit suggests that the basic assumption, i.e., the coexistence of one sensitive and one resistant population during irradiation, might be correct. Especially interesting in this regard are the surviving fractions at 2 Gy. When a simple exponential function (i.e., only the first addend in eq. (4.3)) was fitted to the data (not shown), the data points at 2 Gy both lay above the curve. This indicates a slope that is decreasing with dose, which again is indicative of a resistant subpopulation. Thus, it seems plausible that the large increase in radiosensitivity observed in these experiments was caused by a significant proportion of mitotic cells, and the data do therefore not contradict the possibility of G_2 being a relatively radioresistant phase for T-47D cells.

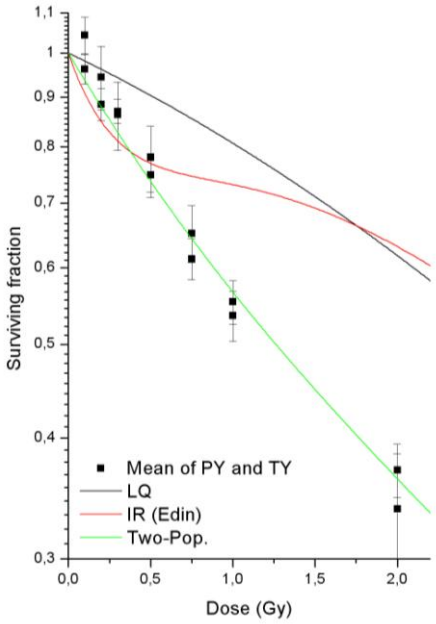

Figure 4.22
Surviving fractions of cells that had been selected in early S phase and were irradiated acutely by ^{60}Co γ-rays 14-15 hours (T-47D) and 14 hours (T-47D-P) after plating were fitted by a two-population model, given by equation (4.3). The data points are the same as in figure 4.21. See the text and figure 4.21 for further details.

The observed multiplicities and the similarities in survival for primed and unprimed cells also indicate that the unprimed cells, despite their longer doubling time, traversed through the S and G_2 phases at the same rate as the T-47D-P cells. Consequently, the difference in doubling time seems to reflect a difference in the length of the G_1 period, as expected.

4.5.4 Dose Response of the G_2-Enriched Populations Obtained by Selection of G_2-Phase Cells

Naturally, G_2-phase cells were also sorted directly and irradiated shortly after plating. The advantage of this procedure was that a high fraction of the cells were guaranteed to be in G_2 at the time of irradiation. The disadvantage was that the cells were irradiated just 15 minutes after plating, i.e., before they had attached to the flask surface and while they

were still in lag phase. Because the time between plating and irradiation was too short for the cells to divide, multiplicity was not measured in these experiments.

The mean surviving fractions are shown in figure 4.23. The radiosensitivity of the unprimed cells is again quite similar to the observed survival of asynchronous cells, and it is not possible to discern any presence of HRS. For the T-47D-P cells the surviving fractions generally tend to lie lower than the LQ curve. It could perhaps be argued that the lowest doses show a weak HRS-like response, but considering the low surviving fractions at 1 Gy and 2 Gy it seems more likely that the dose response follows a linear-quadratic description, and that the radiosensitivity of the G_2 cells is slightly greater than the sensitivity of asynchronous T-47D-P cells. Thus the results correspond well with the findings from the experiments with G_2-enriched populations that were presented in chapter 4.5.2.

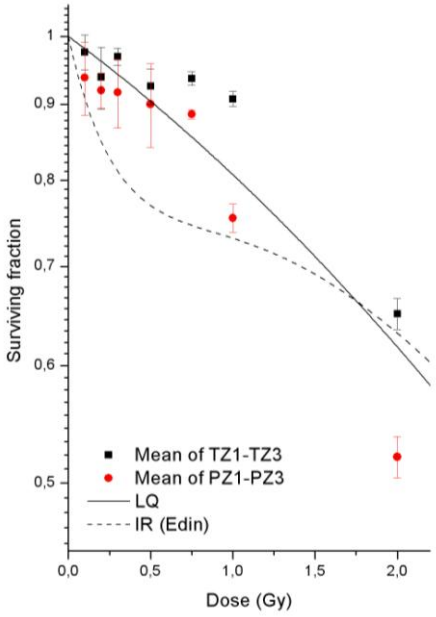

Figure 4.23
Survival of T-47D and T-47D-P cells irradiated with single acute doses of ^{60}Co γ-rays. The cells had been selected in G_2 phase and were irradiated 15 minutes after plating. All T-47D-P cells, including the controls, had been given the same priming treatment (0.3 Gy at 0.3 Gy/h). The curves represent a fit by the LQ model (solid line) to pooled survival data (T1-T24) from unprimed asynchronous cells, and a fit by the IR model (dashed line) to survival data measured by Edin [personal communication] using asynchronous T-47D cells and the same radiation quality. The data points represent mean values of three experiments with T-47D cells (■) and three experiments with T-47D-P cells (●). Standard errors are shown by error bars.

Studies of repair of potentially lethal damage (PLD) have shown that cell survival is enhanced considerably if the cells are allowed to remain in density-inhibited stationary-phase cell cultures for 6 or 12 hours after irradiation, before being subcultured and tested for clonogenicity [Hall and Giaccia, 2006, p. 66-67]. In general the fraction of cells surviving a given radiation dose will be enhanced as a result of PLD repair if postirradiation conditions are suboptimal for growth. Consequently, when cells are irradiated in the lag period immediately after sorting and plating, as was done for the pure G_2 populations in this study, there is a risk that the true surviving fractions of progressing G_2 cells are obscured by PLD repair. It is difficult to assess whether this was the case for the data presented here. It strengthens the reliability of the results that the same survival features (i.e., survival in accordance with the LQ fit to asynchronous cell data for T-47D cells and an increased radiosensitivity in G_2 for T-47D-P cells) were observed when irradiating G_2 cells shortly after plating and when irradiating G_2-enriched populations

many hours after plating. However, the high surviving fractions observed for T-47D cells with more than 90% survival even at a dose of 1 Gy might indicate that low levels of damage have been repaired to a larger extent than in progressing cells. Also, the G_2 fraction among the T-47D-P cells that were irradiated after 24 hours was relatively modest, (31.6 ± 1.4)%, but still resulted in a clear increase in radiosensitivity. On this basis, perhaps an even higher radiosensitivity should have been expected for the pure G_2-cell population.

4.6 Cell-Cycle Distribution 18 Hours after Trypsinization

The cell-cycle distributions of exponentially growing T-47D and T-47D-P cultures were estimated from DNA histograms that were acquired from the cell sorting procedures, as previously described (see Ch. 4.5.1). However, these estimates do not account for the effects of trypsinization. It has been shown that trypsinization entails considerable perturbations of cell-cycle distributions in T-47D cells. Edin et al. [2007] measured the cell-cycle distributions 6 and 24 hours after trypsinization in cells that had been sham-irradiated, irradiated with 0.3 Gy at high dose rate and irradiated with 0.3 Gy at 0.3 Gy/h. The same trend was observed in all three cases: after 6 hours the G_1 fraction had risen to ~75%, while it had decreased to a level that was lower than the starting point, typically ~60%, after 24 hours. Accordingly the fractions of cells in the S and G_2 phases were slightly increased 24 hours after trypsinization.

Since the expression of HRS is ascribed to ineffective arrest of cells that are irradiated in late S or G_2 phase (see Ch. 2.4.4), it was hypothesized that the absence of HRS response in the experiments with asynchronous T-47D cells could be caused by a diminished fraction of G_2 cells at the time of irradiation. This could be an effect of trypsinization or other aspects of the cell handling during plating. To test this hypothesis exponentially growing cell cultures were trypsinized, a single-cell suspension was prepared and the cells were plated. Finally the cell-cycle distribution was measured by flow cytometry 18 hours after trypsinization. Cell-cycle analysis was performed after 18 hours because the average time between trypsinization and irradiation in 24 experiments with asynchronous T-47D cells (experiment T1-T24) was found to be (17.8 ± 0.3) hours. The average cell-cycle distribution as determined from three experiments is given in table 4.11. The measured DNA histograms are printed in appendix C. The average CV was (5.7 ± 0.5)%.

G_0 / G_1	S	G_2/M
61.2 ± 1.2	24.7 ± 1.2	14.0 ± 0.5

Table 4.11: Cell-cycle distribution in T-47D cells 18 hours after trypsinization
The percentages of cells in the different cell-cycle phases 18 hours after trypsinization were determined from DNA histograms measured by flow cytometry. Cell-cycle distributions from individual DNA histograms were obtained by analyses in ModFit. The numbers are given as average ± standard error calculated from 3 experiments.

When compared to the cell-cycle distribution at the time of trypsinization, which is given in table 4.9, a slight decrease in the G_1 fraction accompanied by small increases in the fractions of cells in the S and G_2 phases were observed after 18 hours. This is consistent with the results of Edin et al. [2007]. Thus it is clear that the missing HRS expression in the acutely irradiated T-47D cells was not caused by a diminished fraction of G_2 cells. This result also supports the findings of the previous section (4.5), where no low-dose hypersensitivity was observed in G_2-enriched cell populations.

5 Discussion

5.1 Dose Response of Asynchronous T-47D Cells

The LQ model (equation (2.10)) was fitted to pooled survival data (experiments T1-T24) from asynchronous unprimed T-47D cells in chapter 4.1 (see fig. 4.1), with excellent goodness-of-fit (χ^2/ν = 0.941 obtained by Origin). Although the IR model (equation (2.11)), which was designed to adequately describe low-dose survival in the presence of HRS/IRR, also could be applied to get a good fit, the introduction of two additional parameters was not needed to describe the data, as illustrated by a slight increase in the value of the reduced chi-squared (χ^2/ν = 0.985).

The radiosensitivity of T-47D cells has been extensively studied and is well characterized. Curve-fitting parameters obtained in a number of studies are summarized in table 5.1, and some of the dose-response curves are plotted together in figure 5.1. All the dose-response measurements summarized in table 5.1 were performed on asynchronous T-47D cells, but there are still relatively large differences in the measured survival between the studies. When comparing the results of different studies it is important to keep in mind, however, that a multitude of factors can influence the cellular response. The radiation quality is one of these factors, and especially LET differences between X-rays and ^{60}Co γ-rays are important for the low-dose response [Edin et al., 2008a]. Both X- and γ-rays are, however, relatively sparsely ionizing, and since no other types of radiation were used in these studies the differences in radiation modalities should not alone account for the observed variation in survival. The dose-rate effect, which was described previously (see Ch. 2.3.4), is another factor that has an impact on radiation response. The dose rates applied in the listed studies varied by a factor of ~5-6, but can all be considered as acute irradiations, and the influence of dose rate on the observed differences should be small. Note that the dose rates used in the present study varied by almost a factor of two. We could not observe any sparing effect in the low-dose range of reducing the dose rate from 1.3 to 0.7 Gy/min, and although a minor effect can not be excluded, it was decided to include all the data when performing the curve-fitting. All the high-dose irradiations were performed at 0.7 Gy/min.

Cell-cycle distribution is also important for the estimated values of the α and β parameters, as the measured dose response for an exponentially growing cell population will be a conjunction of responses of subpopulations at different stages of the cell cycle, with different intrinsic radiosensitivities (see Ch. 2.3.4). Thus the most reliable parameter estimates would be obtained using synchronized populations. Finally, survival curve responses will depend on more subtle differences in the experimental conditions, such as temperature, pH, the quality of serum, cell cultivation routines and other aspects of the experimental setup.

The survival curve obtained in the present study is seen to be in good agreement with the results of previous studies (see fig. 5.1). It is clear that except for the discrepancies in the low-dose region, the observed radiation response is quite consistent with the response measured by Edin et al. [2008b; 2008a]. Also the curve-fit by Christiansen [2005] obtained by irradiating T-47D cells with 220 kV_p X-rays at room-temperature

corresponds quite well with the results presented in this thesis. Note, however, that the dosimetry in Christiansen's study might have been incorrect [Edin, personal communication]. The high-dose radiosensitivity as observed in the present study is slightly greater than measured by Edin et al., but compared to the other studies, the cells rather appear to have been more resistant at the higher doses.

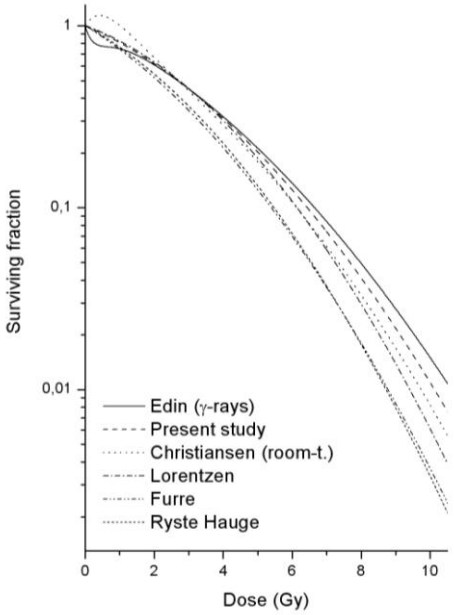

Figure 5.1
Comparison of survival curves obtained by acute irradiation of T-47D cells. The dose rates and radiation qualities used in the different studies are given in table 5.1. The sequence of studies in the figure legend corresponds to the sequence of surviving fractions at 10 Gy, starting from the highest survival.

The value of α/β has, as described in chapter 2.3.3, been shown to characterize early- and late-responding tissues, and is therefore a parameter of clinical importance. It is commonly used to predict the clinical response of fractionated radiotherapy [Hall and Giaccia, 2006, Ch. 22]. In the studies listed in table 5.1, the value of α/β range from 4.6 to 9.3 Gy, and for the present study it was calculated to be (7.1 ± 0.7) Gy (using the Origin-values given in table 4.1). Again the agreement with previous reports is very good, but a value of ~7 Gy is rather low for tumor tissue. Typically tumors have an α/β ratio of around ~10 Gy, although large variations have been detected [Peacock et al., 1992]. It has also been shown that the α/β ratio is dependent on the dose ranges used to obtain the fitted α and β values [Garcia et al., 2007]. Including data from the low-dose range has a significant influence on the determination of these parameters, and is often found to decrease the overall goodness-of-fit. This could be caused by effects at low doses that are not well described by the LQ model, such as a strong linear rather than quadratic component, hypersensitivity and adaptive responses. For three cell lines (a human glioblastoma and two prostate carcinoma lines) examined by Garcia et al. [2007], the value of α/β increased when the low-dose range was omitted (the opposite was true for Chinese hamster cells). In accordance with these reports, an α/β ratio of (8.8 ± 1.3) Gy was found for the T-47D cells in the present study when all data points lower than and including 1 Gy were excluded (curve-fitting details given in table 5.2). This value is also more in line with the value found by Furre et al. [2003], who did not include more than two measurements below 5 Gy.

	Radiation quality	(Gy/ min)	α^* (Gy^{-1})	α_s (Gy^{-1})	d_c (Gy)	β (Gy^{-2})	SF_{10}	α^*/β (Gy)
Ryste Hauge [2000]	220 kV_p X-rays	0.9	0.24± 0.02			0.033± 0.006	0.0033	7.3±1.3
Lorentzen [2001]	80 kV_p X-rays	1.7	0.16± 0.04			0.035± 0.005	0.0061	4.6±1.3
Furre [2003]	5 MV_p linear accelerator	4	0.27± 0.06			0.029± 0.005	0.0037	9.3±2.6
Christiansen [2005]	220 kV_p X-rays (37°C)	0.5	0.29± 0.003	0.24± 0.05	0.35± 0.26	0.049± 0.0004	0.0004	5.9±0.1
Christiansen [2005]	220 kV_p X-rays (room-temp.)	0.5	0.21± 0.01	-0.72± 0.14	0.74± 0.10	0.027± 0.001	0.0082	7.8±0.5
Edin [2008a]	^{60}Co γ-rays	0.7	0.20± 0.01	1.55± 0.20	0.34± 0.04	0.022± 0.002	0.015	9.1±0.9
Edin [2008a]	220 kV_p X-rays	0.5	0.18± 0.02	1.45± 0.41	0.20± 0.06	0.024± 0.001	0.015	7.5±0.9
Present study	^{60}Co γ-rays	0.7-1.3	0.19± 0.01			0.026± 0.002	0.011	7.1±0.7

Table 5.1: Curve-fitting parameters from several studies, obtained by fitting the LQ or IR model to survival data from T-47D cells

All the studies listed in this table were performed on asynchronous cell populations. SF_{10} is the surviving fraction at 10 Gy, calculated using the listed parameter values with equation (2.10) and (2.11).

**When IR parameter values are listed, the LQ parameter α has been replaced by α_r, which was also used for calculating the α/β ratio.*

Program	α (Gy^{-1})	β (Gy^{-2})	χ^2/ν
Origin	0.209 ± 0.021	0.0238 ± 0.0028	0.279

Table 5.2: Parameter values obtained by fitting the LQ model to high-dose data

The LQ model was fitted to the mean surviving fractions at 2, 5, 7.5 and 10 Gy in Origin, using the method of least squares and weighting the errors. χ^2/ν is the reduced chi-squared value, i.e., the value of chi-squared divided by the associated number of degrees of freedom.

5.2 Low-Dose Hypersensitivity in T-47D Cells

Previous reports by Edin et al. [2003; 2007; 2008c; 2008b; 2008a] demonstrated pronounced low-dose hyper-radiosensitivity (HRS) in T-47D cells. It was also shown that a 0.3 Gy priming dose delivered by a ^{60}Co source at low dose rate (0.3 Gy/h) eliminated HRS seemingly permanently [Edin et al., 2007; 2008c; 2008b], while HRS was transiently removed by the same dose when delivered acutely [Edin et al., 2007]. HRS was also abolished in two individual experiments performed on cells that had received a priming dose of ~30 Gy administered at an ultra-low dose rate (0.01 Gy/h) over several months through the incorporation of tritium-labeled valine [Edin, 2003]. The original purpose of the present study was to examine possible dose and dose-rate thresholds for the abolition of HRS by pre-irradiation at such ultra-low dose rates.

Surprisingly, the initial control experiments with unprimed T-47D cells failed to demonstrate the presence of HRS. In a series of experiments designed to elucidate possible mechanisms causing this discrepancy, different aspects of the experimental procedure were changed, and the impact of these changes on the low-dose response of the cells was examined. The effects of preparing single-cell suspensions in different ways, of maintaining the temperature at 37°C during irradiation, of avoiding centrifugation, of diminishing the pipetting error and of reducing the Perspex shielding to avoid modification of the ^{60}Co γ-ray spectrum were all explored. Furthermore, experiments were performed on different cell batches to ensure that the inconsistencies were not caused by spontaneous genetic changes in the cell stock. Despite these repeated investigations of the low-dose response, the presence of HRS was never detected. Rather the mean surviving fractions from 21-24 experiments in the low-dose range seemed to be well fitted by the linear-quadratic model (see fig. 4.1 b)).

A strong association has been demonstrated between the induction of the rapidly induced and transient "early" G_2 checkpoint, in which cells irradiated in G_2 are arrested, and the transition from HRS to increased radioresistance (IRR) [Marples et al., 2003; Marples et al., 2004; Xu et al., 2002]. It is believed that HRS reflects the failure of this checkpoint to prevent radiation-damaged G_2-phase cells from prematurely entering mitosis (see Ch. 2.4.4). Thus the expression of HRS in an asynchronous cell population is dependent on a sufficiently large fraction of cells in late S and G_2 phase, i.e., cells that will progress into mitosis before the later Sinclair checkpoint is induced. The lack of HRS/IRR response in T-47D cells could therefore be caused by a reduced G_2 fraction in the asynchronous cell populations, perhaps as a result of trypsinization, which has been shown to influence the cell-cycle distribution [Edin et al., 2007]. Since the average time interval between trypsinization and irradiation was found to be (17.8 ± 0.3) hours, the cell-cycle distribution 18 hours after trypsinization was measured by flow cytometry. The G_2/M fraction at this time was measured to be (14.0 ± 0.5)%, making it slightly greater than the average G_2/M fraction in exponentially growing cells, which was found to be (12.2 ± 1.0)% (see table 4.11 and table 4.9). This indicated that the elimination of HRS was not caused by a lack of G_2 cells. In concordance with this result, HRS could not be detected in dose-survival measurements on G_2-enriched cell populations (see Ch. 4.5).

Three experiments on asynchronous T-47D cells were also performed in which another person plated the cells. Although the mean-value data points were seen to follow the LQ curve quite well (see fig. 4.12 b)), there were some indications of increased sensitivity to the lowest doses in the first of these experiments (see fig. 4.12 a) (■)). Such a low-dose response, with presence of HRS in some, but not all experiments, is actually similar to the findings of Christiansen [2005] and Fenne [2008], who explored the low-dose response of T-47D cells to 220 kV_p X-irradiation. This is illustrated in figure 5.2. Here the survival data measured by Fenne are plotted against the LQ curve that was fitted to mean surviving fractions from the present study and against the fit by the IR model to survival data measured by Edin et al. [2008a] when irradiating the cells with 220 kV_p X-rays. Note that the HRS "dip" was shallower for this radiation quality than for ^{60}Co γ-rays, as the transition to IRR seemed to be induced at lower doses (as discussed in Ch. 4.1.2). It is very difficult to decide, based on this figure, whether the cells actually exhibited HRS in the study by Fenne [2008]. The mean surviving fractions from the study by Christiansen [2005] were not plotted in figure 5.2. However, from the curve-fitting parameters given in table 5.1, it is seen that $\alpha_s < \alpha_r$ for both irradiation at room-temperature and at 37°C, and this is clearly inconsistent with the presence of HRS. In some individual experiments performed with controlled temperature, very low surviving fractions were seen at the lowest doses, but the variations were large.

Fenne [2008] also studied the growth pattern of T-47D cells by means of time-lapse cinematography, following a control group and a group of cells given a single acute X-ray dose of 0.3 Gy. Three sections of every flask were filmed for 7 days, and the development of every colony-forming unit in these sections was registered. At the end of the 7-day period every unit that was consisting of at least 6 cells and in which a division had occurred within the last 30 hours, was counted as a surviving cell. Using this assay the surviving fraction at 0.3 Gy was found to be 0.952 or 0.970 depending on how the calculation was performed (per section or per flask, respectively)[*]. For comparison, the survival at 0.3 Gy would be 0.943 according to the linear-quadratic fit of the present study. Thus also in this type of assay, in which there was no uncertainty in the number of cells actually plated, the cells seemed to respond according to the LQ model.

In another study [Grinde, 2006] the dose responses of the sublines T-47DsiRb and T-47DsiRbMock were measured. The T-47DsiRb cells had been transfected with a vector containing a gene for inactivation of pRb, along with genes for green fluorescent protein (GFP) and resistance toward the antibiotic geneticin, while T-47DsiRbMock cells had been given a vector where the basepair sequence coding for inactivation of pRb was rearrangerred in such a way that it did not code for any protein. Since the two other genes should have little influence on radiosensitivity, the mock subline was expected to have a dose response similar to the parental T-47D cells. It was found, however, that the HRS was markedly reduced, and although the low-dose sensitivity seemed to be higher than

[*] The surviving fractions originally given in the thesis by Fenne [2008] were 0.888 and 0.895, respectively. These were, however, calculated by first finding the plating efficiency among the irradiated cells, correcting this fraction for multiplicity and then divide by the plating efficiency of controls. This procedure introduces an erroneously large multiplicity correction. The correct procedure would be to first calculate the ratio of plating efficiencies and subsequently correct this fraction for multiplicity (see Ch. 3.4.2).

predicted by the LQ model, the fit by the IR model did not satisfy the criteria for HRS-competent cells (see Ch. 4.1). Possible reasons for the lack of HRS response might be that the cells were grown in medium containing geneticin, which was observed to increase the doubling time, or that the transfection affected the low-dose response in some way even though the pRb function was left intact.

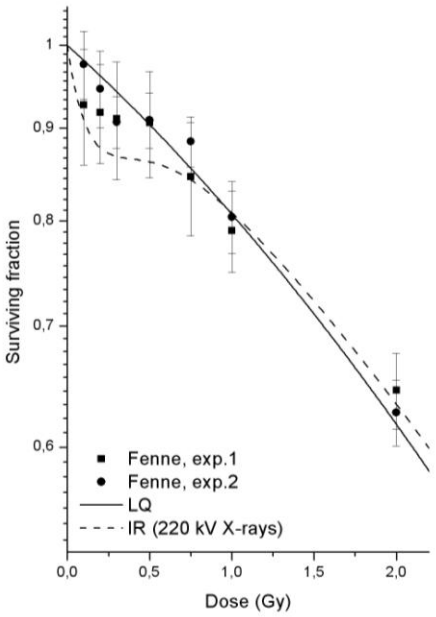

Figure 5.2
Survival of T-47D cells irradiated with single acute doses of 220 kV_p X-rays. The data points represent single observations of two independent experiments performed by Fenne [2008], and the vertical bars are standard errors. The curves represent a fit by the LQ model (solid line) to pooled data (T1-T24) from the present study (using ^{60}Co γ-irradiation), and a fit by the IR model (dashed line) to survival data measured by Edin [personal communication] using the same cell line and 220 kV_p X-rays.

Although these studies performed by students at our group did not convincingly demonstrate an HRS/IRR response pattern in T-47D cells, the low-dose measurements performed by Edin have been very consistent, giving strong evidence that this cell line in fact is HRS proficient. These observations have been corroborated by measurements of the mitotic ratio (ratio of irradiated versus unirradiated mitotic cells) as a function of radiation dose using the method for assessment of anti-phospho-histone H3 (ser28) staining [Edin et al., 2008b]. The mitotic ratio was shown to be unaltered in response to doses below a threshold of ~0.3 Gy, implying that cells irradiated in the G_2 phase are not arrested for doses below this threshold. In other studies there has been a one-to-one correspondence between HRS proficiency and a threshold dose for decrease in the mitotic ratio [Krueger et al., 2007a; Krueger et al., 2007b; Marples et al., 2003]. Consequently, there is little doubt that HRS/IRR is the primary response of T-47D cells to low doses of ionizing radiation. The puzzling aspect is rather what causes the consistent elimination of HRS in the present study and to a certain extent in the measurements of others.

5.3 Statistical Uncertainties in the Measurement of Survival at Low Doses

There are many difficulties involved in making an accurate determination of the initial region of the cell-survival curve. First of all, the biological response to radiation varies, as was discussed in chapter 2.3.4, dramatically through the cell cycle. Thus the survival curve of an asynchronous cell population is in reality a composite of curves relating to cells at different stages of the cycle. Secondly, the endpoint which is observed is loss of

reproductive integrity, and we only score the survivors, i.e., cells with the ability to produce a colony. The number of inactivated cells is normally not known, and neither is the exact number of plated cells. This introduces problems of statistical nature. If the numbers of both surviving and inactivated cells were known, the plating of a cell would be like the flipping of a coin. Only two outcomes would be possible, and the resulting outcome would be registered for every cell. The distribution of survivors from such a process would follow binomial statistics. However, if the exact numbers of plated and inactivated cells are not known, the number of viable cells plated (assuming that the cells are randomly mixed in the suspension they are taken from) will follow a Poisson distribution [Boag, 1975]. An example will be given to illustrate the impact this will have on the statistical uncertainties. Normally in this study, 200 cells were plated per control flask, and the plating efficiency was ~75%. Let us therefore assume that we observe N = 150 survivors in a control flask. In the former case we would know that exactly 200 cells were plated. The plating efficiency (PE) ± standard error and relative uncertainty $(\Delta N/N)$ would be:

$$PE = \frac{150}{200} \pm \frac{\sqrt{200 \cdot 0.75 \cdot 0.25}}{200} = 0.75 \pm 0.031 \quad \Rightarrow \quad \frac{\Delta N}{N} = 0.041$$

In the latter case we only have an estimate of 200 cells being plated. Since Poisson statistics essentially assumes that only colony counts are known, it is artificial to calculate the "plating efficiency". Instead only the number of survivors $N \pm \Delta N$ is given, and we can calculate the relative uncertainty:

$$N = 150 \pm \sqrt{150} = 150 \pm 12.2 \quad \Rightarrow \quad \frac{\Delta N}{N} = 0.082$$

In other words, precise cell counting would reduce the uncertainty by half. For this example only the sampling error was considered, while errors due to pipetting-inaccuracy, non-uniform mixing of the suspension and inadequately controlled variables like pH, temperature, quality of serum and toxic contaminants were ignored [Boag, 1975]. Moreover, a plated single-cell might in some cases give rise to more than one colony as a result of doublet- or colony-division or of cell migration. Up to 7.5% of the seeded cells were observed to form more than one colony in the study by Fenne [2008], thereby influencing the observed plating efficiencies substantially.

In addition to the statistical problems just described, a correction for multiplicity was necessary since the cells were irradiated after overnight attachment. This introduces additional uncertainty, especially when considering the possibility of bystander responses and surviving fractions higher than 1. These issues were discussed in chapter 3.4.2.

It is easy to imagine that small inaccuracies in the volume and homogeneity of the cell suspension administered to each flask would obscure the low-dose measurements considerably. However, from the discussion of the experimental results given in chapter 4.1.7, it should be clear that variations in the quantity of suspension transferred to each flask contributed relatively little to the combined errors. Special attention was also paid to

frequent remixing of the stock suspension in order to keep it homogenous. Since the survival data in addition proved to be quite consistent in this study, inaccuracies in connection with the plating procedure can probably be excluded as a reason for the loss of observable HRS. The main contribution to the experimental uncertainties most likely came from the sampling errors, as illustrated for a control flask in the example above.

Because of the low resolution of the traditional clonogenic assay technique in measuring radiosensitivity at low doses, the HRS phenomenon has normally been investigated using either a microscope relocation technique to detect every plated cell or a fluorescence-activated cell sorter to plate an exact number of cells [Marples et al., 1997]. One should keep in mind, though, the effects caused by colony-forming units that give rise to more than one colony each. If the findings by Fenne [2008] are representative for other cell lines (which remains to be investigated), such effects are likely to obscure the measurements performed by high-precision methods (like those described by Marples et al. [1997]), as well as by conventional methods. It would still be advantageous to know the exact number of plated cells, but the problem of low precision in the measurements can be overcome by performing a large number of experiments with many replicate flasks per experiment. For the unprimed T-47D cells every measured data point (see fig. 4.1) represented the weighted mean of as many as 21-24 experiments. Consequently, the final uncertainties were quite small, and clearly the abrogation of HRS can not be explained by poor statistics.

5.4 Mechanisms for the Elimination of HRS in T-47D Cells

5.4.1 A Model for the Elimination of HRS

The experiments performed by Edin has not only revealed pronounced low-dose hypersensitivity, but also demonstrated that the HRS response can be removed by many different types of pretreatment. Most of these results were reviewed in chapter 2.4.7 and chapter 2.4.8 when relationships between HRS/IRR and two other low-dose phenomena, the radioadaptive response and the bystander effect, were described. On many occasions the removal of HRS was accompanied by surviving fractions that was higher than predicted by the LQ model, and even exceeding 1 for the lowest doses (see Ch. 2.4.9). Table 5.3 summarizes all the types of pretreatment that have been demonstrated to abrogate HRS in T-47D cells.

A model was proposed by Edin et al. [2008b] in an attempt to explain the mechanisms behind the observed elimination of HRS. This model is illustrated in figure 5.3. Panel A displays the situation in which cell conditioned medium is low-dose-rate (LDR) irradiated without the presence of cells. It had been observed that serum had to be present during cell conditioning, and in the model a serum constituent C acts on a receptor on the cell membrane (1), releasing the intracellularly membrane-linked substance A. This substance forms a complex with another substance produced in cells, called B. B is modified to B* when binding to A (2). In unirradiated cells the A-B* complex is secreted into the

Pretreatment	Response
Trypsinization and plating.	HRS reduced temporarily. Almost fully restored 8 hours after plating.
0.3 Gy HDR priming.	LQ survival when challenge-irradiated after 6 hours, but HRS restored after 24 hours.
0.3 Gy LDR priming.	Elevated survival even after more than 2 years of continuous culturing.
24 hours of incubation with ICCM from cells given 0.3 Gy LDR priming. Medium transferred 40 hours after priming. Plated in fresh medium 20 hours before challenge-irradiation.	Elevated survival. HRS was restored 2 weeks after medium transfer. Effect weakened if ICCM was diluted. No effect for HDR priming or if serum was not present during priming.
24 hours of incubation with ICCM from cells given 0.3 Gy LDR priming. Medium transferred up to 14 months after priming. Plated in fresh medium 20 hours before challenge-irradiation.	Possibly elevated survival.
24 hours of incubation with CCM given 0.3 Gy LDR irradiation without cells present. Plated in fresh medium 16-20 hours before challenge-irradiation.	Possibly elevated survival. No effect if medium was HDR irradiated or not cell conditioned or if serum was absent during conditioning. CCM alone also gave no effect.
Cultured for 3-6 weeks in hypoxia box at 4% O_2.	Elevated survival when challenge-irradiated while still hypoxic. Possibly elevated survival when irradiated 5 min. after being flushed with air and 5% CO_2.
Cultured for 4 weeks in hypoxia box at 4% O_2. 48 hours of reoxygenation in CO_2-incubator with air and 5% CO_2 before challenge-irradiation.	LQ survival. HRS restored if cells had been reoxygenated for 2 weeks.
24 hours of incubation with CCM from cells that had been cultured for 4 weeks in hypoxia box at 4% O_2. Plated in fresh medium 18 hours before challenge-irradiation.	LQ survival.

Table 5.3: Pretreatments that have been shown to abolish HRS in T-47D cells
The table displays results from experiments performed by Edin et al. [2007; 2008c; 2008b; 2008a]. Often when HRS was removed, cell survival exceeded the predictions of the LQ model (designated "elevated survival"), but sometimes the data were too sparse to separate between elevated and regular LQ survival.

medium (3). When the medium is LDR irradiated with the cells absent, B* is released from A (4). When unirradiated cells subsequently are exposed to B*, this factor binds to a receptor (5), and initiates a pathway (6) resulting in activation of the early G_2 checkpoint even for the lowest challenge-doses examined.

In panel B LDR irradiation of cells is illustrated. The change in phenotype presumed to occur in T-47D-P cells resulted from this priming procedure. Somehow these cells must be able to continuously produce and secrete B*, since medium transferred from the cells abrogates HRS in recipient unirradiated cells. However, medium transfer only removes HRS if serum is present when the cells are given the priming irradiation. Thus the serum constituent C is again believed to initiate the process by binding to a receptor (1). This causes the release of A, and formation of the A-B* complex (2). This time the cells will be present during LDR irradiation, which means that some of the A-B* compounds will be dissociated intracellularly (3). It is hypothesized that the presence of B* inside the cell triggers an auto-reaction chain persistently modifying B molecules into B* (4). The B* molecules are secreted (5), and will initiate the pathway leading to elimination of HRS by receptor binding (6)-(7).

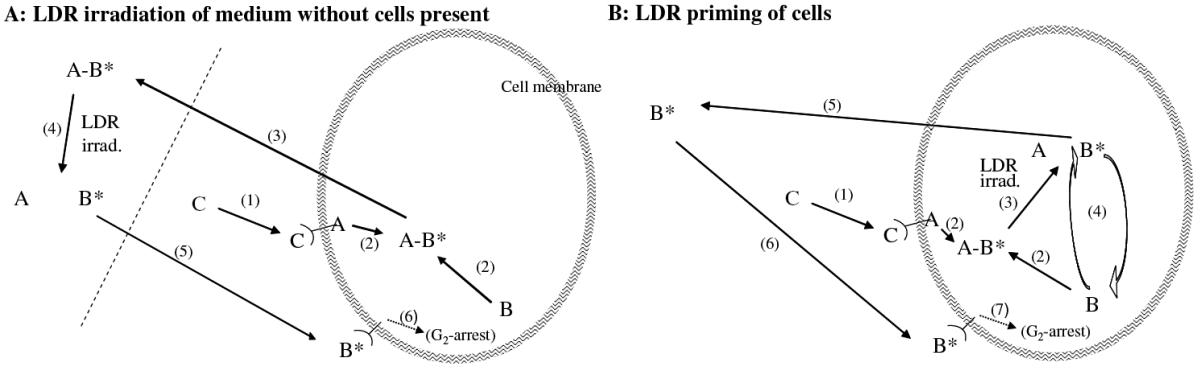

Figure 5.3
Illustration of the model proposed by Edin et al. [2008b] to explain the observed elimination of HRS in T-47D cells. Panel A: LDR irradiation of medium without cells present. The dissociaton of the A-B complex is triggered by LDR irradiation of the medium. This process occurs even in the absence of cells, as indicated by the dashed line. See text for further details. Panel B: B* is released from the A-B* complex intracellularly, inducing an auto-reaction chain modifying all Bs into B*. The B* molecules are subsequently secreted. See text for further details. [Edin et al., 2008b, fig. 8]*

Exposure to the protein synthesis inhibitor BG (4,6-benzylidene-D-glucose) from 1 hour before to 6 hours after LDR priming of cells failed to suppress the abolition of HRS, making it probable that the proposed auto-reaction chain modifying B into B* is independent of enzymes [Edin et al., 2008b]. Growing cells for 3-6 weeks in 4% O_2 was also seen to eliminate HRS, but the effect was temporary, and the cells had restored HRS within 2 weeks [Edin et al., 2008a]. Similar to the observations after LDR priming, medium transferred from cells grown for 4 weeks in 4% O_2 removed HRS in the recipient cells. Thus it seems that both moderate hypoxia and LDR irradiation have the ability to induce or modify bystander-like factors in the medium, factors that are able to abrogate HRS in recipient cells. It was suggested that the hypoxic cells secrete reactive species

with the same effect on the putative A-B* complex as LDR irradiation [Edin et al., 2008a]. According to this hypothesis, the flow of reactive species stops when the cells are reoxygenated, and HRS will then be recovered.

The identity of the B*-factor (or factors) and the signaling pathways involved in the priming processes are not known. However, a few signaling molecules have been seen to play a role in bystander effects and bystander-induced radioadaptive responses in other cell lines. The cytokine transforming growth factor β (TGF-β) has been proposed as a factor that mediates or contributes to radiation-induced bystander responses [Iyer and Lehnert, 2000; Shao et al., 2008b; Shao et al., 2008a]. TGF-β has some interesting characteristics with regard to Edin's model. For instance, TGF-β signaling is necessary for autophosphorylation of ATM and for induction of ATM-kinase activity in response to ionizing radiation [Kirshner et al., 2006]. Moreover, TGF-β is secreted from cells as part of a latent complex, and release from this complex can be triggered by a variety of molecules including radicals like reactive oxygen species (ROS) [Annes et al., 2003]. TGF-β is also known to be a key extracellular sensor and signal of stress responses in irradiated tissues [Barcellos-Hoff, 2005]. Experiments to investigate the possible involvement of TGF-β in elimination of HRS in T-47D cells have recently been started [Edin, personal communication].

Involvement of reactive oxygen and nitrogen species (ROS/RNS) has also been demonstrated to be important for bystander effects and radioadaptive responses [Azzam et al., 2004; Matsumoto et al., 2007]. Especially the radical nitric oxide (NO), which is a key participant in many physiological pathways, appears to play an important role. The participation of NO in radiation-induced bystander responses have been demonstrated in a number of studies using low- and high-LET radiation qualities, low and high doses, medium-transfer or co-cultivation protocols, different cell lines and both beneficial endpoints, such as increase in plating efficiency or increased radioresistance, or non-beneficial endpoints, such as induction of micronuclei or apoptosis [Han et al., 2007; Matsumoto et al., 2000; Matsumoto et al., 2001; Shankar et al., 2006; Shao et al., 2003; Shao et al., 2006; Shao et al., 2001; Shao et al., 2004]. NO and its reaction products (N_2O_3 and $ONOO^-$) can damage DNA through multiple pathways [Burney et al., 1999; Nguyen et al., 1992], and NO has been shown to be important as an early activator for induction of double-strand breaks in bystander cells [Han et al., 2007]. Low levels of DNA damage or DNA discontinuities have been suggested as initiators for the radioadaptive response through the activation of DNA repair systems [Stoilov et al., 2007; Wolff, 1998], and single-strand breaks likely to be caused by ROS/RNS might function as such initiators [Matsumoto et al., 2007]. Induction of the radioadaptive response in bystander cells was abolished by treating ICCM with NO scavengers or inhibitors of NO synthase, which is a group of enzymes necessary for cellular NO generation [Matsumoto et al., 2000; Matsumoto et al., 2001]. This is interesting with regard to our experiments on T-47D cells since, as described in chapter 2.4.7, many inducers of the adaptive response have been observed to also prime for HRS. Furthermore, NO has been demonstrated to stimulate activation of PARP-1, DNA-PK_{CS} and ERK1/2, all of which are proteins necessary for overcoming HRS and for activation of the "early" G_2/M checkpoint (see Ch. 2.4.5) [Leach et al., 2002; Szabo, 2006; Xu et

al., 2000]. Very recent studies also demonstrated that TGF-β was a downstream product of irradiation-induced NO, and TGF-β could further trigger the expression of NO in non-irradiated bystander cells [Shao et al., 2008b; Shao et al., 2008a]. It has been reported that T-47D cells produce a great amount of NO [Kampa et al., 2001], and it was recently shown in another human breast cancer cell line, MCF-7, that NO levels increased in the whole cell population after irradiating only 1% of the cells with a microbeam [Shao et al., 2008c]. Based on these findings, the possible involvement of NO and its reaction products for elimination of HRS in T-47D cells should be investigated.

5.4.2 Possible Reasons for the Loss of HRS in the Present Study

Many different aspects of the experimental procedures were investigated in order to find out why the T-47D cells did not exhibit low-dose hypersensitivity in the present study. These were presented and discussed in a systematic manner in the Results and Analysis section. However, none of the investigations resolved the apparent contradiction between the results presented in this thesis and those of Edin et al. [2007; 2008c; 2008b; 2008a], and the mechanism(s) responsible for removing HRS remains a mystery. From the experiments performed by Edin et al. (summarized in table 5.3), it is clear that the low-dose behavior of T-47D cells is altered as a response to very moderate stress. It also seems that whatever caused the lack of HRS in figure 4.1 (experiments T1-T24), it did not influence cell viability since the plating efficiency was as high as (76 ± 4)%. For comparison Edin et al. [2008c] reported a plating efficiency of (74 ± 3)%.

Unlike the experiments where HRS was eliminated by LDR priming or medium transfer (see table 5.3), the surviving fractions did not exceed 1 at the lowest doses in the present study. This indicates that the full "priming effect" was not induced. The observed survival was quite similar to the low-dose response measured for cells that had been cultured in hypoxic conditions for 4 weeks and reoxygenated for 48 hours prior to challenge-irradiation, and to the response of cells that had been exposed to medium harvested from hypoxic cells [Edin et al., 2008a]. Thus, by examining Edin's model (fig. 5.3, panel A), it seems like the elimination of HRS in the present study was caused by either something inducing the dissociation of the putative A-B* complex, although the concentration of B* did not get high enough to obtain the saturated effect, or by some kind of change in the intracellular environment (initiating a pathway downstream of the B*-receptor binding). Edin et al. [2008a] suggested that hypoxic cells release or secrete reactive species with the same effect on the putative medium complex as LDR irradiation. Perhaps, in the present study, some aspect of the treatment cells were given during plating influenced temporarily the activity or secretion of reactive species.

While the experiments presented in this thesis consistently failed to detect HRS in unprimed T-47D cells, the same cell line consistently exhibited HRS in experiments performed by Edin. This consistency might be an important clue to reveal the causes of the differing responses. The exact same experimental setup has been used in the present study and in the studies by Edin. Whenever a change was made to this setup (as described in Ch. 4.1.1-4.1.8), it was naturally imperative to keep all other aspects of the procedure constant in order to possibly identify the mechanism responsible for removing HRS.

Consistently about 70 minutes were spent on the plating procedure per experiment. The average time was (73.0 ± 1.8) minutes. In contrast, Edin spends only about half this time. The shortest time used for plating in the present study was 57 minutes. Interestingly, this occurred for experiment T14, which was the only experiment that showed an HRS-like response (see fig. 4.8). This might of course be a coincidence, but it is tempting to speculate how the time spent by cells in suspension might influence their radiosensitivity. One factor that could possibly influence the cells by inducing a stress response is the pH of the medium, which during plating will be higher than normal. The pH value of the medium is mainly controlled by the carbon dioxide-bicarbonate buffer system. The dissociation of CO_2 is given by the following equilibrium equation:

$$\mathrm{CO_2 + H_2O \rightleftharpoons H_2CO_3 \rightleftharpoons H^+ + HCO_3^-} \tag{5.1}$$

The concentration of bicarbonate (HCO_3^-) in the medium used by our group is 2.0 g/l of stem solution. This gives a pH slightly lower than physiological pH (7.4) when cells are grown in a humidified incubator with 5% CO_2. The relationship between pH and the concentrations of CO_2 and HCO_3^- is defined by the Henderson-Hasselbalch equation [Taylor, 1962]:

$$\mathrm{pH} = \mathrm{p}K + \log \frac{[\mathrm{HCO_3^-}]}{[\mathrm{CO_2}]} \tag{5.2}$$

where K is the acid dissociation constant and $\mathrm{p}K = -\log K$. The concentration of CO_2 is proportional to the partial pressure of CO_2 in the incubator. During plating, however, the medium is kept in ambient air, which has negligible CO_2 content (~0.04%). Consequently, as the CO_2 that has been previously formed in the medium will gradually diffuse into the surrounding air, it is clear from equations (5.1) and (5.2) that the pH will increase. The question is thus how significant this increase will be, and whether it can be a plausible mechanism for removing HRS.

To investigate these matters, the pH was measured at various stages of the plating procedure. The results of the pH measurements are shown in table 5.4. While the initial pH of ~7.7 was unlikely to affect the low-dose sensitivity of the cells, the final pH of more than 8.1 was higher than expected, and it cannot be excluded that exposure to such alkaline conditions can trigger stress responses in the cells. The activity and perhaps also the generation of reactive species and other sensor molecules are likely to be influenced by the change in pH. Moreover, although the intracellular pH of tumor cells is almost identical or even slightly more basic than that of normal cells, tumors in general have a lower extracellular pH (below 7.0) than surrounding normal tissues due to poor microvasculature [Gerweck and Seetharaman, 1996; Song et al., 2006]. Tumor cells are therefore not adapted to a basic milieu and will probably not tolerate it well. It is an open question whether such stress can have caused the elimination of HRS. Note that the cells were seeded in flasks that contained 4 ml of medium that had been incubated at 5% CO_2 prior to plating, and the exposure to alkaline conditions was therefore not protracted. Nevertheless, the possible impact of exposure to high pH values on low-dose radiosensitivity in T-47D cells should clearly be investigated further.

Stage of the plating procedure:	pH
pH in medium at the start of the experiment:	7.66
pH in suspension of trypsin and medium:	7.39
pH in cell suspension with 12000 cells/ml:	7.82
pH in cell suspension with 200 cells/ml when seeding begins:	7.84
pH in cell suspension with 200 cells/ml 70 min. after experiment start:	8.16 / 8.12*

Table 5.4: Measurements of pH during plating
*The table displays pH values measured at various stages of the plating procedure. The pH increases from 7.66 to more than 8.1 after 70 minutes in ambient air. *The pH was measured twice. The second reading was performed after re-calibration of the pH meter.*

5.5 Fine-Structure in the Low-Dose Response

So far the measured dose response for T-47D cells (fig. 4.1) has been discussed in light of Edin's results and the established LQ and IR models. Curve-fitting was performed in chapter 4.1 using those models, and the LQ model clearly gave a very good fit for the overall dose response. Nevertheless, if one imagines that the low-dose response of T-47D cells was a "tabula rasa", so to speak, and examines the measured surviving fractions without regard to previous results or established models, an interesting pattern emerges. While the survival initially drops a few percent, it remains constant over the dose range 0.1-0.3 Gy.

This is highlighted in figure 5.4. Panel A shows the mean values of the four lowest doses from all 24 experiments (T1-T24) together with a straight line. The straight line was found by fitting the constant-function $S = C$ to the three lowest doses (0.1 – 0.3 Gy) using the method of least squares with error-weighting in Origin. The resulting value of C was 0.971 ± 0.008. Panel B displays the surviving fractions measured at the same doses in single experiments. The constant function was fitted also to these points (0.5 Gy was omitted for the curve-fitting), and C was found to be 0.970 ± 0.006. In addition, the mean surviving fractions from all the six experiment triples that were presented in the Results and Analysis section are plotted together with the line C = 0.971 (panels C-H). It cannot be excluded that this low-dose plateau is a result of statistical fluctuations. The LQ curve is more or less within the error bars of the mean surviving fractions (see fig. 4.1 b)), and as discussed in chapter 5.3, variations in sampling and in plating procedures smother the small variations in survival at low doses. However, the mean surviving fractions in panel A each represent as much as 21 experiments, and it is evident from figure 5.4 that in only one of the six experiment triples, the surviving fraction was highest at 0.1 Gy. It is therefore not unlikely that this deviation from the LQ model is more than a coincidence caused by experimental uncertainties.

The linear-quadratic model, or the molecular theory of cell survival as it was named by Chadwick and Leenhouts [1973], assumes that the lethal lesion is a double-strand break. The lesion may arise by a single event if a single ionizing particle, directly or indirectly, creates breaks in both DNA strands (α term), or by a double event, if it is caused by two independent and adjacent single-strand breaks in the complementary strands (β term).

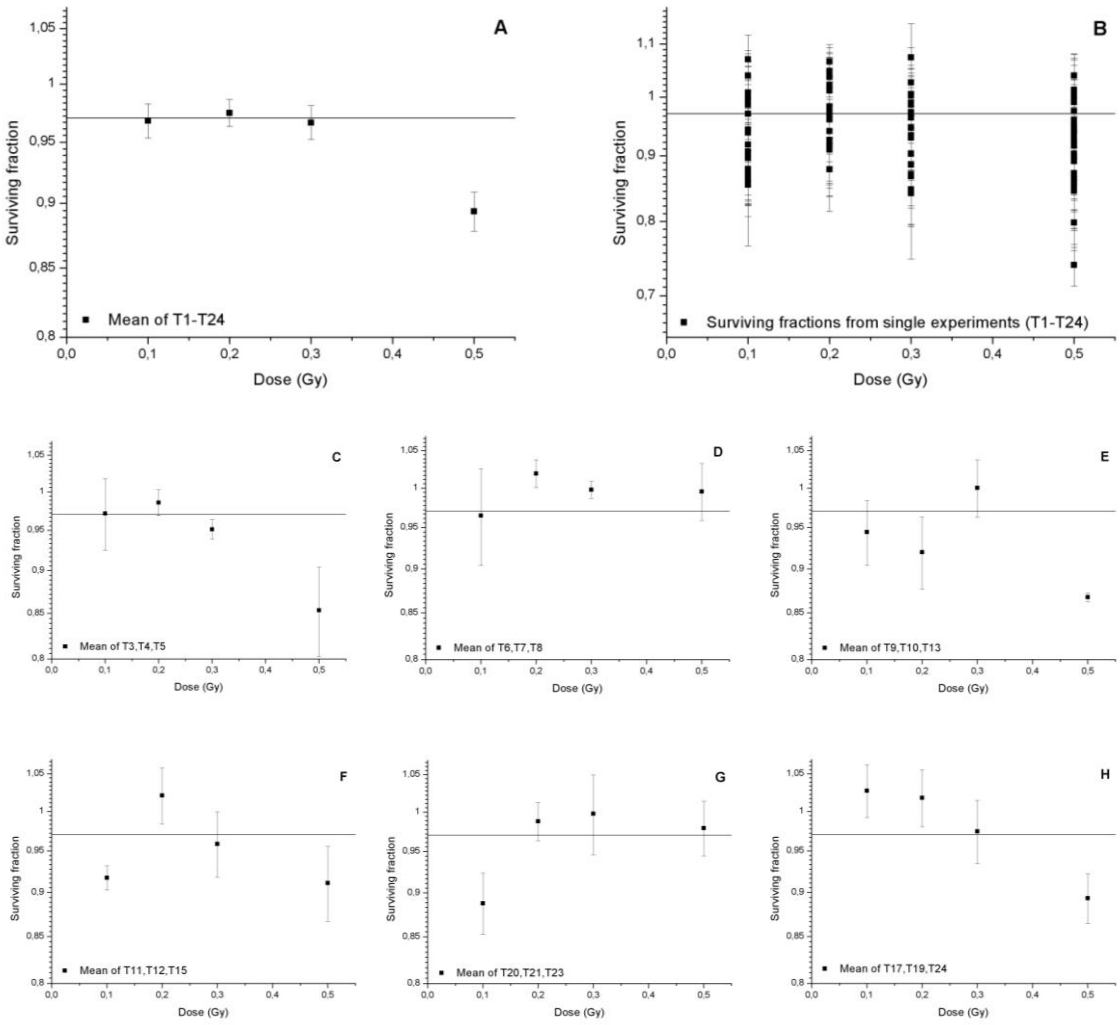

Figure 5.4
The figure displays the surviving fractions of T-47D cells in response to doses in the dose range 0.1-0.5 Gy. The level of survival seems to be constant for the three lowest doses, implying that the effect per unit dose declines over this dose range.

Panel A shows the mean surviving fractions from 21 experiments (0.1-0.3 Gy) and 24 experiments (0.5 Gy). The data points were redrawn from figure 4.1 b). The line C = 0.971 was found by fitting the constant function S = C to the surviving fractions at the three lowest doses. This line is also plotted in panel C-H. Panel B shows all the surviving fractions from single experiments (T1-T24). The line C = 0.970 was found by fitting the constant function S = C to the surviving fractions at the three lowest doses. Panel C shows the mean surviving fractions from the 3 experiments with reduced Perspex shielding (redrawn from figure 4.4 b)). Panel D shows the mean surviving fractions from the 3 experiments with a new cell batch (redrawn from figure 4.5 b)). Panel E shows the mean surviving fractions from the 3 experiments with single-cell suspension prepared without cannula (redrawn from figure 4.6 b)). Panel F shows the mean surviving fractions from the 3 experiments with temperature maintained at 37°C (redrawn from figure 4.7 b)). Panel G shows the mean surviving fractions from the 3 experiments with centrifugation avoided (redrawn from figure 4.9 b)). Panel H shows the mean surviving fractions from the 3 experiments with pipetting error diminished (redrawn from figure 4.10 b)).

The LQ model, given by equation (2.10), applies formally only to synchronized cultures since the parameters α and β vary through the cell cycle, but can successfully be used to describe the survival of an asynchronous cell population as well. Importantly, it predicts that survival, also after low-LET radiation, will have an initial slope, given by the coefficient α. Furthermore, the model describes a survival curve that will be continuously bending, that is, the probability of cell inactivation increases continuously with increasing dose. Although strand-break repair is incorporated into the model, it is only represented by a simple constant embracing all physical recombination processes, chemical restitution processes and biochemical enzymatic repair processes. Thus, modification of the survival curve by dose-dependent activation of repair processes, such as the induction of the "early" G_2/M checkpoint, will not be predicted by this theory. The same applies to other processes, such as radiation-induced increases in plating efficiency as a result of single clonogenic units giving rise to multiple colonies each.

Consequently, the plateau-like low-dose response measured in the present study cannot be fitted well by the LQ model. Although rarely applied today, it should be mentioned that the multitarget model was characterized by zero slope at zero dose, and could theoretically be fitted to an initial plateau region. Such a plateau would not arise from the onset of repair, though, but from the requirement that the dose has to be relatively large before the probability of inactivating all the targets of a cell is non-negligible. However, as seen from figure 5.4, the survival seems to drop initially, i.e., the plateau is formed at a surviving fraction of 97%, and not at zero dose. Clearly, neither the target theory nor the molecular theory can explain the low-dose behavior, and one may speculate about the nature of this response. It does bear some resemblance to the HRS-phenomenon, with a higher effect per unit dose at 0.1 Gy than at 0.2 and 0.3 Gy, but in order to call these cells hypersensitive, the effect would have to be much more pronounced. Since the effect per unit dose at 0.1 Gy was higher than expected from the LQ model, it is possible that what was observed is a small remnant of the primary HRS response. It was described in chapter 2.4.3 how a threshold level of DNA damage is required to initiate the transition towards IRR. Perhaps the treatment that was given the T-47D cells during plating did not remove HRS completely, but caused the IRR transition to set in for much lower doses. Consistent with an incomplete HRS elimination, the surviving fractions did not exceed 1 at the lowest doses as observed by Edin et al. [2007; 2008c; 2008b; 2008a] when priming effects were fully expressed.

In some cases a plated single-cell might give rise to more than one colony as a result of doublet- or colony-division or of cell migration. Up to 7.5% of the seeded cells were observed to form more than one colony in the study by Fenne [2008], and for the unprimed T-47D cells, these effects occurred to a larger extent among cells irradiated with 0.3 Gy than among controls. The mean surviving fraction at 0.3 Gy in the present study was 0.967 (which is similar to the surviving fractions of 0.952 or 0.970 measured by Fenne with time-lapse filming), while the prediction from the LQ curve-fit was 0.943. If we assume that the fractions of colony-forming units giving rise to more than one colony each were the same as in the study by Fenne, and correct the mean surviving fraction for this effect, the survival at 0.3 Gy will be 0.926. Thus, it is clear that such

effects occur frequently enough to account for the observed discrepancy from the LQ model.

5.6 Radiosensitivity of the G_2-Enriched Cell Populations

When cells were selected in the G_1 phase and incubated for 24 hours (T-47D-P) or 29-30 hours (T-47D), the degree of G_2-enrichment at the time of irradiation was poorer than expected with G_2 fractions of (31.6 ± 1.4)% and (42.0 ± 3.5)% for the primed and unprimed cells, respectively. In previous experiments the fraction of T-47D-P cells in G_2/M was around ~50% after the same incubation time (see table 4.5). The large discrepancy is hard to explain, but was discussed in chapter 4.5.2. It is clear from these experiments that to sort a population of G_1 cells and incubate them for a certain time is not a very reliable way to achieve a substantial G_2-enrichment. Although the approach was relatively successful for the unprimed cells, it is hard to determine the true dose response of G_2 cells when large subpopulations of cells in other phases obscure the results. This was especially true for the T-47D-P cells. Whether the increased radiosensitivity for these cells was a consequence of high sensitivity of G_2 cells or a consequence of many cells in late G_1, which is known as a sensitive phase of the cell cycle, or a combination of both, cannot be answered based on the results given in figure 4.20 and table 4.10.

Relatively synchronized cell populations were collected by sorting cells in early S phase. Using this approach we were guaranteed that all the cells would reach G_2 phase more or less at the same time. Thus a very good measure of G_2 radiosensitivity would be obtained if the cells were irradiated at the right time. Unfortunately a 14-hour interval seemed to be 2-3 hours too long, resulting in a large late-G_2/mitotic subpopulation that would attempt dividing without repairing radiation-induced DNA damage (see figure 4.22). The basis for incubating the cells for 14 hours after plating was that the G_2/M fraction was still zero at this time in the experiments previously conducted with selection of G_1 T-47D-P cells (see table 4.7). However, it is likely that the G_2/M fractions given in table 4.7 are somewhat misleading as ModFit sets the G_2/M fraction to zero more or less automatically when the model f_dip_n0, especially designed to handle histograms with indistinct G_2/M peaks, is used (see Ch. 3.6.3). Using a different model and specifying the G_2 range manually generally produced exaggerated estimates for the G_2/M fraction, as seen from artificially low G_2/G_1 ratios (data not shown). Consequently, an actual G_2/M fraction of ~5% would possibly not be detected. Moreover, it is seen from figure 3.4 that although the S-phase gate is placed at an early stage of the phase, it is not placed at the very beginning since this would result in the selection of some G_1 cells. In retrospect it is therefore not surprising that a 14-hour interval turned out to be too long.

By selecting cells in G_2 phase and irradiating them 15 minutes after plating, the cells were guaranteed to be in G_2/M at the time of irradiation, but, as discussed in chapter 4.5.4, irradiating cells in the lag period immediately after plating entail a risk of PLD repair obscuring the results. It was therefore reassuring that the survival data plotted in figure 4.23 (cells selected in G_2) corresponded well with the data plotted in figure 4.20 (cells selected in G_1). However, since G_1 selection produced a relatively poor degree of

enrichment, and irradiation of cells selected in G_2 involved a risk of PLD repair masking the actual sensitivity of progressing cells, the most promising approach was probably collecting cells in early S phase. Unfortunately the cells were irradiated at a time when a large fraction was in mitosis. By reducing the interval between plating and irradiation to about 11-12 hours, this should be a successful method for G_2-enrichment.

It seems clear from these experiments that T-47D cells in G_2 phase are not more sensitive than an asynchronous population as a whole. In addition the S-phase experiments indicated that the radiosensitivity was much higher for mitotic cells. The variation of radiosensitivity with age in the cell cycle was briefly described in chapter 2.3.4. Traditionally, it has been concluded that 1) mitotic cells are generally the most radiosensitive, 2) there is usually a resistant period in early G_1 declining towards S phase, 3) radioresistance increases during S phase, reaching a maximum in late S, and 4) G_2 phase is almost as sensitive as mitosis in most cell lines [Hall and Giaccia, 2006, p. 54; Sinclair, 1968]. While the three first conclusions still persist and have been corroborated in many studies, the latter seem to be an anomaly [Wilson, 2004]. More recent studies have shown that in many cell lines, the cells, after becoming increasingly radioresistant during S phase, remain relatively resistant in G_2 [Biade et al., 1997; Hill et al., 1999]. Considering that irradiated G_2-phase cells will be subject to both nonhomologous end-joining and homologous recombination repair, and that the "early" G_2 checkpoint arrests cells that were damaged in G_2 phase, it appears natural that these cells are quite resistant to radiation-induced injury. Some of the radiosensitivity traditionally attributed to G_2 cells may, due to imperfect synchrony, have been the result of substantial mitotic subpopulations within the irradiated cell populations [Wilson, 2004]. Thus the observation of a radioresistant G_2 phase in T-47D cells is in concordance with data reported for other cell lines. Futhermore, the results of the present study are in agreement with the findings of Furre et al. [2003], who also reported that radiosensitivity for T-47D cells is not higher in G_2 than the average sensitivity in other cell-cycle phases. Note, however, that this conclusion was based on the lack of an inverse dose-rate effect, meaning that although the cells accumulated in G_2 at the same rate (as a function of time), the cell-kill per unit dose was not higher when the dose rate was lowered from 0.94 Gy/h to 0.37 Gy/h. So strictly speaking, what was actually shown by Furre et al. [2003] was that cells *arrested* in G_2 phase are not more radiosensitive than cells in other phases.

Surprisingly the T-47D-P cells seemed to be less radioresistant in G_2 phase than the unprimed cells. At first glance this might seem contradictory to the measurements performed on asynchronous cell populations, which showed that the dose responses of primed and unprimed cells were similar (see fig. 4.13). Later the cell-cycle distribution of exponentially growing T-47D-P cells was shown to differ substantially from the distribution of T-47D cells, probably as a consequence of a shorter G_1 period (see table 4.9). Consequently, there must be some differences between the phase-specific radio-sensitivities of primed and unprimed cells. If there was none, the differences in cell-cycle distributions would be reflected in the survival of the asynchronous populations.

No signs of HRS were seen in the G_2-enriched T-47D cell populations in contrast to the reports of exaggerated HRS responses for G_2-phase cells of other HRS-competent cell

lines [Marples et al., 2003; Short et al., 2003]. It is important to be aware, however, that HRS might have been removed by the cell-sorting procedure itself. We needed quite many cells for every experiment, and while the sorting of G_1-phase cells is very rapid, it is rather time-consuming to sort cells from the other phases, especially S phase. Typically it took about 1.5-2.5 hours to complete the cell sorting. As described in the Materials and Methods (Ch. 3.5.2) the cells were stained with the fluorescent dye Hoechst 33342. In the first description of the use of this staining agent for sorting of viable cells, the dye was reported to not be transported out of the cells at 4°C [Arndt-Jovin and Jovin, 1977]. The cytotoxicity of Hoechst 33342 used on living Chinese hamster V79 cells was later studied by Durand and Olive [1982]. Although causing significant cell-cycle perturbations, the dye was found to be relatively nontoxic. Durand and Olive also investigated the potential interaction of Hoechst 33342 with holding the cells at "ice bath" temperatures (4°C). Protracted exposure to low temperature caused a large decrease in survival for cells exposed to 5 μM Hoechst for 30 min. prior to temperature reduction, as illustrated in figure 5.5. For comparison, cells were incubated at 37°C with 8 μM Hoechst 33342 for 15 min. prior to temperature reduction in the present study.

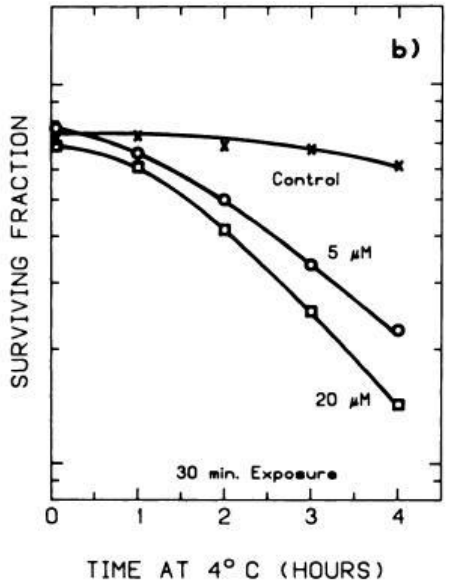

Figure 5.5
Interaction of Hoechst 33342 with reduced temperature. The figure shows survival of V79 cells as a function of time at 4°C for unstained cells and for cells exposed to the indicated concentrations of Hoechst 33342 for 30 min. prior to temperature reduction to 4°C. [Durand and Olive, 1982, fig. 5]

Despite the risk for loss of cell viability, it was decided to hold the cells at 4°C in the experiments with G_2-enrichment to avoid problems with loss of fluorescence. In the study by Durand and Olive [1982] the efflux of Hoechst 33342 appeared to be biphasic with a rapid decrease in mean fluorescence the first 3-4 hours followed by continued loss at a much slower rate that would be consistent with dilution due to cell growth and division. For concentrations of 5 and 10 μM the mean fluorescence seemed to decrease to about 60-70% of the initial intensity after 2 hours.

From the experiments performed by Edin we know that T-47D cells often respond to very moderate stress stimuli by abrogating HRS. Therefore it is not unlikely that the synergistic stress caused by low temperature and staining with Hoechst 33342 eliminated

HRS. Probably this combination also caused the reduction in plating efficiency from ~75-80% in asynchronous cultures to (52 ± 4)%. In other studies where G_2 cells have been sorted to examine low-dose HRS, the same staining agent was used, and exaggerated HRS was still observed [Marples et al., 2003; Short et al., 2003]. However, these studies used a slightly different experimental design, dispensing cells in appropriate numbers directly into Petri dishes or culture flasks. This approach would take even more time, and it would not be possible to remove the sheath buffer (normally PBS) used for sorting. We also included a step with washing in 5 ml of fresh medium after sorting, but this could probably have been omitted. In the studies by Marples and colleagues, the cells were reported to be maintained on 37°C whenever possible throughout the sorting, irradiation and plating procedures. Thus it appears that they avoided "ice bath" treatment, but at the same time they reported problems with obtaining sufficiently large populations of S-phase cells, at least if a high degree of selectivity was demanded (since this requires a narrow gate to avoid overlapping with regions of G_1 and G_2). This indicates that sorting-time was a limitation for their method. In a more recent study by the same group it was reported that they were unable to collect sufficient G_2-phase V79 and MR4 cells by means of FACS (to look for HRS-related apoptosis, which was observed in asynchronous populations), and that they instead used the confluence arrest technique (to demonstrate a lack of apoptosis in G_1-enriched cell populations) because this methodology was less aggressive than chemical synchronization or Hoechst-based cell sorting [Krueger et al., 2007b]. It has also been reported that Hoechst 33342 is specifically toxic to S-phase cells [Siemann and Keng, 1986], but this was not observed in the present study.

5.7 Elevated Low-Dose Survival for T-47D-P cells

5.7.1 Two Hypotheses for Elevated Survival

In chapter 2.4.9 it was described how the survival of LDR-primed cells in experiments performed by Edin et al. [2007; 2008c; 2008b] and Fenne [2008] was not well described by the LQ model. Rather the surviving fractions tended to lie above the LQ curve for doses smaller than 1 Gy, and for the lowest doses, survival even exceeded 1. Time-lapse filming revealed that the elevated survival was not caused by some colony-forming units giving rise to more than one colony each [Fenne, 2008]. In fact seeding of satellite colonies occurred to a larger extent in the controls (given priming only). On this basis two hypotheses were made in an attempt to explain the excess survival:

1) The challenge-irradiation increases the adhesion forces between cells and the flask surface. The improved attachment causes a smaller loss of challenge-irradiated colonies than control colonies during change of medium.
2) The challenge-irradiation recruits plated G_0 cells into the cell cycle. This has to occur rapidly after irradiation since no single-cells were observed to start dividing several days after plating in the time-lapse films [Fenne, 2008].

In the present study we attempted to detect whether low-dose irradiation stimulates T-47D-P cells out of G_0. One possible way to achieve this is by applying a metaphase-inhibitor. Most metaphase-inhibitors interfere with the formation of microtubules in the

cells; thereby preventing the proper attachment of chromosomes to the mitotic spindle and triggering the spindle-attachment checkpoint (see Ch. 2.1.3) to arrest the cells in metaphase. By treating one control group and one irradiated group with a metaphase-inhibitor and subsequently measure the DNA content of the cells at a time when all cells except those in G_0 phase have replicated their chromosomes, the fraction of cells remaining in G_0 would be determined. If this fraction would be lower in the irradiated group, the hypothesis would be strengthened. Test-experiments were conducted with the metaphase-inhibitor colcemid, but the cells did not respond well to this treatment. During preparation for flow cytometry, strings of cells and debris did not pellet in the bottom of the tube, indicating lysed cells. From the few DNA-content measurements that were relatively reliable, it also appeared that a significant fraction of the cells remained in G_1 phase, i.e., the fraction was too large to represent only G_0 cells (data not shown). These observations were supported by other studies, reporting that T-47D cells are sensitive to microtubule-disrupting agents such as nocodazole, and in general fails to arrest in mitosis in response to the metaphase-inhibitors nocodazole, vincristine and colchicine [Li and Benezra, 1996; Blajeski et al., 2002]. Rather, nocodazole treatment seemed to induce premitotic G_1 and G_2 arrests associated with increased expression of p21 in T-47D cells [Blajeski et al., 2002]. Interestingly, Li and Benezra [1996] also showed that T-47D had less than one third of the normal amount of MDM2, which is an important protein for the spindle-attachment checkpoint. They therefore concluded that T-47D cells are defective in this checkpoint. Furthermore, it had been demonstrated in another study that colcemid initiates DNA synthesis, a property that would have biased the measured G_0 fractions [Vasiliev et al., 1971].

Consequently, another experimental design was chosen. This method was described in chapter 3.6, and the results were shown in chapter 4.4. The fraction of G_1-sorted cells remaining in G_0/G_1 phase was measured 14, 15, 16, 17, 23 and 24 hours after plating. After 17 hours many progressing cells had not yet left G_1 phase. Shorter intervals were still investigated because of what seemed to be a radiation-induced G_1 arrest (discussed in Ch. 5.8). It was also observed an increase in the G_0/G_1 fractions from 23 to 24 hours (see table 4.5), indicating that the cells that were in late G_1 at the time of plating now had started to divide and replenish the G_0/G_1 population. However, the increase was relatively small, and it is possible that the fractions after 23 hours might have been close to the minimum. There was no significant difference between the G_0/G_1 fractions in controls and irradiated cell populations at that time (23 and 24 hours, see table 4.8), but as long as the times between 17 and 23 hours after plating were not investigated we cannot know whether the actual minimum G_0/G_1 percentages were lower in the irradiated cultures. The later experiments (PX1-PX3) with G_2-enriched populations also showed that the rate of exit from G_1 phase is extremely sensitive to the experimental conditions, and since we are not guaranteed that all progressing cells have left G_1 before other cells finish mitosis, it is doubtful whether this method has adequate resolution to detect a recruitment of G_0 cells. To complicate things further, the observed G_1 delay in the irradiated populations implies that the minimum G_0/G_1 fraction will occur at different times for the two groups (irradiated and control). The conclusion from these experiments is thus that no recruitment of G_0-phase cells was observed in the irradiated cultures, but the possibility that such recruitment does occur cannot be excluded.

Another matter is whether evidence of elevated survival was found in the measurements of clonogenic survival of asynchronous T-47D-P cells (see fig. 4.13). The two initial experiments with these cells seemed to be in accordance with the results of Edin et al. [2007; 2008c; 2008b] and Fenne [2008], with surviving fractions more or less consistently greater than 1 for the lowest doses (fig. 4.14). As discussed in chapter 4.2, new batches of cells had to be thawed for the follow-up experiments (see appendix A.1). Surprisingly, elevated survival was not observed in those experiments (see fig. 4.16), although this characteristic of the primed cells has previously been successfully recovered after cryostorage and thawing [Edin, personal communication]. The experiments with G_1-selection discussed above were performed on cells from the same batch that was used for the follow-up experiments (P5-P7, fig.4.16). If the mechanisms causing the increased survival had been somehow inactivated, it would of course explain why no differences could be observed between the G_0/G_1 fractions of irradiated cells and of controls.

The lack of elevated survival in figure 4.16 could have been caused by statistical fluctuations, as three of the nine measured surviving fractions in the dose range 0.1-0.3 Gy are actually greater than 1. But all three experiments, and especially the first (P5), failed to show the consistent excess in survival that has been reported previously. It is therefore likely that the measurements reflect true changes in the low-dose response, either because the cells have changed as a result of cryostorage, or because of differences in the experimental conditions. Interestingly, medium was changed during colony growth in the two initial experiments (P1-P2, fig. 4.14), but not in the last three (P5-P7). Thus the results actually support the first hypothesis, and it seems that medium-change might affect colony numbers. But too few measurements were made to draw any conclusions, especially considering the added uncertainty introduced by cryostorage and thawing. Note also that of the two experiments that were excluded (see Ch. 4.2.2 and fig. 4.15), medium was changed in one (P3), but not in the other (P4). No difference in survival could be discerned between those two experiments, and the surviving fractions lay below the LQ curve for both of them.

5.7.2 A Possible Mechanism for Recruitment of G_0 Cells

Edin et al. [2008c] demonstrated that the elevated survival relative to controls (in experiments with priming and ICCM transfer) could not be explained by a low plating efficiency of the control flasks, i.e., the fact that controls were given the same pretreatment as challenge-irradiated flasks was not the reason for the high surviving fractions. Rather than inducing a cytotoxic effect, treatment with ICCM from T-47D cells irradiated with 0.3 Gy caused a significant increase in the plating efficiency compared to cells that received fresh, unirradiated medium at the same time. This bystander effect was independent of the priming dose rate, and the plating efficiency of cells treated with ICCM increased by more than 10% relative to controls. Since plating efficiency of T-47D controls is as high as ~75%, it is very likely that some of the enhancement in survival of ICCM-treated cultures was caused by recruitment of G_0-phase cells.

The involvement of nitric oxide (NO) and its reaction products in radiation-induced bystander responses were briefly discussed in chapter 5.4.1. Similar to the results for T-47D cells, the plating efficiency of recipient cells was enhanced when they were co-cultivated with X-irradiated cells [Shao et al., 2001]. The effect was accompanied by an increased concentration of nitrite (NO_2) in the co-culture medium, and the plating efficiency decreased to control level when a scavenger of NO was added to the medium. Similarly, a significant increase in the percentage of daughter cells (in response to the mitogen con A) was observed in murine lymphocytes after treatment with ICCM from lymphocytes irradiated with only 0.1 Gy of ^{60}Co γ-rays, although the largest effect was observed after 0.5 Gy [Shankar et al., 2006]. Compared to cells incubated with unirradiated CCM, treatment with 0.1 Gy ICCM for 72 hours increased the nitrite concentration by more than a factor of 3. It is possible that NO might play an important role also for the enhanced plating efficiencies observed after ICCM treatment of T-47D cells. This is an attractive hypothesis because it has been reported that upregulation of endogenous NO production induces phosphorylation and inactivation of the tumor suppressor pRb, and consequently increased proliferation in T-47D cells [Radisavljevic, 2004].

As discussed in chapter 2.1.3, pRb is a key player at the G_1 restriction point. Phosphorylation of pRb is required for a cell to enter the cycle from quiescence. Thus, increased NO activity would be an initiator for recruitment of cells out of G_0 phase, and might hypothetically explain the increased plating efficiency of cells exposed to ICCM. Whether the same mechanism can cause the elevated survival in challenge-irradiated T-47D-P cells is more doubtful, and dephosphorylation of pRb as a response to radiation-induced stress would perhaps offset NO-mediated inactivation. As a response to hypoxia and radiation, pRb has been shown to be dephosphorylated and bound in the cell nucleus also in other cell-cycle phases than G_1 [Furre et al., 2003; Åmellem et al., 1996; Åmellem et al., 1998]. However, since upregulated NO secretion is a plausible mechanism for stimulating cells out of G_0, involvement of NO cannot be excluded in the context of the second hypothesis for the elevated survival of T-47D-P cells.

5.8 Radiation-Induced G_1 Arrest in T-47D-P Cells

T-47D-P cells that had been selected in G_1 phase showed a delayed exit from G_1 after irradiation with 0.2 Gy (see fig. 4.19 and table 4.8). This was evident from significantly greater G_0/G_1 fractions in the irradiated cell populations after 14 and 15 hours, and it was also reflected by delayed entry into G_2/M at later times.

As described in chapter 2.1.3, activation of the tumor-suppressor protein p53 is required for a sustained radiation-induced G_1 arrest. T-47D cells contain only mutated single copies of the p53 gene [Casey et al., 1991; Nigro et al., 1989], and several studies have demonstrated a low ability of T-47D cells to arrest in G_1 in response to ionizing radiation [Wosikowski et al., 1995; Siles et al., 1996; Bohnke et al., 2004]. Similarly, Furre et al. [2003] reported that the rate of G_2 accumulation for T-47D cells, whether radiation was given protracted at low dose rates or as an acute dose of 10 Gy, was close to the theoretical maximum rate, i.e., cell-cycle progression was not inhibited in the stages

before G_2. Consequently, it is very surprising that a possible G_1 arrest was observed in the present study.

Although surprising, the observed G_1 delay is not necessarily in contradiction to previous reports. In the study by Siles et al. [1996], a weak G_1 arrest was actually detected for the T-47D clone named T-47D-B8. Moreover, in the other studies G_1 arrest was measured either by looking for differences in cell-cycle distribution of asynchronous cells, or by an assay applying nocodazole to prevent cells from re-entering G_1 (which is not reliable for T-47D cells since this drug has the ability to induce a G_1 arrest by itself in that cell line, see Ch. 5.7.1). The method used in the present study, monitoring the exit from G_1 of a cell population that was selected in that phase, probably has a higher resolution and is more suited to reveal a short G_1 delay. Besides, the previous investigations focused on detecting G_1 arrests after high doses or after protracted LDR irradiation, while we measured the response to a very low acute dose (0.2 Gy). Naturally, the cells might respond quite differently to large doses than to such a small dose.

While the G_0/G_1 fractions in the irradiated cell populations were significantly greater than in controls after 14 and 15 hours, the differences had disappeared after 16 and 17 hours (see table 4.8), implying that the observed G_1 delay was quite short. Since only one radiation dose was examined, it is impossible to say whether the short duration of the arrest simply reflected the low level of damage. It is also a matter of speculation what caused the delay. Perhaps the mutated p53, although being mostly non-functional, possesses a "residual" activity capable of inducing an incomplete G_1 arrest. Another possibility is that a p53-independent pathway is capable of inducing a G_1 arrest in response to low doses of ionizing radiation. Interestingly, a transient radiation-induced p53-independent G_1/S blockage, lasting only a few hours, has been reported (see Ch. 2.1.3). Upon ionizing radiation, DNA damage triggers a cascade of phosphorylation events involving the ATM and Chk2 kinases, followed by a rapid degradation of the Cdc25A phosphatase [Bartek and Lukas, 2001; Mailand et al., 2000; Falck et al., 2001]. The Cdc25A phosphatase is necessary for Cdk2 activation, and thereby entry into S phase.

The independence of p53 and the short duration of the arrest are of course in good agreement with the observed delay in T-47D-P cells. Furthermore, it seems likely that such a transient delay would not be observed in the studies referred to above [Wosikowski et al., 1995; Siles et al., 1996; Bohnke et al., 2004], since these studies looked for a sustained increase in the G_0/G_1 fraction. However, the checkpoint is initiated through ATM-dependent activation of Chk2 (note that this also applies for the p53-dependent pathway). As mentioned previously for the "early" G_2 checkpoint (Ch. 2.4.4), there is a dose threshold for the full induction of ATM activity. Weak ATM phosphorylation is detected after X-ray doses of 0.1 Gy, with a gradual increase in function until maximal activity is reached at ~0.4-0.5 Gy [Bakkenist and Kastan, 2003]. Consistent with this, the "early" G_2 checkpoint is ineffective at doses less than ~0.3 Gy (see Ch. 2.4.4). Thus, a detectable G_1 delay in response to a 0.2 Gy dose (as was given to the T-47D-P cells) triggered by the ATM-Chk2-Cdc25A pathway would be surprising. It is interesting, though, to consider some of the similarities between the p53-independent

G_1 checkpoint and the "early" G_2 checkpoint. Both checkpoints are rapidly activated in response to radiation-induced damage, and both checkpoints are ATM dependent. ATM functions as an activator of the Chk2 kinase during induction of the G_1 arrest, and a similar phosphorylation of Chk2 has been anticipated for the G_2 checkpoint [Wilson, 2004]. In accordance with this, very recent results implicate a role for Chk2 in the context of HRS [Marples et al., 2008]. HRS-negative cell lines, such as T-47D-P, seem to have a dissociation between ATM activity and "early" G_2-phase checkpoint function, thus evading dose-dependent ATM regulatory control [Krueger et al., 2007a]. Since some of the initial steps of the checkpoint pathways seem to be common for the G_1 and G_2 checkpoints, it is not unlikely that also the delay in G_1 can be induced in response to doses below the threshold for full ATM activation. Therefore it should be investigated whether rapid degradation of Cdc25A does occur in response to low-dose irradiation of T-47D-P cells, and whether a similar G_1 delay is observed for the HRS-competent, unprimed T-47D cells.

First, however, the G_1 arrest in the LDR-primed cells has to be confirmed. Although the results presented in chapter 4.4 were quite consistent, rather few measurements were performed. Considering the uncertainties in connection with analysis in ModFit (as discussed in Ch. 4.4), more experiments should be performed to corroborate these results.

5.9 Suggestions for Further Investigations

In the present study several different aspects concerning elimination of HRS were investigated. Firstly, many attempts were made to identify the reasons for HRS abrogation in unprimed T-47D cells. Secondly, since HRS reflects a failure to arrest radiation-damaged G_2 cells, G_2-enriched cell populations were obtained by cell sorting in order to see if the lacking HRS response could be retrieved in such populations. Finally, experiments were performed to elucidate the mechanisms causing the elevated survival in T-47D-P cells and thereby contribute to a better understanding of the processes induced by LDR priming.

Although the mechanisms responsible for removing HRS in the unprimed cells were never identified, it was speculated whether exposure to medium with alkaline pH during plating might play a role. This should be investigated further by monitoring the pH during the plating procedure, and look for differences in the low-dose response of cells plated with or without exposure to higher than normal (up to ~7.7) pH values.

The original purpose of this thesis was to identify possible thresholds in dose and dose rate for elimination of HRS by incorporation of tritium into cellular protein. Since the unprimed T-47D cells did not exhibit HRS only preliminary investigations were performed (see Ch. 4.3). When the reason for HRS removal in unprimed cells is identified, the search for priming-thresholds at ultra-low dose rates should finally be carried out.

HRS was not observed after irradiation of G_2-enriched cell populations, indicating that the removal of HRS was not caused by an insufficient amount of G_2 cells in the

asynchronous cultures. Rather it seems like the "early" G_2 checkpoint might have been activated in some way during plating. Although the experiments with G_2-enrichment did not explain the loss of HRS, they did provide some important insight for future work with this cell line. For instance it was demonstrated that synchronized cell populations of T-47D cells can be obtained by applying a narrow gate in S phase during Hoechst-based cell sorting. This synchronization technique can be very useful for studies of events occurring in S or G_2 phase. Treatment with Hoechst 33342 did not seem to be toxic to these cells, although a reduction in plating efficiency was observed. This reduction was probably caused by keeping the cells in a water/ice-mix, and for future work it is recommended to perform an initial optimization study to check whether the sorting procedure will be so time-consuming that this is necessary.

We were not able to determine the mechanisms causing elevated low-dose survival for T-47D-P cells. No recruitment of G_0 cells into the cell cycle could be observed when monitoring the exit out of G_1 phase by cells originally selected in G_1. However, the measurements were not precise enough to exclude the possibility that such recruitment does occur. Measurements of dose response by clonogenic assay indicated that change of medium might be required for the surviving fractions to exceed 1. This supports the hypothesis that improved attachment to the flask surface causes the effect, but very few experiments were performed, and no conclusions can be drawn on this basis. Since it has proved difficult to test the hypothesis of G_0 recruitment, future studies should probably focus on experiments designed to strengthen or falsify the other hypothesis. Two types of experiments can be performed for this purpose. The present study supported the findings of Edin et al. [2008c], that medium change did not seem to influence final surviving fraction in unprimed cells, and omitting change of medium did not inhibit colony growth or reduce plating efficiency as long as only 200 cells were plated per flask. The straight-forward approach will therefore be to plate two experiments in parallel, and change medium during colony growth in only one of them. By repeating this process until the statistical uncertainties are small enough to detect the presence or loss of elevated survival, it will be clear whether the effect is caused by medium change. Unfortunately, it is still a risk that the colony loss will be greater in controls than in challenge-irradiated flasks during fixation and staining, but loosened colonies were hardly ever detected during these procedures in the work with the present study, despite a large number of experiments and careful examination of the flasks. The second possible experimental approach involves the use of manipulation force microscopy, a type of atomic force microscopy. The use of this method to measure cell adhesion forces has been described by Sagvolden et al. [1999]. The force microscope uses a cantilever to exert forces on and eventually displace a cell. The cantilever acts as a spring (with known compliances), and subnanometer deflections of the cantilever can be detected by measuring the position of a reflected laser beam, resulting in piconewton force sensitivity. By measuring the force needed to break all cellular bonds to the surface for both challenge-irradiated and control T-47D-P cells, it can be determined whether a small irradiation dose improves the surface attachment.

When G_1-phase T-47D-P cells were irradiated with 0.2 Gy of ^{60}Co γ-rays their entry into S phase was delayed. Since T-47D cells have mutated p53, it was surprising that such a

low level of radiation-induced damage could halt cell-cycle progression in G_1. It should be investigated whether G_1-phase T-47D-P cells consistently are arrested in response to low radiation doses and whether the arrest is activated also in response to higher doses. Moreover, it should be investigated whether unprimed T-47D cells respond in a similar manner. The method used in the present study, with selection of G_1 cells and measurements of DNA content after different times of incubation, is very suited for such investigations. If these follow-up experiments confirm a G_1 arrest, one should explore whether p53 is involved despite being mutated, or whether the rapid p53-independent pathway might induce the arrest. The former can be investigated for instance by using the p53 inhibitor pifithrin [Komarov et al., 1999]. Abrogation of the G_1 delay by treating the cells with pifithrin would imply that p53 is required for the response. The latter can be explored by performing Western blotting during the first hour post-irradiation. If a pronounced degradation of Cdc25A is detected, it will be a strong indication for the involvement of the rapid pathway.

6 Conclusion

The main findings of the present study are:

- Contrary to previous reports, T-47D cells did not exhibit low-dose HRS in response to acute ^{60}Co γ-irradiation. The reason for this contradiction was not identified, but it was speculated whether exposure to alkaline conditions during plating might be involved. This hypothesis was not tested, however.

- The radiosensitivitity of T-47D cells in G_2 phase is not higher than the average sensitivity in other phases of the cell cycle. The radiosensitivity of T-47D-P cells appears to be slightly increased in G_2 phase.

- Flow-cytometric DNA content analysis revealed a substantially lower fraction of G_0/G_1 cells in exponentially growing T-47D-P cells compared to unprimed T-47D cells. This difference is thought to reflect the shorter doubling time of the primed cells.

- Contrary to previous reports, a consistent trend of elevated low-dose survival for T-47D-P cells was not observed. However, surviving fractions at the lowest doses tended to exceed 1 when medium was changed during colony growth, although the data are much too sparse to establish a connection between elevated survival and change of medium.

- Attempts were made to detect stimulation of G_0-phase T-47D-P cells into the cell cycle in response to a radiation dose of 0.2 Gy. No recruitment of G_0 cells was observed, but the measurements were not precise enough to exclude the possibility that such recruitment does occur.

- T-47D-P cells that had been selected in G_1 phase and irradiated with 0.2 Gy showed a delayed entry into S phase, indicating a radiation-induced G_1 arrest despite the mutated p53 status of these cells.

For most of these findings, supplementary investigations are needed in order to draw any conclusions.

References

Alberts B, Johnson A, Lewis J, Raff M, Roberts K, Walter P (2002) *Molecular Biology of the Cell, 4th edition*. Garland Science: New York

Annes JP, Munger JS, Rifkin DB (2003) Making sense of latent TGF beta activation. *Journal of Cell Science* **116**: 217-224

Arndt-Jovin DJ, Jovin TM (1977) Analysis and sorting of living cells according to deoxyribonucleic acid content. *J Histochem Cytochem* **25**: 585-589

Attix FH (1986) *Introduction to Radiological Physics and Radiation Dosimetry*. John Wiley & Sons: New York

Azzam EI, de Toledo SM, Little JB (2004) Stress signaling from irradiated to non-irradiated cells. *Current Cancer Drug Targets* **4**: 53-64

Bakkenist CJ, Kastan MB (2003) DNA damage activates ATM through intermolecular autophosphorylation and dimer dissociation. *Nature* **421**: 499-506

Barcellos-Hoff MH (2005) Integrative radiation carcinogenesis: interactions between cell and tissue responses to DNA damage. *Seminars in Cancer Biology* **15**: 138-148

Bartek J, Lukas J (2001) Mammalian G1- and S-phase checkpoints in response to DNA damage. *Current Opinion in Cell Biology* **13**: 738-747

Ben-Porath I, Weinberg RA (2005) The signals and pathways activating cellular senescence. *International Journal of Biochemistry & Cell Biology* **37**: 961-976

Berkovich E, Monnat RJ, Kastan MB (2007) Roles of ATM and NBS1 in chromatin structure modulation and DNA double-strand break repair. *Nature Cell Biology* **9**: 683-U137

Biade S, Stobbe CC, Chapman JD (1997) The intrinsic radiosensitivity of some human tumor cells throughout their cell cycles. *Radiation Research* **147**: 416-421

Bjørhovde I (2006) *Undersøkingar av celler sin respons på intern bestråling med lågenergetiske elektron ved ultralåge doseratar*. Cand. Scient. thesis: University of Oslo

Blajeski AL, Phan VA, Kottke TJ, Kaufmann SH (2002) G(1) and G(2) cell-cycle arrest following microtubule depolymerization in human breast cancer cells. *Journal of Clinical Investigation* **110**: 91-99

Boag JW (1975) The statistical treatment of cell survival data. In *Cell Survival after Low Doses of Radiation: Theoretical and Clinical Implications*, Alper T (ed) pp 40-53. John Wiley & Sons: London

Bohnke A, Westphal F, Schmidt A, El-Awady RA, hm-Daphi J (2004) Role of p53 mutations, protein function and DNA damage for the radiosensitivity of human tumour cells. *Int J Radiat Biol* **80**: 53-63

Bonner WA, Hulett HR, Sweet RG, Herzenberg LA (1972) Fluorescence activated cell sorting. *Rev Sci Instrum* **43**: 404-409

Bonner WM (2004) Phenomena leading to cell survival values which deviate from linear-quadratic models. *Mutation Research-Fundamental and Molecular Mechanisms of Mutagenesis* **568**: 33-39

Bryant PE (1985) Enzymatic Restriction of Mammalian-Cell Dna - Evidence for Double-Strand Breaks As Potentially Lethal Lesions. *International Journal of Radiation Biology* **48**: 55-60

Burma S, Chen BPC, Chen DJ (2006) Role of non-homologous end joining (NHEJ) in maintaining genomic integrity. *Dna Repair* **5**: 1042-1048

Burney S, Caulfield JL, Niles JC, Wishnok JS, Tannenbaum SR (1999) The chemistry of DNA damage from nitric oxide and peroxynitrite. *Mutation Research-Fundamental and Molecular Mechanisms of Mutagenesis* **424**: 37-49

Cao S, Skog S, Tribukait B (1983) Comparison Between Protracted and Conventional Dose-Rates of Irradiation on the Growth of the Bp8 Mouse Ascites Sarcoma. *Acta Radiologica Oncology* **22**: 35-47

Casey G, Lohsueh M, Lopez ME, Vogelstein B, Stanbridge EJ (1991) Growth Suppression of Human Breast-Cancer Cells by the Introduction of A Wild-Type P53 Gene. *Oncogene* **6**: 1791-1797

Chadwick KH, Leenhouts HP (1973) Molecular Theory of Cell Survival. *Physics in Medicine and Biology* **18**: 78-87

Chalmers A, Johnston P, Woodcock M, Joiner M, Marples B (2004) PARP-1, PARP-2, and the cellular response to low doses of ionizing radiation. *International Journal of Radiation Oncology Biology Physics* **58**: 410-419

Chandna S, Dwarakanath BS, Khaitan D, Mathew TL, Jain V (2002) Low-dose radiation hypersensitivity in human tumor cell lines: Effects of cell-cell contact and nutritional deprivation. *Radiation Research* **157**: 516-525

Chen J (2004) On the difference between reference radiations used in radiobiology. *International Journal of Radiation Biology* **80**: 577-580

Christiansen K (2005) *Adaptive effekter av små røntgenstråledoser for celler dyrket i kultur*. Cand. Scient. thesis: University of Oslo

Cohen-Jonathan E, Bernhard EJ, McKenna WG (1999) How does radiation kill cells? *Current Opinion in Chemical Biology* **3**: 77-83

Collis SJ, DeWeese TL, Jeggo PA, Parker AR (2005) The life and death of DNA-PK. *Oncogene* **24**: 949-961

Collis SJ, Schwaninger JM, Ntambi AJ, Keller TW, Nelson WG, Dillehay LE, DeWeese TL (2004) Evasion of early cellular response mechanisms following low level radiation-induced DNA damage. *Journal of Biological Chemistry* **279**: 49624-49632

Cregan SP, Brown DL, Mitchel REJ (1999) Apoptosis and the adaptive response in human lymphocytes. *International Journal of Radiation Biology* **75**: 1087-1094

Cummins RJ, Mothersill C, Seymour CB, Johns H, Joiner MC (1999) The effect of microcolony size, at time of irradiation, on colony forming ability. *International Journal of Radiation Biology* **75**: 225-232

Dertinger H, Jung H (1970) *Molecular radiaton biology*. Springer Verlag: Berlin - Heidelberg

Dey S, Spring PM, Arnold S, Valentino J, Chendil D, Regine WF, Mohiuddin M, Ahmed MM (2003) Low-dose fractionated radiation potentiates the effects of paclitaxel in wild-type and mutant p53 head and neck tumor cell lines. *Clinical Cancer Research* **9**: 1557-1565

Dimova EG, Bryant PE, Chankova SG (2008) "Adaptive response" - Some underlying mechanisms and open questions. *Genetics and Molecular Biology* **31**: 396-408

Dionet C, Tchirkov A, Alard JP, Arnold J, Dhermain J, Rapp M, Bodez V, Tamain JC, Monbel I, Malet P, Kwiatkowski F, Donnarieix D, Veyre A, Verrelle P (2000) Effects of low-dose neutrons applied at reduced dose rate on human melanoma cells. *Radiation Research* **154**: 406-411

Durand RE (1986) Use of a cell sorter for assays of cell clonogenicity. *Cancer Res* **46**: 2775-2778

Durand RE, Olive PL (1982) Cytotoxicity, Mutagenicity and DNA damage by Hoechst 33342. *J Histochem Cytochem* **30**: 111-116

Edin NFJ (2003) *Hyper-radiosensitivity and induced radioresistance (HRS/IRR) - The effect of using different dose-rates for pre-exposure on the hyper-radiosensitivity in T-47D cells*. Cand. Scient thesis: University of Oslo

Edin NFJ, Olsen DR, Sandvik JA, Malinen E, Pettersen EO (2008a) *Low dose hyper-radiosensitivity in T-47D cells is eliminated by chronic moderate hypoxia but returns after reoxygenation*. Article in PhD-thesis of Edin NFJ: University of Oslo

Edin NFJ, Olsen DR, Stokke T, Pettersen EO (2007) Recovery of low-dose hyper-radiosensitivity following a small priming dose depends on priming dose-rate. *Int J Low Radiation* **4**: 69-86

Edin NFJ, Olsen DR, Stokke T, Sandvik JA, Ebbesen P, Pettersen EO (2008b) Mechanisms of the elimination of low dose hyper-radiosensitivity in T-47D cells by low dose-rate priming. *International Journal of Radiation Biology* submitted

Edin NFJ, Sandvik JA, Olsen DR, Pettersen EO (2008c) The elimination of low-dose hyper-radiosensitivity by transfer of irradiated cell conditioned medium depends on dose-rate. *Radiation Research* in press

Elkind MM, Whitmore GF (1967) Survival Curve Theory. In *The Radiobiology of Cultured Mammalian Cells*, Elkind MM, Whitmore GF (eds) pp 7-52. Gordon and Breach: New York

Enns L, Bogen KT, Wizniak J, Murtha AD, Weinfeld M (2004) Low-dose radiation hypersensitivity is associated with p53-dependent apoptosis. *Molecular Cancer Research* **2**: 557-566

Falck J, Mailand N, Syljuasen RG, Bartek J, Lukas J (2001) The ATM-Chk2-Cdc25A checkpoint pathway guards against radioresistant DNA synthesis. *Nature* **410**: 842-847

Feinendegen LE (1967) *Tritium-labeled molecules in biology and medicine*. Academic Press Inc.: New York

Feinendegen LE (1999) The role of adaptive responses following exposure to ionizing radiation. *Human & Experimental Toxicology* **18**: 426-432

Fenne S (2008) *Effekt av små røntgendoser på humane celler - Individuelle celleresponser målt ved bruk av "time-lapse" cinematografi og koloni-metoden*. Master of Science thesis: University of Oslo

Furre T, Furre IE, Koritzinsky M, Amellem O, Pettersen EO (2003) Lack of inverse dose-rate effect and binding of the retinoblastoma gene product in the nucleus of human cancer T-47D cells arrested in G2 by ionizing radiation. *International Journal of Radiation Biology* **79**: 413-422

Furre T, Koritzinsky M, Olsen DR, Pettersen EO (1999) Inverse dose-rate effect due to pre-mitotic accumulation during continuous low dose-rate irradiation of cervix carcinoma cells. *International Journal of Radiation Biology* **75**: 699-707

Garcia LM, Wilkins DE, Raaphorst GP (2007) alpha/beta ratio: A dose range dependence study. *International Journal of Radiation Oncology Biology Physics* **67**: 587-593

Gerweck LE, Seetharaman K (1996) Cellular pH gradient in tumor versus normal tissue: potential exploitation for the treatment of cancer. *Cancer Res* **56**: 1194-1198

Goddu SM, Howell RW, Bouchet LG, Bolch WE, Rao DV (1997) *MIRD Cellular S values: Self-absorbed dose per unit cumulated activity for selected radionuclides and monoenergetic electron and alpha particle emitters incorporated into different cell compartments*. Society of Nuclear Medicine: Reston, VA

Goodhead DT (1994) Initial Events in the Cellular Effects of Ionizing-Radiations - Clustered Damage in Dna. *International Journal of Radiation Biology* **65**: 7-17

Goodhead DT (1989) The Initial Physical Damage Produced by Ionizing-Radiations. *International Journal of Radiation Biology* **56**: 623-634

Grinde MT (2006) *Forsøk på inaktivering av RB-funksjonen til T-47D-celler ved bruk av vektorbasert siRNA-teknikk*. Master of Science thesis: University of Oslo

Hall EJ, Giaccia AJ (2006) *Radiobiology for the Radiologist, 6th edition*. Lippincott Williams & Wilkins: Philadelphia

Han W, Wu L, Chen S, Bao L, Zhang L, Jiang E, Zhao Y, Xu A, Hei TK, Yu Z (2007) Constitutive nitric oxide acting as a possible intercellular signaling molecule in the initiation of radiation-induced DNA double strand breaks in non-irradiated bystander cells. *Oncogene* **26**: 2330-2339

Hartwell LH, Weinert TA (1989) Checkpoints - Controls That Ensure the Order of Cell-Cycle Events. *Science* **246**: 629-634

Henriksen T, Maillie HD (2003) *Radiation & Health*. Taylor & Francis: London

Herceg Z, Wang ZQ (2001) Functions of poly(ADP-ribose) polymerase (PARP) in DNA repair, genomic integrity and cell death. *Mutation Research-Fundamental and Molecular Mechanisms of Mutagenesis* **477**: 97-110

Hill AA, Wan F, Acheson DK, Skarsgard LD (1999) Lack of correlation between G(1) arrest and radiation age-response in three synchronized human tumour cell lines. *International Journal of Radiation Biology* **75**: 1395-1408

Hirao A, Kong YY, Matsuoka S, Wakeham A, Ruland J, Yoshida H, Liu D, Elledge SJ, Mak TW (2000) DNA damage-induced activation of p53 by the checkpoint kinase Chk2. *Science* **287**: 1824-1827

Honore HB, Bentzen SM (2006) A modelling study of the potential influence of low dose hypersensitivity on radiation treatment planning. *Radiotherapy and Oncology* **79**: 115-121

Howard A, Pelc SR (1953) Synthesis of deoxyribonucleic acid in normal and irradiated cells and its relation to chromosome breakage. *Heredity* **6 (suppl)**: 261-273

Howell RW (1994) The Mird Schema - from Organ to Cellular Dimensions. *Journal of Nuclear Medicine* **35**: 531-533

International Commission on Radiation Protection (ICRP) (1983) *Radionuclide transformations: energy and intensity of emissions*. ICRP Publication 38, Pergamon Press: New York

Iwasaki A (1994) Characteristics of Co-60 Gamma-Ray Spr (Scatter-Primary Ratio), Sf (Scatter Factor), Beta (Dose-Kerma Ratio), and D(Max) (Depth of Maximum Dose). *Physics in Medicine and Biology* **39**: 1081-1088

Iyer R, Lehnert BE (2002) Low dose, low-LET ionizing radiation-induced radioadaptation and associated early responses in unirradiated cells. *Mutation Research-Fundamental and Molecular Mechanisms of Mutagenesis* **503**: 1-9

Iyer R, Lehnert BE (2000) Factors underlying the cell growth-related bystander responses to alpha particles. *Cancer Research* **60**: 1290-1298

Jaenicke RU, Sprengart ML, Wati MR, Porter AG (1998) Caspase-3 is required for DNA fragmentation and morphological changes associated with apoptosis. *Journal of Biological Chemistry* **273**: 9357-9360

Joiner MC, Johns H (1988) Renal Damage in the Mouse - the Response to Very Small Doses Per Fraction. *Radiation Research* **114**: 385-398

Joiner MC, Lambin P, Malaise EP, Robson T, Arrand JE, Skov KA, Marples B (1996) Hypersensitivity to very-low single radiation doses: Its relationship to the adaptive response and induced radioresistance. *Mutation Research-Fundamental and Molecular Mechanisms of Mutagenesis* **358**: 171-183

Joiner MC, Marples B, Lambin P, Short SC, Turesson I (2001) Low-dose hypersensitivity: Current status and possible mechanisms. *International Journal of Radiation Oncology Biology Physics* **49**: 379-389

Kampa M, Hatzoglou A, Notas G, Niniraki M, Kouroumalis E, Castanas E (2001) Opioids are non-competitive inhibitors of nitric oxide synthase in T47D human breast cancer cells. *Cell Death and Differentiation* **8**: 943-952

Kastan MB (2001) Checking two steps. *Nature* **410**: 766-767

Kastan MB, Bartek J (2004) Cell-cycle checkpoints and cancer. *Nature* **432**: 316-323

Kastan MB, Lim DS (2000) The many substrates and functions of ATM. *Nature Reviews Molecular Cell Biology* **1**: 179-186

Kastan MB, Onyekwere O, Sidransky D, Vogelstein B, Craig RW (1991) Participation of P53 Protein in the Cellular-Response to Dna Damage. *Cancer Research* **51**: 6304-6311

Keydar I, Chen L, Karby S, Weiss FR, Delarea J, Radu M, Chaitcik S, Brenner HJ (1979) Establishment and Characterization of A Cell-Line of Human-Breast Carcinoma Origin. *European Journal of Cancer* **15**: 659-670

Kirshner J, Jobling MF, Pajares MJ, Ravani SA, Glick AB, Lavin MJ, Koslov S, Shiloh Y, Barcellos-Hoff MH (2006) Inhibition of transforming growth factor-beta 1 signaling attenuates ataxia telanglectasia mutated activity in response to genotoxic stress. *Cancer Research* **66**: 10861-+

Komarov PG, Komarova EA, Kondratov RV, Christov-Tselkov K, Coon JS, Chernov MV, Gudkov AV (1999) A chemical inhibitor of p53 that protects mice from the side effects of cancer therapy. *Science* **285**: 1733-1737

Krause M, Hessel F, Wohlfarth J, Zips D, Hoinkis C, Foest H, Petersen C, Short SC, Joiner MC, Baumann M (2003) Ultrafractionation in A7 human malignant glioma in nude mice. *International Journal of Radiation Biology* **79**: 377-383

Krause M, Prager J, Wohlfarth J, Hessel F, Dorner D, Haase M, Joiner MC, Baumann M (2005) Ultrafractionation does not improve the results of radiotherapy in radioresistant murine DDL1 lymphoma. *Strahlentherapie und Onkologie* **181**: 540-544

Krueger SA, Collis SJ, Joiner MC, Wilson GD, Marples B (2007a) Transition in survival from low-dose HYPER-RADIOSENSITIVITY to increased radioresistance is independent of activation of atm ser1981 activity. *International Journal of Radiation Oncology Biology Physics* **69**: 1262-1271

Krueger SA, Joiner MC, Weinfeld M, Piasentin E, Marples B (2007b) Role of apoptosis in low-dose hyper-radiosensitivity. *Radiation Research* **167**: 260-267

Leach JK, Black SM, Schmidt-Ullrich RK, Mikkelson RB (2002) Activation of constitutive nitric-oxide sythase activity is an early signaling event induced by ionizing radiation. *Journal of Biological Chemistry* **277**: 15400-15406

Li Y, Benezra R (1996) Identification of a human mitotic checkpoint gene: hsMAD2. *Science* **274**: 246-248

Lorentzen H (2001) *Effect of the protein synthesis inhibitor P-1013 on repair after x-irradiation of human cells in culture*. Cand. Scient. thesis, University of Oslo:

Maguire P, Mothersill C, McClean B, Seymour C, Lyng FM (2007) Modulation of radiation responses by pre-exposure to irradiated cell conditioned medium. *Radiation Research* **167**: 485-492

Mailand N, Falck J, Lukas C, Syljuasen RG, Welcker M, Bartek J, Lukas L (2000) Rapid destruction of human Cdc25A in response to DNA damage. *Science* **288**: 1425-1429

Marples B, Adomat H, Koch CJ, Skov KA (1996) Response of V79 cells to low doses of X-rays and negative pi-mesons: Clonogenic survival and DNA strand breaks. *International Journal of Radiation Biology* **70**: 429-436

Marples B, Cann NE, Mitchell CR, Johnston PJ, Joiner MC (2002) Evidence for the involvement of DNA-dependent protein kinase in the phenomena of low dose hyper-

radiosensitivity and increased radioresistance. *International Journal of Radiation Biology* **78**: 1139-1147

Marples B, Collis SJ (2008) Low-dose hyper-radiosensitivity: Past, present, and future. *International Journal of Radiation Oncology Biology Physics* **70**: 1310-1318

Marples B, Joiner MC (1995) The Elimination of Low-Dose Hypersensitivity in Chinese-Hamster V79-379A Cells by Pretreatment with X-Rays Or Hydrogen-Peroxide. *Radiation Research* **141**: 160-169

Marples B, Joiner MC (2000) Modification of survival by DNA repair modifiers: a probable explanation for the phenomenon of increased radioresistance. *International Journal of Radiation Biology* **76**: 305-312

Marples B, Joiner MC (1993) The Response of Chinese-Hamster V79 Cells to Low Radiation-Doses - Evidence of Enhanced Sensitivity of the Whole Cell-Population. *Radiation Research* **133**: 41-51

Marples B, Krueger SA, Schoenherr D, Joiner MC, Martinez AA, Wilson GD (2008) Cell-cycle checkpoint control and radiosensitivity after low-dose X-irradiation: Implications for IMRT. *International Journal of Radiation Oncology Biology Physics* **72**: S694

Marples B, Lambin P, Skov KA, Joiner MC (1997) Low dose hyper-radiosensitivity and increased radioresistance in mammalian cells. *International Journal of Radiation Biology* **71**: 721-735

Marples B, Skov KA (1996) Small doses of high-linear energy transfer radiation increase the radioresistance of Chinese hamster V79 cells to subsequent X irradiation. *Radiation Research* **146**: 382-387

Marples B, Wouters BG, Collis SJ, Chalmers AJ, Joiner MC (2004) Low-dose hyper-radiosensitivity: A consequence of ineffective cell cycle arrest of radiation-damaged G(2)-phase cells. *Radiation Research* **161**: 247-255

Marples B, Wouters BG, Joiner MC (2003) An association between the radiation-induced arrest of G(2)-phase cells and low-dose hyper-radiosensitivity: A plausible underlying mechanism? *Radiation Research* **160**: 38-45

Matsumoto H, Hamada N, Takahashi A, Kobayashi Y, Ohnishi T (2007) Vanguards of paradigm shift in radiation biology: Radiation-induced adaptive and bystander responses. *Journal of Radiation Research* **48**: 97-106

Matsumoto H, Hayashi S, Hatashita M, Ohnishi K, Shioura H, Ohtsubo T, Kitai R, Ohnishi T, Kano E (2001) Induction of radioresistance by a nitric oxide-mediated bystander effect. *Radiation Research* **155**: 387-396

Matsumoto H, Hayashi S, Hatashita M, Shioura H, Ohtsubo T, Kitai R, Ohnishi T, Yukawa O, Furusawa Y, Kano E (2000) Induction of radioresistance to accelerated carbon-ion beams in recipient cells by nitric oxide excreted from irradiated donor cells of human glioblastoma. *International Journal of Radiation Biology* **76**: 1649-1657

Mayles P, Nahum A, Rosenwald JC (2007) *Handbook of Radiotherapy Physics: Theory and Practice*. Taylor & Francis:

Melvik JE (1983) *Effekt av cisplatin på celleoverlevelse, cellesyklusprogresjon og strålefølsomhet hos mammalske celler i kultur*. Cand. Real. thesis: University of Oslo

Metcalfe P, Kron T, Hoban P (1997) *The Physics of Radiotherapy X-Rays from Linear Accelerators*. Medical Physics Publishing: Madison, WI

Mitchell CR, Folkard M, Joiner MC (2002) Effects of exposure to low-dose-rate Co-60 gamma rays on human tumor cells in vitro. *Radiation Research* **158**: 311-318

Mitchell CR, Joiner MC (2002) Effect of subsequent acute-dose irradiation on cell survival in vitro following low dose-rate exposures. *International Journal of Radiation Biology* **78**: 981-990

Mitchell JB, Bedford JS, Bailey SM (1979) Dose-Rate Effects on the Cell-Cycle and Survival of S3-Hela and V79-Cells. *Radiation Research* **79**: 520-536

Morstin K, Kopec M, Olko P, Schmitz T, Feinendegen LE (1993) Microdosimetry of Tritium. *Health Physics* **65**: 648-656

Mothersill C, Seymour C (1997b) Survival of human epithelial cells irradiated with cobalt 60 as microcolonies or single cells. *International Journal of Radiation Biology* **72**: 597-606

Mothersill C, Seymour C (1997a) Medium from irradiated human epithelial cells but not human fibroblasts reduces the clonogenic survival of unirradiated cells. *International Journal of Radiation Biology* **71**: 421-427

Mothersill C, Seymour C (2001) Radiation-induced bystander effects: Past history and future directions. *Radiation Research* **155**: 759-767

Mothersill C, Seymour CB, Joiner MC (2002) Relationship between radiation-induced low-dose hypersensitivity and the bystander effect. *Radiation Research* **157**: 526-532

Mothersill C, Seymour RJ, Seymour CB (2004) Bystander effects in repair-deficient cell lines. *Radiation Research* **161**: 256-263

Moussa H, Mitchell SA, Grenman R, Joiner MC (2000) Cell-cell contact increases radioresistance in head and neck carcinoma cell lines. *International Journal of Radiation Biology* **76**: 1245-1253

Nguyen T, Brunson D, Crespi CL, Penman BW, Wishnok JS, Tannenbaum SR (1992) Dna Damage and Mutation in Human-Cells Exposed to Nitric-Oxide Invitro. *Proceedings of the National Academy of Sciences of the United States of America* **89**: 3030-3034

Nigro JM, Baker SJ, Preisinger AC, Jessup JM, Hostetter R, Cleary K, Bigner SH, Davidson N, Baylin S, Devilee P, Glover T, Collins FS, Weston A, Modali R, Harris CC, Vogelstein B (1989) Mutations in the P53 Gene Occur in Diverse Human-Tumor Types. *Nature* **342**: 705-708

OConnor PM, Jackman J, Bae I, Myers TG, Fan SJ, Mutoh M, Scudiero DA, Monks A, Sausville EA, Weinstein JN, Friend S, Fornace AJ, Kohn KW (1997) Characterization of the p53 tumor suppressor pathway in cell lines of the National Cancer Institute anticancer drug screen and correlations with the growth-inhibitory potency of 123 anticancer agents. *Cancer Research* **57**: 4285-4300

Opstad HK (2005) *Matematisk modellering av cellers hypersensitivitet for små doser ved bestråling med pulset doserate*. Cand. Scient. thesis, University of Oslo:

Orear J (1982) *Notes on statistics for physicists, revised*. Laboratory for Nuclear Studies, Cornell University: Ithaca, NY

Pallavicini MG, Lalande ME, Miller RG, Hill RP (1979) Cell cycle distribution of chronically hypoxic cells and determination of the clonogenic potential of cells accumulated in G2 + M phases after irradiation of a solid tumor in vivo. *Cancer Res* **39**: 1891-1897

Palmer GM, Keely PJ, Breslin TM, Ramanujam N (2003) Autofluorescence spectroscopy of normal and malignant human breast cell lines. *Photochemistry and Photobiology* **78**: 462-469

Peacock JH, Eady JJ, Edwards SM, Mcmillan TJ, Steel GG (1992) The Intrinsic Alpha Beta Ratio for Human Tumor-Cells - Is It A Constant. *International Journal of Radiation Biology* **61**: 479-487

Pettersen EO, Bjorhovde I, Sovik A, Edin NFJ, Zachar V, Hole EO, Sandvik JA, Ebbesen P (2007) Response of chronic hypoxic cells to low dose-rate irradiation. *International Journal of Radiation Biology* **83**: 331-345

Pohlit W, Drenkard S (1985) Quantitative-Determination of the Contribution of Indirect and Direct-Radiation Action to the Production of Lethal Lesions in Mammalian-Cells. *Radiation Protection Dosimetry* **13**: 195-198

Pouget JP, Mather SJ (2001) General aspects of the cellular response to low- and high-LET radiation. *European Journal of Nuclear Medicine* **28**: 541-561

Puck TT, Marcus PI (1956) Action of X-Rays on Mammalian Cells. *Journal of Experimental Medicine* **103**: 653-&

Radford IR (2002) DNA lesion complexity and induction of apoptosis by ionizing radiation. *International Journal of Radiation Biology* **78**: 457-466

Radisavljevic Z (2004) Inactivated tumor suppressor Rb by nitric oxide promotes mitosis in human breast cancer cells. *Journal of Cellular Biochemistry* **92**: 1-5

Reddel RR, Alexander IE, Koga M, Shine J, Sutherland RL (1988) Genetic Instability and the Development of Steroid-Hormone Insensitivity in Cultured T-47D Human-Breast Cancer-Cells. *Cancer Research* **48**: 4340-4347

Roos WP, Kaina B (2006) DNA damage-induced cell death by apoptosis. *Trends in Molecular Medicine* **12**: 440-450

Ryste Hauge IH (2000) *Aktivering av pRB og innflytelse på strålefølsomhet for humane celler in vitro av behandling med benzaldehydderivatet P-1013*. Cand. Scient thesis: University of Oslo

Sagvolden G, Giaever I, Pettersen EO, Feder J (1999) Cell adhesion force microscopy. *Proc Natl Acad Sci U S A* **96**: 471-476

Schwartz JL (2007) Variability: The common factor linking low dose-induced genomic instability, adaptation and bystander effects. *Mutation Research-Fundamental and Molecular Mechanisms of Mutagenesis* **616**: 196-200

Shadley JD, Wiencke JK (1989) Induction of the Adaptive Response by X-Rays Is Dependent on Radiation Intensity. *International Journal of Radiation Biology* **56**: 107-118

Shall S, de Murcia G (2000) Poly(ADP-ribose) polymerase-1: what have we learned from the deficient mouse model? *Mutation Research-Dna Repair* **460**: 1-15

Shankar B, Pandey R, Sainis K (2006) Radiation-induced bystander effects and adaptive response in murine lymphocytes. *International Journal of Radiation Biology* **82**: 537-548

Shao C, Folkard M, Prise KM (2008a) Role of TGF-beta 1 and nitric oxide in the bystander response of irradiated glioma cells. *Oncogene* **27**: 434-440

Shao C, Lyng FM, Folkard M, Prise KM (2006) Calcium fluxes modulate the radiation-induced bystander responses in targeted glioma and fibroblast cells. *Radiat Res* **166**: 479-487

Shao C, Prise KM, Folkard M (2008b) Signaling factors for irradiated glioma cells induced bystander responses in fibroblasts. *Mutation Research-Fundamental and Molecular Mechanisms of Mutagenesis* **638**: 139-145

Shao C, Stewart V, Folkard M, Michael BA, Prise KM (2003) Nitric oxide-mediated signaling in the bystander response of individually targeted glioma cells. *Cancer Research* **63**: 8437-8442

Shao CL, Aoki M, Furusawa Y (2004) Bystander effect in lymphoma cells vicinal to irradiated neoplastic epithelial cells: Nitric oxide is involved. *Journal of Radiation Research* **45**: 97-103

Shao CL, Aoki M, Furusawa Y (2001) Medium-mediated bystander effects on HSG cells co-cultivated with cells irradiated by X-rays or a 290 MeV/u carbon beam. *Journal of Radiation Research* **42**: 305-316

Shao CL, Folkard M, Held KD, Prise KM (2008c) Estrogen enhanced cell-cell signalling in breast cancer cells exposed to targeted irradiation. *Bmc Cancer* **8**:

Short SC, Bourne S, Martindale C, Woodcock M, Jackson SP (2005) DNA damage responses at low radiation doses. *Radiation Research* **164**: 292-302

Short SC, Kelly J, Mayes CR, Woodcock M, Joiner MC (2001) Low-dose hypersensitivity after fractionated low-dose irradiation in vitro. *International Journal of Radiation Biology* **77**: 655-664

Short SC, Woodcock M, Marples B, Joiner MC (2003) Effects of cell cycle phase on low-dose hyper-radiosensitivity. *Int J Radiat Biol* **79**: 99-105

Shrivastav M, De Haro LP, Nickoloff JA (2008) Regulation of DNA double-strand break repair pathway choice. *Cell Research* **18**: 134-147

Siemann DW, Keng PC (1986) Cell cycle specific toxicity of the Hoechst 33342 stain in untreated or irradiated murine tumor cells. *Cancer Res* **46**: 3556-3559

Siles E, Villalobos M, Valenzuela MT, Nunez MI, Gordon A, Mcmillan TJ, Pedraza V, Ruiz de Almodovar JM (1996) Relationship between p53 status and radiosensitivity in human tumour cell lines. *Br J Cancer* **73**: 581-588

Simonsson M, Qvarnstrom F, Nyman J, Johansson KA, Garmo H, Turesson I (2008) Low-dose hypersensitive gammaH2AX response and infrequent apoptosis in epidermis from radiotherapy patients. *Radiother Oncol* **88**: 388-397

Sinclair WK (1968) Cyclic X-Ray Responses in Mammalian Cells in Vitro. *Radiation Research* **33**: 620-643

Sinclair WK (1966) *The Shape of Radiation Survival Curves of Mammalian Cells Cultured In Vitro. I: Biophysical Aspects of Radiation Quality*. (Technical Report Series No. 58), International Atomic Energy Agency: Vienna

Skarsgard LD, Skwarchuk MW, Wouters BG, Durand RE (1996) Substructure in the radiation survival response at low dose in cells of human tumor cell lines. *Radiat Res* **146**: 388-398

Skov KA (1999) Radioresponsiveness at low doses: hyper-radiosensitivity and increased radioresistance in mammalian cells. *Mutation Research-Fundamental and Molecular Mechanisms of Mutagenesis* **430**: 241-253

Skov KA, Koch CJ, Marples B (1995) Further investigations into the nature of the trigger of increased radioresistance: the effect of 14C and 3H thymidine incorporation on low dose hypersensitivity. In *Proceedings of workshop on "Radiation Damage in DNA: Relationships at early times".*, Zimbrick J, Fucarielli A (eds) pp 441-447. Batelle Publishing: Columbus, Ohio

Skov KA, Marples B, Matthews JB, Joiner MC, Zhou H (1994) A preliminary investigation into the extent of increased radioresistance or hyper-radiosensitivity in cells of hamster cell lines known to be deficient in DNA repair. *Radiat Res* **138**: S126-S129

Song CW, Griffin R, Park HJ (2006) Influence of Tumor pH on Therapeutic Response. In *Cancer Drug Resistance*, Teicher BA (ed) pp 21-42. Humana Press: Totowa, NJ

Spring PM, Arnold SM, Shajahan S, Brown B, Dey S, Lele SM, Valentino J, Jones R, Mohiuddin M, Ahmed MM (2004) Low dose fractionated radiation potentiates the effects of taxotere in nude mice xenografts of squamous cell carcinoma of head and neck. *Cell Cycle* **3**: 479-485

Steel GG (1997) *Basic Clinical Radiobiology*. Arnold: London

Stoilov LM, Mullenders LHF, Darroudi F, Natarajan AT (2007) Adaptive response to DNA and chromosomal damage induced by X-rays in human blood lymphocytes. *Mutagenesis* **22**: 117-122

Stokke T, Erikstein BK, Smedshammer L, Boye E, Steen HB (1993) The Retinoblastoma Gene-Product Is Bound in the Nucleus in Early G1-Phase. *Experimental Cell Research* **204**: 147-155

Straume T, Carsten AL (1993) Tritium Radiobiology and Relative Biological Effectiveness. *Health Physics* **65**: 657-672

Szabo C (2006) Poly(ADP-ribose) polymerase activation by reactive nitrogen species - Relevance for the pathogenesis of inflammation. *Nitric Oxide-Biology and Chemistry* **14**: 169-179

Szumiel I (2005) Adaptive response: stimulated DNA repair or decreased damage fixation? *International Journal of Radiation Biology* **81**: 233-241

Søvik Å (2002) *Lavdoseratebestråling av humane celler i kultur. Dosimetri og effektmålinger.* Cand. Scient. thesis: University of Oslo

Taylor AC (1962) Responses of cells to pH changes in the medium. *J Cell Biol* **15**: 201-209

Thomas C, Charrier J, Massart C, Cherel M, Fertil B, Barbet J, Foray N (2008) Low-dose hyper-radiosensitivity of progressive and regressive cells isolated from a rat colon tumour: Impact of DNA repair. *International Journal of Radiation Biology* **84**: 533-548

Vaganay-Juery S, Muller C, Marangoni E, Abdulkarim B, Deutsch E, Lambin P, Calsou P, Eschwege F, Salles B, Joiner M, Bourhis J (2000) Decreased DNA-PK activity in human cancer cells exhibiting hypersensitivity to low dose irradiation. *British Journal of Cancer* **83**: 514-+

Vasiliev JM, Gelfand IM, Guelstei VI (1971) Initiation of Dna Synthesis in Cell Cultures by Colcemid. *Proceedings of the National Academy of Sciences of the United States of America* **68**: 977-&

Vines AM, Lyng FM, McClean B, Seymour C, Mothersill CE (2008) Bystander signal production and response are independent processes which are cell line dependent. *International Journal of Radiation Biology* **84**: 83-90

Ward JF (1988) Dna Damage Produced by Ionizing-Radiation in Mammalian-Cells - Identities, Mechanisms of Formation, and Reparability. *Progress in Nucleic Acid Research and Molecular Biology* **35**: 95-125

Watson JV (1991) *Introduction to Flow Cytometry*. Cambridge University Press: Cambridge

Williams RS, Williams JS, Tainer JA (2007) Mre11-Rad50-Nbs1 is a keystone complex connecting DNA repair machinery, double-strand break signaling, and the chromatin template. *Biochemistry and Cell Biology-Biochimie et Biologie Cellulaire* **85**: 509-520

Wilson GD (2004) Radiation and the cell cycle, revisited. *Cancer and Metastasis Reviews* **23**: 209-225

Wilson GD, Marples B (2007) Flow cytometry in radiation research: past, present and future. *Radiat Res* **168**: 391-403

Wolff S (1998) The adaptive response in radiobiology: Evolving insights and implications. *Environmental Health Perspectives* **106**: 277-283

Wosikowski K, Regis JT, Robey RW, Alvarez M, Buters JT, Gudas JM, Bates SE (1995) Normal p53 status and function despite the development of drug resistance in human breast cancer cells. *Cell Growth Differ* **6**: 1395-1403

Wouters BG, Skarsgard LD (1997) Low-dose radiation sensitivity and induced radioresistance to cell killing in HT-29 cells is distinct from the "adaptive response" and cannot be explained by a subpopulation of sensitive cells. *Radiation Research* **148**: 435-442

Xu B, Kim ST, Lim DS, Kastan MB (2002) Two molecularly distinct G(2)/M checkpoints are induced by ionizing irradiation. *Molecular and Cellular Biology* **22**: 1049-1059

Xu WM, Liu LZ, Smith GCM, Charles IG (2000) Nitric oxide upregulates expression of DNA-PKcs to protect cells from DNA-damaging anti-tumour agents. *Nature Cell Biology* **2**: 339-345

Yan Y, Black CP, Cowan KH (2007) Irradiation-induced G2/M checkpoint response requires ERK1/2 activation. *Oncogene* **26**: 4689-4698

Zhao S, Weng YC, Yuan SSF, Lin YT, Hsu HC, Lin SCJ, Gerbino E, Song MH, Zdzienicka MZ, Gatti RA, Shay JW, Ziv Y, Shiloh Y, Lee EYHP (2000) Functional link between ataxia-telangiectasia and Nijmegen breakage syndrome gene products. *Nature* **405**: 473-477

Åmellem Ø, Sandvik JA, Stokke T, Pettersen EO (1998) The retinoblastoma protein-associated cell cycle arrest in S-phase under moderate hypoxia is disrupted in cells expressing HPV18 E7 oncoprotein. *British Journal of Cancer* **77**: 862-872

Åmellem Ø, Stokke T, Sandvik JA, Pettersen EO (1996) The retinoblastoma gene product is reversibly dephosphorylated and bound in the nucleus in S and G(2) phases during hypoxic stress. *Experimental Cell Research* **227**: 106-115

Appendix A: Dose-Survival Measurements on Asynchronous Cell Populations

A.1 List of Cell Batches

Batch nr.	Cell line	Date of thawing/priming
t1	T-47D	Thawed May 26th, 2006
t2	T-47D	Thawed October 5th, 2007
t3	T-47D	Thawed March 18th, 2008
t4	T-47D	Thawed August 20th, 2008
p1	T-47D-P	LDR-primed with 0.3 Gy August 17th, 2005. Cultured continuously since then, except for 42 days in cryostorage from Nov. 9th – Dec. 21st, 2006
p2	T-47D-P	Thawed March 18th, 2008. These were cells from batch p1 that had been kept in cryostorage since November 9th, 2006.
p3	T-47D-P	Thawed April 11th, 2008. These were cells from batch p1 that had been kept in cryostorage for just 2 weeks (in addition to the period in late 2006).

A.2 List of Experiments

Experiment	Cell batch	Priming dose	Challenge doses	Irr. setup (Ch. 3.3.2)	Comments
T1, T2	t1	-	0.1 – 2 Gy	A	7 cm Perspex shielding
T3, T4, T5	t1	-	0.1 – 2 Gy	B	Reduced Perspex shielding (1 cm)
T6, T7, T8	t2	-	0.1 – 2 Gy	B	New cell batch
T9, T10, T13	t2 (T13 - t3)	-	0.1 – 2 Gy	B (T13 – C)	Single-cell suspension prepared with 2-ml pipette
T11, T12, T15	t3	-	0.1 – 2 Gy	C	Temperature maintained at 37°C. Cells kept longer in trypsin and pumped very gently
T14, T20, T21, T23	t3	-	0.1 – 2 Gy	C	No centrifugation to remove trypsin
T17, T19, T24	t3	-	0.1 – 2 Gy	C	Pipetting error minimized
T16, T18, T22	t3	-	0.5 – 10 Gy	C	Measurements of high-dose response
A1, A2, A3	t3	-	0.1 – 2 Gy	C	Plating performed by another person
H1	t1	(65 ± 17) Gy	0.1 – 2 Gy	A	Grown in medium with tritium-labeled valine for 26 weeks
H2	t2	(0.3 ± 0.1) Gy	0.1 – 2 Gy	B	48 hours of tritium incorporation
H3	t2	(0.9 ± 0.2) Gy	0.1 – 2 Gy	B	96 hours of tritium incorporation
H4	t2	(2.0 ± 0.3) Gy	0.1 – 2 Gy	B	1 week (168 hours) of tritium incorporation
P1, P2	p1	0.3 Gy	0.1 – 2 Gy	B	Medium changed after one week.
P3	p2	0.3 Gy	0.1 – 2 Gy	B	The cells were thawed only 4 weeks prior to experiment. Medium changed after one week.
P4	p2	0.3 Gy	0.2 – 2 Gy	C	Same as for P3, but medium was not changed.
P5, P6, P7	p3	0.3 Gy	0.1 – 2 Gy	C	The cells were thawed 9-11 weeks prior to experiments. Medium was not changed.

A.3 Experimental Raw Data

All the raw data from the experiments listed in appendix A.2 are given in this section. The raw data of experiments with similar procedures are listed together, and the survival data from the individual experiments are plotted as a function of dose, with standard errors shown as error bars.

A.3.1 Initial Experiments with Unprimed Cells

Experiment T1	September 4, 2007								
Plating efficiency PE =	**1.047**				**Multiplicity M =**	**1.243**			
Dose (Gy)	**C**	**C**	**0.1**	**0.2**	**0.3**	**0.5**	**0.75**	**1**	**2**
flask 1	218	204	190	193	222	189	166	177	145
flask 2	203	217	218	197	187	210	186	187	157
flask 3	200	197	219	191	209	194	197	173	148
flask 4	215	224	203	198	166	188	186	182	160
flask 5	198	218	213		169	200	173	182	150
Number of cells seeded per flask	200	200	200	200	200	200	200	200	200
Mean number of colonies per flask: N		209.4	208.6	194.75	190.6	196.2	181.6	180.2	152
Standard error: ΔN		3.149	5.446	1.652	10.975	4.055	5.446	2.396	2.811
Surviving fraction: F			0.996	0.930	0.910	0.937	0.867	0.861	0.726
Standard error: ΔF			0.030	0.016	0.054	0.024	0.029	0.017	0.017
Surviving fraction corrected for multiplicity: S			0.995	0.910	0.886	0.919	0.834	0.826	0.672
Standard error: ΔS			0.040	0.020	0.067	0.030	0.035	0.021	0.020

Experiment T2	September 10, 2007								
Plating efficiency PE =	**0.892**				**Multiplicity M =**	**1.516**			
Dose (Gy)	**C**	**C**	**0.1**	**0.2**	**0.3**	**0.5**	**0.75**	**1**	**2**
flask 1	210	229	187	206	207	214	172	172	139
flask 2	235	202	217	231	214	216	197	184	187
flask 3	182	226	230	193	176	226	206	170	136
flask 4	232	238	195	212	222	212	222	202	134
flask 5	191	196		208	196	200	216	192	179
Number of cells seeded per flask	240	240	240	240	240	240	240	240	240
Mean number of colonies per flask: N		214.1	207.3	210.0	203.0	213.6	202.6	184.0	155.0
Standard error: ΔN		6.452	9.886	6.140	7.987	4.167	8.761	6.033	11.528
Surviving fraction: F			0.968	0.981	0.948	0.998	0.946	0.859	0.724
Standard error: ΔF			0.055	0.041	0.047	0.036	0.050	0.038	0.058
Surviving fraction corrected for multiplicity: S			0.938	0.962	0.903	0.995	0.900	0.767	0.600
Standard error: ΔS			0.100	0.079	0.081	0.073	0.085	0.053	0.065

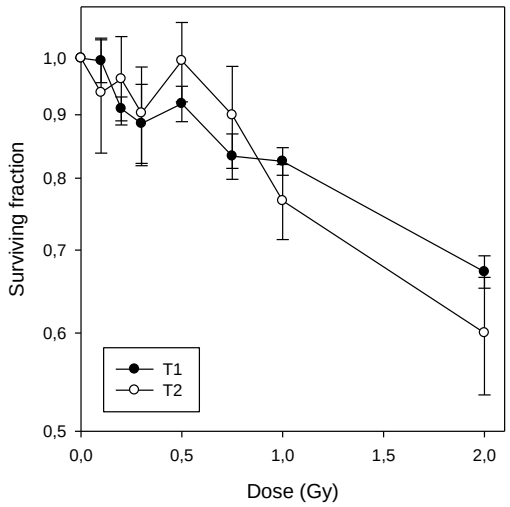

Acute irradiation of T-47D cells. The ^{60}Co source was shielded with 7 cm Perspex during irradiation. The dose rate was 1.0 Gy/min.

A.3.2 Reduced Perspex Shielding

Experiment T3	November 14, 2007								
Plating efficiency PE =	**0.639**			**Multiplicity M =**		**1.275**			
Dose (Gy)	**C**	**C**	**0.1**	**0.2**	**0.3**	**0.5**	**0.75**	**1**	**2**
flask 1	125	129	107	132	118	107	115	104	61
flask 2	124	117	113	126	122	104	109	90	64
flask 3	138	140	125	113	113	111	118	96	61
flask 4	140	115	108	134	125	116	121	107	60
flask 5	125	124	120	123	127	100	109	93	56
Number of cells seeded per flask	200	200	200	200	200	200	200	200	200
Mean number of colonies per flask: N		127.7	114.6	125.6	121	107.6	114.4	98	60.4
Standard error: ΔN		2.844	3.473	3.723	2.510	2.768	2.400	3.240	1.288
Surviving fraction: F			0.897	0.984	0.948	0.843	0.896	0.767	0.473
Standard error: ΔF			0.034	0.036	0.029	0.029	0.027	0.031	0.015
Surviving fraction corrected for multiplicity: S			0.865	0.978	0.930	0.798	0.863	0.711	0.407
Standard error: ΔS			0.042	0.049	0.038	0.035	0.035	0.035	0.015

Experiment T4	November 21, 2007								
Plating efficiency PE =	**0.790**			**Multiplicity M =**		**1.488**			
Dose (Gy)	**C**	**C**	**0.1**	**0.2**	**0.3**	**0.5**	**0.75**	**1**	**2**
flask 1	147	153	182	168	142	160	134	121	92
flask 2	168	157	144	188	152	147	135	138	102
flask 3	160	138	163	157	168	136	135	137	96
flask 4	157	157	158	145	142	145	156	118	92
flask 5	172	170	149	146	163	153	143	113	99
Number of cells seeded per flask	200	200	200	200	200	200	200	200	200
Mean number of colonies per flask: N		157.9	159.2	160.8	153.4	148.2	140.6	125.4	96.2
Standard error: ΔN		3.321	6.598	7.984	5.325	4.017	4.179	5.105	1.960
Surviving fraction: F			1.008	1.018	0.972	0.939	0.890	0.794	0.609
Standard error: ΔF			0.047	0.055	0.039	0.032	0.032	0.036	0.018
Surviving fraction corrected for multiplicity: S			1.008	1.018	0.947	0.891	0.818	0.690	0.487
Standard error: ΔS			0.047	0.055	0.070	0.052	0.047	0.045	0.019

Experiment T5	November 21, 2007								
Plating efficiency PE =	**1.042**				**Multiplicity M =**	**1.419**			
Dose (Gy)	**C**	**C**	**0.1**	**0.2**	**0.3**	**0.5**	**0.75**	**1**	**2**
flask 1	225	205	207	197	198	180	192	192	129
flask 2	202	189	213	227	200	213	172	169	148
flask 3	208	200	217	195	207	211	211	197	133
flask 4	220	226	194	193	210	204	165	194	144
flask 5	195	213	213	205	210	218	186	154	128
Number of cells seeded per flask	200	200	200	200	200	200	200	200	200
Mean number of colonies per flask: N		208.3	208.8	203.4	205	205.2	185.2	181.2	136.4
Standard error: ΔN		3.972	4.030	6.242	2.530	6.689	8.046	8.423	4.057
Surviving fraction: F			1.002	0.976	0.984	0.985	0.889	0.870	0.655
Standard error: ΔF			0.027	0.035	0.022	0.037	0.042	0.044	0.023
Surviving fraction corrected for multiplicity: S			1.002	0.961	0.973	0.975	0.830	0.804	0.551
Standard error: ΔS			0.027	0.057	0.037	0.062	0.059	0.059	0.025

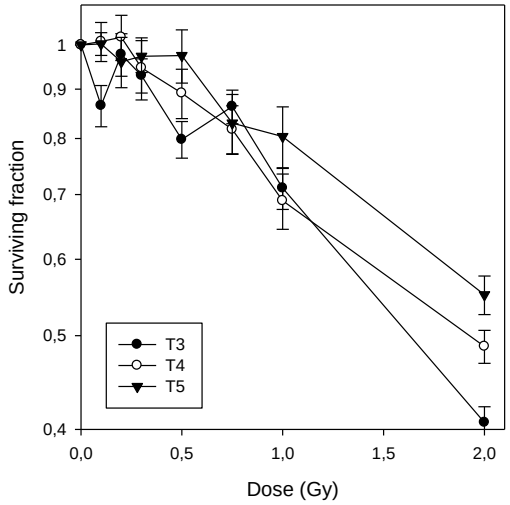

Acute irradiation of T-47D cells. The Perspex shielding was reduced to 1 cm, giving a dose rate of 1.3 Gy/min.

A.3.3 New Batch of Cells

Experiment T6	January 29, 2008								
Plating efficiency PE =	**0.775**				**Multiplicity M =**	**1.397**			
Dose (Gy)	**C**	**C**	**0.1**	**0.2**	**0.3**	**0.5**	**0.75**	**1**	**2**
flask 1	152	142	172	158	156	147	138	132	120
flask 2	132	146	153	163	151	156	152	136	122
flask 3	167	171	152	159	162	173	166	156	120
flask 4	158	158	168	159	153	158	140	136	107
flask 5	167	156	184	164	155	171	147	144	118
Number of cells seeded per flask	200	200	200	200	200	200	200	200	200
Mean number of colonies per flask: N		154.9	165.8	160.6	155.4	161	148.6	140.8	117.4
Standard error: ΔN		3.874	6.037	1.208	1.860	4.868	5.016	4.271	2.676
Surviving fraction: F			1.070	1.037	1.003	1.039	0.959	0.909	0.758
Standard error: ΔF			0.047	0.027	0.028	0.041	0.040	0.036	0.026
Surviving fraction corrected for multiplicity: S			1.070	1.037	1.003	1.039	0.935	0.862	0.670
Standard error: ΔS			0.047	0.027	0.028	0.041	0.062	0.050	0.031

Experiment T7	January 29, 2008								
Plating efficiency PE =	**0.708**				**Multiplicity M =**	**1.303**			
Dose (Gy)	**C**	**C**	**0.1**	**0.2**	**0.3**	**0.5**	**0.75**	**1**	**2**
flask 1	140	133	135	140	154	130	110	132	101
flask 2	144	145	119	127	141	143	145	119	96
flask 3	147	138	130	155	133	122	121	120	112
flask 4	149	125	129	146	151	150	117	119	91
flask 5	136	159	124	130	122	120	147	125	95
Number of cells seeded per flask	200	200	200	200	200	200	200	200	200
Mean number of colonies per flask: N		141.6	127.4	139.6	140.2	133	128	123	99
Standard error: ΔN		2.982	2.731	5.144	5.877	5.865	7.563	2.510	3.619
Surviving fraction: F			0.900	0.986	0.990	0.939	0.904	0.869	0.699
Standard error: ΔF			0.027	0.042	0.046	0.046	0.057	0.025	0.029
Surviving fraction corrected for multiplicity: S			0.864	0.980	0.986	0.916	0.870	0.825	0.628
Standard error: ΔS			0.035	0.059	0.066	0.061	0.073	0.032	0.033

Experiment T8	February 7, 2008								
Plating efficiency PE =	**1.029**				**Multiplicity M =**	**1.495**			
Dose (Gy)	**C**	**C**	**0.1**	**0.2**	**0.3**	**0.5**	**0.75**	**1**	**2**
flask 1	202	208	207	190	230	179	204	189	151
flask 2	201	204	199	210	208	233	203	186	130
flask 3	222	196	217	212	210	208	171	197	157
flask 4	216	204	187	204	179	203	165	162	157
flask 5	199		219		183	180	216	212	140
Number of cells seeded per flask	200	200	200	200	200	200	200	200	200
Mean number of colonies per flask: N		205.8	205.8	204.0	202.0	200.6	191.8	189.2	147.0
Standard error: ΔN		2.783	5.919	4.967	9.418	10.003	10.027	8.157	5.263
Surviving fraction: F			1.000	0.991	0.982	0.975	0.932	0.919	0.714
Standard error: ΔF			0.032	0.028	0.048	0.050	0.050	0.042	0.027
Surviving fraction corrected for multiplicity: S			1.000	0.983	0.965	0.952	0.880	0.860	0.595
Standard error: ΔS			0.032	0.053	0.088	0.091	0.081	0.065	0.031

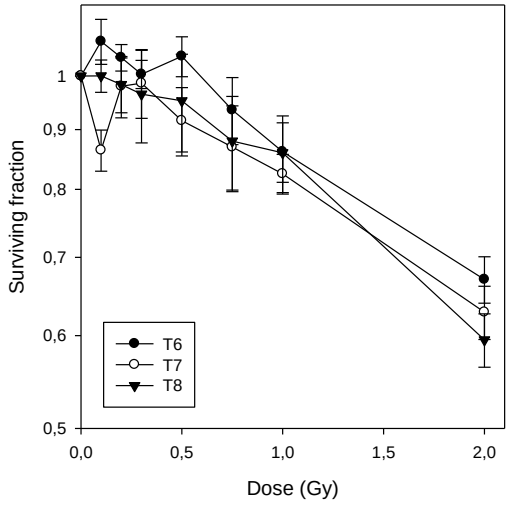

Acute irradiation of T-47D cells. These three experiments used cells from a different batch than in the first five experiments (T1-T5).

A.3.4 Single-Cell Suspension Prepared without Syringe and Cannula

Experiment T9	March 5, 2008								
Plating efficiency PE =	**0.626**			**Multiplicity M =**		**1.447**			
Dose (Gy)	**C**	**C**	**0.1**	**0.2**	**0.3**	**0.5**	**0.75**	**1**	**2**
flask 1	144	121	109	130	122	104	117	116	78
flask 2	137	124	123	111	130	101	115	117	66
flask 3	122	116	120	108	120	120	106	90	82
flask 4	139	122	112	130	121	119	99	94	82
flask 5	120	106	114	114	113	126	119	94	71
Number of cells seeded per flask	200	200	200	200	200	200	200	200	200
Mean number of colonies per flask: N		125.1	115.6	118.6	121.2	114	111.2	102.2	75.8
Standard error: ΔN		3.656	2.581	4.750	2.709	4.868	3.774	5.886	3.169
Surviving fraction: F			0.924	0.948	0.969	0.911	0.889	0.817	0.606
Standard error: ΔF			0.034	0.047	0.036	0.047	0.040	0.053	0.031
Surviving fraction corrected for multiplicity: S			0.875	0.912	0.946	0.856	0.824	0.729	0.494
Standard error: ΔS			0.051	0.075	0.059	0.069	0.056	0.067	0.032

Experiment T10	March 5, 2008								
Plating efficiency PE =	**0.476**			**Multiplicity M =**		**1.353**			
Dose (Gy)	**C**	**C**	**0.1**	**0.2**	**0.3**	**0.5**	**0.75**	**1**	**2**
flask 1	94	96	112	83	116	85	79	88	56
flask 2	102	84	90	89	83	87	89	80	72
flask 3	88	105	92	87	100	84	98	86	65
flask 4	107	84	88	89	110	87	71	73	54
flask 5	105	87	95	88	102	91	66	87	60
Number of cells seeded per flask	200	200	200	200	200	200	200	200	200
Mean number of colonies per flask: N		95.2	95.4	87.2	102.2	86.8	80.6	82.8	61.4
Standard error: ΔN		2.886	4.308	1.114	5.589	1.200	5.836	2.818	3.250
Surviving fraction: F			1.002	0.916	1.074	0.912	0.847	0.870	0.645
Standard error: ΔF			0.055	0.030	0.067	0.030	0.066	0.040	0.039
Surviving fraction corrected for multiplicity: S			1.002	0.878	1.074	0.872	0.788	0.817	0.558
Standard error: ΔS			0.055	0.041	0.067	0.041	0.084	0.051	0.042

Experiment T13	April 23, 2008								
Plating efficiency PE =	**0.442**			**Multiplicity M =**		**1.427**			
Dose (Gy)	**C**	**C**	**0.1**	**0.2**	**0.3**	**0.5**	**0.75**	**1**	**2**
flask 1	101	82	89	96	86	89	79	88	66
flask 2	76	98	80	102	89	69	65	55	73
flask 3	98	93	84	87	86	79	91	90	60
flask 4	73	77	92	90	102	97	81	71	74
flask 5	90	95	93	76	76	69	80	65	79
Number of cells seeded per flask	200	200	200	200	200	200	200	200	200
Mean number of colonies per flask: N		88.3	87.6	90.2	87.8	80.6	79.2	73.8	70.4
Standard error: ΔN		3.287	2.462	4.386	4.176	5.528	4.152	6.719	3.326
Surviving fraction: F			0.992	1.022	0.994	0.913	0.897	0.836	0.797
Standard error: ΔF			0.046	0.063	0.060	0.071	0.058	0.082	0.048
Surviving fraction corrected for multiplicity: S			0.986	1.022	0.990	0.862	0.839	0.757	0.709
Standard error: ΔS			0.079	0.063	0.103	0.103	0.081	0.106	0.059

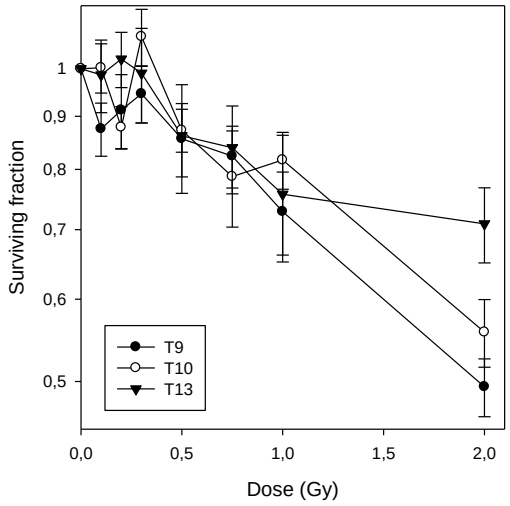

Acute irradiation of T-47D cells. The single-cell suspension to be plated was prepared by gentle pumping with a 2-ml pipette.

A.3.5 Temperature Maintained at 37°C

Experiment T11	April 18, 2008								
Plating efficiency PE =	**0.719**			**Multiplicity M =**		**1.303**			
Dose (Gy)	**C**	**C**	**0.1**	**0.2**	**0.3**	**0.5**	**0.75**	**1**	**2**
flask 1	152	129	144	140	135	131	121	139	105
flask 2	146	139	131	132	123	176	113	121	119
flask 3	143	148	145	128	148	140	144	138	115
flask 4	150	156	125	159	103	136	136	154	118
flask 5	142	132	125	129	141	131	138	116	108
Number of cells seeded per flask	200	200	200	200	200	200	200	200	200
Mean number of colonies per flask: N		143.7	134	137.6	130	142.8	130.4	133.6	113
Standard error: ΔN		2.712	4.427	5.750	7.899	8.470	5.767	6.831	2.775
Surviving fraction: F			0.932	0.958	0.905	0.994	0.907	0.930	0.786
Standard error: ΔF			0.035	0.044	0.058	0.062	0.044	0.051	0.024
Surviving fraction corrected for multiplicity: S			0.907	0.941	0.871	0.991	0.874	0.903	0.726
Standard error: ΔS			0.047	0.060	0.074	0.088	0.057	0.067	0.029

Experiment T12	April 18, 2008								
Plating efficiency PE =	**0.920**			**Multiplicity M =**		**1.353**			
Dose (Gy)	**C**	**C**	**0.1**	**0.2**	**0.3**	**0.5**	**0.75**	**1**	**2**
flask 1	209	198	189	184	170	200	155	179	143
flask 2	194	187	180	188	189	170	154	169	134
flask 3	188	180	177	182	200	170	160	153	144
flask 4	187	151	178	170	183	185	164	163	160
flask 5	162	184	161	183	183	170	172	167	172
Number of cells seeded per flask	200	200	200	200	200	200	200	200	200
Mean number of colonies per flask: N		184	177	181.4	185	179	161	166.2	150.6
Standard error: ΔN		5.317	4.528	3.027	4.868	6.000	3.286	4.224	6.794
Surviving fraction: F			0.962	0.986	1.005	0.973	0.875	0.903	0.818
Standard error: ΔF			0.037	0.033	0.039	0.043	0.031	0.035	0.044
Surviving fraction corrected for multiplicity: S			0.943	0.978	1.005	0.959	0.824	0.861	0.753
Standard error: ΔS			0.054	0.050	0.039	0.064	0.041	0.047	0.054

Experiment T15	May 1, 2008								
Plating efficiency PE =	**0.749**			**Multiplicity M =**		**1.430**			
Dose (Gy)	**C**	**C**	**0.1**	**0.2**	**0.3**	**0.5**	**0.75**	**1**	**2**
flask 1	153	134	153	155	159	133	141	137	112
flask 2	158	142	147	165	132	127	149	157	111
flask 3	168	147	135	167	142	124	130	134	121
flask 4	128	152	126	152	138	148	127	144	117
flask 5	159	157		159	134	143	157	145	130
Number of cells seeded per flask	200	200	200	200	200	200	200	200	200
Mean number of colonies per flask: N		149.8	140.25	159.6	141	135	140.8	143.4	118.2
Standard error: ΔN		3.864	6.047	2.857	4.817	4.593	5.643	3.982	3.455
Surviving fraction: F			0.936	1.065	0.941	0.901	0.940	0.957	0.789
Standard error: ΔF			0.047	0.033	0.040	0.038	0.045	0.036	0.031
Surviving fraction corrected for multiplicity: S			0.896	1.065	0.904	0.845	0.902	0.929	0.698
Standard error: ΔS			0.071	0.033	0.062	0.055	0.069	0.058	0.038

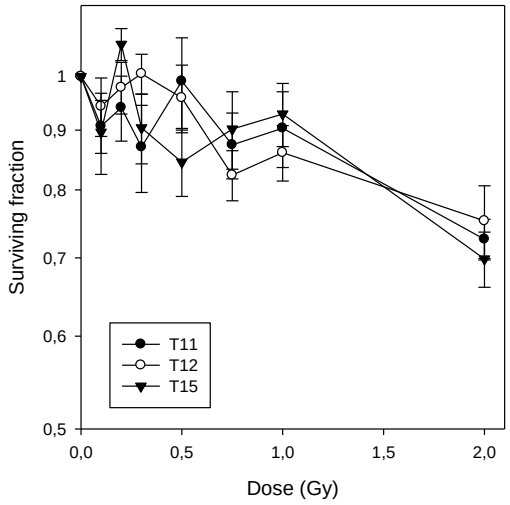

Acute irradiation of T-47D cells. The temperature was maintained at 37°C during irradiation. The cells were also kept longer in trypsin (~10 min) and pumped very gently in order to prepare the single-cell suspension for plating.

A.3.6 Centrifugation Avoided

Experiment T14	April 23, 2008								
Plating efficiency PE =	**1.025**			**Multiplicity M =**		**1.467**			
Dose (Gy)	**C**	**C**	**0.1**	**0.2**	**0.3**	**0.5**	**0.75**	**1**	**2**
flask 1	210	189	175	175	183	178	177	152	159
flask 2	198	198	191	209	178	166	177	182	132
flask 3	196	218	216	203	186	164	189	188	154
flask 4	222	214	212	169	173	172	191	184	166
flask 5	208	196	175	195	206		194	173	141
Number of cells seeded per flask	200	200	200	200	200	200	200	200	200
Mean number of colonies per flask: N		204.9	193.8	190.2	185.2	170	185.6	175.8	150.4
Standard error: ΔN		3.478	8.772	7.813	5.652	3.162	3.600	6.437	6.153
Surviving fraction: F			0.946	0.928	0.904	0.830	0.906	0.858	0.734
Standard error: ΔF			0.046	0.041	0.032	0.021	0.023	0.035	0.033
Surviving fraction corrected for multiplicity: S			0.906	0.878	0.842	0.740	0.844	0.777	0.625
Standard error: ΔS			0.074	0.064	0.047	0.028	0.035	0.047	0.038

Experiment T20 May 29, 2008

Plating efficiency PE =	**0.612**			**Multiplicity M =**		**1.436**			
Dose (Gy)	**C**	**C**	**0.1**	**0.2**	**0.3**	**0.5**	**0.75**	**1**	**2**
flask 1	144	125	123	112	118	108	119	108	95
flask 2	114	99	114	129	118	127	102	126	102
flask 3	126	109	86	118	126	128	91	115	93
flask 4	135	122	115	119	103	99	102	109	89
flask 5	122	128	118	107	123	112	115	125	104
Number of cells seeded per flask	200	200	200	200	200	200	200	200	200
Mean number of colonies per flask: N		122.4	111.2	117	117.6	114.8	105.8	116.6	96.6
Standard error: ΔN		4.047	6.492	3.701	3.957	5.598	5.034	3.829	2.804
Surviving fraction: F			0.908	0.956	0.961	0.938	0.864	0.953	0.789
Standard error: ΔF			0.061	0.044	0.045	0.055	0.050	0.044	0.035
Surviving fraction corrected for multiplicity: S			0.854	0.926	0.934	0.898	0.793	0.921	0.697
Standard error: ΔS			0.088	0.070	0.073	0.085	0.068	0.070	0.043

Experiment T21 June 5, 2008

Plating efficiency PE =	**0.659**			**Multiplicity M =**		**1.637**			
Dose (Gy)	**C**	**C**	**0.1**	**0.2**	**0.3**	**0.5**	**0.75**	**1**	**2**
flask 1	134	126	114	137	140	122	124	137	97
flask 2	131	127	128	132	135	121	142	118	104
flask 3	123	127	145	119	132	130	117	109	98
flask 4	121	156	134	137	130	148	125	139	110
flask 5	142		131	142	140	118	136	142	115
Number of cells seeded per flask	200	200	200	200	200	200	200	200	200
Mean number of colonies per flask: N		131.9	130.4	133.4	135.4	127.8	128.8	129	104.8
Standard error: ΔN		3.668	5.006	3.932	2.040	5.426	4.488	6.535	3.455
Surviving fraction: F			0.989	1.011	1.027	0.969	0.977	0.978	0.795
Standard error: ΔF			0.047	0.041	0.032	0.049	0.044	0.057	0.034
Surviving fraction corrected for multiplicity: S			0.970	1.011	1.027	0.925	0.941	0.945	0.650
Standard error: ΔS			0.117	0.041	0.032	0.107	0.100	0.131	0.043

Experiment T23 June 12, 2008

Plating efficiency PE =	**0.736**			**Multiplicity M =**		**1.619**			
Dose (Gy)	**C**	**C**	**0.1**	**0.2**	**0.3**	**0.5**	**0.75**	**1**	**2**
flask 1	132	144	137	131	139	137	150	139	116
flask 2	160	161	138	154	161	140	158	119	115
flask 3	132	151	147	148	136	158	115	144	111
flask 4	130	166	147	162	129	147	129	135	129
flask 5	137	158	126	132	117	163	109	130	138
Number of cells seeded per flask	200	200	200	200	200	200	200	200	200
Mean number of colonies per flask: N		147.1	139	145.4	136.4	149	132.2	133.4	121.8
Standard error: ΔN		4.360	3.886	6.096	7.222	5.030	9.557	4.273	5.054
Surviving fraction: F			0.945	0.988	0.927	1.013	0.899	0.907	0.828
Standard error: ΔF			0.039	0.051	0.056	0.046	0.070	0.040	0.042
Surviving fraction corrected for multiplicity: S			0.879	0.971	0.847	1.013	0.799	0.813	0.697
Standard error: ΔS			0.073	0.122	0.099	0.046	0.112	0.065	0.056

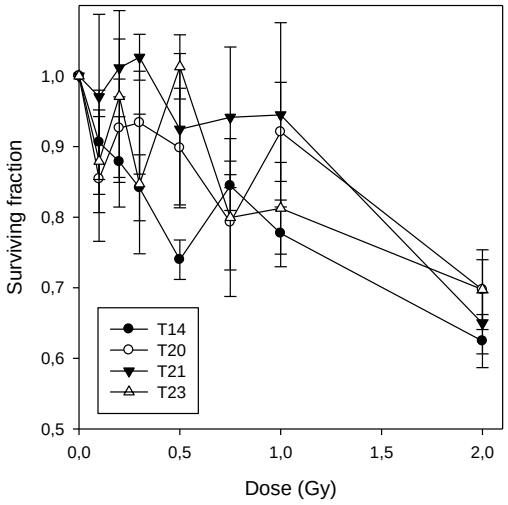

Acute irradiation of T-47D cells. Four experiments were performed where centrifugation to remove trypsin was avoided.

A.3.7 Pipetting Error Diminished

Experiment T17	May 16, 2008								
Plating efficiency PE =	**0.559**			**Multiplicity M =**		**1.593**			
Dose (Gy)	**C**	**C**	**0.1**	**0.2**	**0.3**	**0.5**	**0.75**	**1**	**2**
flask 1	107	126	110	126	112	115	117	118	119
flask 2	99	116	108	109	114	114	112	108	111
flask 3	105	126	100	108	100	106	101	118	95
flask 4	104	119	99	106	97	112	97	104	95
flask 5	104		121	102	100	99	113	94	99
Number of cells seeded per flask	200	200	200	200	200	200	200	200	200
Mean number of colonies per flask: N		111.8	107.6	110.2	104.6	109.2	108.0	108.4	103.8
Standard error: ΔN		3.390	3.982	4.128	3.487	2.990	3.821	4.534	4.800
Surviving fraction: F			0.963	0.986	0.936	0.977	0.966	0.970	0.929
Standard error: ΔF			0.046	0.048	0.042	0.040	0.045	0.050	0.051
Surviving fraction corrected for multiplicity: S			0.918	0.967	0.868	0.947	0.925	0.932	0.855
Standard error: ΔS			0.091	0.107	0.075	0.085	0.091	0.103	0.089

Experiment T19	May 29, 2008								
Plating efficiency PE =	**1.041**			**Multiplicity M =**		**1.568**			
Dose (Gy)	**C**	**C**	**0.1**	**0.2**	**0.3**	**0.5**	**0.75**	**1**	**2**
flask 1	200	207	227	204	216	198	202	211	164
flask 2	229	216	209	194	199	176	175	204	181
flask 3	198	176	207	184	217	209	199	198	148
flask 4	198	220	183	207	192	180	212	210	171
flask 5	230	208	209	212	200	199	196	201	178
Number of cells seeded per flask	200	200	200	200	200	200	200	200	200
Mean number of colonies per flask: N		208.2	207	200.2	204.8	192.4	196.8	204.8	168.4
Standard error: ΔN		5.187	7.014	5.004	4.974	6.218	6.078	2.518	5.887
Surviving fraction: F			0.994	0.962	0.984	0.924	0.945	0.984	0.809
Standard error: ΔF			0.042	0.034	0.034	0.038	0.038	0.027	0.035
Surviving fraction corrected for multiplicity: S			0.987	0.920	0.964	0.853	0.889	0.964	0.687
Standard error: ΔS			0.094	0.065	0.072	0.063	0.067	0.058	0.045

Experiment T24	July 1, 2008								
Plating efficiency PE =	**0.618**				**Multiplicity M =**	**1.675**			
Dose (Gy)	**C**	**C**	**0.1**	**0.2**	**0.3**	**0.5**	**0.75**	**1**	**2**
flask 1	126	132	124	138	139	134	121	128	110
flask 2	112	120	127	128	118	124	120	114	108
flask 3	126	134	136	121	123	107	119	132	110
flask 4	116	121	131	136	118	128	127	128	98
flask 5	119	129	124	124	121	108	108	112	110
Number of cells seeded per flask	200	200	200	200	200	200	200	200	200
Mean number of colonies per flask: N		123.5	128.4	129.4	123.8	120.2	119	122.8	107.2
Standard error: ΔN		2.242	2.293	3.311	3.917	5.426	3.082	4.079	2.332
Surviving fraction: F			1.040	1.048	1.002	0.973	0.964	0.994	0.868
Standard error: ΔF			0.026	0.033	0.037	0.047	0.030	0.038	0.025
Surviving fraction corrected for multiplicity: S			1.040	1.048	1.002	0.928	0.906	0.983	0.737
Standard error: ΔS			0.026	0.033	0.037	0.112	0.068	0.108	0.037

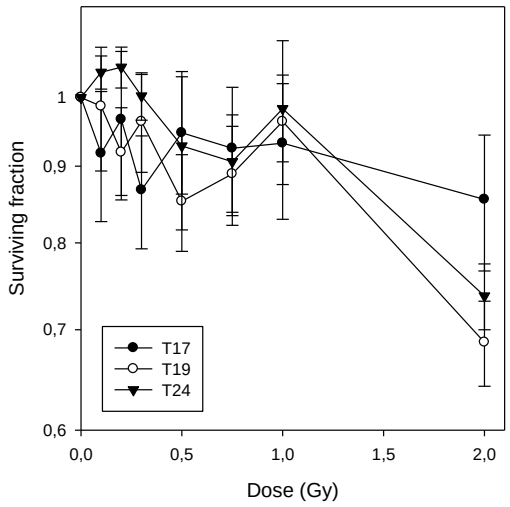

Acute irradiation of T-47D cells. By reducing the cell concentration in the stock suspension from 200 to 50 cells/ml, the pipetting error was diminished.

A.3.8 Radiosensitivity in the High-Dose Range

Experiment T16	May 1, 2008							
Plating efficiency PE =	**0.463**			**Multiplicity M =**	**1.414**			
Dose (Gy)	**C**	**C**	**0.5**	**1**	**2**	**5**	**7.5**	**10**
flask 1	90	93	86	76	89	84	98	59
flask 2	82	105	106	80	74	103	119	63
flask 3	111	91	100	100	72	98	130	56
flask 4	100	88	79	91	66	94	98	76
flask 5	73		94	101	73	109	124	52
Number of cells seeded per flask	200	200	200	200	200	600	2000	6000
Mean number of colonies per flask: N		92.6	93.0	89.6	74.8	97.6	113.8	61.2
Standard error: ΔN		3.863	4.817	5.085	3.813	4.226	6.681	4.116
Surviving fraction: F			1.005	0.968	0.808	0.352	0.123	0.022
Standard error: ΔF			0.0668	0.0682	0.0532	0.0211	0.0089	0.0017
Surviving fraction corrected for multiplicity: S			1.005	0.947	0.726	0.270	0.089	0.016
Standard error: ΔS			0.0668	0.1084	0.0659	0.0184	0.0069	0.0013

Experiment T18	May 16, 2008							
Plating efficiency PE =	**0.677**				**Multiplicity M =**	**1.369**		
Dose (Gy)	**C**	**C**	**0.5**	**1**	**2**	**5**	**7.5**	**10**
flask 1	129	139	119	118	108	146	109	62
flask 2	132	131	140	141	114	106	115	66
flask 3	137	134	128	126	106	116	114	57
flask 4	139	133	128	112	121	141	112	59
flask 5	140	140	134	127	105	134	103	62
Number of cells seeded per flask	200	200	200	200	200	600	2000	6000
Mean number of colonies per flask: N		135.4	129.8	124.8	110.8	128.6	110.6	61.2
Standard error: ΔN		1.293	3.499	4.893	2.990	7.600	2.159	1.530
Surviving fraction: F			0.959	0.922	0.818	0.317	0.082	0.015
Standard error: ΔF			0.02741	0.03719	0.02342	0.01895	0.00177	0.00040
Surviving fraction corrected for multiplicity: S			0.937	0.884	0.749	0.248	0.061	0.011
Standard error: ΔS			0.04054	0.05207	0.02952	0.01666	0.00186	0.00038

Experiment T22	June 5, 2008							
Plating efficiency PE =	**1.092**				**Multiplicity M =**	**1.458**		
Dose (Gy)	**C**	**C**	**0.5**	**1**	**2**	**5**	**7.5**	**10**
flask 1	218	204	203	210	164	185	153	106
flask 2	240	207	197	182	194	166	151	92
flask 3	234	207	212	206	163	169	184	103
flask 4	201	217	206	189	184	162	137	86
flask 5	230	225	212	190	163	160	140	96
Number of cells seeded per flask	200	200	200	200	200	600	2000	6000
Mean number of colonies per flask: N		218.3	206	195.4	173.6	168.4	153	96.6
Standard error: ΔN		4.295	2.846	5.363	6.485	4.434	8.337	3.628
Surviving fraction: F			0.944	0.895	0.795	0.257	0.070	0.015
Standard error: ΔF			0.02269	0.03023	0.03358	0.00845	0.00406	0.00063
Surviving fraction corrected for multiplicity: S			0.904	0.831	0.699	0.187	0.049	0.010
Standard error: ΔS			0.03624	0.04378	0.04177	0.00747	0.00304	0.00048

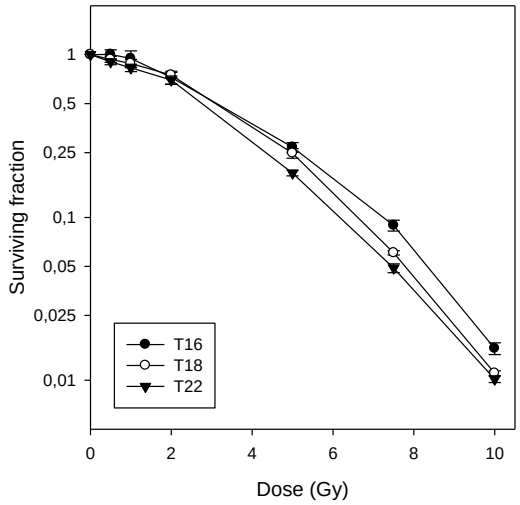

Acute irradiation of T-47D cells. The cells were irradiated with doses up to 10 Gy to determine the high-dose response.

A.3.9 Plating Performed by another Person

Experiment A1	May 21, 2008								
Plating efficiency PE =	**0.472**			**Multiplicity M =**		**1.834**			
Dose (Gy)	**C**	**C**	**0.1**	**0.2**	**0.3**	**0.5**	**0.75**	**1**	**2**
flask 1	90	111	80	77	99	94	89	76	59
flask 2	86	88	108	75	81	97	118	89	69
flask 3	92	106	83	83	85	103	88	78	76
flask 4	90	87	83	105	84	93	89	85	59
flask 5	107	87	77	103	95	85	82	88	66
Number of cells seeded per flask	200	200	200	200	200	200	200	200	200
Mean number of colonies per flask: N		94.4	86.2	88.6	88.8	94.4	93.2	83.2	65.8
Standard error: ΔN		3.045	5.562	6.431	3.470	2.926	6.336	2.634	3.216
Surviving fraction: F			0.913	0.939	0.941	1.000	0.987	0.881	0.697
Standard error: ΔF			0.066	0.075	0.048	0.045	0.074	0.040	0.041
Surviving fraction corrected for multiplicity: S			0.762	0.810	0.815	1.000	0.941	0.709	0.489
Standard error: ΔS			0.117	0.155	0.101	0.045	0.281	0.062	0.041

Experiment A2	June 30, 2008								
Plating efficiency PE =	**1.224**			**Multiplicity M =**		**2.122**			
Dose (Gy)	**C**	**C**	**0.1**	**0.2**	**0.3**	**0.5**	**0.75**	**1**	**2**
flask 1	263	231	244	248	260	263	234	247	223
flask 2	263	260	270	262	271	253	227	250	217
flask 3	265	225	250	258	245	248	256	210	212
flask 4	249	233	244	236	241	257	256	216	221
flask 5	238	220	255	227	234	231	232	224	205
Number of cells seeded per flask	200	200	200	200	200	200	200	200	200
Mean number of colonies per flask: N		244.7	252.6	246.2	250.2	250.4	241	229.4	215.6
Standard error: ΔN		5.479	4.812	6.576	6.719	5.437	6.229	8.122	3.250
Surviving fraction: F			1.032	1.006	1.022	1.023	0.985	0.937	0.881
Standard error: ΔF			0.030	0.035	0.036	0.032	0.034	0.039	0.024
Surviving fraction corrected for multiplicity: S			1.032	1.006	1.022	1.023	0.817	0.703	0.616
Standard error: ΔS			0.030	0.035	0.036	0.032	0.118	0.073	0.034

Experiment A3	June 30, 2008								
Plating efficiency PE =	**0.806**			**Multiplicity M =**		**1.635**			
Dose (Gy)	**C**	**C**	**0.1**	**0.2**	**0.3**	**0.5**	**0.75**	**1**	**2**
flask 1	162	172	173	165	164	152	167	179	132
flask 2	157	170	143	153	153	148	164	140	105
flask 3	169	155	160	152	162	176	146	143	122
flask 4	150	147	163	138	153	150	143	136	136
flask 5	159	170	151	166	147	169	147	141	149
Number of cells seeded per flask	200	200	200	200	200	200	200	200	200
Mean number of colonies per flask: N		161.1	158	154.8	155.8	159	153.4	147.8	128.8
Standard error: ΔN		2.830	5.138	5.113	3.153	5.657	5.006	7.883	7.358
Surviving fraction: F			0.981	0.961	0.967	0.987	0.952	0.917	0.800
Standard error: ΔF			0.036	0.036	0.026	0.039	0.035	0.052	0.048
Surviving fraction corrected for multiplicity: S			0.951	0.908	0.921	0.966	0.890	0.826	0.656
Standard error: ΔS			0.085	0.075	0.056	0.096	0.070	0.088	0.060

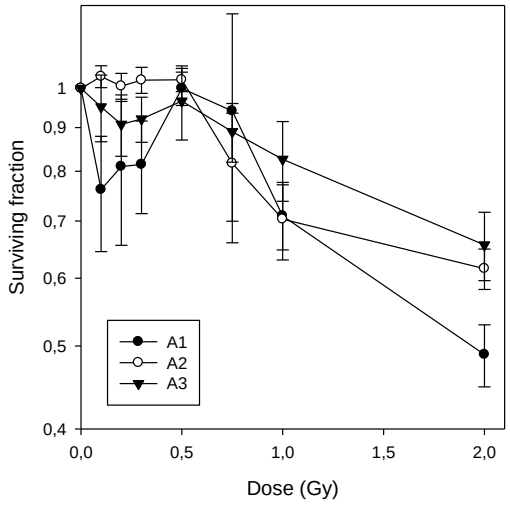

Acute irradiation of T-47D cells. In these three experiments, the cells were plated by another person (P. Mikolajewska, PhD-student, DNR).

A.3.10 Priming Dose Given by Incorporation of Tritium-Labeled Valine

Experiment H1	September 26, 2007								
Plating efficiency PE =	**0.641**			**Multiplicity M =**		**1.603**			
Dose (Gy)	**C**	**C**	**0.1**	**0.2**	**0.3**	**0.5**	**0.75**	**1**	**2**
flask 1	152	153	142	132	123	146	125	118	77
flask 2	125	124	141	124	112	118	120	106	109
flask 3	119	134	126	130	120	120	124	94	80
flask 4	115	129	137	108	134	129	114	104	96
flask 5	118	113	124	129	116	125	127	118	84
Number of cells seeded per flask	200	200	200	200	200	200	200	200	200
Mean number of colonies per flask: N		128.2	134	124.6	121	127.6	122	108	89.2
Standard error: ΔN		4.519	3.782	4.354	3.742	4.986	2.302	4.561	5.911
Surviving fraction: F			1.045	0.972	0.944	0.995	0.952	0.842	0.696
Standard error: ΔF			0.047	0.048	0.044	0.052	0.038	0.046	0.052
Surviving fraction corrected for multiplicity: S			1.045	0.936	0.880	0.988	0.895	0.721	0.546
Standard error: ΔS			0.047	0.102	0.082	0.127	0.073	0.064	0.056

Experiment H2	February 20, 2008								
Plating efficiency PE =	**0.524**			**Multiplicity M =**		**1.354**			
Dose (Gy)	**C**	**C**	**0.1**	**0.2**	**0.3**	**0.5**	**0.75**	**1**	**2**
flask 1	109	103	96	100	103	101	112	108	65
flask 2	111	112	120	109	104	102	90	74	85
flask 3	97	100	103	128	118	93	119	92	70
flask 4	100	113	102	89	130	102	100	86	89
flask 5	109	93	127	131	98	109	88	81	73
Number of cells seeded per flask	200	200	200	200	200	200	200	200	200
Mean number of colonies per flask: N		104.7	109.6	111.4	110.6	101.4	101.8	88.2	76.4
Standard error: ΔN		2.216	5.904	8.054	5.879	2.542	6.053	5.765	4.556
Surviving fraction: F			1.047	1.064	1.056	0.968	0.972	0.842	0.730
Standard error: ΔF			0.061	0.080	0.060	0.032	0.061	0.058	0.046
Surviving fraction corrected for multiplicity: S			1.047	1.064	1.056	0.952	0.958	0.782	0.649
Standard error: ΔS			0.061	0.080	0.060	0.047	0.091	0.073	0.052

Experiment H3	February 22, 2008								
Plating efficiency PE =	**0.499**			**Multiplicity M =**		**1.320**			
Dose (Gy)	**C**	**C**	**0.1**	**0.2**	**0.3**	**0.5**	**0.75**	**1**	**2**
flask 1	105	89	98	94	96	78	91	103	54
flask 2	90	97	102	96	107	103	98	78	72
flask 3	120	102	102	99	90	102	84	100	54
flask 4	92	99	99	88	83	87	71	80	73
flask 5	101	103		109	84	114	77	77	68
Number of cells seeded per flask	200	200	200	200	200	200	200	200	200
Mean number of colonies per flask: N		99.8	100.25	97.2	92	96.8	84.2	87.6	64.2
Standard error: ΔN		2.855	1.031	3.455	4.416	6.367	4.810	5.715	4.247
Surviving fraction: F			1.005	0.974	0.922	0.970	0.844	0.878	0.643
Standard error: ΔF			0.031	0.044	0.052	0.070	0.054	0.063	0.046
Surviving fraction corrected for multiplicity: S			1.005	0.962	0.891	0.957	0.791	0.833	0.565
Standard error: ΔS			0.031	0.063	0.069	0.098	0.067	0.080	0.049

Experiment H4	February 25, 2008								
Plating efficiency PE =	**0.509**			**Multiplicity M =**		**1.322**			
Dose (Gy)	**C**	**C**	**0.1**	**0.2**	**0.3**	**0.5**	**0.75**	**1**	**2**
flask 1	110	97	106	111	99	90	86	77	74
flask 2	108	106	117	111	106	118	97	79	68
flask 3	115	114	106	104	93	101	85	97	76
flask 4	91	93	111	103	93	114	73	83	59
flask 5	83	100	100	97	117	109	87	94	74
Number of cells seeded per flask	200	200	200	200	200	200	200	200	200
Mean number of colonies per flask: N		101.7	108	105.2	101.6	106.4	85.6	86	70.2
Standard error: ΔN		3.367	3.182	2.653	4.534	4.986	3.816	4.025	3.105
Surviving fraction: F			1.062	1.034	0.999	1.046	0.842	0.846	0.690
Standard error: ΔF			0.047	0.043	0.056	0.060	0.047	0.048	0.038
Surviving fraction corrected for multiplicity: S			1.062	1.034	0.999	1.046	0.788	0.793	0.614
Standard error: ΔS			0.047	0.043	0.082	0.060	0.058	0.060	0.042

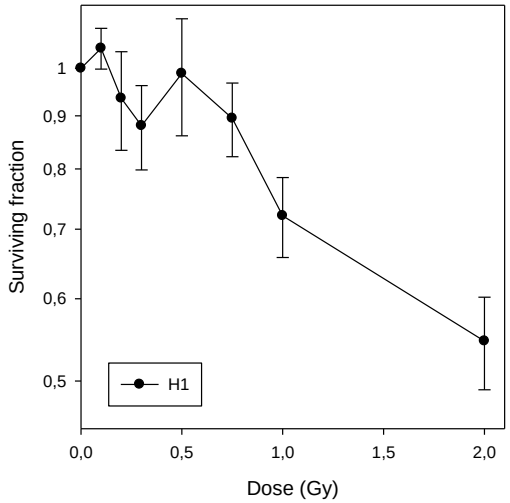

Acute irradiation of T-47D cells that had been primed by incorporation of tritium-labeled valine. The priming dose rate was (0.015 ± 0.004) Gy/h under steady-state conditions. Experiment H1 had been given a (65 ± 17) Gy priming dose.

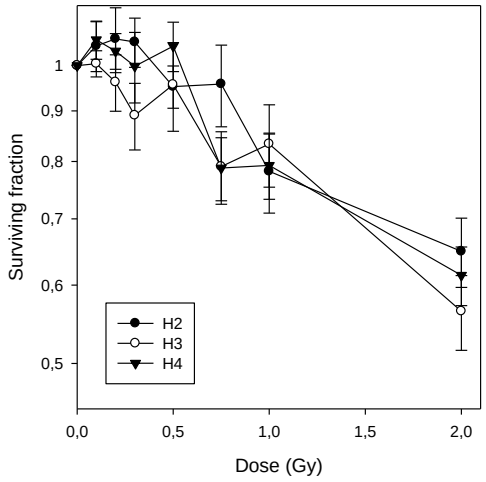

Acute irradiation of T-47D cells that had been primed by incorporation of tritium-labeled valine. The priming dose rate was (0.015 ± 0.004) Gy/h under steady-state conditions. Experiments H2, H3 and H4 had been primed with (0.3 ± 0.1) Gy, (0.9 ± 0.2) Gy and (2.0 ± 0.5) Gy, respectively.

A.3.11 Initial Experiments with ^{60}Co LDR-Primed Cells

Experiment P1*	January 23, 2008							
Plating efficiency PE =	**0.482**		**Multiplicity M =**		**1.474**			
Dose (Gy)	**C**	**0.1**	**0.2**	**0.3**	**0.5**	**0.75**	**1**	**2**
flask 1	84	82	104	104	101	101	75	64
flask 2	93	110	105	84	107	110	100	72
flask 3	95	98	102	111	104	94	87	72
flask 4	105	113	94	85	90	91	96	65
flask 5	105	114	100	113	105	102	89	64
Number of cells seeded per flask	200	200	200	200	200	200	200	200
Mean number of colonies per flask: N	96.4	103.4	101	99.4	101.4	99.6	89.4	67.4
Standard error: ΔN	3.970	6.063	1.949	6.266	3.010	3.326	4.297	1.887
Surviving fraction: F		1.073	1.048	1.031	1.052	1.033	0.927	0.699
Standard error: ΔF		0.077	0.048	0.078	0.053	0.055	0.059	0.035
Surviving fraction corrected for multiplicity: S		1.073	1.048	1.031	1.052	1.033	0.876	0.584
Standard error: ΔS		0.077	0.048	0.078	0.053	0.055	0.091	0.039

Experiment P2	February 7, 2008								
Plating efficiency PE =	**0.7325**			**Multiplicity M =**		**1.528**			
Dose (Gy)	**C**	**C**	**0.1**	**0.2**	**0.3**	**0.5**	**0.75**	**1**	**2**
flask 1	142	149	151	160	162	154	146	126	101
flask 2	143	135	140	153	170	143	115	141	100
flask 3	139	173	144	136	149	145	126	138	96
flask 4	146	159	147	158	143	160	121	137	100
flask 5	147	132	132	152	136	125	127	129	106
Number of cells seeded per flask	200	200	200	200	200	200	200	200	200
Mean number of colonies per flask: N		146.5	142.8	151.8	152	145.4	127	134.2	100.6
Standard error: ΔN		3.795	3.247	4.224	6.205	5.955	5.206	2.853	1.600
Surviving fraction: F			0.975	1.036	1.038	0.992	0.867	0.916	0.687
Standard error: ΔF			0.034	0.039	0.050	0.048	0.042	0.031	0.021
Surviving fraction corrected for multiplicity: S			0.949	1.036	1.038	0.984	0.775	0.848	0.556
Standard error: ΔS			0.064	0.039	0.050	0.098	0.060	0.049	0.024

* Only one control group was plated because too few cell flasks were available at the time of experiment.

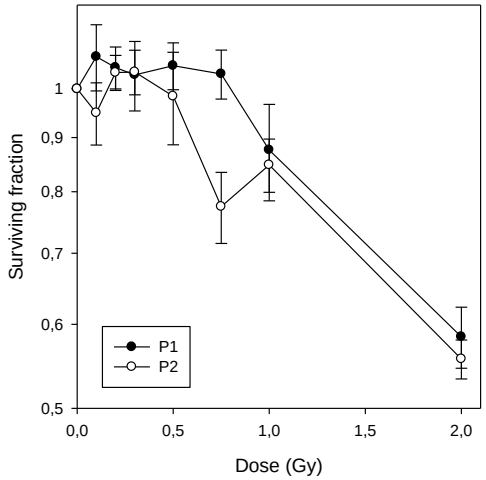

Acute irradiation of T-47D-P cells. The cells had been given a 0.3 Gy priming dose at 0.3 Gy/h on August 17th, 2005. In these two experiments (P1 and P2) the medium was changed after one week of colony growth.

A.3.12 New Batch of T-47D-P Cells

Experiment P3	April 16, 2008								
Plating efficiency PE =	**0.788**			**Multiplicity M =**		**1.756**			
Dose (Gy)	**C**	**C**	**0.1**	**0.2**	**0.3**	**0.5**	**0.75**	**1**	**2**
flask 1	166	166	175	153	157	145	141	173	127
flask 2	164	151	135	172	160	145	134	133	118
flask 3	155	133	155	156	140	159	144	141	111
flask 4	167	151	165	129	156	138	136	155	130
flask 5	169	153	140	132	150	162		133	124
Number of cells seeded per flask	200	200	200	200	200	200	200	200	200
Mean number of colonies per flask: N		157.5	154	148.4	152.6	149.8	138.75	147	122
Standard error: ΔN		3.528	7.483	8.004	3.544	4.576	2.287	7.642	3.391
Surviving fraction: F			0.978	0.942	0.969	0.951	0.881	0.933	0.775
Standard error: ΔF			0.052	0.055	0.031	0.036	0.025	0.053	0.028
Surviving fraction corrected for multiplicity: S			0.926	0.841	0.902	0.860	0.733	0.823	0.592
Standard error: ΔS			0.147	0.114	0.080	0.080	0.039	0.104	0.033

Experiment P4*	April 16, 2008							
Plating efficiency PE =	**1.203**		**Multiplicity M =**		**1.744**			
Dose (Gy)	**C**	**C**	**0.2**	**0.3**	**0.5**	**0.75**	**1**	**2**
flask 1	261	273	228	233	218	221	233	178
flask 2	244	233	224	243	225	230	218	165
flask 3	244	222	225	241	243	231	229	185
flask 4	211	236	227	229	234	229	219	172
flask 5	241	240	222	222	205	236	220	185
Number of cells seeded per flask	200	200	200	200	200	200	200	200
Mean number of colonies per flask: N		240.5	225.2	233.6	225	229.4	223.8	177
Standard error: ΔN		5.568	1.068	3.868	6.535	2.421	3.023	3.860
Surviving fraction: F			0.936	0.971	0.936	0.954	0.931	0.736
Standard error: ΔF			0.022	0.028	0.035	0.024	0.025	0.023
Surviving fraction corrected for multiplicity: S			0.833	0.911	0.831	0.869	0.821	0.552
Standard error: ΔS			0.045	0.071	0.069	0.054	0.049	0.027

* In another experiment additional cells were by mistake seeded in the cell flasks irradiated with 0.1 Gy. These flasks were therefore discarded.

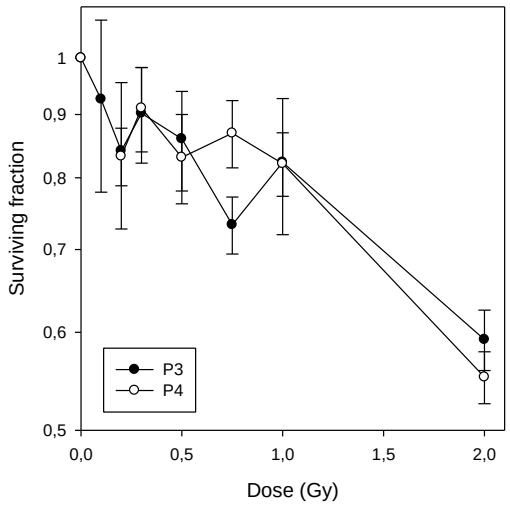

Acute irradiation of T-47D-P cells. The cell batch used for these experiments (P3 and P4) had been thawed only 4 weeks prior to plating. Medium was changed after 1 week of colony growth in experiment P3, but not in experiment P4. The temperature was kept at 37°C during irradiation in experiment P4.

A.3.13 Challenge Irradiation of Primed Cells with Temperature at 37°C

Experiment P5	June 13, 2008								
Plating efficiency PE =	**0.479**			**Multiplicity M =**		**1.611**			
Dose (Gy)	**C**	**C**	**0.1**	**0.2**	**0.3**	**0.5**	**0.75**	**1**	**2**
flask 1	103	113	80	68	84	89	95	94	76
flask 2	94	102	98	97	86	88	95	87	65
flask 3	91	97	81	86	79	92	105	97	77
flask 4	87	92	86	97	93	95	94	77	76
flask 5	83	96	85	81	95	101	98	101	88
Number of cells seeded per flask	200	200	200	200	200	200	200	200	200
Mean number of colonies per flask: N		95.8	86	85.8	87.4	93	97.4	91.2	76.4
Standard error: ΔN		2.728	3.209	5.435	2.943	2.345	2.015	4.224	3.641
Surviving fraction: F			0.898	0.896	0.912	0.971	1.017	0.952	0.797
Standard error: ΔF			0.042	0.062	0.040	0.037	0.036	0.052	0.044
Surviving fraction corrected for multiplicity: S			0.800	0.797	0.824	0.932	1.017	0.894	0.660
Standard error: ΔS			0.067	0.098	0.067	0.078	0.036	0.100	0.056

Experiment P6	June 26, 2008								
Plating efficiency PE =	**1.069**			**Multiplicity M =**		**1.696**			
Dose (Gy)	**C**	**C**	**0.1**	**0.2**	**0.3**	**0.5**	**0.75**	**1**	**2**
flask 1	208	206	211	213	207	188	217	181	152
flask 2	218	222	220	211	225	205	207	187	150
flask 3	196	223	218	212	191	213	214	184	145
flask 4	214	215	219	214	221	197	195	190	166
flask 5	220	215	202	222	213	230	214	209	173
Number of cells seeded per flask	200	200	200	200	200	200	200	200	200
Mean number of colonies per flask: N		213.7	214	214.4	211.4	206.6	209.4	190.2	157.2
Standard error: ΔN		2.629	3.391	1.965	5.980	7.174	3.957	4.934	5.267
Surviving fraction: F			1.001	1.003	0.989	0.967	0.980	0.890	0.736
Standard error: ΔF			0.020	0.015	0.031	0.036	0.022	0.026	0.026
Surviving fraction corrected for multiplicity: S			1.001	1.003	0.967	0.909	0.942	0.765	0.565
Standard error: ΔS			0.020	0.015	0.087	0.083	0.058	0.041	0.030

Experiment P7	June 26, 2008								
Plating efficiency PE =	**0.767**				**Multiplicity M =**	**1.626**			
Dose (Gy)	**C**	**C**	**0.1**	**0.2**	**0.3**	**0.5**	**0.75**	**1**	**2**
flask 1	162	156	167	132	154	165	145	144	143
flask 2	153	129	160	148	146	134	139	139	122
flask 3	175	158	150	152	148	179	143	142	132
flask 4	146	137	157	158	133	137	123	135	127
flask 5	162	155	149	157	150	144	142	152	125
Number of cells seeded per flask	200	200	200	200	200	200	200	200	200
Mean number of colonies per flask: N		153.3	156.6	149.4	146.2	151.8	138.4	142.4	129.8
Standard error: ΔN		4.169	3.326	4.707	3.555	8.691	3.970	2.839	3.680
Surviving fraction: F			1.022	0.975	0.954	0.990	0.903	0.929	0.847
Standard error: ΔF			0.035	0.041	0.035	0.063	0.036	0.031	0.033
Surviving fraction corrected for multiplicity: S			1.022	0.938	0.895	0.975	0.804	0.848	0.721
Standard error: ΔS			0.035	0.090	0.069	0.155	0.058	0.056	0.047

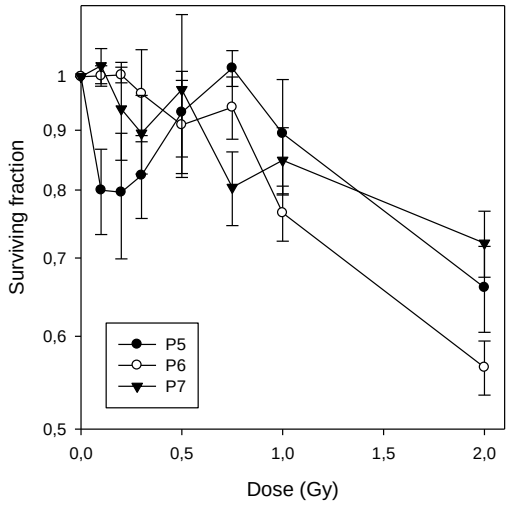

Acute irradiation of T-47D-P cells. The cell batch used for these experiments (P5-P7) had been thawed 9-11 weeks prior to plating. The temperature was kept at 37°C during irradiation. Medium was not changed during the colony growth period.

A.3.14 Mean Values of Experiments P1-P7

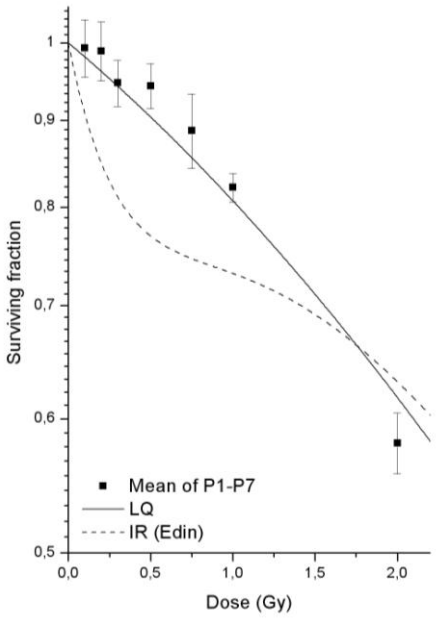

Survival of T-47D-P cells irradiated with single acute doses of ^{60}Co γ-rays. All the cells, including the controls, had been given the same priming treatment (0.3 Gy at 0.3 Gy/h). The curves represent a fit by the LQ model (solid line) to pooled survival data (T1-T24) from unprimed cells, and a fit by the IR model (dashed line) to survival data measured by Edin [personal communication] using unprimed T-47D cells and the same radiation quality. The data points represent mean values of seven experiments (P1-P7). Standard errors are shown by error bars.

Appendix B: Dose-Survival Measurements on G_2-Enriched Cell Populations

B.1 List of Experiments

Experiment	Cell batch	Priming dose	Challenge doses	Irr. setup (Ch. 3.3.2)	Comments
TX1-TX3	t4	-	0.1 – 2 Gy	C	Cells were selected in G_1 and incubated for 29-30 hours before irradiation
TY1-TY3	t4	-	0.1 – 2 Gy	C	Cells were selected in early S phase and incubated for 14-15 hours before irradiation
TZ1-TZ3	t4	-	0.1 – 2 Gy	C (TZ2 – B)	Cells were selected in G_2 and incubated for 15 min. before irradiation
PX1-PX3	p3	0.3 Gy	0.1 – 2 Gy	C	Cells were selected in G_1 and incubated for 24 hours before irradiation
PY1-PY3	p3	0.3 Gy	0.1 – 2 Gy	C	Cells were selected in early S phase and incubated for 14 hours before irradiation
PZ1-PZ3	p3	0.3 Gy	0.1 – 2 Gy	C	Cells were selected in G_2 and incubated for 15 min. before irradiation

As described in chapter 3.5, populations of G_1-, S- and G_2-phase cells were collected simultaneously. Thus experiments TX1, TY1 and TZ1 were performed together, TX2, TY2 and TZ2 were performed together and so forth. Some small changes in the experimental design were introduced after the first experiments:

1) Except for the first experiments with T-47D-P cells (PX1, PY1, PZ1), medium was changed after one week to ensure removal of all Hoechst dye.
2) Multiplicity was counted for all PX, TX, PY and TY experiments except PX1, PY1 and PX2.
3) Some of the experiments (PY3, TY1, TX2, TY3) were plated by Patrycja Mikolajewska, thereby reducing the time the cell samples were kept on ice.

B.2 Experimental Raw Data

All the raw data from the experiments listed in appendix B.1 are given in this section*. The raw data of experiments with similar procedures are listed together, and the survival data from the individual experiments are plotted as a function of dose, with standard errors shown as error bars.

B.2.1 Unprimed Cells Selected in G_1 Phase and Incubated for 30 Hours

Experiment TX1	October 2, 2008								
Plating efficiency PE =	**0.539**			**Multiplicity M =**		**1.129**			
Dose (Gy)	**C**	**C**	**0.1**	**0.2**	**0.3**	**0.5**	**0.75**	**1**	**2**
flask 1	86	87	81	98	82	77	75	73	65
flask 2	86	81	97	89	88	98	84	73	67
flask 3	88	90	90	83	91	83	62	87	56
flask 4	95	99	92	83	93	100	81	67	65
flask 5	95	93	101	87	97	87	80	81	63
Number of cells seeded per flask	167	167	167	167	167	167	167	167	167
Mean number of colonies per flask: N	90	92,2	88	90,2	89	76,4	76,2	63,2	90
Standard error: ΔN	1,719	3,397	2,757	2,518	4,393	3,881	3,499	1,908	1,719
Surviving fraction: F			1,0244	0,9778	1,0022	0,9889	0,8489	0,8467	0,7022
Standard error: ΔF			0,0425	0,0359	0,0339	0,0523	0,0461	0,0421	0,0251
Surviving fraction corrected for multiplicity: S			1,0244	0,9746	1,0022	0,9873	0,8308	0,8283	0,6739
Standard error: ΔS			0,0425	0,0409	0,0339	0,0599	0,0506	0,0462	0,0272

Experiment TX2	October 8, 2008								
Plating efficiency PE =	**0.333**			**Multiplicity M =**		**1.284**			
Dose (Gy)	**C**	**C**	**0.1**	**0.2**	**0.3**	**0.5**	**0.75**	**1**	**2**
flask 1	52	50	37	54	59	33	50	51	35
flask 2	68	49	45	45	64	44	32	38	45
flask 3	66	53	49	50	50	47	40	47	38
flask 4	62	58	54	42	53	57	44	38	29
flask 5	42	56	51	62	32	55	68	41	29
Number of cells seeded per flask	167	167	167	167	167	167	167	167	167
Mean number of colonies per flask: N		55,6	47,2	50,6	51,6	47,2	46,8	43	35,2
Standard error: ΔN		2,557	2,939	3,516	5,464	4,294	6,053	2,588	3,007
Surviving fraction: F			0,849	0,910	0,928	0,849	0,842	0,773	0,633
Standard error: ΔF			0,066	0,076	0,107	0,087	0,116	0,059	0,061
Surviving fraction corrected for multiplicity: S			0,804	0,880	0,903	0,804	0,796	0,716	0,563
Standard error: ΔS			0,080	0,097	0,139	0,105	0,139	0,067	0,064

* Note that except for the last two series of experiments with unprimed cells, the concentration of cells in the stock suspensions was not determined by counting in Bürker chamber since the exact number of sorted cells was known. However, a relatively large percentage of the cells were lost during removal of buffer solution and washing with fresh medium. This resulted in artificially low plating efficiencies. From the experiments where the cell concentrations were measured, it was found that in average 20% of the cells had been lost. In the raw data listed here the plating efficiencies have been corrected for this cell loss.

Experiment TX3	October 15, 2008								
Plating efficiency PE =	**0.797**			**Multiplicity M =**		**1.244**			
Dose (Gy)	**C**	**C**	**0.1**	**0.2**	**0.3**	**0.5**	**0.75**	**1**	**2**
flask 1	165	170	158	159	162	147	140	134	125
flask 2	154	165	174	149	155	150	127	134	116
flask 3	149	157	145	143	149	154	152	134	120
flask 4	164	160	165	168	171	179	160	111	131
flask 5		150	167	151	152	163	155	150	133
Number of cells seeded per flask	200	200	200	200	200	200	200	200	200
Mean number of colonies per flask: N		159,3	161,8	154	157,8	158,6	146,8	132,6	125
Standard error: ΔN		2,438	4,913	4,336	3,942	5,767	5,945	6,226	3,209
Surviving fraction: F			1,015	0,967	0,990	0,995	0,921	0,832	0,785
Standard error: ΔF			0,035	0,031	0,029	0,039	0,040	0,041	0,023
Surviving fraction corrected for multiplicity: S			1,015	0,956	0,987	0,994	0,899	0,792	0,737
Standard error: ΔS			0,035	0,040	0,038	0,052	0,050	0,048	0,027

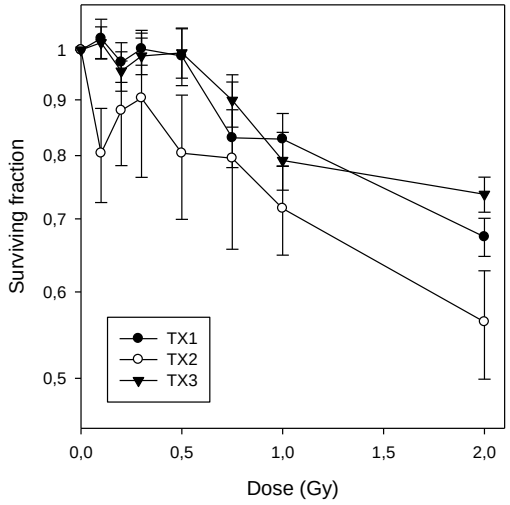

Acute irradiation of T-47D cells. The cells were selected in G_1 phase, incubated for 29-30 hours and subsequently irradiated.

B.2.2 Unprimed Cells Selected in S Phase and Incubated for 15 Hours

Experiment TY1	October 2, 2008								
Plating efficiency PE =	**0.234**			**Multiplicity M =**		**1.288**			
Dose (Gy)	**C**	**C**	**0.1**	**0.2**	**0.3**	**0.5**	**0.75**	**1**	**2**
flask 1	36	26	27	32	31	32	27	19	27
flask 2	41	37	40	36	38	28	17	23	17
flask 3	38	44	45	45	29	17	24	27	20
flask 4	41	46	32	42	27	28	25	25	20
flask 5	43	38	48	35	21		28	18	13
Number of cells seeded per flask	167	167	167	167	167	167	167	167	167
Mean number of colonies per flask: N		39	38,4	38	29,2	26,25	24,2	22,4	19,4
Standard error: ΔN		1,770	3,932	2,387	2,764	3,224	1,934	1,720	2,293
Surviving fraction: F			0,985	0,974	0,749	0,673	0,621	0,574	0,497
Standard error: ΔF			0,110	0,076	0,079	0,088	0,057	0,051	0,063
Surviving fraction corrected for multiplicity: S			0,979	0,964	0,687	0,604	0,549	0,502	0,427
Standard error: ΔS			0,152	0,103	0,088	0,094	0,059	0,052	0,061

Experiment TY2	October 8, 2008								
Plating efficiency PE =	**0.857**			**Multiplicity M =**		**1.165**			
Dose (Gy)	**C**	**C**	**0.1**	**0.2**	**0.3**	**0.5**	**0.75**	**1**	**2**
flask 1	154	173	206	142	136	152	107	96	49
flask 2	173	168	159	160	136	143	112	87	67
flask 3	182	188	185	159	152	129	112	90	68
flask 4	182	171	186	153	163	140	128	109	82
flask 5	159	163	157	134	170	147	130	114	62
Number of cells seeded per flask	200	200	200	200	200	200	200	200	200
Mean number of colonies per flask: N		171,3	178,6	149,6	151,4	142,2	117,8	99,2	65,6
Standard error: ΔN		3,406	9,212	5,046	6,911	3,865	4,673	5,286	5,316
Surviving fraction: F			1,043	0,873	0,884	0,830	0,688	0,579	0,383
Standard error: ΔF			0,058	0,034	0,044	0,028	0,031	0,033	0,032
Surviving fraction corrected for multiplicity: S			1,043	0,853	0,865	0,804	0,650	0,538	0,346
Standard error: ΔS			0,058	0,039	0,050	0,032	0,033	0,034	0,031

Experiment TY3	October 15, 2008								
Plating efficiency PE =	**0.830**			**Multiplicity M =**		**1.204**			
Dose (Gy)	**C**	**C**	**0.1**	**0.2**	**0.3**	**0.5**	**0.75**	**1**	**2**
flask 1	172	154	152	146	169	162	129	124	75
flask 2	172	180	156	158	153	135	125	108	58
flask 3	139	166	162	175	145	119	129	101	81
flask 4	171	165	151	165	145	131	105	95	89
flask 5	145	195	158	140	162	114	127	110	58
Number of cells seeded per flask	200	200	200	200	200	200	200	200	200
Mean number of colonies per flask: N		165,9	155,8	156,8	154,8	132,2	123	107,6	72,2
Standard error: ΔN		5,216	2,010	6,320	4,737	8,375	4,561	4,885	6,208
Surviving fraction: F			0,939	0,945	0,933	0,797	0,741	0,649	0,435
Standard error: ΔF			0,032	0,048	0,041	0,056	0,036	0,036	0,040
Surviving fraction corrected for multiplicity: S			0,925	0,932	0,918	0,760	0,698	0,600	0,387
Standard error: ΔS			0,039	0,059	0,049	0,063	0,040	0,038	0,039

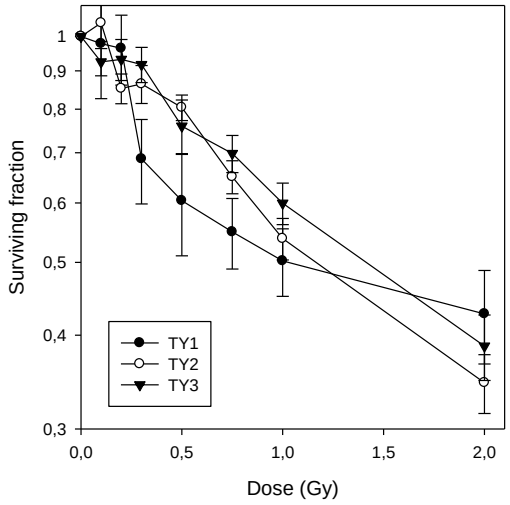

Acute irradiation of T-47D cells. The cells were selected in S phase, incubated for 14-15 hours and subsequently irradiated.

B.2.3 Unprimed Cells Selected and Irradiated in G_2 Phase

Experiment TZ1	October 2, 2008								
Plating efficiency PE =	**0.541**			**Multiplicity M =**	**-**				
Dose (Gy)	**C**	**C**	**0.1**	**0.2**	**0.3**	**0.5**	**0.75**	**1**	**2**
flask 1	100	94	90	85	80	95	81	81	60
flask 2	82	83	82	67	79	86	86	86	62
flask 3	85	85	76	72	105	83	86	69	51
flask 4	90	100	89	83	85	74	84	89	65
flask 5	85	99	82	79	95	108	83	79	64
Number of cells seeded per flask	167	167	167	167	167	167	167	167	167
Mean number of colonies per flask: N		90,3	83,8	77,2	88,8	89,2	84	80,8	60,4
Standard error: ΔN		2,319	2,577	3,382	4,944	5,774	0,949	3,441	2,502
Surviving fraction: F			0,928	0,855	0,983	0,988	0,930	0,895	0,669
Standard error: ΔF			0,037	0,043	0,060	0,069	0,026	0,044	0,033

Experiment TZ2	October 8, 2008								
Plating efficiency PE =	**0.508**			**Multiplicity M =**	**-**				
Dose (Gy)	**C**	**C**	**0.1**	**0.2**	**0.3**	**0.5**	**0.75**	**1**	**2**
flask 1	112	120	104	113	95	93	103	90	60
flask 2	111	87	99	98	100	91	89	95	75
flask 3	96	94	99	108	102	87	95	82	66
flask 4	101	98	93	99	96	102	92	98	53
flask 5	100	97	113	93	108	91	98	107	77
Number of cells seeded per flask	200	200	200	200	200	200	200	200	200
Mean number of colonies per flask: N		101,6	101,6	102,2	100,2	92,8	95,4	94,4	66,2
Standard error: ΔN		3,117	3,341	3,625	2,332	2,498	2,421	4,155	4,510
Surviving fraction: F			1	1,006	0,986	0,913	0,939	0,929	0,652
Standard error: ΔF			0,045	0,047	0,038	0,037	0,037	0,050	0,049

Experiment TZ3	October 15, 2008								
Plating efficiency PE =	**0.537**			**Multiplicity M =**	**-**				
Dose (Gy)	**C**	**C**	**0.1**	**0.2**	**0.3**	**0.5**	**0.75**	**1**	**2**
flask 1	93	108	106	101	99	94	87	104	70
flask 2	100	125	103	93	95	117	106	88	51
flask 3	113	109	102	110	98	102	113	87	70
flask 4	99	102	115	112	112	80	96	99	76
flask 5	115	110	117	101	104	95	115	107	64
Number of cells seeded per flask	200	200	200	200	200	200	200	200	200
Mean number of colonies per flask: N		107,4	108,6	103,4	101,6	97,6	103,4	97	66,2
Standard error: ΔN		2,926	3,108	3,444	2,977	6,022	5,278	4,087	4,247
Surviving fraction: F			1,011	0,963	0,946	0,909	0,963	0,903	0,616
Standard error: ΔF			0,040	0,041	0,038	0,061	0,056	0,045	0,043

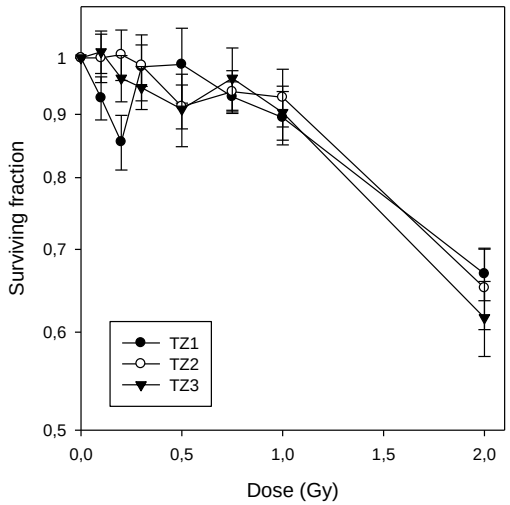

Acute irradiation of T-47D cells. The cells were selected in G_2 phase, incubated for15 minutes and subsequently irradiated.

B.2.4 Primed Cells Selected in G_1 Phase and Incubated for 24 Hours

Experiment PX1	August 27, 2008								
Plating efficiency PE =	**0.489**			**Multiplicity M =**	**-**				
Dose (Gy)	**C**	**C**	**0.1**	**0.2**	**0.3**	**0.5**	**0.75**	**1**	**2**
flask 1	88	80	87	73	69	70	57	59	44
flask 2	90	75	81	80	74	68	66	58	36
flask 3	100	81	67	71	74	73	66	53	35
flask 4	75	85	80	67	84	65	60	51	48
flask 5	69	74	86	87	84	63	65	54	44
Number of cells seeded per flask	167	167	167	167	167	167	167	167	167
Mean number of colonies per flask: N		81,7	80,2	75,6	77	67,8	62,8	55	41,4
Standard error: ΔN		2,921	3,569	3,544	3,000	1,772	1,828	1,517	2,522
Surviving fraction: F			0,982	0,925	0,942	0,830	0,769	0,673	0,507
Standard error: ΔF			0,056	0,055	0,050	0,037	0,035	0,030	0,036

Experiment PX2	September 3, 2008								
Plating efficiency PE =	**0.562**			**Multiplicity M =**	**-**				
Dose (Gy)	**C**	**C**	**0.1**	**0.2**	**0.3**	**0.5**	**0.75**	**1**	**2**
flask 1	101	92	108	83	74	83	64	67	59
flask 2	86	82	84	86	93	82	62	77	59
flask 3	95	97	91	91	71	78	69	75	46
flask 4	89	104	101	94	90	89	84	74	53
flask 5	103	89	91	81	103	86	74	73	56
Number of cells seeded per flask	167	167	167	167	167	167	167	167	167
Mean number of colonies per flask: N		93,8	95	87	86,2	83,6	70,6	73,2	54,6
Standard error: ΔN		2,361	4,231	2,429	6,012	1,860	3,945	1,685	2,421
Surviving fraction: F			1,013	0,928	0,919	0,891	0,753	0,780	0,582
Standard error: ΔF			0,052	0,035	0,068	0,030	0,046	0,027	0,030

Experiment PX3	September 15, 2008								
Plating efficiency PE =	**0.523**			**Multiplicity M =**		**1.096**			
Dose (Gy)	**C**	**C**	**0.1**	**0.2**	**0.3**	**0.5**	**0.75**	**1**	**2**
flask 1	103	96	99	83	78	81	67	64	40
flask 2	81	89	70	74	89	62	63	55	50
flask 3	73	91	86	79	73	68	58	53	39
flask 4	79	88	96	79	78	94	68	69	62
flask 5	90	84	98	80	73	72	67	69	48
Number of cells seeded per flask	167	167	167	167	167	167	167	167	167
Mean number of colonies per flask: N		87,4	89,8	79	78,2	75,4	64,6	62	47,8
Standard error: ΔN		2,729	5,463	1,449	2,922	5,582	1,860	3,406	4,152
Surviving fraction: F			1,027	0,904	0,895	0,863	0,739	0,709	0,547
Standard error: ΔF			0,070	0,033	0,044	0,069	0,031	0,045	0,050
Surviving fraction corrected for multiplicity: S			1,027	0,895	0,885	0,850	0,720	0,689	0,523
Standard error: ΔS			0,070	0,036	0,047	0,074	0,033	0,047	0,051

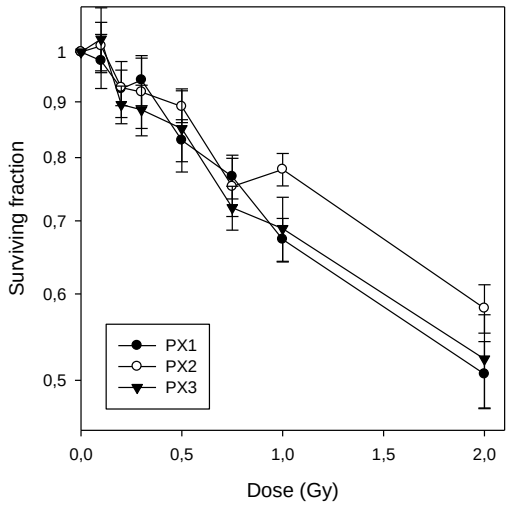

Acute irradiation of T-47D-P cells. The cells had been given a 0.3 Gy priming dose at 0.3 Gy/h on August 17th, 2005. In experiments PX1-PX3 the cells were selected in G_1 phase, incubated for 24 hours and subsequently irradiated.

B.2.5 Unprimed Cells Selected in S Phase and Incubated for 15 Hours

Experiment PY1	August 27, 2008								
Plating efficiency PE =	**0.212**			**Multiplicity M =**		**-**			
Dose (Gy)	**C**	**C**	**0.1**	**0.2**	**0.3**	**0.5**	**0.75**	**1**	**2**
flask 1	34	43	41	33	31	20	18	22	14
flask 2	39	28	51	19	38	30	29	27	20
flask 3	30	31	46	31	28	38	27	19	12
flask 4	37	36	32	24	25	32	18	26	15
flask 5		40	32	39	44	31	19	16	19
Number of cells seeded per flask	167	167	167	167	167	167	167	167	167
Mean number of colonies per flask: N		35,33	40,4	29,2	33,2	30,2	22,2	22	16
Standard error: ΔN		1,667	3,776	3,499	3,455	2,905	2,396	2,074	1,517
Surviving fraction: F			1,143	0,826	0,940	0,855	0,628	0,623	0,453
Standard error: ΔF			0,120	0,106	0,107	0,092	0,074	0,066	0,048

Experiment PY2	September 3, 2008								
Plating efficiency PE =	**0.536**				**Multiplicity M =**	**1.110**			
Dose (Gy)	**C**	**C**	**0.1**	**0.2**	**0.3**	**0.5**	**0.75**	**1**	**2**
flask 1	101	91	101	94	81	60	65	45	29
flask 2	110	78	78	93	73	72	59	57	35
flask 3	88	91	109	103	82	79	63	51	33
flask 4	84	75	76	90	75	59	56	45	32
flask 5	87	90	79	92	78	73		51	29
Number of cells seeded per flask	167	167	167	167	167	167	167	167	167
Mean number of colonies per flask: N		89,5	88,6	94,4	77,8	68,6	60,75	49,8	31,6
Standard error: ΔN		3,229	6,831	2,249	1,715	3,906	2,016	2,245	1,166
Surviving fraction: F			0,990	1,055	0,869	0,766	0,679	0,556	0,353
Standard error: ΔF			0,084	0,046	0,037	0,052	0,033	0,032	0,018
Surviving fraction corrected for multiplicity: S			0,989	1,055	0,856	0,746	0,654	0,529	0,329
Standard error: ΔS			0,094	0,046	0,040	0,055	0,035	0,033	0,019

Experiment PY3	September 15, 2008								
Plating efficiency PE =	**0.494**				**Multiplicity M =**	**1.092**			
Dose (Gy)	**C**	**C**	**0.1**	**0.2**	**0.3**	**0.5**	**0.75**	**1**	**2**
flask 1	90	79	78	75	85	66	48	46	39
flask 2	100	67	98	65	69	57	47	41	24
flask 3	82	74	87	69	79	64	38	41	22
flask 4	75	81	83	75	72	65	54	48	26
flask 5	95	82	83	75	63	56	51	49	20
Number of cells seeded per flask	167	167	167	167	167	167	167	167	167
Mean number of colonies per flask: N		82,5	85,8	71,8	73,6	61,6	47,6	45	26,2
Standard error: ΔN		3,167	3,367	2,059	3,842	2,112	2,694	1,703	3,353
Surviving fraction: F			1,040	0,870	0,892	0,747	0,577	0,545	0,318
Standard error: ΔF			0,057	0,042	0,058	0,038	0,039	0,029	0,042
Surviving fraction corrected for multiplicity: S			1,040	0,859	0,883	0,728	0,554	0,523	0,298
Standard error: ΔS			0,057	0,045	0,062	0,041	0,041	0,030	0,041

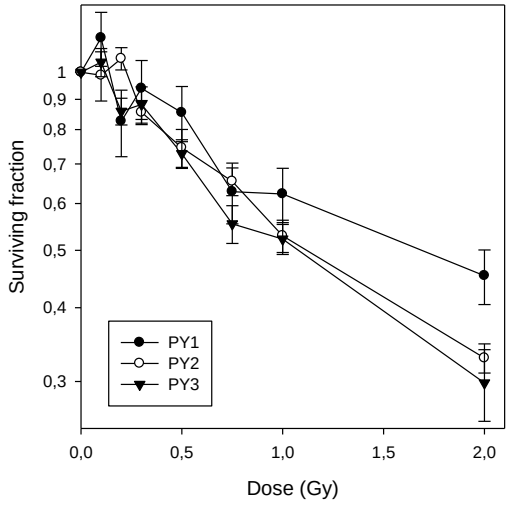

Acute irradiation of T-47D-P cells. The cells were selected in S phase, incubated for 14 hours and subsequently irradiated.

B.2.3 Primed Cells Selected and Irradiated in G_2 Phase

Experiment PZ1	August 27, 2008								
Plating efficiency PE =	**0.334**			**Multiplicity M =**		**-**			
Dose (Gy)	**C**	**C**	**0.1**	**0.2**	**0.3**	**0.5**	**0.75**	**1**	**2**
flask 1	50	56	53	46	61	57	61	41	29
flask 2	58	56	48	74	56	62	41	42	23
flask 3	57	53	52	55	48	48	43	47	26
flask 4	54	56	51	51	54	57	48	41	39
flask 5	66	52	51	47	67	60	54	44	33
Number of cells seeded per flask	167	167	167	167	167	167	167	167	167
Mean number of colonies per flask: N		55,8	51	54,6	57,2	56,8	49,4	43	30
Standard error: ΔN		1,373	0,837	5,105	3,216	2,396	3,669	1,140	2,793
Surviving fraction: F			0,914	0,978	1,025	1,018	0,885	0,771	0,538
Standard error: ΔF			0,027	0,095	0,063	0,050	0,069	0,028	0,052

Experiment PZ2	September 3, 2008								
Plating efficiency PE =	**0.594**			**Multiplicity M =**		**-**			
Dose (Gy)	**C**	**C**	**0.1**	**0.2**	**0.3**	**0.5**	**0.75**	**1**	**2**
flask 1	87	105	80	107	80	77	94	64	42
flask 2	102	91	97	90	89	91	79	75	65
flask 3	91	111	84	73	79	80	96	82	55
flask 4	107	92	76	99	83	90	91	57	47
flask 5	93	113	100	87	94	81	82	76	60
Number of cells seeded per flask	167	167	167	167	167	167	167	167	167
Mean number of colonies per flask: N		99,2	87,4	91,2	85	83,8	88,4	70,8	53,8
Standard error: ΔN		2,992	4,729	5,748	2,846	2,818	3,356	4,510	4,188
Surviving fraction: F			0,881	0,919	0,857	0,845	0,891	0,714	0,542
Standard error: ΔF			0,055	0,064	0,039	0,038	0,043	0,050	0,045

Experiment PZ3	September 15, 2008								
Plating efficiency PE =	**0.444**			**Multiplicity M =**		**-**			
Dose (Gy)	**C**	**C**	**0.1**	**0.2**	**0.3**	**0.5**	**0.75**	**1**	**2**
flask 1	60	73	82	61	76	52	52	54	34
flask 2	68	78	82	62	64	74	64	57	43
flask 3	61	84	73	81	80	63	84	45	43
flask 4	81	85	76	67	67	49	65	59	33
flask 5	81	71	78	61		74	58	61	29
Number of cells seeded per flask	167	167	167	167	167	167	167	167	167
Mean number of colonies per flask: N		74,2	78,2	66,4	71,75	62,4	64,6	55,2	36,4
Standard error: ΔN		2,878	1,744	3,816	3,750	5,278	5,381	2,800	2,821
Surviving fraction: F			1,054	0,895	0,967	0,841	0,871	0,744	0,491
Standard error: ΔF			0,047	0,062	0,063	0,078	0,080	0,048	0,043

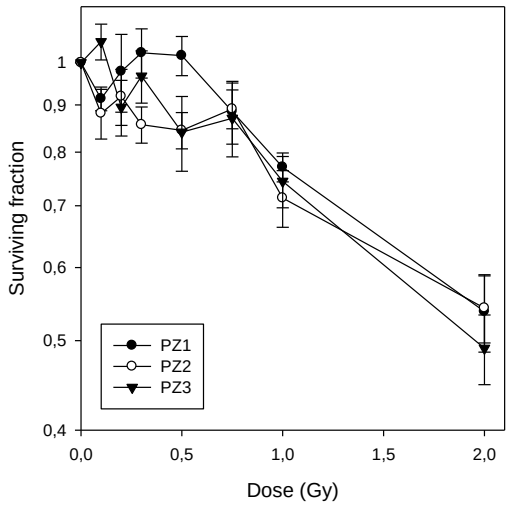

Acute irradiation of T-47D-P cells. The cells were selected in G_2 phase, incubated for15 minutes and subsequently irradiated.

Appendix C: DNA histograms

C.1 Selection of G_1-phase T-47D-P cells

Experiment 1

(DNA histograms for the initial cell-cycle distribution and a test sample of the sorted cells were not saved for the first experiment.)

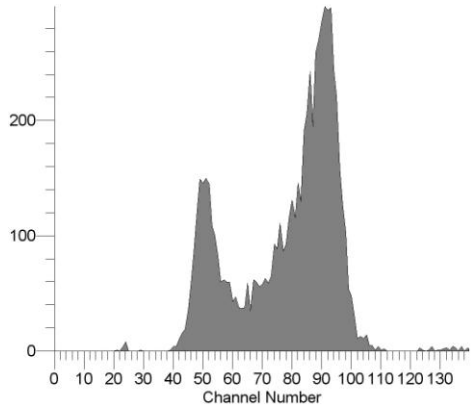

23hours, control A
G_0/G_1: 15.2% S: 36.7% G_2/M: 48.1%
CV: 5.46 G_2/G_1-ratio: 1.81

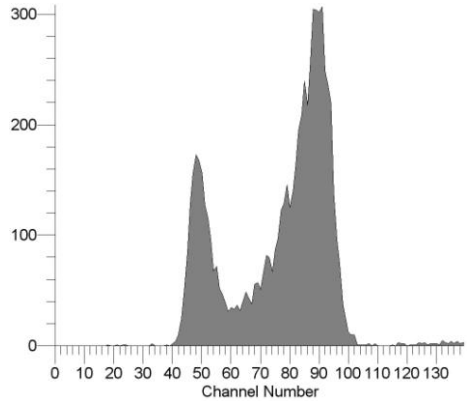

23 hours, control B
G_0/G_1: 17.6% S: 34.7% G_2/M: 47.7%
CV: 5.17 G_2/G_1-ratio: 1.83

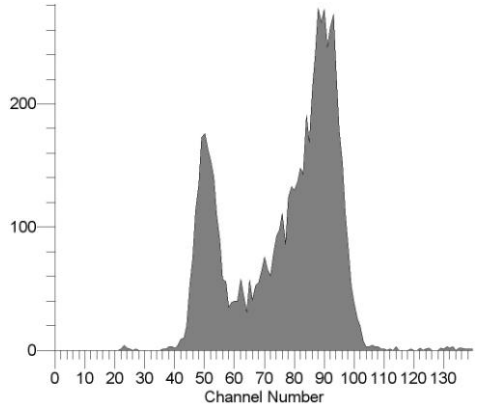

23hours, irradiated A
G_0/G_1: 18.9% S: 38.6% G_2/M: 42.5%
CV: 5.41 G_2/G_1-ratio: 1.80

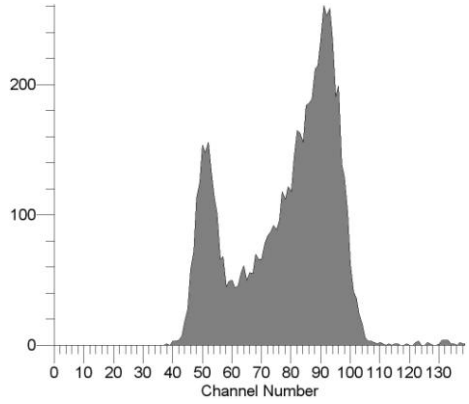

23 hours, irradiated B
G_0/G_1: 16.3% S: 46.4% G_2/M: 37.3%
CV: 5.57 G_2/G_1-ratio: 1.81

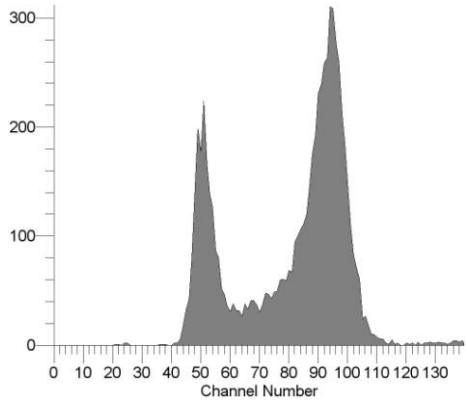

24 hours, control A
G_0/G_1: 20.4% S: 28.7% G_2/M: 50.9%
CV: 5.50 G_2/G_1-ratio: 1.86

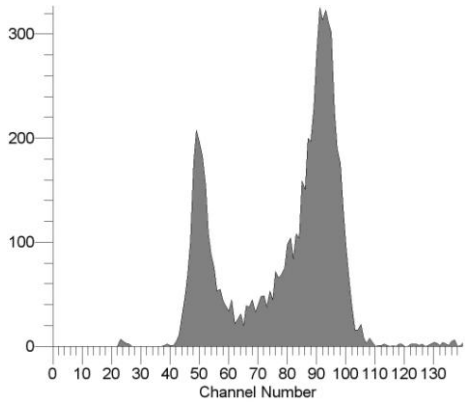

24 hours, control B
G_0/G_1: 19.5% S: 28.7% G_2/M: 51.8%
CV: 5.12 G_2/G_1-ratio: 1.86

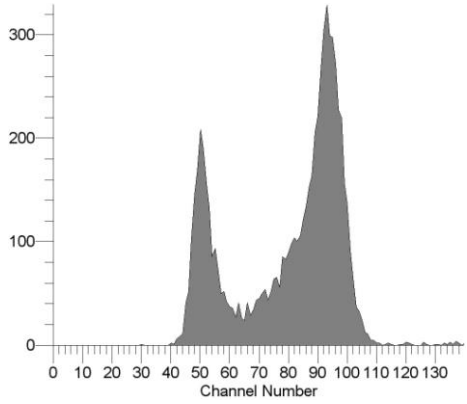

24 hours, irradiated A
G_0/G_1: 19.3% S: 32.5% G_2/M: 48.2%
CV: 5.21 G_2/G_1-ratio: 1.86

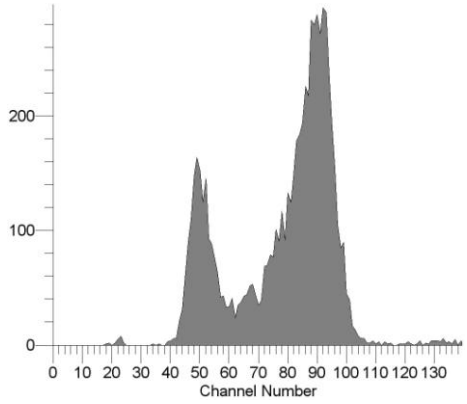

24 hours, irradiated B
G_0/G_1: 17.3% S: 30.1% G_2/M: 52.7%
CV: 5.88 G_2/G_1-ratio: 1.82

Experiment 2

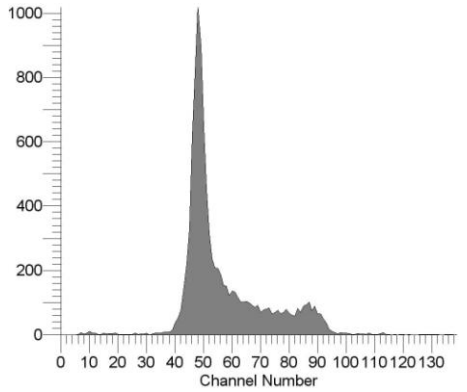

Initial cell-cycle distribution
G_0/G_1: 49.9% S: 39.4% G_2/M: 10.7%
CV: 5.02 G_2/G_1-ratio: 1.80

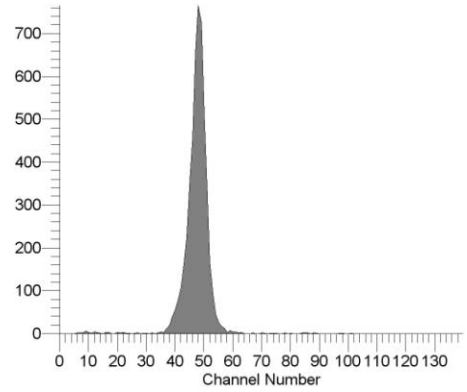

Sorted G_1-phase cells
G_0/G_1: 98.9% S: 1.0% G_2/M: 0.1%
CV: 5.81 G_2/G_1-ratio: 2.00

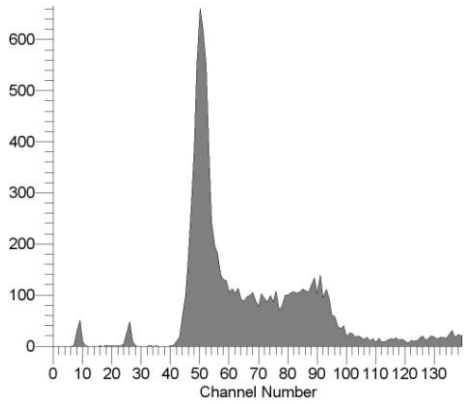

15 hours, control A
G_0/G_1: 42.7% S: 44.7% G_2/M: 12.7%
CV: 5.32 G_2/G_1-ratio: 1.81

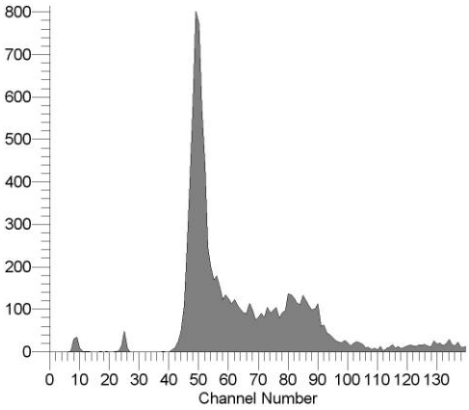

15 hours, control B
G_0/G_1: 43.7% S: 44.6% G_2/M: 11.7%
CV: 4.61 G_2/G_1-ratio: 1.77

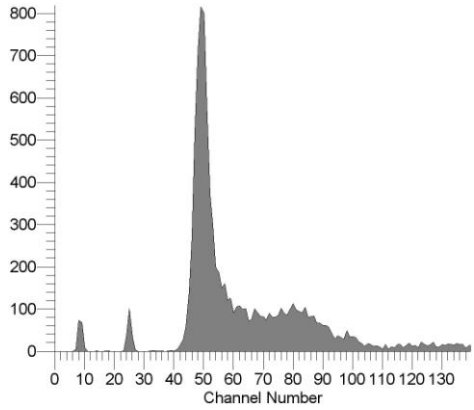

15 hours, irradiated A
G_0/G_1: 49.6% S: 44.2% G_2/M: 6.3%
CV: 4.72 G_2/G_1-ratio: 1.81

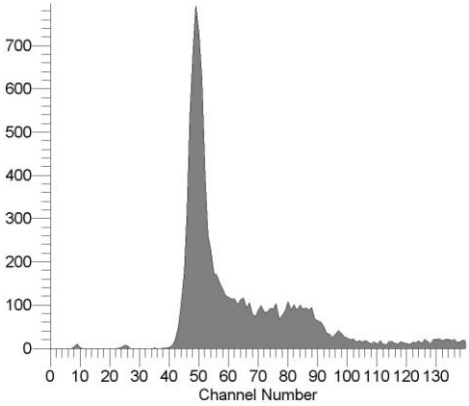

15 hours, irradiated B
G_0/G_1: 47.6% S: 43.2% G_2/M: 9.2%
CV: 5.05 G_2/G_1-ratio: 1.79

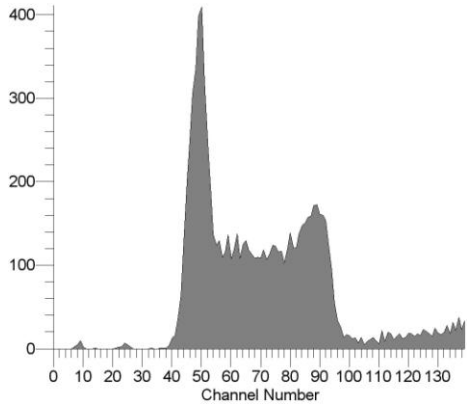

17 hours, control A
G_0/G_1: 27.1% S: 54.3% G_2/M: 18.6%
CV: 5.74 G_2/G_1-ratio: 1.83

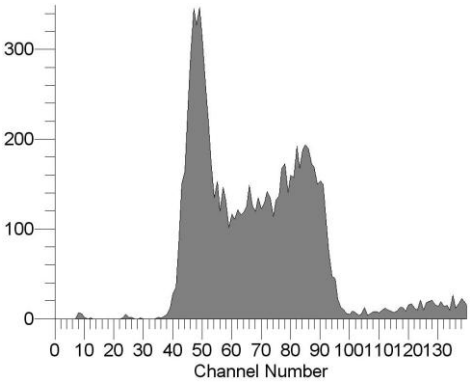

17 hours, control B
G_0/G_1: 24.7% S: 47.1% G_2/M: 28.2%
CV: 6.69 G_2/G_1-ratio: 1.78

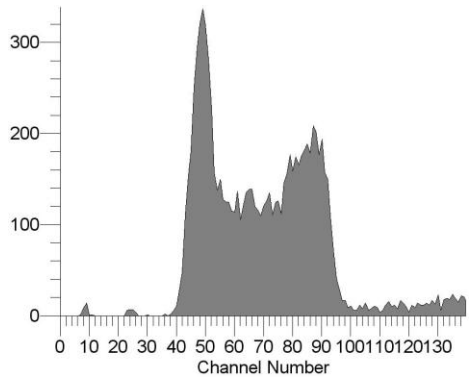

17 hours, irradiated A
G_0/G_1: 22.3% S: 52.6% G_2/M: 25.0%
CV: 6.11 G_2/G_1-ratio: 1.82

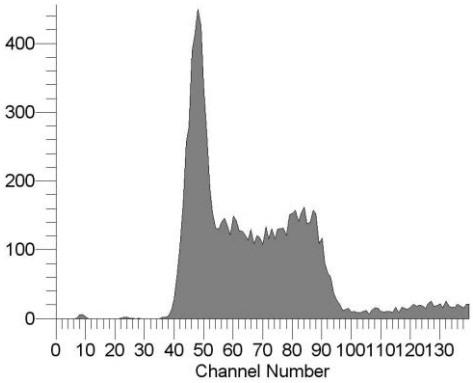

17 hours, irradiated B
G_0/G_1: 30.9% S: 52.4% G_2/M: 16.7%
CV: 6.48 G_2/G_1-ratio: 1.82

Experiment 3

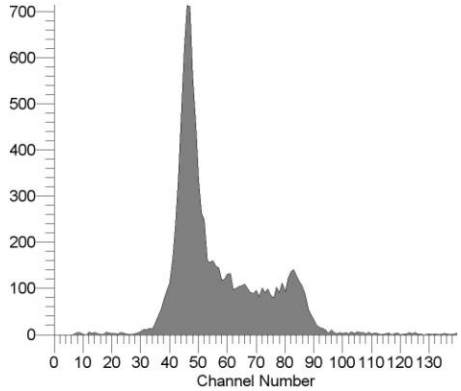

Initial cell-cycle distribution
G_0/G_1: 44.3% S: 38.3% G_2/M: 17.4%
CV: 6.66 G_2/G_1-ratio: 1.77

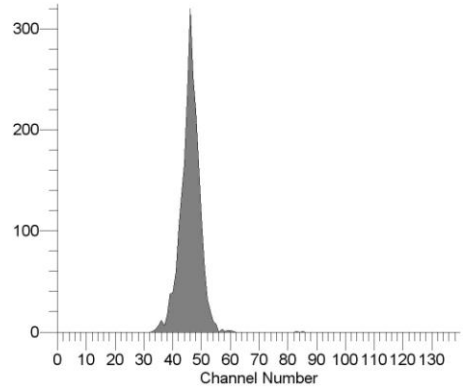

Sorted G_1-phase cells
G_0/G_1: 100.0% S: 0.0% G_2/M: 0.0%
CV: 6.71 G_2/G_1-ratio: 2.00

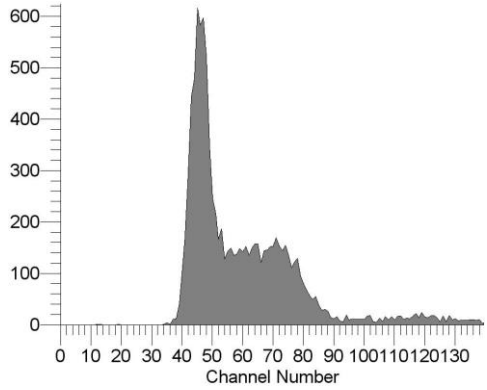

14 hours, control A
G_0/G_1: 37.6% S: 62.4% G_2/M: 0.0%
CV: 5.84 G_2/G_1-ratio: 2.00

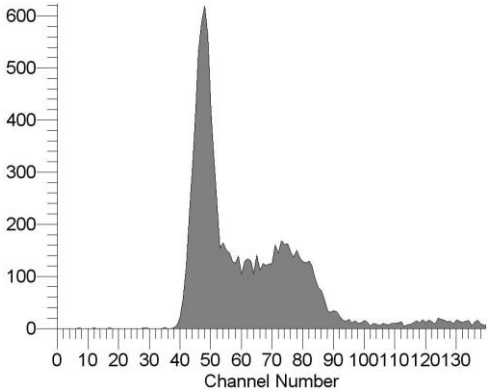

14 hours, control B
G_0/G_1: 38.3% S: 61.7% G_2/M: 0.0%
CV: 5.65 G_2/G_1-ratio: 2.00

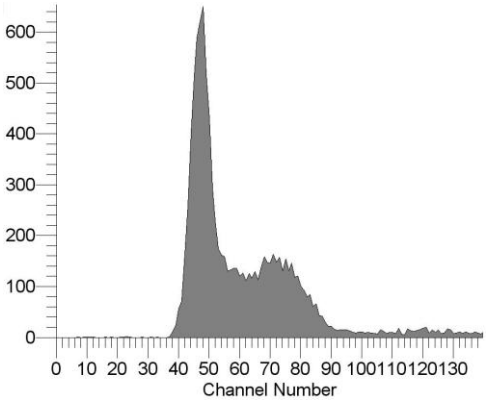

14 hours, irradiated A
G_0/G_1: 41.1% S: 58.9% G_2/M: 0.0%
CV: 6.03 G_2/G_1-ratio: 2.00

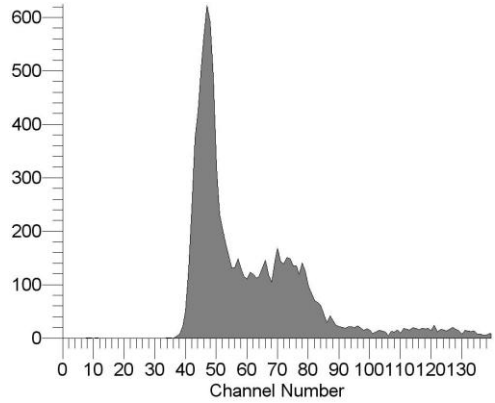

14 hours, irradiated B
G_0/G_1: 41.4% S: 58.4% G_2/M: 0.2%
CV: 6.18 G_2/G_1-ratio: 2.00

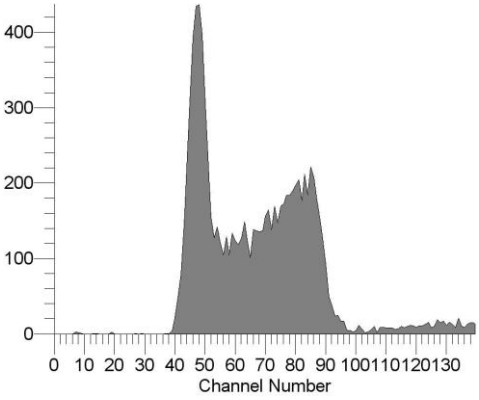

16 hours, control A
G_0/G_1: 29.6% S: 52.3% G_2/M: 18.1%
CV: 5.86 G_2/G_1-ratio: 1.78

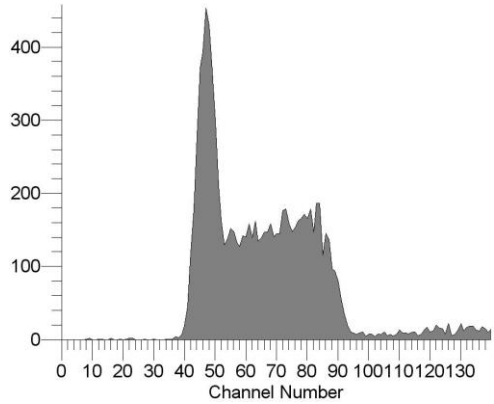

16 hours, control B
G_0/G_1: 29.1% S: 55.0% G_2/M: 15.8%
CV: 6.05 G_2/G_1-ratio: 1.77

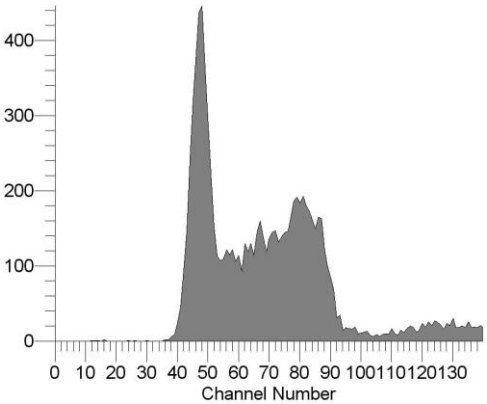

16 hours, irradiated A
G_0/G_1: 30.9% S: 54.3% G_2/M: 14.8%
CV: 5.84 G_2/G_1-ratio: 1.80

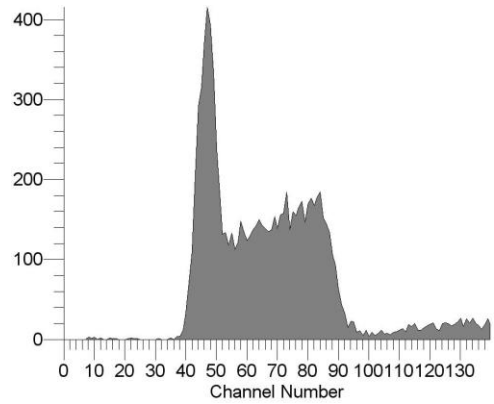

16 hours, irradiated B
G_0/G_1: 28.6% S: 56.8% G_2/M: 14.6%
CV: 6.23 G_2/G_1-ratio: 1.79

C.2 G_2-Enriched Cell Populations

T-47D experiments:

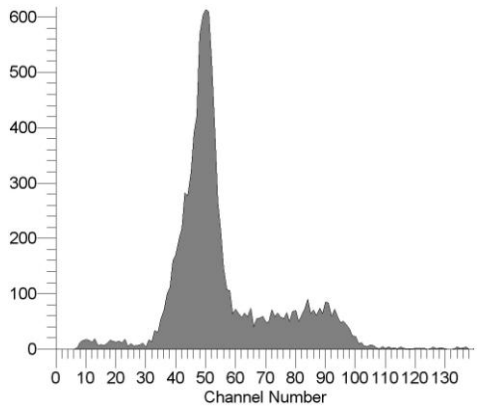

Initial cell-cycle distribution 1
G_0/G_1: 68.2% S: 21.6% G_2/M: 10.2%
CV: 8.44 G_2/G_1-ratio: 1.80

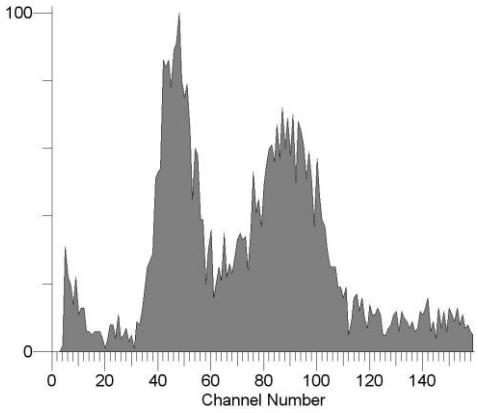

TX1
G_0/G_1: 35.3% S: 19.9% G_2/M: 44.8%
CV: 13.17 G_2/G_1-ratio: 1.96

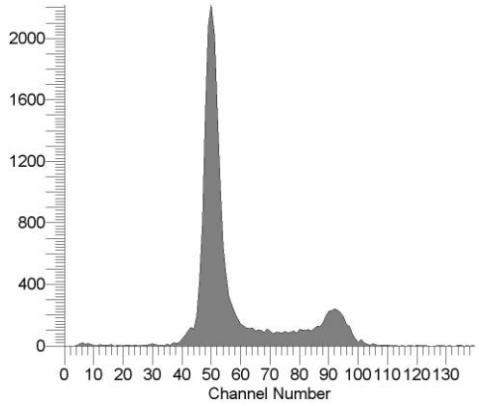

Initial cell-cycle distribution 2
G_0/G_1: 64.8% S: 22.3% G_2/M: 12.9%
CV: 4.74 G_2/G_1-ratio: 1.83

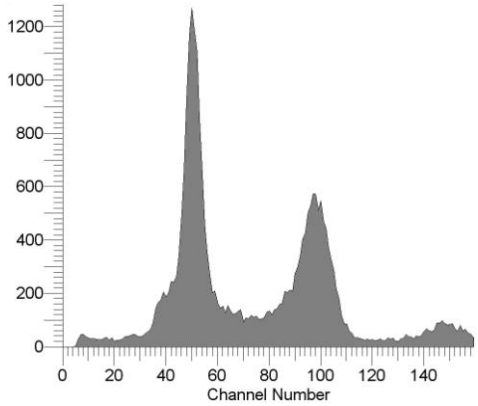

TX2
G_0/G_1: 41.7% S: 23.3% G_2/M: 35.0%
CV: 6.79 G_2/G_1-ratio: 1.95

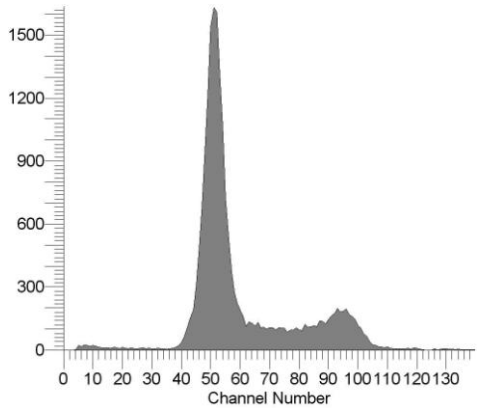

Initial cell-cycle distribution 3
G_0/G_1: 63.9% S: 22.6% G_2/M: 13.5%
CV: 6.48 G_2/G_1-ratio: 1.85

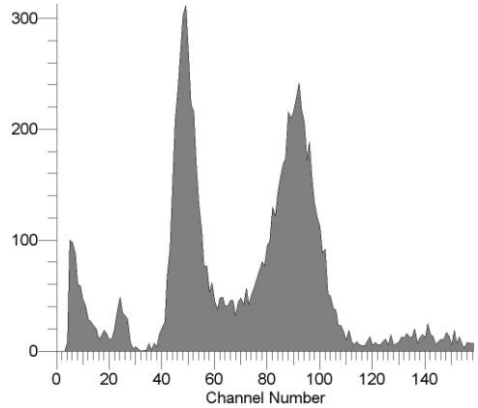

TX3
G_0/G_1: 31.9% S: 22.0% G_2/M: 46.1%
CV: 7.70 G_2/G_1-ratio: 1.89

T-47D-P experiments:

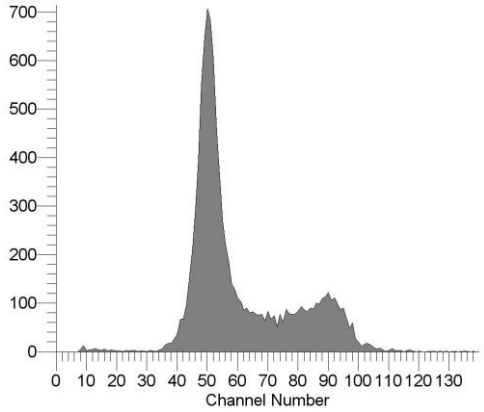

Initial cell-cycle distribution 1
G_0/G_1: 53.4% S: 28.1% G_2/M: 18.5%
CV: 7.12 G_2/G_1-ratio: 1.78

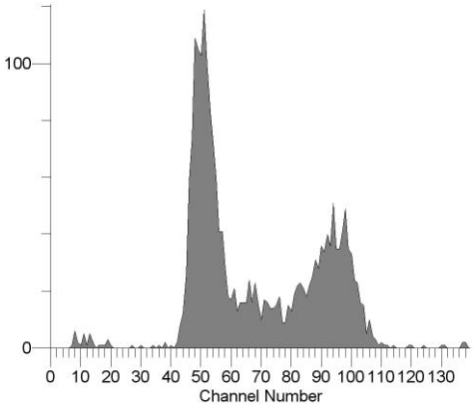

PX1
G_0/G_1: 40.8% S: 30.3% G_2/M: 28.9%
CV: 6.11 G_2/G_1-ratio: 1.88

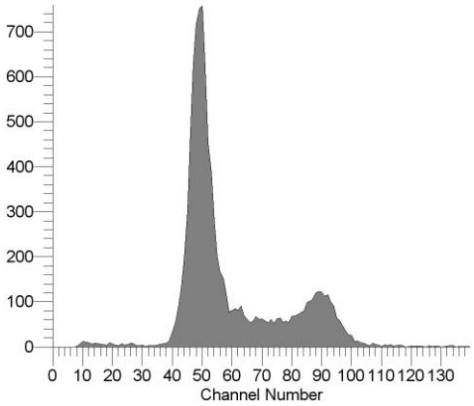

Initial cell-cycle distribution 2
G_0/G_1: 56.7% S: 24.6% G_2/M: 18.7%
CV: 6.64 G_2/G_1-ratio: 1.82

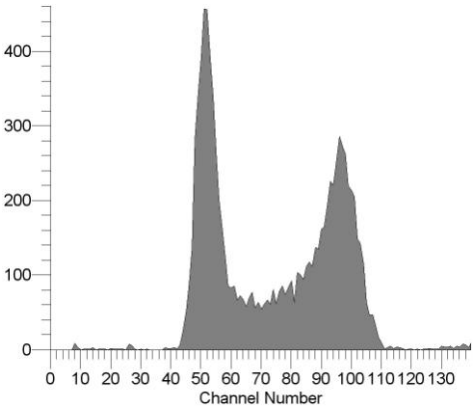

PX2
G_0/G_1: 33.2% S: 33.9% G_2/M: 32.9%
CV: 5.44 G_2/G_1-ratio: 1.88

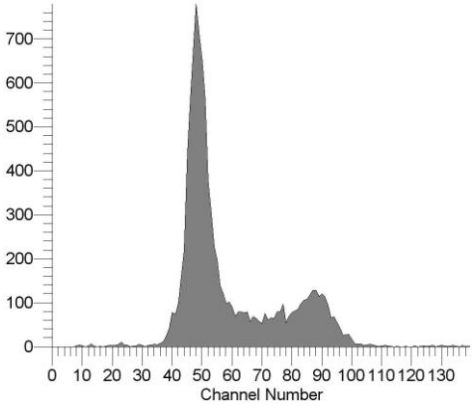

Initial cell-cycle distribution 3
G_0/G_1: 55.3% S: 26.0% G_2/M: 18.7%
CV: 6.77 G_2/G_1-ratio: 1.81

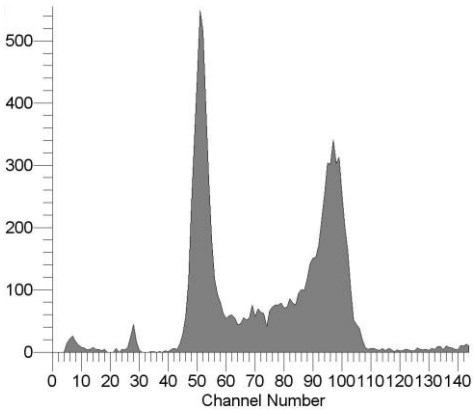

PX3
G_0/G_1: 33.6% S: 33.3% G_2/M: 33.1%
CV: 4.47 G_2/G_1-ratio: 1.89

C.3 Cell-Cycle Distribution 18 Hours after Trypsinization

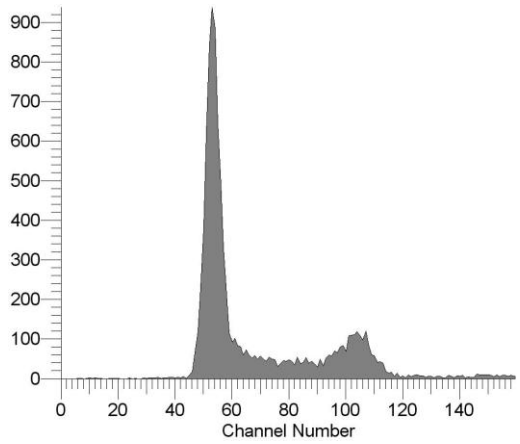

Cell-cycle distribution 1
G_0/G_1: 60.3% S: 26.5% G_2/M: 13.3%
CV: 4.81 G_2/G_1-ratio: 1.96

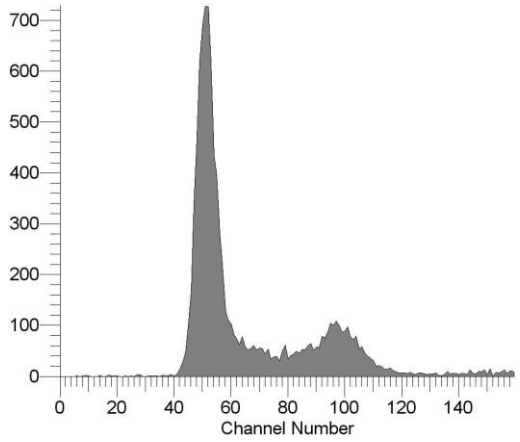

Cell-cycle distribution 2
G_0/G_1: 59.8% S: 25.3% G_2/M: 15.0%
CV: 6.21 G_2/G_1-ratio: 1.94

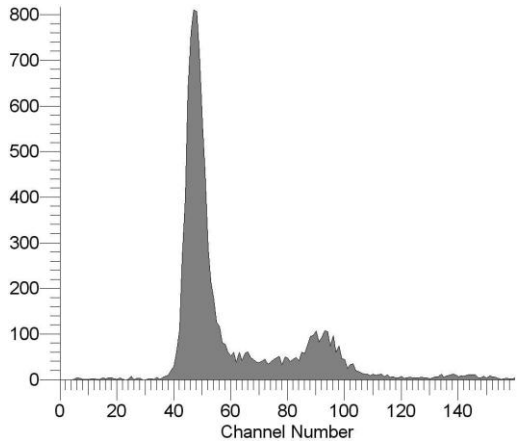

Cell-cycle distribution 3
G_0/G_1: 63.6% S: 22.5% G_2/M: 13.9%
CV: 6.21 G_2/G_1-ratio: 1.94

Appendix D: List of Chemicals

Below is a list of chemicals used in this study. The list is in alphabetical order and states the manufacturer of each chemical.

Chemical	Manufacturer
DNA prep LPR	Becton Dickinson (USA)
DNA prep stain (with 50 μg/ml propidium iodide)	Becton Dickinson (USA)
EDTA	Fluka (Switzerland)
Ethanol 96%	Arcus AS (Norway)
Fetal bovine serum	Euroclone (UK)
Glucose	Sigma (USA)
Hoechst 33342 (562 μg/ml)	Riedel de Haën (Germany)
Insulin	Sigma (USA)
KCl	Merck (Germany)
L-glutamine	Sigma (USA)
L-valine	Sigma (USA)
L-[3,4(n)-^{3}H]valine	Amersham, GE Healthcare (UK)
Methylene blue	Merck (Germany)
Milli-Q water	Millipore (USA)
NaCl	Riedel de Haën (Germany)
$NaHCO_3$	Norsk Medisinaldepot AS (Norway)
PBS	Euroclone (UK)
Penicillin-Streptomycin (5000 IU/ml-5000 μg/ml)	Euroclone (UK)
Phenol red	Merck (Germany)
RPMI 1640 powder with L-glutamine	JHR Biosciences (USA)
RPMI stem solution	Euroclone (UK)
Trypsin powder	Roche (Germany)

Appendix E: Recipes

RPMI 1640 medium

Stem solution, 1 liter	
RPMI 1640 powder	10.43 g
$NaHCO_3$	2.00 g
Milli-Q water	1.00 l

RPMI medium with serum, 1 liter	
RPMI 1640 stem solution	880 ml
Fetal calf serum	100 ml
Penicillin/streptomycin	10 ml
Insulin (200 units/l)	2 ml
L-glutamine	10 ml

Trypsin

Trypsin stem solution, 1 liter	
NaCl	8.00 g
KCl	0.40 g
Glucose	1.00 g
$NaHCO_3$	0.35 g
Phenol red	0.002 g
Milli-Q water	1.00 l

Trypsin with EDTA, 1 liter	
Trypsin stem solution	1.00 l
EDTA	200 mg
Trypsin powder	500 mg

L-glutamine, 35 ml

L-glutamine	1.0227 g
RPMI stem solution	35 ml

PBS, 1 liter

NaCl	8.000 g
KCl	0.201 g
KH_2PO_4	0.204 g
$NaHPO_4 \cdot 12H_2$	2.858 g
Milli-Q water	1.00 l

Appendix F: Medium with Tritium-Labeled Valine

Three components were mixed to obtain medium with the desired concentration (1.0 mM) and specific activity (1.6 Ci/mol) of valine. These components were:

1) 100 ml of RPMI 1640 full-medium (with serum).
2) Tritium-labeled valine solution diluted with water (Milli-Q, Millipore, MA, USA).
3) Cold valine solution with a valine-concentration of 126.87 mM (arbitrarily chosen).

The tritium-labeled valine solution was purchased in a small bottle with the activity measured to be 1.0 mCi/ml on June 19th, 2006, according to the specifications (Amersham, GE healthcare, Buckinghamshire, UK). To calculate the amount of cold valine needed, it was decided to dilute tritium-labeled valine solution with Milli-Q water to a total volume of 1.00 ml.

Valine has an atomic weight of 117.1 g/mol. RPMI 1640 contains 20 mg valine per litre, yielding a valine concentration of 0.171 mM. Be aware, however, that only 88 out of 100 ml of the RPMI full-medium have this valine concentration. It should also be noted that the activity of 1.0 mCi/ml in the tritium-labeled valine solution corresponded to an activity of 35 Ci/(mmol valine), resulting in a valine concentration of 0.0286 mM. This small amount of valine is negligible since less than 1 ml of the solution is added to the medium. Thus the required volume V_{CV} of cold valine needed to give a total concentration of 1.0 mM can be found by solving the following equation:

$$1.0\mathrm{mM} \cdot (101\mathrm{ml} + V_{CV}) - 0.171\mathrm{mM} \cdot 88\mathrm{ml} = 126.87\mathrm{mM} \cdot V_{CV}$$

From this it follows that $V_{CV} = 0.683\mathrm{ml}$ of the cold valine solution has to be added to the medium.

Next, it is necessary to find the required volume V_{TL} of tritium-labeled valine solution in order to obtain a specific activity of 1.6 Ci/mol. Radioactive decay has to be corrected for, since tritium has a relatively short half-life of 12.32 years. The experiments H2-H4 were started February 18th, 2008, which was 1.67 years after the activity was measured to be 1.0 mCi/ml. Consequently, the activity per unit volume was

$$A_V = 1.0\mathrm{mCi/ml} \cdot e^{-1.67 \cdot \ln 2/12.32} = 0.910\mathrm{mCi/ml}$$

at that time. The required volume V_{TL} could then be obtained from

$$\frac{0.910\mathrm{mCi/ml} \cdot V_{TL}}{1.0\mathrm{mM} \cdot 101.7\mathrm{ml}} = 1.6\mathrm{Ci/mol}$$

The solution to this equation is $V_{TL} = 0.179\mathrm{ml}$.

Thus 0.179 ml of the tritium-labeled valine solution was diluted with 0.821 ml of Milli-Q water, and added to the medium.

The recipes for cold valine solution (126.87 mM) and medium with tritium-labeled valine (1.6 Ci/mol) are given below:

Cold Valine (126.87 mM)

L-valine powder	0.742 g
RPMI stem solution	50 ml

Medium with Tritium-Labeled Valine (1.6 Ci/mol)

RPMI medium with serum	100 ml
Cold valine (126.87 mM)	0.683 ml
Tritium-labeled valine (0.910 mCi/ml)	0.179 ml
Milli-Q water	0.821 ml

Appendix G: Calculation of Doses from Incorporated Tritium

According to the dosimetry model introduced by Goddu et al. [1997], the absorbed dose in the nucleus from incorporated radionuclides is given by

$$D_N = \widetilde{A_C}\left[f_N S(N \leftarrow N) + f_{Cy} S(N \leftarrow Cy)\right] \tag{G.1}$$

where $\widetilde{A_C}$ is the integrated intracellular activity (i.e., the number of disintegrations per cell during the irradiation), $S(N \leftarrow N)$ is the dose to the nucleus per unit activity in the nucleus, $S(N \leftarrow Cy)$ is the dose to the nucleus per unit activity in the cytoplasm, and f_N and f_{Cy} are the fractions of intracellular activity in the nucleus and the cytoplasm, respectively. The cellular S values are functions of the cell radius R_C and the radius of the nucleus R_N, and have been calculated by Goddu et al. [1997].

By computer-aided image analysis Ingunn Bjørhovde [2006] measured the cell diameter to be 14±1 μm and the nucleus diameter to be 11±1 μm for T-47D cells. The corresponding S values are

$$S(N \leftarrow N) = 8.61 \cdot 10^{-4}\mathrm{Gy/(Bq\,s)}$$
$$S(N \leftarrow Cy) = 1.99 \cdot 10^{-4}\mathrm{Gy/(Bq\,s)}$$

Åste Søvik [2002] found that the tritium-incorporation data (plots of activity per cell as a function of incorporation time) can be fitted by the function

$$y = \frac{at}{b+t} \tag{G.2}$$

where y is the activity per cell, t is the time, and a and b are constants. The function satisfies the boundary conditions $y(t=0) = 0$ and $y(t \to \infty) \to a$ (positive constant). The incorporation kinetics in T-47D cells was measured by Bjørhovde [2006] using a scintillation counter (Packard TRI-CARB2100TR, Perkin Elmer, USA). She performed two experiments and found the following values:

$$a_1 = 0.01231\mathrm{Bq} \quad \wedge \quad b_1 = 106.68913\mathrm{h}$$
$$a_2 = 0.00902\mathrm{Bq} \quad \wedge \quad b_2 = 23.09813\mathrm{h}$$

When these values are known, the integrated activity $\widetilde{A_C}$ at any time t can be found by integrating the function in eq. (G.2):

$$\widetilde{A_C}(t) = \int_0^t \frac{at'}{b+t'}dt' = \Big[at' - ab\ln(b+t')\Big]_0^t = at - ab\ln\left(1+\frac{t}{b}\right) \tag{G.3}$$

Bjørhovde also measured the activity per cell, A_C, and the activity per nucleus, A_N, by scintillation counting. The measurements were performed when steady-state conditions were reached. From these results the fractions f_N and f_{Cy} could be calculated:

$$f_N = \frac{A_N}{A_C} \quad \wedge \quad f_{Cy} = 1 - f_N$$

The measured values were:

$$f_N = 0.60 \pm 0.05$$
$$f_{Cy} = 0.40 \pm 0.05$$

Using the values listed above, it is now straight-forward to calculate the absorbed dose D_N to the nucleus at any given time t from eq. (G.1).

The standard error is given by

$$\Delta D_N = \sqrt{\left(\frac{\partial D_N}{\partial \widetilde{A_C}} \cdot \Delta \widetilde{A_C}\right)^2 + \left(\frac{\partial D_N}{\partial f_N} \cdot \Delta f_N\right)^2} \qquad \text{(G.4)}$$

$$= \sqrt{\Big(f_N S(N \leftarrow N) + (1 - f_N) S(N \leftarrow Cy)\Big)^2 \Delta \widetilde{A_C}^2 + \Big(\widetilde{A_C}\big(S(N \leftarrow N) - S(N \leftarrow Cy)\big)\Big)^2 \Delta f_N^2}$$

The experiments H2-H4 were grown in medium with tritium-labeled valine for 48, 96 and 168 hours respectively. Since the cells were grown in medium with the same specific activity (1.6 Ci/mol)[1], the values measured by Bjørhovde can be used with equations (G.1) and (G.4) to calculate the absorbed doses given in chapter 3.3.3.

For incorporation times far exceeding 100 hours, which is the approximate time for steady state to occur, another approach can be used. Bjørhovde found that the dose rate under steady-state conditions is (0.015 ± 0.004) Gy/h, and she calculated the total dose after 100 hours of irradiation to be (1.0 ± 0.2) Gy. Thus the absorbed dose can be found as the sum of the total dose after the first 100 hours and the number of additional hours multiplied by the dose rate under steady-state conditions. This approach was used to calculate the dose for experiments H1 and H4 (see Ch. 3.3.3).

[1] Bjørhovde [2006] calculated that the specific activity in the medium used for her experiments had been reduced from 1.6 Ci/mol to 1.5 Ci/mol because of radioactive decay. However, she had not taken into consideration that only 88% of the RPMI 1640 full-medium (with serum) has a valine concentration of 0.171 mM. Thus she added too little cold valine, resulting in a total valine concentration of 0.97 mM rather than the intended 1.0 mM. If the (reduced) activity is divided by the actual valine content, it turns out that the specific activity was in fact 1.6 Ci/mol.

Appendix H: Exposure-Time Calculations

Since the dose rates for the different irradiation setups were found by irradiating small TLD dosimeters in the setup concerned, these dose rates only needed to be corrected for reduction in activity of the ^{60}Co source. Thus, if the dose rate $\dot{D}$ was measured to be 1.38 Gy/min on August 21st, 2007 (setup B), and the cells are supposed to be irradiated with 0.1 Gy on January 24th, 2008, i.e., 156 days later, the exposure time t is given by

$$t = \frac{D_{initial}}{\dot{D}} = \frac{0.1\text{Gy}}{1.38\text{Gy/min} \cdot e^{-\ln 2 \cdot \frac{156}{1925.1}}} = \frac{0.1\text{Gy}}{1.305\text{Gy/min}} = 0.0767\text{min}$$

However, the exact dose given will deviate slightly from $D_{initial}$. There are two reasons for this discrepancy:

1) The temporal resolution of the ^{60}Co unit's dose delivery system is limited to decimal-seconds (one-hundredth of a minute). So in this example, the cell sample will be irradiated for $t_{actual} = 0.08\text{min}$.
2) The intrinsic temporal inaccuracy in the shutter mechanism of the ^{60}Co unit. For low doses the shutter mechanism is not able to open and close fast enough to deliver the specified dose with high accuracy. This is called the shutter effect.

The shutter effect for the Theratron 780C/T1000 (MDS Nordion, Canada) used in these experiments has been determined by observing the response of an ionization chamber irradiated at a fixed position in a fixed field for different exposure times. The relative response per unit time of the chamber, normalized to the response from a 1 minute exposure, is a measure of the shutter effect. The measurements were performed by T. Furre and C. Lervåg irradiating a Farmer 23 chamber in a water tank at 6 mm physical depth, with SSD = 80 cm and field size 12 × 12 (display), corresponding to approximately 10 × 10 cm^2 at dose-max. Although different SSDs, field sizes and depths were used in irradiation setup A, B and C (see Ch. 3.3.2), it is reasonable to assume that the measured relative responses after different exposure times are valid also for these setups. The measurements are shown in figure H.1.

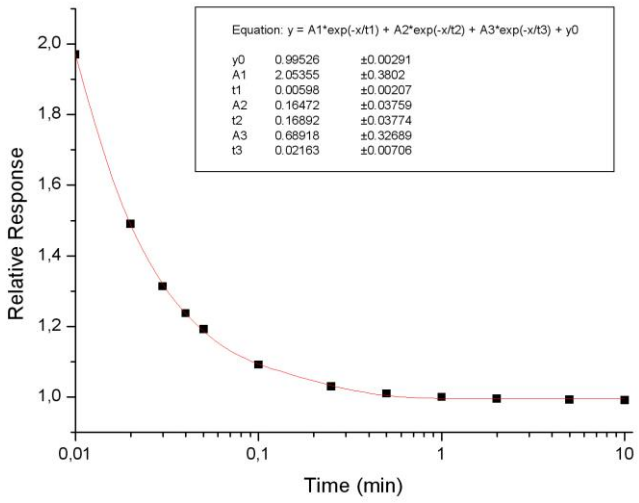

Figure H.1
The figure shows the relative response per unit time at a fixed position in a fixed field, as a function of irradiation time. The measured data has been fitted by a third-order exponential decay function in Origin. Also shown are the parameters determined by the curve fitting.

An excellent interpolation between the measured data points was obtained in Origin (version 7) by fitting the data with a third-order exponential decay function. Using this function, a correction factor for the shutter effect can be found for all irradiation times. For an exposure time of 0.08 min, the correction factor $k_{shutter}$ equals 1.115.

The exact dose given in the example above can then be calculated as follows:

$$D_{exact} = \dot{D} \cdot t_{actual} \cdot k_{shutter} = 1.305\mathrm{Gy/min} \cdot 0.08\mathrm{min} \cdot 1.115 = 0.116\mathrm{Gy}$$

In other words, the actual dose delivered in this case is 16% higher than intended. However, as can be seen from figure H.1, the shutter effect decreases rapidly with increasing exposure time, and this example (from experiment P1) was chosen because it represents the maximal relative error in dose delivery from the experiments of this thesis. Even though the relative errors are large in a few cases for the lowest doses given, the absolute errors are relatively modest, and corrections for the effects described here are not performed in the presentations of graphs and experimental raw data elsewhere in this thesis.